EXHIBIT 22

GASTROENTEROLOGY 1994;106:1076-10[illegible]

SPECIAL REPORTS AND REVIEWS

Gene Therapy: Applications to the Treatment of Gastrointestinal and Liver Diseases

ALAN G. Y. CHANG and GEORGE Y. WU

Department of Medicine, Division of Gastroenterology-Hepatology, University of Connecticut School of Medicine, Farmington, Connecticut

There has been much progress in our understanding of molecular mechanisms in the pathogenesis of inherited metabolic disorders. In addition, powerful new molecular techniques have made possible phenotypic alterations by delivery of foreign genes to target cells. As a result, concepts and methods that would have been considered purely science fiction 10 years ago can now be found in human clinical trials engaged in the treatment of these disorders. In this review, we have attempted to provide an introduction and survey of the topic of gene therapy, with specific examples of laboratory and clinical achievements to date, and highlights on potentials for applications in digestive diseases.

Gene therapy, the introduction of new genetic material into an affected cell or organism to correct a disease phenotype, is rapidly evolving into a potential method of treatment for human illness. Advances in molecular biology have led to the identification of genetic defects in many disease processes and have given scientists the ability to create functionally normal copies of the involved gene.

The term "gene replacement" therapy refers to the specific replacement of an abnormal gene with a normal copy. In this method, homologous or site-specific recombination is required. It increases the probability that the transferred gene will function correctly by substitution of a normal for an abnormal gene at the corresponding site on the chromosome. This targeted insertion reduces the likelihood of disruption of other cellular genes, an event that can occur with random insertion.[1] However, site-specific recombination is relatively inefficient, with over 1000 copies of the gene randomly spliced into the genome for every one that is inserted properly.[1,2] Because of this inefficiency, most of the current work in gene therapy involves "gene augmentation," which is achieved by transferring a functionally normal copy into a cell with a defective or absent gene without physically replacing the defective gene itself. Gene augmentation can be useful for treatment of single gene, recessive disorders, and for dominant diseases in which expression of a wild-type gene will override the abnormal dominant phenotype.[3]

To date, efforts to develop human gene therapy systems have focused solely on somatic cells. Ethical concerns regarding the possibility of introducing exogenous genetic material into the gene pool have kept germ cells from being used as target tissues for gene therapy.[4]

Methods of clinical gene transfer into human cells are based on two general approaches: ex vivo and in vivo strategies. In ex vivo methods, the target cells are harvested from the host and grown in culture. Then, the desired genetic material is introduced into the cells in culture, and the cells are subsequently transplanted back to the affected host. In contrast, in vivo techniques seek to avoid this multistep process by directly introducing the normal gene into the host to deliver the gene to a specific target tissue or organ.

Although gene therapy is still in its infancy, with most studies to date confined to the laboratory, clinical applications are being explored. Following the pioneering studies on adenosine deaminase deficiency treated with transfer of the adenosine deaminase gene into lymphocytes,[5] several other trials of gene therapy are in progress, and many others have recently been approved.[6-8] Applications to gastrointestinal and liver diseases will be discussed below.

Strategies for Gene Transfer

Ex Vivo Gene Transfer

Ex vivo gene transfer has been studied extensively using hepatocytes. Liver cells can theoretically be obtained through liver biopsy, partial hepatectomy, and from specimens otherwise harvested for orthotopic liver transplantation.[9] They are then purified and grown in culture.[10-13] Adult liver cells transiently undergo active proliferation, allowing in vitro gene transfer, even with vectors that require active cell division for efficacy.[12]

Abbreviations used in this paper: CF, cystic fibrosis; CFTR, cystic fibrosis transmembrane conductance regulator; FH, familial hypercholesterolemia; GCSF, granulocyte colony-stimulating factor; HSV, herpes simplex virus; LDL, low-density lipoprotein; OTC, ornithine transcarbamylase; PAH, phenylalanine hydroxylase; WHHL, Watanabe heritable hyperlipidemic.

0016-5085/94/$3.00

Calcium phosphate coprecipitated with DNA, first described in 1973,[14] results in the formation of insoluble calcium phosphate–DNA complexes. When added to cell cultures, these complexes are endocytosed into the cells after coming in contact with their membranes. This method is relatively simple, rapid, and has been applied to hepatoma and hepatocyte cell lines. However, it is inefficient, with stable transfection frequencies less than 1%.[15,16] Stable transfection efficiency has been improved up to 50% by using plasmid DNA and varying the pH of buffer in which the calcium phosphate–DNA complex formed.[17] Poor survival, especially in primary cultures of hepatocytes, has been a problem.

Liposomes are vesicular structures composed of a spherical phospholipid bilayer surrounding an inner aqueous medium. They can be used to package material for delivery to cells,[18–20] which then take up the liposomes by endocytosis. In vitro efficiency of liposome-mediated gene transfer is roughly comparable with calcium phosphate precipitation methods using plasmid DNA.[20]

Other nonviral methods include diethylaminoethyl dextran,[21] polybrene,[22] electroporation,[23–25] and sonication loading.[26] These methods have been originally developed for in vitro gene transfer.

Viruses have evolved to transfer their genetic material into eukaryotic cells efficiently. Therefore, it is not surprising that viral vectors, primarily retroviruses, have proven to be more efficient than the above methods for gene transfer.[27,28] To produce retroviral transfection vectors, a packaging cell line containing genes that produce envelope components, but lack a packaging signal (ψ), is constructed.[6] A recombinant plasmid is prepared containing a complementary DNA of the retrovirus that has been rendered replication-defective by insertion of a gene of interest in place of the genes for packaging.[6] The ψ sequence allows the RNA transcript of the recombinant plasmid to be packaged into viral particles that are then secreted into the culture media.[6] Following exposure and entry into cells, viral reverse transcriptase then converts viral RNA to double-stranded DNA, which then stably integrates into the host genome, allowing synthesis of viral proteins.[29] Integration of this newly formed double-stranded DNA into the host DNA requires active cell division.

Other viral vectors, such as adenovirus, adenoassociated virus,[6,30,31] herpesvirus,[31–33] and hepatitis B virus (HBV)[34,35] have been used to transfer genes into hepatocytes or hepatoma cell lines in vitro and have the potential for advantages and disadvantages in gene transfer for ex vivo gene therapy (Table 1).

The final step in ex vivo gene transfer to liver cells requires reintroduction of transfected hepatocytes into the host. Therefore, the recent advances in hepatocyte transplantation are very important in ex vivo methods of gene delivery. Many different locations for transplantation of hepatocytes have been used, including intraperitoneally via a microcarrier system[36–38] or in gel beads,[39] on a hepatocyte-coated cell support matrix implanted next to liver tissue,[40] or intrasplenically through direct injection.[41–46] In addition, transplanted hepatocytes have been directly injected intravascularly into portal[45,47] and umbilical veins.[48] Comparisons of these routes reveal that the most effective methods for hepatocyte survival involve intraportal and intrasplenic introduction of the cells[45,47,49,50] with intraportal methods requiring fewer hepatocytes than intrasplenic transplantation.[45]

Experience with hepatocyte transplantation in humans is limited, though initial success has been achieved infusing transfected hepatocytes into the portal circulation via an indwelling catheter placed initially at the time of surgical harvest of the liver cells.[51]

In Vivo Gene Transfer

In vivo gene transfer methods offer the advantage of avoiding the multistep process of ex vivo gene delivery, including the need to obtain and culture cells. However, it adds the challenge of targeting the delivery system to a specific tissue to ensure that the transferred genetic material arrives at the target in sufficient quantities and does not affect other organ systems.

Calcium phosphate–DNA coprecipitation. Direct injection of calcium phosphate–DNA precipitates into mouse liver and spleen has been shown to result in successful transfection and active viral replication.[52] DNA precipitated with calcium phosphate can also be injected intraperitoneally with subsequent expression of the transfected gene in liver and spleen.[53]

Particle bombardment. By coating tiny gold beads with plasmid DNA and using a high-voltage discharge between two electrodes, particle bombardment can successfully transfer genetic material to the liver, as well as other organ systems.[54] This method can be used in vivo during surgical procedures or in vitro for bombardment of tissue cultures.[54]

Liposomes. Although liposomes can be used for in vitro gene transfer as previously discussed, in vivo usage is potentially more attractive. Intravenously injected liposomes containing rat insulin gene are taken up primarily by the liver and spleen.[55] Hepatic uptake accounts for 40%–60% of an injected dose of liposomes, with most of the vesicles taken up by Kupffer cells.[20] Improvement in hepatocyte uptake can be achieved by incorporating lactosyl-ceramide into the phospholipid bilayer; this galactose-terminal asialoganglioside is specifically recognized by a receptor highly selective for hepatocytes.[20] In addition, by introducing desired DNA with added nuclear proteins in the liposomes, DNA expression in hepatocytes transfected in vivo can be increased more than fivefold when compared with DNA in liposomes without the nuclear proteins.[55] The nuclear proteins facilitate foreign DNA migration into the nu-

Table 1. Characteristics of Common Viral Vectors

Virus	Advantages	Disadvantages
Retrovirus	Extensive experience using this virus is available Efficient Integrates genome	Need for active cell replication Potential risk of insertional mutagenesis Potential for development of replication-competent (helper) virus (depending on the construct)
Adenovirus[6]	Able to concentrate to high titers Can infect nonreplicating cells No packaging cell lines	Presence of many adenoviral genes in vectors can stimulate immunity, affecting ability to give repeated doses
Adenoassociated virus (AAV)	Less risk of insertional mutagenesis Nonpathogenic (ubiquitous in humans)[30,31] Can infect nonreplicating cells	Lack of information on long-term consequences of integration and gene expression from the AAV provirus[30] Requires co-infection with helper adenovirus or herpes virus for replication[31]
Herpes virus	Can infect nonreplicating cells Large genome (150 kb), can potentially transfer large, intact genes[31]	Little information on long-term fate or stability of gene expression Could potentially become latent in neural cells[31]
HBV (Hepadnavirus)	Hepatotropic[35] Tendency to integrate in vivo	Little information or experience with its usage

cleus of hepatocytes, thus enhancing its transcription and translation, even in nondividing cells.[56]

Viral vectors. Viral vectors can be used for in vivo gene transfer in addition to the in vitro methods previously discussed. It is difficult, however, to direct viruses to infect a single organ or tissue as is desired for in vivo use. This problem can be circumvented by temporarily excluding the liver, or target organ, from circulation surgically. Retroviruses, as discussed above, need actively dividing cells to allow integration of viral DNA into the host genome. Adult hepatocytes in vivo, however, are largely quiescent. By performing a partial hepatectomy, adult liver cells can be stimulated to divide and allow retroviral-mediated transfection.[57] Retroviruses have been shown to persist in up to 5% of hepatocytes for at least 3 months after two-thirds hepatectomy, removal of the liver from the circulation, injection of viruses into the portal vein, and restoration of normal blood flow.[57]

Concerns with use of retroviruses include insertional mutagenesis and abnormal regulation of the foreign gene due to insertion adjacent to undesirable enhancer-promoter regions. Another potential concern with the use of defective retroviral vectors is the potential appearance of wild-type replication-competent virus in the packaging cells. This can result from recombination events in which the intact ψ sequence from the recombinant virus inserts upstream from the gag, pol, env sequence integrated in the host cell genome. However, novel packaging cell lines are now available that should greatly decrease the likelihood of recombination.[58,59]

Another limitation to the use of retrovirus vectors in vivo is the inability to produce retroviral vector titers greater than 10^6 infectious units per milliliter. Titers 10- to 1000-fold higher are necessary for many in vivo applications.

Adenoviruses can infect nondividing cells and do not require partial hepatectomy before portal vein injection with concomitant temporarily blocked hepatic inflow and outflow. Transfection efficiency rates of 30%–50% persisting for 3 weeks using this method have been achieved in rats.[60]

Receptor-mediated methods. Cell-surface receptors can also be used to target DNA delivery to specific organs. Hepatocytes are particularly well suited for this route of gene delivery because they possess receptors that recognize galactose-terminal (asialo-) glycoproteins. These receptors bind this class of circulating glycoproteins, with subsequent internalization by endocytosis in membrane-bound vesicles (endosomes).[61] Intracellular segregation leads to return of the receptor to the cell membrane for reuse and transport of the glycoprotein to lysosomes for degradation.[62]

A variety of agents can be delivered to hepatocytes using asialoglycoproteins as vehicles.[63–65] These agents were covalently coupled to the glycoproteins.[66] However, covalent bonding between DNA and the asialoglycoprotein could cause damage to the base pairs and result in altered transcription.[66] To prevent this potential problem, a vehicle consisting of a polycation, poly-L-lysine, covalently bound to a naturally occurring asialoglycoprotein, asialoorosomucoid, has been created. The polycation binds negatively charged DNA in an electrostatic, nondamaging manner.[66,67]

This soluble DNA carrier system delivers its foreign genes specifically to the liver after intravenous injection, as shown in a rat model.[67] Foreign gene expression can be made to persist at least 11 weeks postinjection by

DNA Sequencing by Capillary Electrophoresis with Replaceable Linear Polyacrylamide and Laser-Induced Fluorescence Detection

Marie C. Ruiz-Martinez, Jan Berka,† Alexei Belenkii, Frantisek Foret,‡ Arthur W. Miller,§ and Barry L. Karger*

Barnett Institute, Northeastern University, 360 Huntington Avenue, Boston, Massachusetts 02115

Replaceable linear polyacrylamide (LPA) has been utilized as a sieving matrix for DNA sequencing by capillary electrophoresis (CE). Difficulties associated with cross-linked polyacrylamide gel stability have been overcome for the routine application of CE to DNA sequencing. A simple laser-induced fluorescence (LIF) detection system based on a single laser and two photomultipliers (PMT) has been adopted for this work. Sequencing information for four bases has been obtained from two fluorescent dyes and two peak height ratios, detected in two optical channels. FAM- and JOE-labeled M13 (-21) primers have been chosen because both dyes are efficiently excited with a low-power argon ion laser, can be optically separated, and exhibit minimal dye-based shifts in DNA fragment mobilities. Addition of denaturants to the electrophoresis running buffer (1 × TBE, 3.5 M urea, 30% formamide) and column operation at 32 °C permitted the resolution of difficult compressed sites in the sequence of phage M13mp18. Careful examination of the polymerization reaction of LPA has led to methodology that has proven to be reproducible for obtaining DNA sequencing information of M13mp18 phage for 350 nucleotides in close to 30 min.

INTRODUCTION

High-speed DNA sequencing methods are under rapid development, both for the needs of the Human Genome Project and for general sequencing applications. At present, high-resolution electrophoretic techniques are the standard procedures for the separation of DNA sequencing reaction products. The limited throughput of standard gel electrophoretic techniques, however, remains a barrier for the sequencing of large genomes. Furthermore, rapid, automatable methods that are cost effective for clinical, forensic, and general molecular biological applications are required.

Since the first reports on ultrahigh resolution of DNA mixtures using capillary gel electrophoresis,[1] CE has been successfully applied to different kinds of DNA analysis, including the following: DNA sequencing,[2-6] separation of restriction fragments,[7-14] synthetic oligonucleotides,[6,15] and PCR products.[6,16-18] The relatively low currents in fused silica capillary columns enable high electric fields to be applied without damage to the separation matrix from overheating. Large electric field strengths result in an order of magnitude increase in separation speed over conventional methods. The overall throughput of CE can be further increased by analyzing many samples in parallel, e.g., through the use of capillary arrays.[19-21] A related modification of standard slab gel electrophoresis has been described utilizing horizontal ultrathin slab gels.[22,23]

In the case of CE, adoption for DNA sequencing has been limited. Problems related to the stability of gel-filled capillaries with sequencing reaction products hinder the full automation of CE-based systems. The instability of cross-linked gels in capillary columns is manifested by either formation of bubbles or a steady decline of current, caused by a resistivity increase normally at the injection end of the capillary. These problems make the gel-filled capillaries useable for only a few injections, even when the capillary end is trimmed after each run. Although the effects of formation of anomalous conductivity zones, resulting in ion depletion at the gel/liquid interface,[24] can be reduced by adding denaturant and acrylamide monomers to the buffer reser-

* Author to whom reprint requests and correspondence should be sent.
† On leave from The Institute of Pathological Physiology, School of Medicine, Masaryk University, Brno, Czech Republic.
‡ On leave from The Institute of Analytical Chemistry, Veveri 97, Brno, Czech Republic.
§ College of Computer Science, Northeastern University.

(1) Cohen, A. S.; Najarian, D. R.; Paulus, A.; Guttman, A.; Smith, J. A.; Karger, B. L. *Proc. Natl. Acad. Sci. U.S.A.* 1988, *85*, 9660-9663.
(2) Drossman, H.; Luckey, J. A.; Kostichka, A. J.; D'Cunha, J.; Smith, L. M. *Anal. Chem.* 1990, *62*, 900-903.
(3) Cohen, A. S.; Najarian, D. R.; Karger, B. L. *J. Chromatogr.* 1990, *516*, 49-60.
(4) Luckey, J. A.; Drossman, H.; Kostichka, A. J.; Mead, D. A.; D'Cunha, J.; Norris, T. B.; Smith, L. M. *Nucleic Acids Res.* 1990, *18*, 4417-4421.
(5) Karger, A. E.; Harris, J. M.; Gesteland, R. F. *Nucleic Acids Res.* 1991, *19*, 4955-4963.
(6) Swerdlow, H.; Zhang, J. Z.; Chen, D. Y.; Harke, H. R.; Grey, R.; Wu, S.; Dovichi, N. J. *Anal. Chem.* 1991, *63*, 2835-2841.
(7) Heiger, D. N.; Cohen, A. S.; Karger, B. L. *J. Chromatogr.* 1990, *516*, 33-48.
(8) Grossman, P. D.; Soane, D. S. *J. Chromatogr.* 1991, *559*, 257-266.
(9) Motsch, S. R.; Kleemis, M. H.; Schomburg, G. *J. High Resolut. Chromatogr.* 1991, *14*, 629-632.
(10) Bocek, P.; Chrambach, A. *Electrophoresis* 1992, *13*, 31-34.
(11) Guttman, A.; Wanders, B.; Cooke, N. *Anal. Chem.* 1992, *64*, 2348-2351.
(12) Stege, M.; Lagu, A. *Anal. Chem.* 1991, *63*, 1233-1236.
(13) MacCrehan, W. A.; Rasmussen, H. T.; Northrop, D. M. *J. Liq. Chromatogr.* 1992, *15*, 1063-1080.
(14) Baba, Y.; Matsuura, T.; Wakamoto, K.; Tsukako, M. *J. Chromatogr.* 1991, *558*, 273-284.
(15) Paulus, A.; Ohms, J. I. *J. Chromatogr.* 1990, *507*, 1113-1123.
(16) Schwartz, H. E.; Ulfelder, K.; Sunzeri, F. J.; Busch, M. P.; Brownlee, R. G. *J. Chromatogr.* 1991, *559*, 267-283.
(17) McCord, B. R.; McClure, D. L.; Jung, J. M. *J. Liq. Chromatogr.*, in press.
(18) Nathakarnkitkool, S.; Oefner, P. J.; Bartsch, G.; Chin, M. A.; Bonn, G. K. *Electrophoresis* 1992, *13*, 18-30.
(19) Huang, X. C.; Quesada, M. A.; Mathies, R. A. *Anal. Chem.* 1992, *64*, 2149-54.
(20) Kambara, H.; Takahashi, S. *Nature* 1993, *361*, 565-566.
(21) Taylor, J. A.; Yeung, E. A. *Anal. Chem.* 1993, *65*, 956-960.
(22) Kostichka, A. J.; Marchbanks, M. L.; Brumley, R. L., Jr.; Drossman, H.; Smith, L. M. *Bio/Technology* 1992, *10*, 78-81.
(23) Ansorge, W.; Voss, H.; Wiemann, S.; Schwager, C. H.; Sproat, B.; Zimmermann, J.; Stegemann, J.; Erfle, H.; Hewitt, N.; Rupp, T. *Electrophoresis* 1992, *13*, 616-619.
(24) Spencer, M. *Electrophoresis* 1983, *4*, 36-41.

0003-2700/93/0365-2851$04.00/0

voirs,[25] cross-linked or high % T nonreplaceable linear polyacrylamide-filled capillaries still cannot generally be used for more than 5–10 sequencing runs without a significant loss in signal and resolution.[26,27] In addition, the cross-linked gel columns cannot be used above room temperature. To permit multiple consecutive DNA sequencing runs on the same capillary, additional methods for sample purification, including DNA template removal, have been described.[25,28] Despite these developments, there is still a critical need for improved column design for routine use.

In this work, low- to moderate-viscosity linear polyacrylamide (LPA) matrices for DNA sequencing analysis have been developed in order to overcome the problems of gel stability. The advantage of such matrices is that, along with providing powerful separation, the LPA can be replaced after each run. In effect, this means that each sequencing run is conducted on a fresh column. Furthermore, the denaturing agent of the running buffer has been modified from the typical 7 M urea to 3.5 M urea plus 30% (v/v) formamide in order to reduce the viscosity of the medium while enhancing the denaturing ability of the buffer with the addition of formamide.[29] With replaceable LPA, the most laborious and time-consuming steps in CE, i.e., the preparation and alignment of the separation column, are reduced to a simple reloading of the sieving medium.[30]

The sequencing strategy utilizes modification of Sanger–Coulson dideoxy sequencing chemistry to achieve approximately equal product amounts,[31,32] along with a single-laser, two-fluorescent-dye primer approach, related to that recently reported;[33] however, on-column detection has been used instead of the flow sheath cuvette. Such a simple and relatively inexpensive system can be accessible to many laboratories. Moreover, this system is, in principle, compatible with a capillary array arrangement. Of course, other sequencing strategies, e.g., four-dye-labeled primers or terminators, could be incorporated into the replaceable matrix format. In principle, CE using replaceable LPA matrices should also be compatible with membrane collection/multiplexing schemes.[34]

EXPERIMENTAL SECTION

Instrumentation. The instrumental design using one laser and two photomultiplier tubes (PMTs) is illustrated in Figure 1. The power supply (point 16 in Figure 1) was 60 kV dc (Model PS/MK30, Glassman, Whitehouse Station, NJ). Laser light from the 488-nm emission of a low-power argon ion laser (7 mW) (point 1) (Model 532, Omnichrom, Chino, CA) was first passed through a narrow band-pass filter (488 nm) (point 2) (Melles Griot, Irvine, CA), and then the intensity of the light was decreased by a neutral density filter (Melles Griot) (point 3) to 1.2 mW. The laser light was next reflected by a 45° mirror (point 4) (Newport, Fountain Valley, CA) and focused by an achromatic lens (focal length 20 mm) (point 5) (Melles Griot) onto a detection window of a horizontally positioned fused silica capillary of dimensions 75-μm i.d., 360-μm o.d. (point 6) (Polymicro Technologies, Inc., Phoenix, AZ). The detection window (3 mm in length) was formed

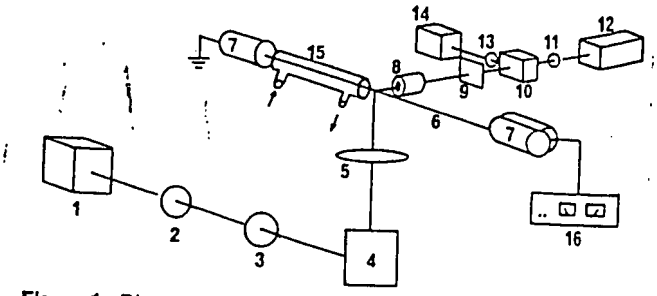

Figure 1. Diagram of the DNA sequencing instrument. Details of the component parts can be found in the Experimental Section.

by stripping the polyimide coating off the capillary with a razor blade. The buffer reservoirs (point 7) were positioned at the same height and refilled daily with fresh, filtered buffer. At the anodic end, a double buffer reservoir filled with 1 × TBE, which separated the capillary from the electrode chamber, was utilized to protect the capillary from water electrolysis products which can react with gel or buffer components, causing an increase of background fluorescence noise during prolonged operation under high electric fields.[35]

At the cathodic end, a single buffer reservoir filled with 1 × TBE, 7 M urea buffer was used. The capillary was placed inside a stainless steel tube of 380-μm i.d., which was then inserted into a water jacket 10 cm in length (point 15). For capillaries with an effective length of 18 cm, about 4 cm of the column protruded from the water jacket at the cathodic end for insertion into the buffer reservoir and another 4 cm of the capillary protruded from the end of the water jacket to the detection window. The water jacket was controlled by a circulating bath at 32 °C.

Light emitted from the capillary was collected by a 40× microscope objective (Oriel, Stamford, CT) (point 8) and passed through a high-pass, 488-nm reflecting filter (Melles Griot) (point 9), followed by a visible spectrum 50/50 beam splitter (Type BS-550-S, Corion, Holliston, MA) (point 10). The fluorescence signal transmitted through the beam splitter was filtered by an interference filter (515 ± 10 nm) (point 11) (Corion), which isolated the emission from the DNA fragments that were fluorescently labeled with the primer FAM (Applied Biosystems, Foster City, CA), for detection by a PMT (Hamamatsu Type 647, Hamamatsu Photonics K.K., Japan) (point 12). The light reflected from the beam splitter was filtered by a 550 ± 10-nm interference filter (Corion) (point 13), which isolated the emission of DNA fragments that were fluorescently labeled with the primer JOE (Applied Biosytems), for detection by a second PMT (Hamamatsu Type 928) (point 14). The signals were collected at a 10-Hz sampling rate by a Perkin-Elmer Nelson data acquisition system using Turbochrom software (Version 3.2) running on an IBM compatible 486 DX-2 personal computer. The residual FAM emission in the JOE channel was subtracted by computer data processing. Finally, the sequence was coded and analyzed by the software described in the Appendix section.

DNA Sequencing Reaction and Sample Preparation. Two commercially available labeled primers FAM and JOE (-21) M13 were utilized (Applied Biosystems). One picomole of fluorescent dye-labeled primer, FAM or JOE, was annealed to 0.5 pmol of M13mp18 single-stranded DNA template (New England Biolabs, Inc., Beverly, MA) in 1 × sequencing buffer (USB, Cleveland, OH) by heating the solution to 65 °C and cooling it to 20 °C for 30 min. Nucleotide termination mixtures containing 720 μM portions of each of the deoxynucleotides (dNTP) (USB) and a 7.2 μM portion of a single dideoxynucleotide (ddNTP) (USB) were prepared. The proper product ratio, 3:1, was obtained by mixing 16.5 μL of the termination mixture ddC and 3.5 μL of the termination mixture ddT for the JOE-primed sequencing reaction. For the FAM-primed sequencing reaction, 12 μL of the termination mixture ddA plus 8 μL of the termination mixture ddG were mixed to obtain the product ratio of 3:1, respectively.

(25) Swerdlow, H.; Dew-Jager, K.; Brady, K.; Grey, R.; Dovichi, N. J.; Gesteland, R. *Electrophoresis* **1992**, *13*, 475–83.
(26) Smith, L. M. *Nature* **1991**, *349*, 812–813.
(27) Pentoney, S. L.; Konrad, K. D.; Kaye, W. *Electrophoresis* **1992**, *13*, 467–74.
(28) Tong, X.; Smith, L. M. *Anal. Chem.* **1992**, *64*, 2672–2677.
(29) Rocheleau, M. J.; Grey, R. J.; Chen, D. Y.; Harke, H. R.; Dovichi, N. J. *Electrophoresis* **1992**, *13*, 484–486.
(30) Sudor, J.; Foret, F.; Bocek, P. *Electrophoresis* **1991**, *12*, 1056–1058.
(31) Tabor, S.; Richardson, C. S. *J. Biol. Chem.* **1990**, *265*, 8322–6.
(32) Ansorge, W.; Zimmermann, J.; Schwager, C.; Stegeman, T.; Erfle, H.; Voss, H. *Nucleic Acids Res.* **1990**, *18*(11), 3419–3420.
(33) Chen, D. Y.; Harke, H. R.; Dovichi, N. J. *Nucleic Acids Res.* **1992**, *20*, 4873–80.
(34) Church, G. M.; Kieffer-Higgins, S. *Science* **1988**, *240*, 185–188.
(35) Carson, S.; Cohen, A. S.; Belenkii, A.; Ruiz-Martinez, M. C.; Berka, J.; Karger, B. L. *Anal. Chem.*, in press.

Chain extension and termination reactions were initiated in the presence of 5.5 mM DTT (USB) and 1 × Mn buffer (USB) by the addition of 1 μL (13 units) of Sequenase (Version 2.0 USB) and 1 μL (0.005 units) of inorganic pyrophosphatase (USB). After 10 min of incubation at 37 °C, the reactions were terminated by ammonium acetate/ethanol precipitation at −20 °C for 2 h. DNA was then washed twice with 70% ethanol, dried under vacuum, and resuspended in 5 μL of 95% formamide:5% (50 mM) EDTA. The FAM- and JOE-labeled fragments were mixed in equal amounts, and the sample was heated to 95 °C for 5 min, followed by chilling on ice before electrokinetic injection into the capillary.

Capillaries and Linear Polyacrylamide Preparation. The capillaries were coated with LPA as previously described by Hjerten et al.[36] The replaceable LPA matrices were prepared as follows: 0.60 g of acrylamide (ultrapure, ICN, Costamesa, CA) was dissolved in 10 mL of 1 × TBE, 30% formamide, 3.5 M urea buffer, filtered (0.2-μm pore size), and degassed. The monomer solutions were typically polymerized by addition at room temperature of 2 μL of 10% (w/v) ammonium persulfate (ICN) and 1 μL of 100% TEMED (Bio-Rad, Richmond, CA) per milliliter of monomer solution (i.e., final concentration of APS = 0.02% (w/v), TEMED = 0.1% (v/v)). (Recently, the polymerization procedure has been optimized for milliliter volume sizes.) The solutions were filled into 100-μL gas-tight syringes (Rainin, Woburn, MA) and then placed in either a cooling water bath thermostated at 10 °C or a refrigerator set at 0 °C. Polyacrylamide-filled syringes were stored in the refrigerator (0 °C) and could be used for at least 10 days.

The LPA matrix was replaced in the capillary before each run by connecting the 100-μL syringe needle to the capillary with a short piece of Teflon tubing. After fresh polymer matrix was loaded into the column, the capillary was electrodialyzed for 10 min at a constant electric field of 250 V/cm in order to decrease the background fluorescence. Electrodialysis can be conducted on the polymer matrix directly; however, in this work, it was more practical to electrodialyze the matrix in the capillary prior to DNA sequencing analysis.

The electrophoretic conditions for separation of the reaction products of DNA sequencing were as follows: electric field = 250 V/cm, current = 7 μA, effective capillary length = 18 cm, total length = 33 cm, column temperature = 32 °C (10 cm of the capillary effective length heated). The whole analysis time, including the replacement of the matrix and electrodialysis, was about 45 min, with separation achieved in close to 30 min.

Viscosity and Oxygen Content Measurements. The viscosity of the polymer networks were measured by means of a falling ball, size 3, tantalum ball viscometer (Gilmont, Barrington, IL) in a water bath at a constant temperature of 18 °C. The oxygen concentration of the acrylamide solutions was measured at 20 °C by a dissolved oxygen meter with RTD/polarographic oxygen sensor (Type G-05505-00, Cole Palmer, Niles, IL).

RESULTS AND DISCUSSION

As noted in the Introduction, several reports have discussed the lack of the stability of gel-filled capillaries as an impediment to the routine application of CE to DNA sequencing. If sufficient resolution were achievable, low to moderate-viscosity LPA networks would permit the use of replaceable sieving matrices for the separation of DNA sequencing reaction products. Previously, this laboratory showed that LPA (9% T) provided single-base resolution of polyadenylic acids,[7] but this matrix was too viscous to allow easy replacement from the capillary. In the present work, we therefore studied lower percentages of LPA for the single-base separation of DNA fragments. The sequencing strategy utilized a simple base coding and a single-laser, two-PMT instrument that could be easily incorporated into a practical setting.

Instrument Configuration. The instrumentation design was related to that recently described using one laser and two PMTs.[33] The difference between that system and the present one was that the detection of fluorescence was on-column and not with a sheath flow cuvette. Previous studies from this laboratory showed similar detection levels of dye-labeled DNA fragments with on-column detection, as reported for the sheath flow cuvette.[35] For the detection of small fragments (e.g., up to 300–400 bases in length), the four-dye-labeling approach (each dye specific for one base), which provides the best spectral resolution, was not required because of sufficient electrophoretic separation for the low-base-number fragments. The sequencing information was further encoded using different relative peak heights for two bases, each detected in one of two channels, FAM or JOE. The selection of these two-dye-labeled primers was based in part on their negligible electrophoretic migration difference for the same base length. Indeed, the software used to analyze the raw data determined that the difference in mobility between the two primers was about 0.7 s, in agreement with that recently reported.[19] Furthermore, FAM and JOE primers permitted the use of a low-power argon ion laser, since both dyes were efficiently excited at 488 nm.

Table I. Detection System Specification

	FAM channel	JOE channel
λ excitation	488 nm	488 nm
λ emission max	535 nm	557 nm
λ detection	515 ± 10 nm	550 ± 10 nm
FAM emission	100%	30 ± 3%
JOE emission	<3%	100%

Table I presents the system configuration and the percent cross-talk between the emissions in the FAM and JOE spectral channels. The emission wavelength maxima of FAM and JOE are 535 and 557 nm, respectively, but in this work the FAM detection band was shifted to 515 ± 10 nm in order to eliminate the overlap of the JOE signal in the FAM channel. The JOE emission in the FAM channel was then below 3%, which was negligible for our purposes. The JOE channel (detected at 550 ± 10-nm band, determined by a filter), contained 30 ± 3% interference of the FAM emission, and this interference was removed by software. In addition, due to the high migration velocity of the DNA fragments in this separation protocol, the sampling rate for data acquisition was selected to be 10 Hz.

DNA Sequencing Reaction. Various DNA sequencing protocols have been developed using T7 DNA polymerase, manganese, and inorganic pyrophosphatase for sequencing reactions where of (a) single-dye-based coding of bases with four different peak heights,[31,32] or (b) single-dye-based coding of three bases by peak height ratios plus one base coded by a gap,[27,32] (c) two-dye binary coding of three bases with one base coded by a gap and with two optical channels,[19] or (d) two-dye and two peak height ratio coding of four bases with two optical channels[33] have been used. For this work we selected approach d for simplicity while maintaining good discriminating power.

We found that the use of a 100:1 concentration ratio of dNTPs:ddNTPs resulted in good signal-to-noise ratio, even for small peak-coded bases, in the range up to at least 350 nucleotides. For peak height ratio coding, the adjustment of volumes of the dNTP/ddNTP termination mixtures was straightforward for a given batch of reagents. Ratios from 2.5:1 to 3:1 produced a low base identification error. Moreover, a second sequencing run using inverted peak height ratios could be easily accomplished for sequence confirmation. The volumes of the particular dNTPs/ddNTP termination mixes necessary for the inverted ratio were simply inverted in the appropriate manner.

Linear Polyacrylamide Matrix. The LPA composition was optimized in order to provide reproducible and rapid separation of DNA fragments for a minimum of 300 bases.

(36) Hjerten, S. *J. Chromatogr.* **1985**, *347*, 191–8.

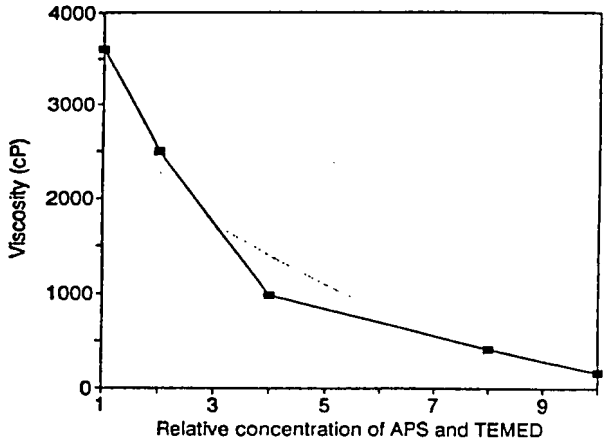

Figure 2. Viscosity of 6% T matrix as a function of concentration of APS and TEMED. Buffer: 1 × TBE, 30% formamide, 3.5 M urea. See Table II for concentrations of APS and TEMED.

Low- to moderate-viscosity LPA allowed faster separations than those reported[6,37] using high % T LPA filled capillaries. The following polymerization parameters were optimized: buffer composition, oxygen content in the monomer solution, radical initiator and catalyst concentration, and polymerization temperature.

For the facile replacement of the polyacrylamide matrix, the composition of the denaturant in the buffer was first altered to include formamide in conjunction with a smaller concentration of urea than previously used.[35] As a denaturing agent, formamide added several advantages, including decreased viscosity of the polymer network relative to 7 M urea and increased decompression of sequences with the secondary structures.[29] On the other hand, formamide or urea decomposition during prolonged electrophoretic runs, especially those performed above room temperature, could potentially lead to an increase in current and thus affect separation reproducibility. This decomposition did not play a role during 30–60-min analyses, and the replacement of fresh polymer after each run did not allow denaturant decomposition to affect the separation.

Oxygen is known to be a radical quencher which inhibits acrylamide polymerization.[38] Thus, minimizing the oxygen concentration in the monomer solution is critical for the efficient and reproducible synthesis of polyacrylamide chains. Although the common laboratory protocols for polyacrylamide slab gel preparation recommend only vacuum degassing of the monomer solution, bubbling with helium is a more efficient technique for the oxygen removal. Bubbling a 10-mL solution with helium for 2 h gave a reproducible oxygen content of less than 2 ppm.

Experiments were next undertaken to optimize the amount of radical initiator, ammonium persulfate (APS), and catalyst, N,N,N′,N′-tetramethylethylenediamine (TEMED). The relative proportions of both compounds were kept constant, but the total concentration was varied for the synthesis of polyacrylamide using the same monomer concentration (6% T). In this study, the reaction was allowed to take place at room temperature for a period of 48 h to assure that no more reaction was occurring.

In order to characterize the LPA obtained, the viscosities of the matrices were measured at 18 °C, as described in the Experimental Section, and the results are shown in Figure 2. It can be seen that the viscosity increases by 22.5-fold with a 10-fold decrease in APS/TEMED concentration. It is known

(37) Huang, X. C.; Quesada, M. A.; Mathies, R. A. *Anal. Chem.* 1992, *64*, 967–970.
(38) Chrambach, A.; Rodbard, D. *Science* 1971, *172*, 440–50.

Table II. Viscosity of Linear Polyacrylamide vs Concentration of Radical Initiator and Its Effect on Separation[a]

η (cp)	TEMED (v/v) (%)	APS (w/v) (%)	N/m	α (226–227)	Rs (226–227)	t (227) (min)
3600	0.05	0.01	3.7×10^6	1.0036	0.54	64.8
2500	0.10	0.02	2.7×10^6	1.0034	0.49	50.8
980	0.20	0.04	2.5×10^6	1.0031	0.44	45.5
160	0.50	0.10	1.2×10^6	1.0030	0.40	43.8

[a] η, viscosity; N/m, number of theoretical plates per meter; α, selectivity; Rs, resolution; t, migration time. Electrophoretic conditions: capillary effective length, 24 cm (total length 40 cm); constant electric field, 200 V/cm; running temperature, 25 °C; 1 × TBE; pH = 8.4; 30% formamide; 3.5 M urea.

that the polymer molecular weight is related to the viscosity of matrix. As the concentrations of TEMED and APS are reduced, fewer acrylamide primary chains are initiated for the same concentration of monomer;[39] therefore, longer fibers or higher molecular weight polymers are produced. The lowest concentration of TEMED/APS, 0.05% (v/v)/0.1% (w/v), while yielding the highest viscosity, was not routinely used because of difficulty in reproducing the polymerization; however, it was a useful matrix to explore trends.

The pressure drop required to replace the LPA matrix of 2500 cp in the separation capillary was calculated with the assumption that the network behaved as a Newtonian fluid,

$$\Delta P = 8LQ\eta/\pi R^4 \quad (1)$$

where ΔP = the required pressure to replace the matrix (Pa), L = the length of the capillary (m), Q = the flow rate of the network (m^3/s), η = the viscosity of the polymer (Pa s), and R = the radius of the capillary (m).[40] The pressure required for replacement of the matrix at room temperature in a 33-cm-long capillary in 3 min was calculated to be 84 atm (1.25×10^3 psi). This pressure can be obtained using a 100-μL gas-tight syringe connected to the capillary with a short piece of Teflon tubing. Syringe pumps could also be employed in an automated system.

We next examined the LPA matrices in Figure 2, all at 6% T monomer concentrations, and the results are shown in Table II. In this case, ddTTP was used as terminator for the sequence reaction with M13mp18. It can be seen that both efficiency and the ratio of mobilities for T226/T227 increase as the viscosity and thus the polymer molecular weight of the matrix increases. The price to pay for the resultant improved resolution is slower migration time; however, an increase in electric field and a decrease in column length leads to a more rapid separation (see Figure 5).

Similar trends of improved resolution with increased matrix viscosity for a given monomer concentration can be seen in Figure 3. In this case, the TEMED/APS were maintained constant at 0.10% (v/v)/0.02% (w/v), and the temperature of polymerization was varied from 18 to 10 to 0 °C. Sufficient time for the reaction to go to completion was allowed. Spectrophotometric determination of residual free acrylamide[41] after 48 h of polymerization confirmed that the degree of polymerization was more than 94%. It can be seen that the resolution increased as the temperature of polymerization was decreased. The lowest temperature (0 °C) also yielded the greatest viscosity and presumably the longest fibers. For convenience, we used 10 °C in our sequencing studies, since the matrix could still be replaced in the capillary in 2–3 min. The molecular weight of this LPA was determined by light scattering to be approximately 1×10^6.

(39) Nossal, R. *Macromolecules* 1985, *18*, 49–54.
(40) *Unified Separation Science*; Giddings, J. C., Ed.; John Wiley & Sons, Inc.: New York, 1991; p 60.
(41) MacWilliams, D. C.; Kaufman, D. C.; Waling, B. F. *Anal. Chem.* 1965, *37*, 1546–1552.

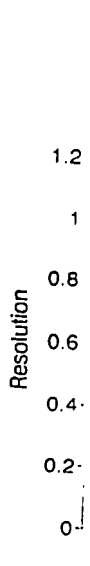

Figure 3. R networks pc capillary eff electric field TBE, 30% f

Work is weight of v lamide stan II and Figu with incre studied), in slabs.[42] It i well above t dependent lecular weig become less presented b of the netw (<10^6 Da) w of 100 bp d resolution w for fiber mo linked gels. molecular w it may well b linked gels polymer ne detail in a s

Separati Critical to products by efficiency p causes of dis et al.[46] deter after filling polymer net the beginnin system was d and poor eff the vertical drop that co distorting th capillary sho improve the capillary posi

(42) Bode, H
(43) deGenn
University Pres
(44) Bae, Y.
(45) Smirnov
manuscript in
(46) Wicar, S
J. Microcol. Sep

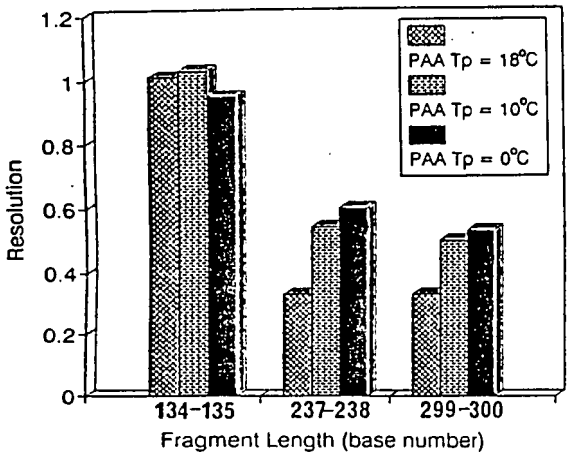

Figure 3. Resolution vs base number for 6% T linear polyacrylamide networks polymerized at three different temperatures. Conditions: capillary effective length = 18 cm (total length = 33 cm), constant electric field = 250 V/cm, running temperature = 32 °C, 6% T, 1 × TBE, 30% formamide, 3.5 M urea.

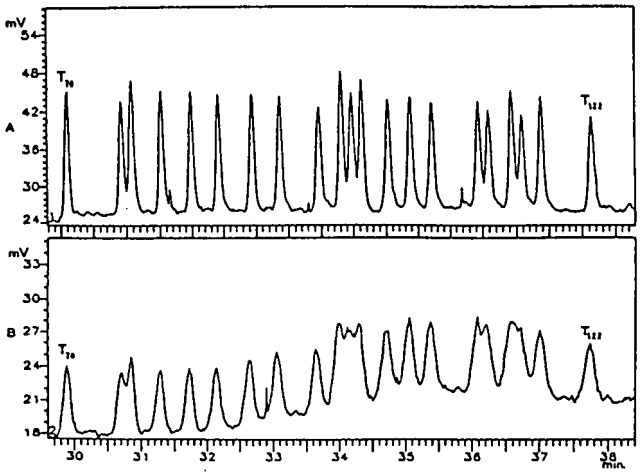

Figure 4. The effect of capillary column orientation on the separation of the FAM–ddT DNA sequencing fragments: (A) horizontal capillary and (B) vertical capillary. Conditions: capillary effective length = 20 cm (total length = 33 cm), constant electric field = 200 V/cm, room temperature. The network composition was 6% T in 1 × TBE, 30% formamide, 3.5 M urea.

Work is continuing on determining the role of molecular weight of various polymerized matrices and linear polyacrylamide standards on separation; however, the results of Table II and Figure 3 show a clear trend to improved resolution with increasing polymer size (within the polymer range studied), in agreement with the earlier conclusion of Bode on slabs.[42] It is known that when the polymer concentration is well above the entanglement threshold, the mesh size will be dependent on polymer concentration but not polymer molecular weight.[43] However, the flexibility of the fibers should become less as the molecular weight increases. As recently presented by Bae and Soane,[44] the relaxation time in a mesh of the network for polymers of moderate molecular weight ($<10^6$ Da) was found to be comparable to the residence time of 100 bp ds fragments. They predicted that above 100 bp, resolution would decrease. Moreover, the relaxation time for fiber movement was 1 order of magnitude lower for cross-linked gels. Given the increased viscosity with higher molecular weight polymers for a fixed monomer concentration, it may well be that such matrices approach more closely cross-linked gels than lower molecular weight non-cross-linked polymer networks. These ideas will be discussed in more detail in a separate paper.[45]

Separation of DNA Sequencing Reaction Products. Critical to the separation of DNA sequencing reaction products by CE is the production of columns with the highest efficiency possible. Recent reports have identified several causes of dispersion in capillary gel electrophoresis. Wicar et al.[46] determined that coiling (or uncoiling) the capillary after filling it with LPA can distort the structure of the polymer networks, especially for low-viscosity matrices. At the beginning of our studies with 6% T LPA, the instrumental system was designed with the capillary in a vertical position, and poor efficiencies were obtained. It was theorized that the vertical position of the capillary could create a pressure drop that could influence flow of the polymer network, thus distorting the mesh structure. Horizontal positioning of the capillary should then remove this pressure drop and should improve the separation. Figure 4 shows the effect of the capillary position on the separation of DNA fragments. The clear advantage of horizontal columns can be seen. This result also suggests that no electroosmotic flow at the capillary walls should occur, or the polymer network structure may be distorted.

We next optimized separation conditions for the M13mp18 DNA sequencing reaction products, using the 6% T LPA matrix, with polymerization at 10 °C and the TEMED/APS concentrations of 0.10% (v/v)/0.02% (w/v), respectively. As shown in Figure 5, where a full sequence is run, these conditions included E = 250 V/cm, effective length = 18 cm, and column temperature = 32 °C. The red lines represent the JOE channel with C > T (3:1) and the blue lines the FAM channel with A > G (3:1). As can be seen in this figure, the sequence is read to 350 bases in 30.5 min. The sequence can be read by eye up to 300-310 bases, with the software adding approximately 50 bases.

For sequence accuracy, a second run is typically made, in which the ratios of each channel are inverted. As noted in the Appendix, if there is an ambiguity, the software calls the base from the run with the higher ratio. With this approach, no errors are found up to 350 bases for M13mp18, a known sequence.

The importance of the two runs is best seen in Figure 6, where the electropherograms are shown for G57-A74 and A230-G249. The partial compressions at G59-G60, G66-A67, and especially G234-G236 are clarified when G > A (3:1). Another approach to minimize ambiguity for severe compressions is to elevate the column temperature to >50 °C to alleviate strand curvature. LPA can be successfully operated at elevated temperatures, whereas cross-linked gels would collapse under such heat. Furthermore, replacing LPA after the run minimizes column fouling due to formamide or urea decomposition at the elevated temperatures. The rapid separation and ease of refilling allows different column conditions to be used, when necessary, to increase sequence accuracy. For general purposes, 32 °C is preferred, since at higher column temperatures some increase in peak widths was observed.

We next explored the reproducibility of sequencing runs. Precise control of the capillary column temperature is important to obtain good reproducibility. Without temperature control, due to laboratory temperature fluctuations, the run-to-run reproducibility was 4% RSD in migration time (n = 9). With temperature control, the migration time reproducibility was 1.2% RSD (n = 4), see Table IIIA. Note also that the maximum number of bases read was always in

(42) Bode, H. J. *Anal. Biochem.* 1977, *83*, 364–371.
(43) deGennes, P. G. *Scaling Concepts in Polymer Physics*; Cornell University Press: Ithaca, NY, 1979.
(44) Bae, Y. C.; Soane, D. *J. Chromatogr.*, in press.
(45) Smirnov, I.; Foret, F.; Ruiz-Martinez, M.; Berka, J.; Karger, B. L., manuscript in preparation.
(46) Wicar, S.; Vilenchik, M.; Belenkii, A.; Cohen, A. S.; Karger, B. L. *J. Microcol. Sep.* 1992, *4*, 339–348.

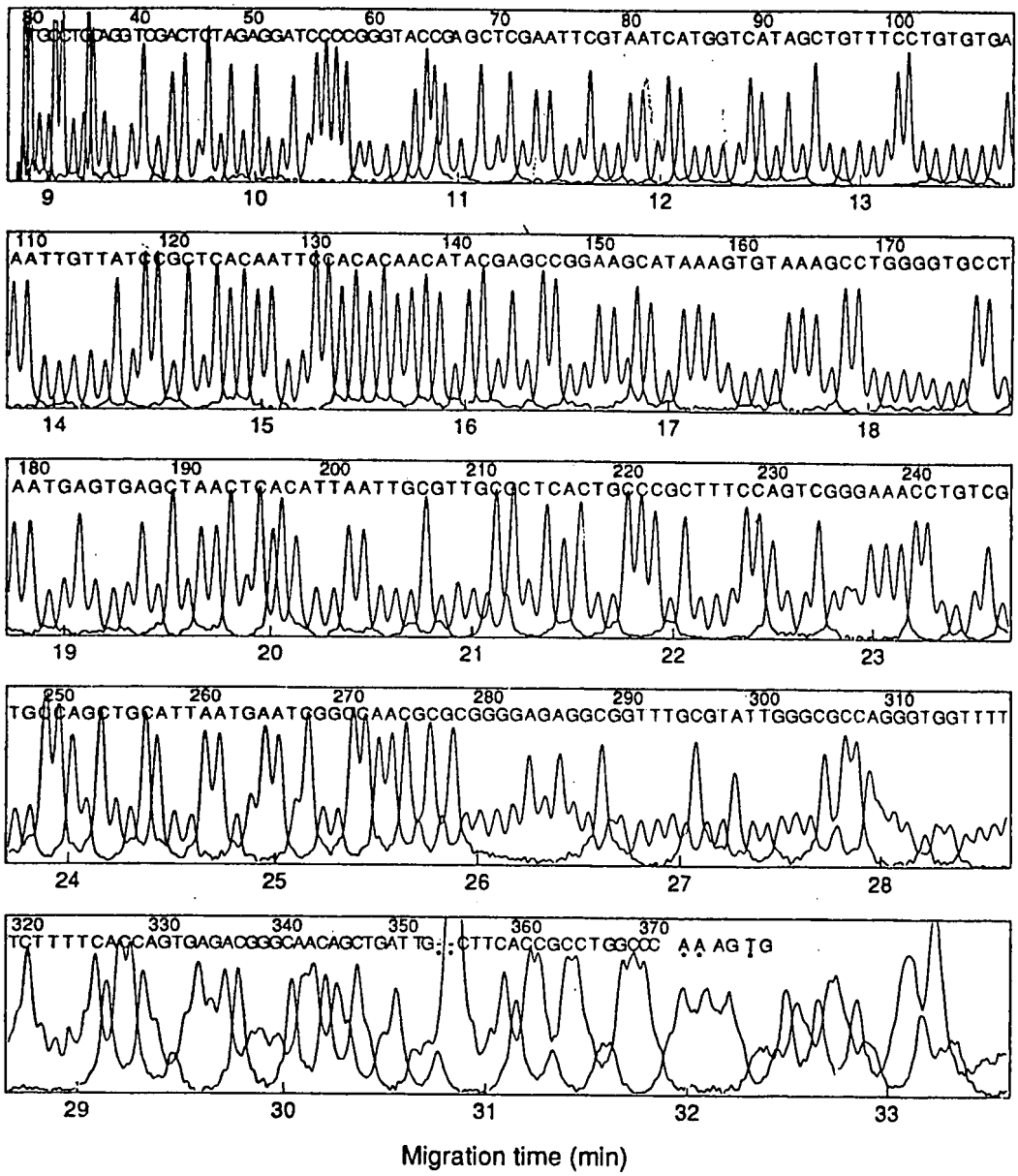

Figure 5. Sequencing of M13mp18. Red, JOE C > T; blue, FAM A > G. Electrophoretic conditions similar to those in Figure 3, except column temperature = 32 °C and the 6% T matrix was polymerized at 10 °C with 0.1% TEMED, 0.02% APS. Asterisks represent software miscalls.

excess of 350. After each run, the matrix was replaced in the column. We next polymerized eight different batches of 6% TLPA, and the reproducibility in migration time from batch to batch with the same capillary was 2.4% RSD Table IIIB. Again, all batches permitted sequencing out to at least 350 bases.

It should be noted that in Table III, the reproducibilities were run on a single-coated capillary. Whenever the capillary was changed due to coating degradation, the variation in migration time from capillary to capillary was approximately 5% RSD. However, the separation was maintained, and the sequence could always be read out to 350 bases or more.

CONCLUSIONS

A simple approach for DNA sequencing by high-performance capillary electrophoresis using a replaceable linear polyacrylamide matrix with a one-laser, two-photomultiplier system and peak height base encoding has been demonstrated. The linear polyacrylamide composition and the polymerization procedure were optimized to provide highly reproducible separation of the single-stranded fragments. DNA sequencing information was accurately obtained for 350 bases in roughly 30 min. The facile replacement of linear polyacrylamide from the capillary column overcame problems associated with the stability of capillary cross-linked gels.

The protocol of this work is applicable to recently described DNA sequencing techniques, for example, sequencing methods based on subcloning of DNA fragments to phage or plasmid vectors for which dye-labeled primers are available. Single-stranded DNA templates produced by asymmetric PCR amplification can be used as well, permitting, for instance, the sequence analysis of eucaryotic exons with average length of about 150 nucleotides for mutation mapping. A recently reported novel technique called partial-digest sequencing[47] that permits DNA of 4–6 kb in length to be sequenced by 200–300-bp-long sequencing steps without subcloning or the preparation of oligonucleotide primers is another promising technique in which the developed methodology can be directly applied. For all these methods, the instrument and matrix preparation are sufficiently straightforward that the procedure could be easily adopted in a laboratory setting.

(47) Wright, W. E. *BioTechniques* **1992**, *13*, 772–779.

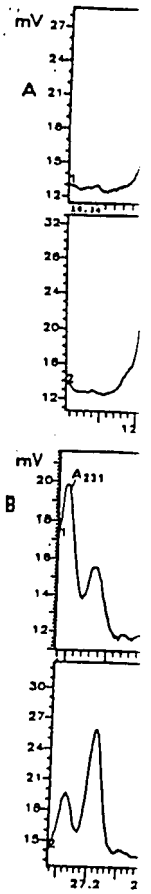

Figure 6. Two e
and A > G com
ratios. The se
presented. Note
59–61 triplet, of
Conditions: sam

Table III. Rep
Polyacrylamid

run no.	R (136/
1	1.1
2	0.9
3	0.9
4	0.9

batch no.	I (136
1	1
2	1.
3	1.
4	0.
5	1.
6	0.
7	0.
8	0.

[a] RSD of the n
[b] migration time

Current wor
sequence readi
the replaceable
sequencing run
minators and a
spectral resolu

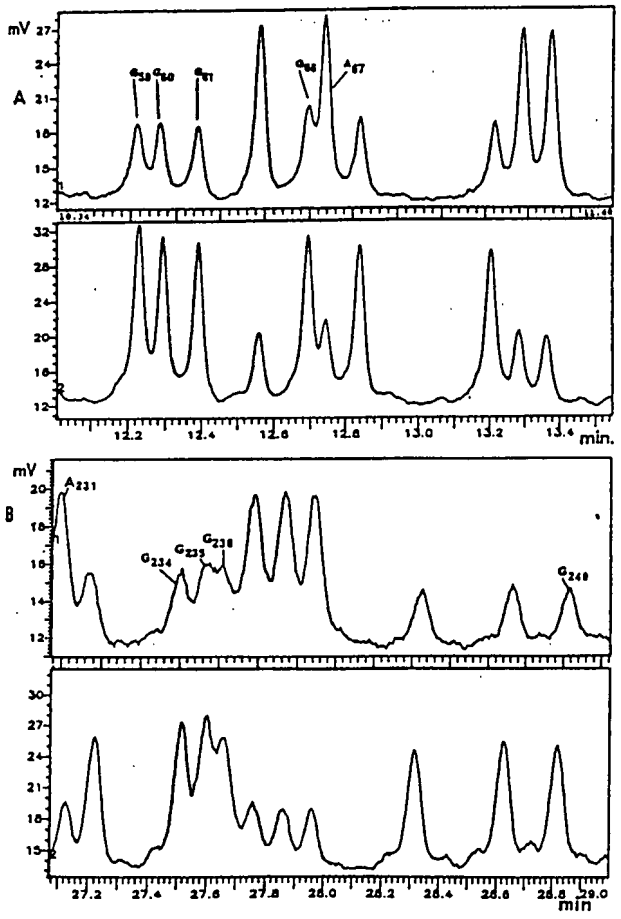

Figure 6. Two electrophoretic regions of the M13mp18, FAM G > A and A > G complementary sequencing reactions with inverted peak ratios. The separation of bases G59–A74 and A230–G248 are presented. Note the partial compressions of GG 59–60 of the GGG 59–61 triplet, of G66/A67, and G234/G235 of the GGG 234–236 triplet. Conditions: same as in Figure 3 except LPA polymerized at 0 °C.

Table III. Reproducibility for the Same Batch of Linear Polyacrylamide and from Batch to Batch

A. For the Same Batch[a]

run no.	RS (136/137)	t (136) (min)	t (299) (min)	maximum no. of bases read
1	1.10	16.6	27.6	369
2	0.96	16.2	26.9	364
3	0.98	15.9	27.0	359
4	0.94	16.0	27.0	355

B. From Batch to Batch[b]

batch no.	Rs (136/137)	t (136) (min)	t (299) (min)	maximum no. of bases read
1	1.26	16.1	27.6	370
2	1.25	16.2	27.4	369
3	1.24	16.1	27.5	360
4	0.97	17.4	28.9	357
5	1.10	16.6	27.6	369
6	0.96	16.2	26.9	364
7	0.98	15.9	27.0	359
8	0.99	16.8	27.0	367

[a] RSD of the migration time of base 299 = 1.2%. Rs, resolution; t, migration time. [b] RSD of the migration time of base 299 = 2.4%.

Current work involves extending the base number for sequence reading in excess of 500 by further optimization of the replaceable polymer network. For these longer base sequencing runs, we are utilizing fluorescently labeled terminators and an intensified diode array detector for high spectral resolution.[35] Such an approach should be fully compatible with recent primer walking strategies.[48] Results from these studies will be presented at a later date.

ACKNOWLEDGMENT

The authors thank NIH under the Human Genome Project Grant HG 00023 for support of this work. The authors wish also to acknowledge Dr. Dieter Schmalzing for discussions concerning polymerization optimization and Steve Carson for assistance in construction of the LIF detection instrument. This work is contribution no. 557 from the Barnett Institute.

APPENDIX

Sequencing Program. The program was written with the commercial programming package MATLAB (The MathWorks, Inc., Natick, MA). The software first converted the data to MATLAB binary format. The next step was spike removal. Spikes were detected as regions where the first derivative of the signal exceeded 10 times the standard deviation of that derivative for the channel. In each such region, a 1-s section at the highest signal value was excised and replaced by a straight line across the resulting gap. After spikes were removed, noise was reduced by a low-pass Fourier filter.

An arbitrary point high on the trailing edge of the primer peaks was selected as the position to begin sequencing, and a base line was estimated for each channel. For this estimate, the lowest signal point in each 2-min section of the data for a channel was found. The base line was then set as the shortest curve connecting the starting point and the final time point that passed through the 2-min minima and underlay all the intervening data.[49]

After base line subtraction, the data consisted of a $2 \times n$ matrix **Y**, each row containing all the n time points for one channel. The 30% cross-talk of JOE in the FAM channel was removed by solving the matrix equation $\mathbf{Y} = \mathbf{RC}$, where **R** was the 2×2 matrix containing the response of each dye in each channel and **C** was the $2 \times n$ solution in which each row held the isolated fluorescence of a single dye. Thresholds for peak slope and peak width were derived from the derivative of each row of **C**. The slope threshold decreased in rough proportion to peak height as base number increased, while the width threshold increased. These thresholds were used to locate approximate peak positions, whose neighborhoods were then searched for precise positions of peak maxima and peak boundaries.[50] Peak area was calculated as the area bounded by the dye signal, the base line, and perpendiculars dropped to the base line at the peak boundaries.

Peaks for a given dye were classified on the basis of peak area. Let the base known to produce the taller peaks be *A* and the other base be *B*. Peaks corresponding to *A* were chosen by first dividing the electrophoretic time profile for the dye into 1-min sections and selecting the peak with greatest area in each. An estimate of maximum peak versus time was constructed by interpolating linearly between values calculated for the selected peaks. Each such value was computed as the median of the areas of a selected peak and its two nearest selected neighbors on each side. Once maximum peak area at all times had been estimated, the ratio of peak area to that value was determined for all peaks. Peaks with ratios of 0.6 or greater were assigned to base *A*. These peaks were removed from consideration, and the process was repeated to assign the remaining peaks to *B* or to error. Peaks assigned to error were then deleted or merged with neighboring peaks.

(48) Kieleczawa, J.; Dunn, J. J.; Studier, F. W. *Science* 1992, *258*, 1787–1791.
(49) Dyson, N. *Chromatographic Integration Methods*; The Bath Press: Bath, U.K., 1990.
(50) Pearson, W. R.; Miller, W. *Methods Enzymol.* 1992, *210*, 575–601.

The entire classification process was repeated until no peaks were assigned to error.

The resulting sequence was aligned with the one from the inverse-labeling experiment, using the sequence comparison program FASTA.[51] Where the two sequences differed, the consensus base was taken as that from the run with the higher ratio labeling for the specific peak. An ASCII text report and a Postscript summary plot were then generated (Figure 5). Figure 5 further illustrates an option whereby the consensus sequence was compared with the known sequence, and miscalls were marked by asterisks.

Sequence ambiguities occurred at the approximate rate of 1% up to 350 bases; however, from the known sequence, these ambiguities were correctly resolved by the consensus procedure (i.e., the higher ratio assignment). Work is continuing on software improvements.

The present program is available on request or by anonymous ftp from ftp.ccs.neu.edu in directory /pub/miller. It requires MATLAB release 4.1 and the MATLAB toolboxes for signal processing and for optimization.

RECEIVED for review May 12, 1993. Accepted July 13, 1993.*

(51) Pearson, W. R. *Methods Enzymol.* 1990, *183*, 63–98.

* Abstract published in *Advance ACS Abstracts*, September 1, 1993.

High-Sensitivity DNA Detection with a Laser-Excited Confocal Fluorescence Gel Scanner

M.A. Quesada, H.S. Rye, J.C. Gingrich[1], A.N. Glazer and R.A. Mathies
University of California, Berkeley, and [1]Human Genome Center, Lawrence Berkeley Laboratory

ABSTRACT

A high-sensitivity, laser-excited confocal fluorescence gel scanner has been developed and applied to the detection of fluorescently labeled DNA. An argon ion laser (1–10 mW at 488 nm) is focused in the gel with a high-numerical aperture microscope objective. The laser-excited fluorescence is gathered by the objective and focused on a confocal spatial filter, followed by a spectral filter and photodetector. The gel is placed on a computer-controlled scan stage, and the scanned image of the gel fluorescence is stored and analyzed in a computer. This scanner has been used to detect DNA separated on sequencing gels, agarose mapping gels and pulsed field gels. Sanger sequencing gels were run on M13mp18 DNA using a fluoresceinated primer. The 400-μm-thick gels, loaded with 30 fmol of DNA fragments in 3-mm lanes, were scanned at 78-μm resolution. The high resolution of our scanner coupled with image processing allows us to read up to approximately 300 bases in four adjacent sequencing lanes. The minimum band size that could be detected and read was approximately 200 μm. This instrument has a limiting detection sensitivity of approximately 10 amol of fluorescein-labeled DNA in a 1 × 3-mm band. In applications to agarose mapping gels, we have exploited the fact that DNA can be prestained with ethidium homodimer, followed by electrophoresis and fluorescence detection to achieve picogram sensitivity (8). We have also developed methods using both ethidium homodimer and thiazole orange staining which permit two-color detection of DNA in one lane. Finally, these methods have been used to perform high-sensitivity detection of DNA separated on pulsed field gels. This fluorescence gel scanner is advantageous because it has high detection sensitivity, the off-line detection apparatus is not tied to the electrophoresis system, and it immediately provides a quantitative image for data analysis and display.

INTRODUCTION

Fluorescence is a highly sensitive technique for the detection of biomolecules. Hirschfeld first pointed out that the number of fluorescent photons emitted by a fluorophore is given by the ratio of the fluorescence quantum yield Q_f to the photodestruction quantum yield Q_d (11). For typical values of Q_f (ca. 1) and Q_d (ca. 10^{-5}), an individual fluorophore will produce 10^5 photons (14–16), which is sufficient to rival the sensitivity of radioactivity. Laser-excited fluorescence is now widely used in flow cytometry (20), in capillary electrophoresis (3,9,30), in confocal (5,17,22) and epifluorescence (10,12,27) microscopy, and in DNA sequencing (1,2,4,6,18,25,26). In all of the DNA sequencing applications, the fluorescence detector is dedicated to the electrophoresis apparatus (for recent reviews see References 23, 28 and 29). Capillary electrophoresis DNA sequencing is relatively rapid and has very high molar sensitivity because of the small sample volume (4,6,26). However, further development will be needed to conveniently run a large number of capillaries in parallel to achieve high throughput. Dedicated slab gel readers can detect up to 24 lanes at a time, each of which can be four-color; however, the electrophoresis runs can last as long as 14 h (1, 18,25). For large-scale DNA sequencing projects, such as the Human Genome Initiative, further technological improvement is needed.

We have developed a laser-excited confocal fluorescence gel scanner which provides a number of improvements on the existing technology. The exciting laser beam is focused in the gel by a high-numerical aperture microscope objective. The same objective gathers the fluorescence and passes it to a confocal spatial filter that rejects stray light and substrate emission. The gel is then scanned by using a motor-driven stage. The advantages of this system are as follows: a) attomole sensitivity, b) optimum control of laser excitation intensity and photodestruction, 3) low background due to confocal detection, d) high spatial resolution, e) off-line detection which permits efficient utilization of the detection system and f) the production of convenient and familiar gel images for quantitative analysis and display. Preliminary descriptions of our apparatus and its application to agarose gels and DNA sequencing have appeared (8,13). We present here a more detailed description of this apparatus, along with examples of its utility for reading DNA sequencing, DNA mapping and pulsed field gels. This confocal fluorescence gel scanner should be useful in a wide variety of biotechnology applications.

MATERIALS AND METHODS

Scanning Confocal Fluorescence Imaging System

Fluorescence detection was performed with the system shown in Figure 1. A 150-mm focal length lens was used to focus the exciting light from a Spectra-Physics 2020 argon ion laser (Mountain View, CA) at the excitation spatial filter which was 150 mm (the parfocal distance) from the objective lens. This served to match the

divergence of the excitation and detection beams at the beam splitter. A long-pass dichroic beam splitter (480 DM, Omega Optical, Brattleboro, VT) reflected 96% of the s-polarized laser beam down through a 40 × 0.60 NA Zeiss long-working-length objective (Carl Zeiss, Thornwood, NY) onto the sample (beam diameter ca. 5 µm). The objective is corrected for a 1.5-mm coverslip, so the laser was focused through the top 1.5-mm glass plate onto the gel. The fluorescence emission was collected by the objective and passed through the beam splitter (92% transmission) to the photodetector. The fluorescence emission was focused through a 200- or 400-µm-diameter spatial filter (Melles Griot, Irvine, CA) to effect confocal detection. For fluorescein and thiazole orange (TO), two long-pass color filters (Schott GG-495 [Esco Products, Oakridge, NJ], 50% transmission cutoff at 495 nm) and a bandpass discrimination filter (Omega Optical, 530 DF 60, 80% transmission at 530 ± 30 nm) were used. The ethidium homodimer (EthD) fluorescence emission required the use of a single long-pass filter (Schott, RG 610, 50% transmission at 610 nm). The output of the cooled phototube (RCA 31034A [Burle Industries, Lancaster, PA] in a Products for Research TE-104RF housing [Danvers, MA]) was detected with a PAR 1105/1120 photon counter (Princeton, NJ), converted to volts with a Teledyne 4736 frequency-to-voltage converter (Dedham, MA) and stored in an IBM PS/2 computer after digitization with a 12-bit Metra Byte DASH16-F ADC (Taunton, MA). For the pulsed field gels, which have intense signals, the output of the photomultiplier was passed directly to a Stanford Research Systems amplifier (SR560) (Sunnyvale, CA) and then digitized by the Metra-Byte ADC. A computer-controlled dc servo motor-driven XY translation stage (Design Components 4000; Franklin, MA) with a 6" × 6" travel and 2.5-µm resolution was used to translate the gel past the laser beam. Scanning was done in a line-scan/step/line-scan sequence with a line-scan rate of 6 cm/s, a step-size of 78 µm and a pixel-size of 78 µm. The fluorescence was sampled six times over the 78-µm pixel with the ADC, and the maximum value was stored. The IBM PS/2 computer was used to control the XY translation stage and to acquire and display images with an IBM 8514A graphics adaptor and monitor. The fluorescence images were pseudo-color displayed in real time and stored for post-data collection processing with an Apple Macintosh® IIci.

The unprocessed binary data files are composed of 12-bit pixels arrayed in FTS file format. These IBM DOS™ files are then converted to 8-bit Macintosh TIFF files after subtracting the typically large background. The resulting images were analyzed with the NIH image processing program. Image 1.29. After setting a threshold and contrast enhancing, each file was plotted on a Hewlett Packard PaintJet® color printer. For DNA sequencing, each lane was reduced to its one-dimensional equivalent by averaging the pixel intensities across the appropriate lane widths.

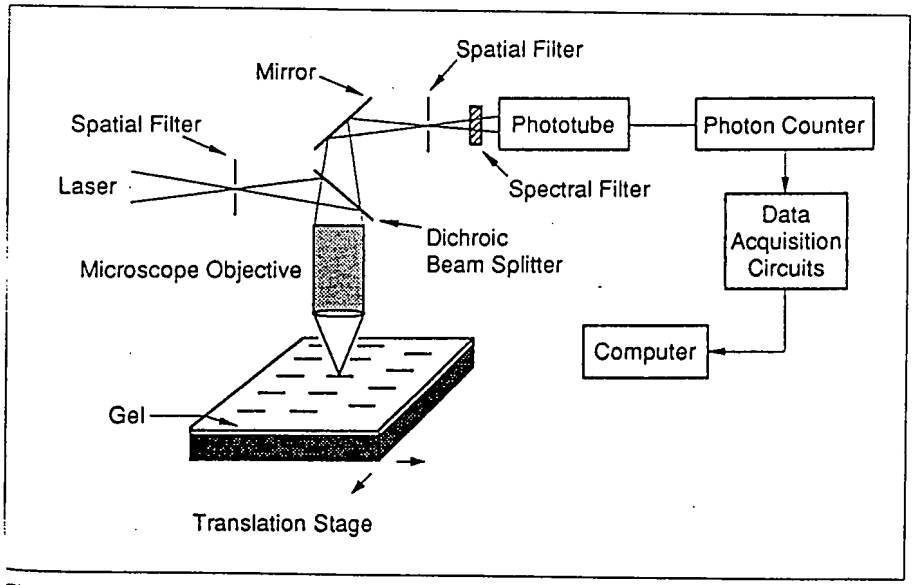

Figure 1. Laser-excited confocal fluorescence gel scanner. The 488-nm exciting laser light is brought to a focus at the excitation spatial filter and then reflected by a long-pass dichroic beamsplitter to the long-working-length microscope objective. The fluorescence is collected by the objective, passed back through the beamsplitter and reflected by a mirror to a focus at the detection spatial filter. Spectral filters are used to eliminate residual Rayleigh and Raman scattering. The output of the phototube is passed through the data aquisition circuits and stored as an image on a computer. A computer-controlled XY translation stage is used to sweep the gel past the laser beam.

Sample Preparation for Sequencing

Chain-terminated M13mp18 DNA sequence fragments were produced using a United States Biochemical Sequenase® 2.0 sequencing kit (Lot No. 66381). The Applied Biosystems "FAM" fluorescein-tagged primer (Lot No. A9E007) (Foster City, CA) was employed in the primer-template annealing step using a 1:1 (primer: template) molar stoichiometry in the following manner: 1.25 µl of FAM, 2.0 µl of the Sequenase reaction buffer, 5.0 µl of the control M13mp18 single-stranded DNA and 1.75 µl of deionized water were combined in a centrifuge tube, heated to 65°C for 2–3 min and then allowed to cool to room temperature (or less than 30°C) for 30 min. Meanwhile, into each of four separate G-, A-, T- and C-labeled centrifuge tubes was added 0.5 µl of the sequence extending mixture, followed by the addition of 2.0 µl of the appropriate dideoxy termination mixture. These four tubes were then mixed and allowed to come to 37°C in a heating block. When 30 min had elapsed and the temperature of the annealing reaction mixture had dropped below 30°C, 1 µl of 0.1 M dithiothreitol (DTT), 2.0 µl of the diluted labeling mixture, 0.5 µl of 10 µM dATP and 2.0 µl of the diluted Sequenase 2.0 polymerase were added, and the mixture was incubated for 4 min at room temperature. Aliquots (3.5 µl) of this mixture were then added to each of the labeled tubes and allowed to incubate for an additional 5 min at 37°C. Stop solution (4 µl) was then

Research Report

added to each of the tubes, mixed thoroughly and stored on ice. Just prior to loading, each of the four labeled tubes was heated to 80°C for 2 min.

Sequencing Gel Electrophoresis

Three-microliter aliquots of DNA sample (30 fmol) were added to 3-mm-wide wells in 400–μ-thick, 19-cm-long HydroLink Seq™ (AT Biochem, Malvern, PA) sequencing gels. The HydroLink gel system (gel dilution 75%) was pre-electrophoresed for 15 min and then run for an additional 3.5 h until the xylene cyanole tracking dye migrated off the gel. All runs were conducted with 8 W of constant power on a vertical gel electrophoresis system at 45°C. A 6" × 9" × 3/16" piece of standard float glass (rabbit-ear cut) was used for the bottom plate along with a 6" × 9" × 1/16" piece of polished BK-7 glass (Esco) for the top plate. Subsequent irradiation and imaging occurred through BK-7 plate.

Two-Color Detection Using DNA-Dye Intercalation Complexes

Double-stranded plasmids M13-mp18 and pBR322 were obtained from GIBCO BRL/Life Technologies, Gaithersburg, MD. Both M13mp18 and pBR322 (3–5 μg) were cut at a single site with *Hin*dIII (6–10 units) using the Boehringer Mannheim restriction kit (Indianapolis, IN). The linear double-stranded DNA was then extracted with phenol and recovered by precipitation with sodium acetate/ethanol. Analysis by agarose gel electrophoresis showed nearly complete single cutting of the plasmids.

EthD was obtained from Molecular Probes (Eugene, OR). TO was a generous gift of Dr. Diether Recktenwald of Becton-Dickinson (San Jose, CA). EthD was prepared as a 1 mg/ml stock solution in 0.04 M Tris-acetate/1 mM EDTA, pH 8.2 (TAE buffer), and TO as a concentrated solution at 0.7 mg/ml in methanol. Prior to use, the TO solution was diluted to 0.1 mg/ml in TAE buffer. Agarose gels were prepared from ultrapure agarose (GIBCO BRL), and Ficoll (type 400) was obtained from Sigma Chemical, St. Louis, MO.

Mixtures of DNA, EthD and/or TO at various DNA:dye ratios were prepared in 4 mM Tris-acetate/0.1 mM EDTA, pH 8.2, under reduced illumination at 23°C. All diluted samples of DNA or dye solutions were also prepared in this buffer. All double-stranded mixtures were incubated for at least 30 min prior to application to gels. Ficoll (15% wt/vol in H_2O) was added to each sample at a ratio of one part of Ficoll to 3 parts sample (by volume) just prior to loading. Vertical (0.9%, wt/vol) agarose gels, 1-mm-thick, 7-cm long with 5-mm-wide wells, were prepared in TAE buffer. Aliquots of sample solutions were applied to the wells, and electrophoresis was performed in TAE buffer in a Bio-Rad Mini-Protean II gel apparatus (Richmond, CA) at 8.6

V/cm in the dark. Where detection of DNA with TO was desired, the dye was added to the electrophoresis buffer at a concentration of 0.05 μg TO/ml. The best results were obtained by first pre-running the gel with TO in the buffer for 1.3 h and then running the gels for 1.3 h after sample application without changing the buffer. Gels run with no dye added to the buffer were pre-run for 1–2 h to decrease background fluorescence and then run for 1 h after application of samples.

Pulsed Field Gel Electrophoresis and Detection

Yeast (*S. cerevisiae*) cells were grown by conventional methods (21) and harvested by centrifugation. The cells were washed twice and suspended with a 50-mM solution of disodium EDTA (pH = 8) to yield a final concentration of 5×10^9 cells per ml. Fivefold serial dilutions of this mixture were made up to give the indicated approximate loads. The cells were then mixed 1:1 with a 1% InCert agarose solution (FMC BioProducts, Rockland, ME) and processed as described in (24). The 5-mm-thick, 1% agarose gel was run using clamped hexagonal electric field (CHEF) pulsed field electrophoresis (run time, 40 h; switching time, 50 s). The gel was post-stained for 30 min with 100 ng/ml of EthD. It was then rinsed for an additional 30 min with 0.5 × TBE (89 mM Tris, 89 mM boric acid, 2 mM EDTA, pH = 8.0) and then stained overnight in 81 ng/ml of TO.

RESULTS

Slab Gel DNA Sequencing

A 1.9 × 14-cm scanned portion of the FAM-tagged M13mp18 DNA sequencing gel is shown in Figure 2. It was obtained by sweeping the 1.2-mW, 488-nm beam (focused in the center of the 400-μm-thick HydroLink sequencing gel). The step size was 78 μm such that each pixel represents a 78-μm square. With a scan speed of 6 cm/s, the 2 × 14-cm image can be obtained in ca. 15 min. The M13mp18 sequence shown corresponds to the region 70–500 bases beyond the primer. The exploded 1.9 × 3-cm region of Figure 2 shows that the typical band width in the center of the gel is 500 μm and bands as small as 200-μm half width can be read at the top of the gel. Each band in this gel contains about 50 amol of fluorescein-labeled DNA fragments, and using the instrumental configuration presented here, the limiting sensitivity is about 10 amol.

By averaging the pixels across the width of each lane and superimposing the one-dimensional line plots for all five lanes, we determined the M13mp18 sequence by reading up the resulting line graph. Figure 3 presents the M13mp18 DNA sequence from

71–295 bases beyond the primer. For the conditions used here, the signal-to-noise ratio varied between 5 and 30.

Two-Color Detection of DNA on Agarose Gels

DNA-EthD and DNA-TO complexes are well suited to fluorescence detection of DNA on gels (19). One can either detect TO or EthD separately, or TO can be used together with EthD as a sensitizer of ethidium fluorescence. These different applications are summarized schematically in Figure 4. Because EthD forms nearly irreversible complexes with DNA, the DNA can be prestained with EthD, followed by electrophoresis and detection at 620 nm. In contrast, TO does not form complexes that are stable to electrophoresis, so TO must be added to the running buffer, followed by detection at 530 nm. However, since the free dye has a very low quantum yield, TO is also a sensitive fluorescence stain for DNA. Finally, since the emission of TO overlaps well with the absorption of EthD, the emission of EthD bound to DNA may be sensitized by secondary staining with TO. TO has a much larger absorption at 488 nm than EthD, so this dramatically enhances the sensitivity. Examples of these modes of detection are shown below.

The scans shown in Figure 5 document that the preformed DNA-EthD complex, together with TO staining during electrophoresis, can be used effectively as a probe in situations requiring two-color detection of DNA. Lane 1 contains M13mp18 prestained with EthD, while lane 2 contains pBR322 prestained with TO. It is evident that EthD can be detected at 620 nm and TO at 530 nm with little cross talk. When EthD-prestained M13mp18 is run together with TO-labeled pBR322 in lanes 3 and 4, the two samples can be separately detected by the appropriate choice of detection wavelength. The modest cross talk indicates that little EthD migrates to the pBR322 and that TO does not displace EthD from M13mp18.

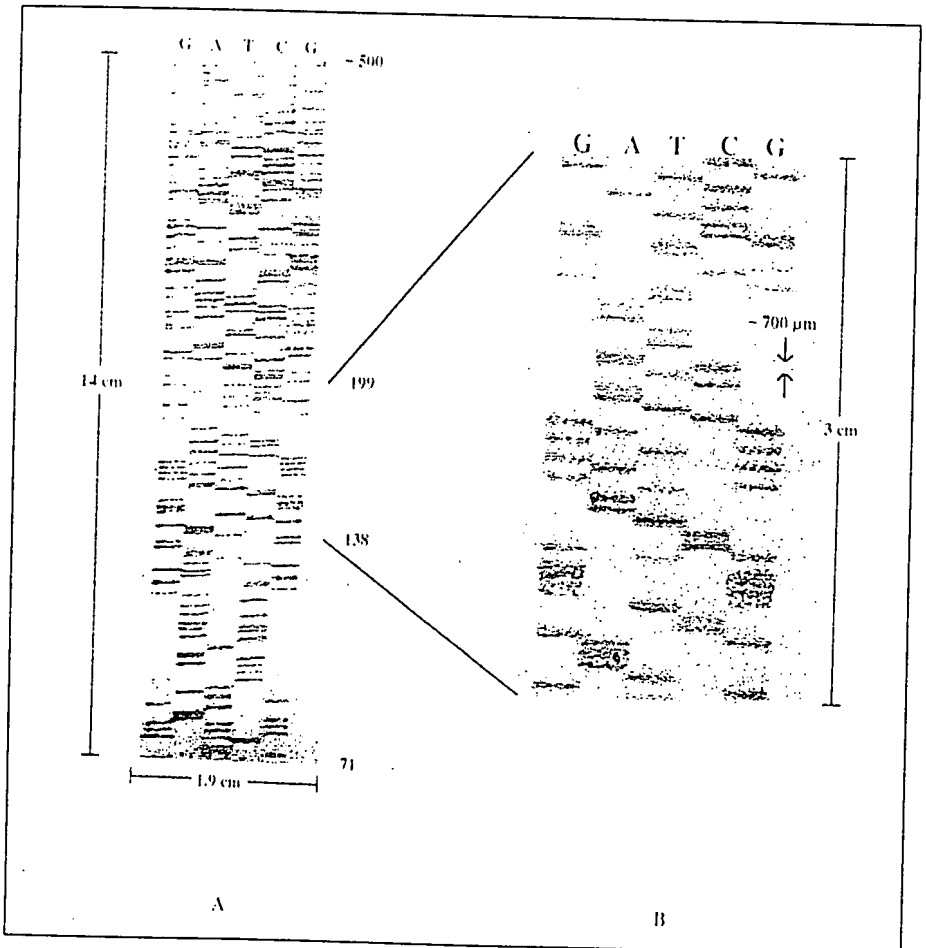

Figure 2. Image obtained from scanning an M13mp18 DNA sequencing gel. Fluorescent primer-labeled DNA fragments (30 fmol per 3-mm lane) were loaded on a 14 cm × 19 cm × 400-µm 10% T HydroLink sequencing gel in a GATCG pattern. The gel was run as described in Materials and Methods. The left panel presents a 1.9 × 14-cm portion of the gel spanning the M13 sequence from 70–500 bases above the primer. The right panel is an expanded view of the M13 sequence from 138–199 bases beyond the primer. The average band size and separation are on the order of 500 µm, and the bands at the top of the gel are ca. 200-µm half width.

Detection of DNA in Pulsed Field Electrophoresis

The application of our scanning methods to pulsed field gels is illustrated in Figure 6. Because of the high signal and background intensities in these gels, the analog photomultiplier output was sent through an amplifer to the computer. The yeast DNA was preincubated with EthD following the usual procedures. However, there was apparently sufficient loss of the EthD during the 40-h run that only modest 1-µg sensitivity was achieved. To increase the sensitivity, the pulsed field gel was post-stained with EthD and then washed to remove excess dye. Then the EthD fluorescence was enhanced by staining with TO, followed by scanning the gel. Figure 6 reveals that the lower molecular weight bands are detectable even in the 8-ng lane, and the compressed bands can be detected even in the 0.3-ng lane. Thus, although the long pulsed field runs require a different staining procedure, very sensitive detection of DNA on pulsed field gels can be accomplished with the confocal fluorescence scanning system.

DISCUSSION

An off-line, laser-excited, confocal fluorescence gel scanner has been developed which has both high-sensitivity and high-spatial resolution. High-spatial resolution is accomplished by using a tightly focused laser as the excitation source coupled to a high-resolution scan stage. High sensitivity arises from the use of laser excitation, confocal detection and a microscope objective for excitation and detection. Confocal detection provides rejection

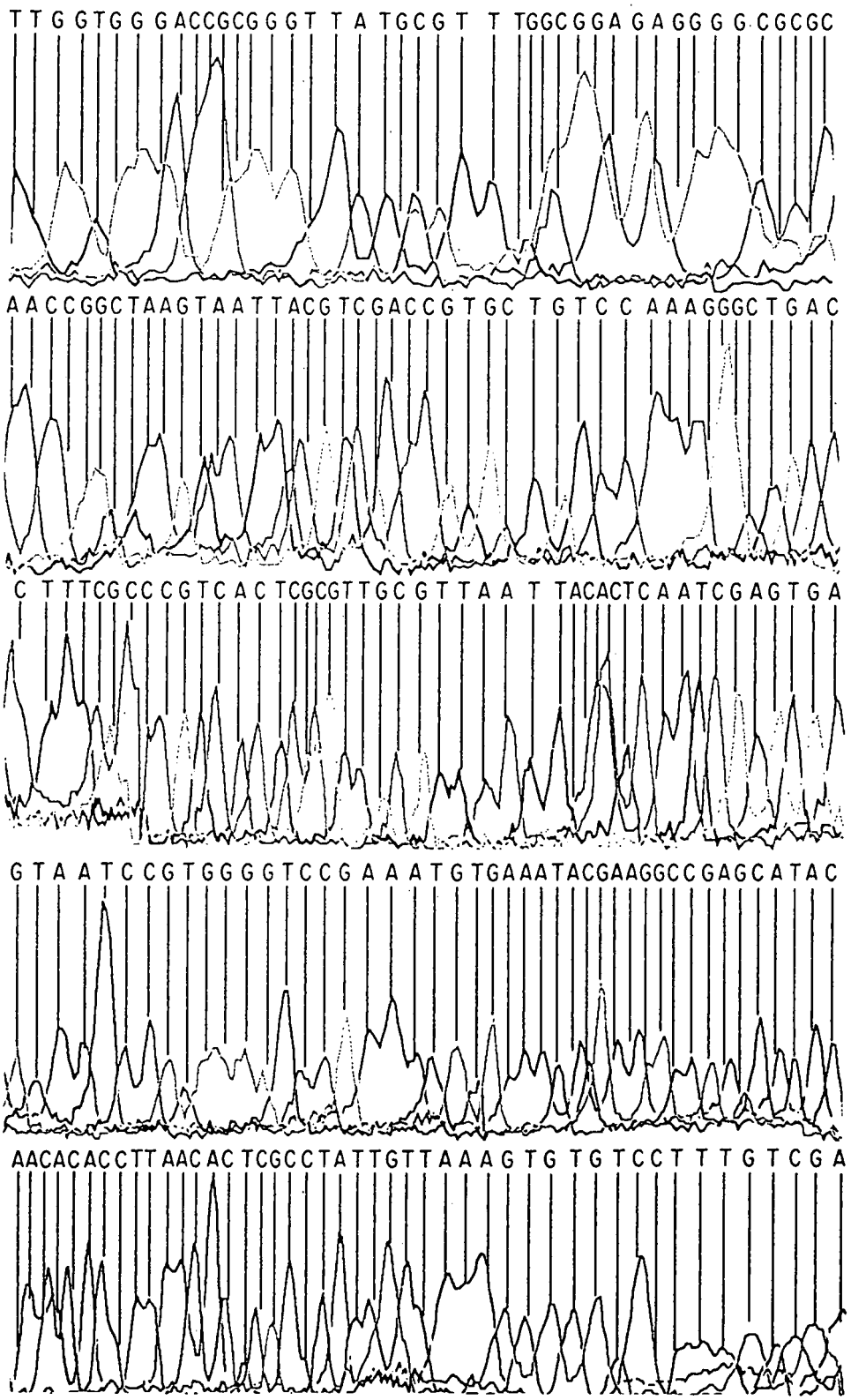

Figure 3. Representative sequence of M13mp18 DNA from 71–295 bases. Each lane of data in Figure 2 was reduced to a one-dimensional line plot by averaging the pixels across the width of each lane using Image 1.29. The colors used are red and yellow (G), green (A), black (T) and blue (C).

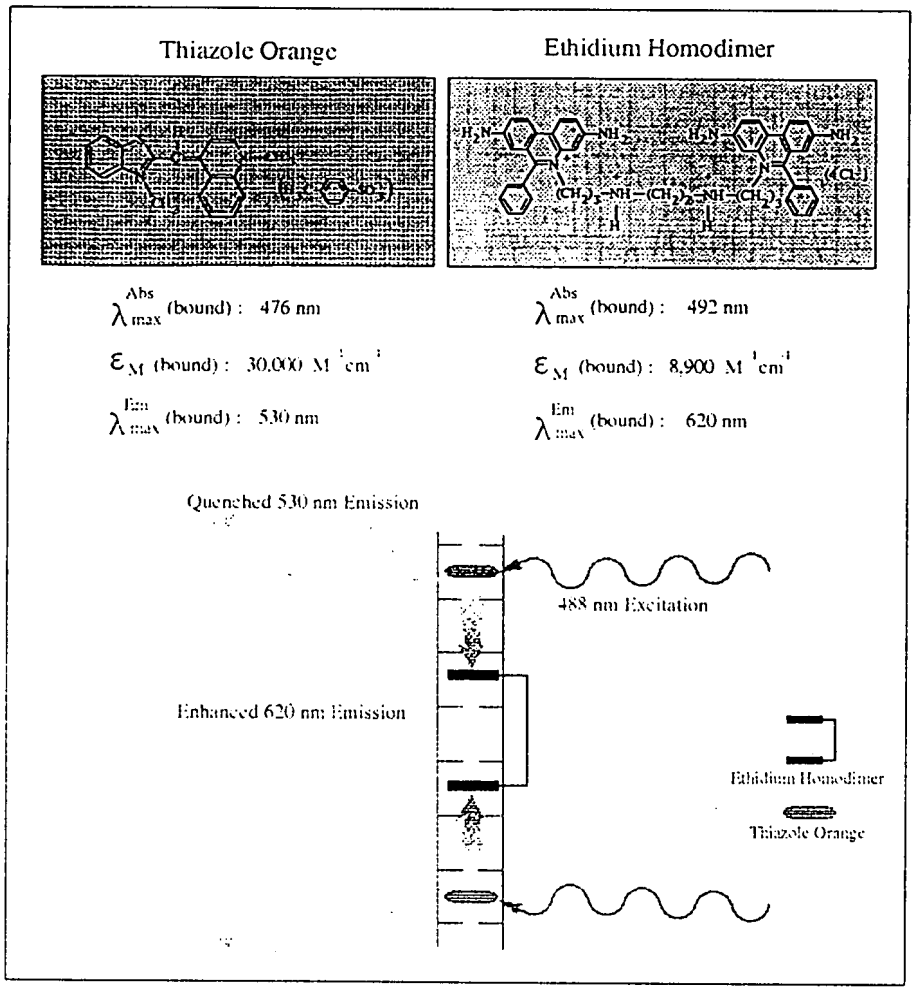

Figure 4. Energy transfer between thiazole orange and ethidium homodimer can be used to enhance sensitivity. The fluorescence of EthD is enhanced by staining with TO because TO has a strong absorption at 488 nm and its excitation energy is efficiently transferred to ethidium. The background is low because the strongly Stokes-shifted emission of EthD is far from the exciting line and because the TO in the buffer is nonfluorescent.

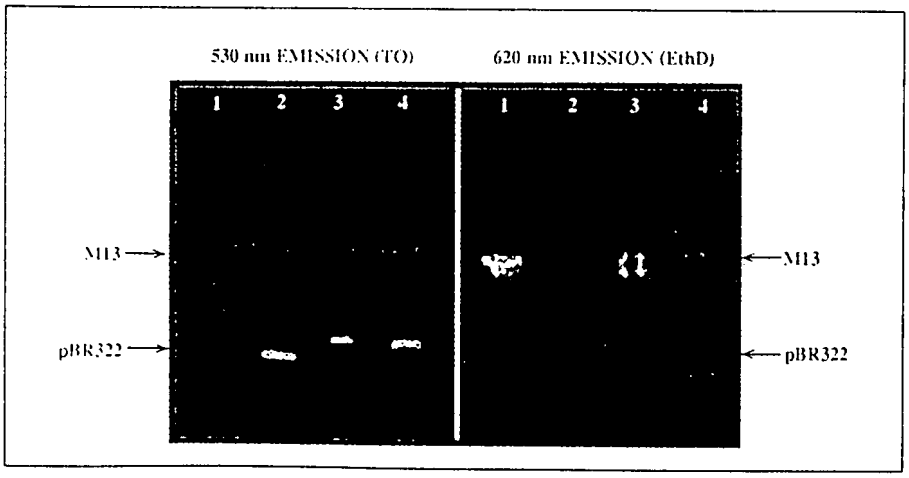

Figure 5. Two-color detection of DNA on agarose gels. Preformed linearized M13mp18 double-stranded DNA-EthD complex and linearized pBR322 can be separately detected on an agarose gel after electrophoresis in buffer containing 1.65×10^{-7} M TO. Fluorescence of intercalated TO is detected at 530 nm and that of intercalated EthD at 620 nm. Lane 1, preformed M13mp18 DNA-EthD complex; lane 2, preformed pBR322 DNA-TO complex; lane 3, preformed M13mp18 DNA-EthD complex mixed with unlabeled pBR322 DNA; lane 4, preformed M13mp18 DNA-EthD complex mixed with preformed pBR322 DNA-TO complex (Figure adapted from Rye et al. [19]).

of the fluorescence and scatter from the glass substrates and of general stray light. Only fluorescence from the labeled and excited molecules in the gel is detected. The microscope objective provides very high light gathering efficiency and precise and efficient imaging of the gel fluorescence through the detection spatial filter. The use of an argon ion laser provides high intensity illumination that also increases sensitivity. This optical and scanning arrangement also provides for optimal selection of the light intensity and illumination time parameters as discussed in Reference 14.

We have shown in Figure 2 that DNA may be sequenced efficiently, rapidly and with high sensitivity using slab gels and the confocal scanner. This is important in the context of efforts to automate DNA sequencing for the Human Genome Project. The ability to scan a large number of DNA slab gels independent of the electrophoresis system increases the overall throughput because the scanner is not tied up during the slow electrophoresis step. Because of the high-sensitivity and high-spatial resolution of the scanning system, it is evident that efforts to miniaturize slab sequencing gels and to improve gel resolution will be profitable. For example, the techniques developed by Gelfi et al. (7) to sequence up to 600 bases on modified HydroLink gels could be immediately coupled to our detection system. Further reduction of the lane width and the electrophoresis run length, as demonstrated here, will result in much higher sequence information density on the gels which could still be read easily with our scanner. High-sensitivity detection implies that the enhanced throughput will not require increased amounts of sample. Finally, our approach is advantageous because the preparation of DNA and the data images are immediately familiar to users of traditional autoradiography.

The confocal gel scanner has also helped us to develop new protocols for fluorescence labeling with intercalating dyes and new procedures for detecting DNA in gels. EthD staining of DNA prior to agarose gel electrophoresis is both convenient and sensitive. This procedure has enabled us to

obtain highly sensitive (30 pg DNA/band) detection. It should be possible to develop other polycationic intercalating oligomers of dye molecules to produce a wide range of highly fluorescent reagents for the detection of DNA. Post-staining of DNA with TO is also a sensitive detection method with 20-pg sensitivity. In addition, by using EthD and TO in concert, it is possible to perform two-color detection of different samples of DNA. This would permit the electrophoresis of size standards in the same lane for accurate molecular weight determination or the multiplex detection of different DNA samples. It should be relatively easy to modify our detection optics to perform simultaneous multi-color detection. Finally, by sequentially post-staining yeast DNA with EthD and then TO, we have obtained greater than 100-fold improvement in the detection sensitivity on pulsed field gels over trans-illumination methods using ethidium bromide. These examples show that the confocal fluorescence scanner is a useful tool in the detection of DNA separated on a variety of gel media.

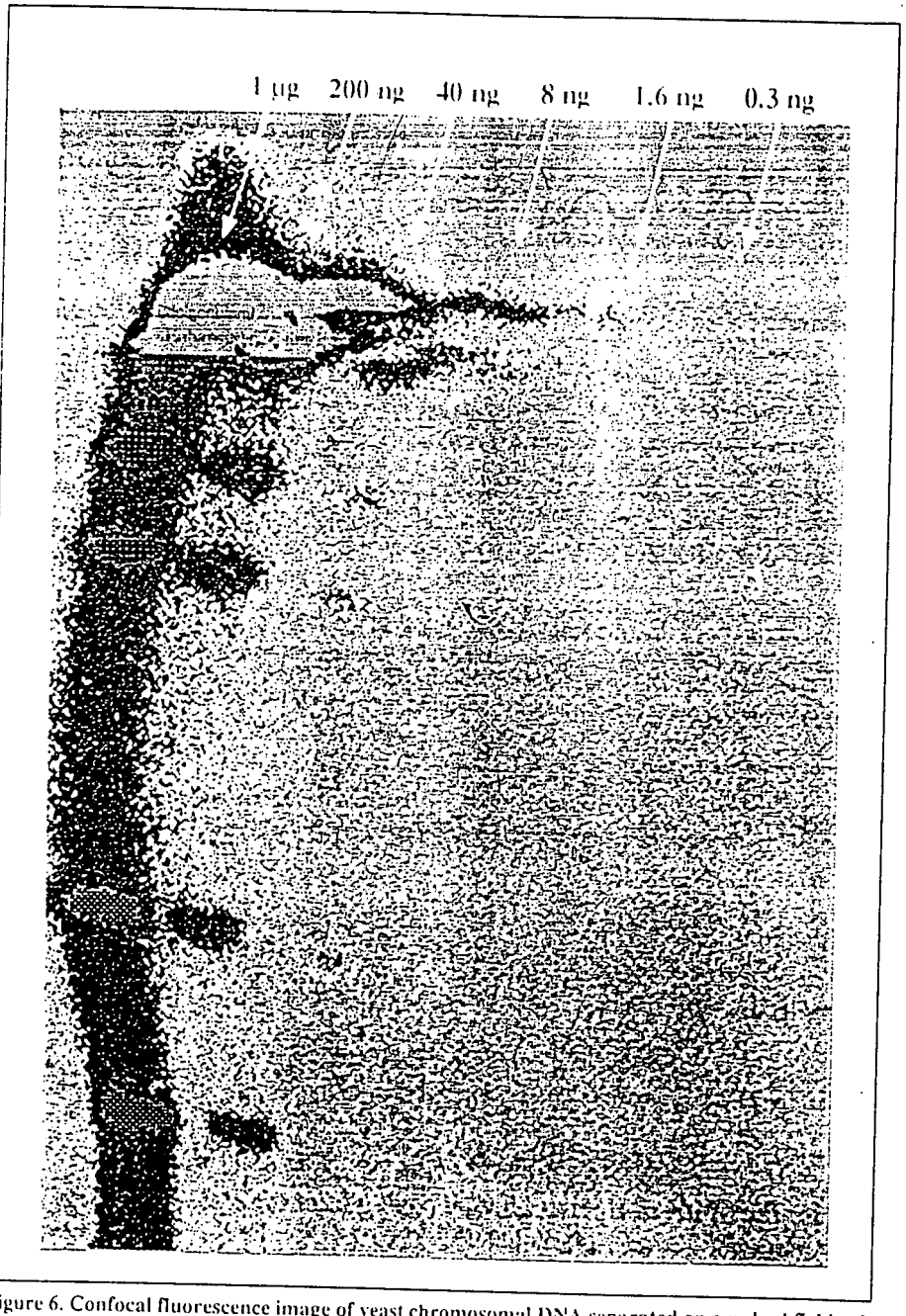

Figure 6. Confocal fluorescence image of yeast chromosomal DNA separated on a pulsed field gel. The serially diluted yeast DNA was loaded in lanes having approximately 1 µg, 200 ng, 40 ng, 8 ng, 1.6 ng and 0.3 ng of total DNA per lane. The CHEF pulsed field gel was post-stained with EthD followed by TO as a sensitizer as described in Materials and Methods.

The versatility and efficiency of our confocal fluorescence gel scanner enables DNA detection in diverse gel separation media. Some of the future possibilities include enhanced DNA sequencing throughput by multi-color detection from a single lane and miniaturization of the slab gels. The two-color intercalation dye experiments lay the groundwork for the use of stable DNA-dye intercalation complexes carrying hundreds of chromophores in multi-color applications such as the physical mapping of chromosomes. Finally, since recent efforts to obtain pulsed field gel separations of DNA in excess of 10 Mb in size have been slowed by low detection sensitivity, one may easily envision that our fluorescence scanner will also contribute to progress in this area. Confocal fluorescence gel scanning will be a valuable new technology in DNA research.

ACKNOWLEDGMENTS

We thank Colleen Sheridan for valuable assistance in running the DNA sequencing gels. H.S.R. is the recipient of a predoctoral fellowship from the Department of Health and Human Services Training Grant GM 07232. This research was supported in part by a grant from the Lucille P. Markey Charitable Trust, by the National Science Foundation (DMB 88-16727 and BBS 87-20382) and by the Director, Office of Energy Research, Office of Health and Environmental Research, Physical and Technological Research Division of the U.S. Department of Energy under contract DE-FG-03-88ER60706.

REFERENCES

1. Ansorge, W., B. Sproat, J. Stegemann, C. Schwager and M. Zenke. 1987. Automated DNA sequencing: ultrasensitive detection of fluorescent bands during electrophoresis. Nucleic Acids Res. 15:4593-4602.
2. Brumbaugh, J.A., L.R. Middendorf, D.L. Grone and J.L. Ruth. 1988. Continuous on-

line DNA sequencing using oligodeoxynucleotide primers with multiple fluorophores. Proc. Natl. Acad. Sci. USA *85*:5610-5614.
3. **Cheng, Y.-F. and N.J. Dovichi.** 1988. Subattomole amino acid analysis by capillary zone electrophoresis and laser-induced fluorescence. Science *242*:562-564.
4. **Cohen, A.S., D.R. Najarian and B.L. Karger.** 1990. Separation and analysis of DNA sequence reaction products by capillary gel electrophoresis. J. Chromotogr. *516*:49-60.
5. **Denk, W., J.H. Strickler and W.W. Webb.** 1990. Two-photon laser scanning fluorescence microscopy. Science *248*:73-76.
6. **Drossman, H., J.A. Luckey, A.J. Kostichka, J. D'Cunha and L.M. Smith.** 1990. High-speed separations of DNA sequencing reactions by capillary electrophoresis. Anal. Chem. *62*:900-903.
7. **Gelfi, C., A. Canali, P.C. Righetti, P. Vezzoni, C. Smith, M. Mellon, T. Jain and R. Shorr.** 1990. DNA sequencing in HydroLink matrices: Extension of reading ability to >600 nucleotides. Electrophoresis *11*:595-600.
8. **Glazer, A.N., K. Peck and R.A. Mathies.** 1990. A stable double-stranded DNA-ethidium homodimer complex: Application to picogram fluorescence detection of DNA in agarose gels. Proc. Natl. Acad. Sci. USA *87*:3851-3855.
9. **Gordon, M.J., X. Huang, S.L. Pentoney Jr. and R.N. Zare.** 1988. Capillary electrophoresis. Science *242*:224-228.
10. **Hiraoka, Y., J.W. Sedat and D.A. Agard.** 1987. The use of a charge-coupled device for quantitative optical microscopy of biological structures. Science *238*:36-41.
11. **Hirschfeld, T.** 1976. Quantum efficiency independence of the time integrated emission from a fluorescent molecule. Appl. Optics *15*: 3135-3139.
12. **Jovin, T.M. and D. Arndt-Jovin.** 1989. Luminescence digital imaging microscopy. Annu. Rev. Biophys. Biophys. Chem. *18*:271-308.
13. **Mathies, R.A., K. Peck and L. Stryer.** 1990. High-sensitivity single molecule fluorescence detection, p. 52-59. *In* L.C. Smith (Ed.), Bioimaging and Two-Dimensional Spectroscopy. SPIE—The International Society for Optical Engineering, Bellingham, WA.
14. **Mathies, R.A., K. Peck and L. Stryer.** 1990. Optimization of high-sensitivity fluorescence detection. Anal. Chem. *62*:1786-1791.
15. **Mathies, R.A. and L. Stryer.** 1986. Single-molecule fluorescence detection: A feasibility study using phycoerythrin, p. 129-140. *In* D.L. Taylor, A.S. Waggoner, F. Lanni, R.F. Murphy and R. Birge (Eds.), Applications of Fluorescence in the Biomedical Sciences. Alan R. Liss, New York.
16. **Nguyen, D.C., R.A. Keller, J.H. Jett and J.C. Martin.** 1987. Detection of single molecules of phycoerythrin in hydrodynamically focused flows by laser-induced fluorescence. Anal. Chem. *59*:2158-2161.
17. **Pawley, J.** 1990. Handbook of Biological Confocal Microscopy. Plenum Press, New York.
18. **Prober, J.M., G.L. Trainor, R.J. Dam, F.W. Hobbs, C.W. Robertson, R.J. Zagursky, A.J. Cocuzza, M.A. Jensen and K. Baumeister.** 1987. A system for rapid DNA sequencing with fluorescent chain-terminating dideoxynucleotides. Science *238*:336-341.
19. **Rye, H.S., M.A. Quesada, K. Peck, R.A. Mathies and A.N. Glazer.** 1991. High-sensitivity two-color detection of double-stranded DNA with a confocal fluorescence gel scanner using ethidium homodimer and thiazole orange. Nucleic Acids Res. *19*:327-333.
20. **Shapiro, H.M.** 1988. Practical Flow Cytometry, Second Edition. A.R. Liss, New York.
21. **Sherman, F., G.R. Fink and J.B. Hicks.** 1986. Laboratory Course Manual for Methods in Yeast Genetics. Cold Spring Harbor Laboratory, Cold Spring Harbor, NY.
22. **Shuman, H., J.M. Murray and C. DiLullo.** 1989. Confocal microscopy: an overview. BioTechniques *7*:154-163.
23. **Smith, L.M.** 1990. Automated DNA sequencing and the analysis of the human genome. Genome *31*:929-937.
24. **Smith, C.L., S.R. Klco and C.R. Cantor.** 1988. Pulsed field gel electrophoresis and the technology of large DNA molecules, p. 41-72. *In* K. Davies (Ed.), Genome Analysis: A Practical Approach. IRL Press, Oxford, England.
25. **Smith, L.M., J.Z. Sanders, R.J. Kaiser, P. Hughes, C. Dodd, C.R. Connell, C. Heiner, S.B.H. Kent and L.E. Hood.** 1986. Fluorescence detection in automated DNA sequence analysis. Nature *321*:674-679.
26. **Swerdlow, H., S. Wu, H. Harke and N.J. Dovichi.** 1990. Capillary gel electrophoresis for DNA sequencing. Laser-induced fluorescence detection with the sheath flow cuvette. J. Chromatogr. *516*:61-67.
27. **Taylor, D.L., A.S. Waggoner, R.F. Murphy, F. Lanni and R.R. Birge, (Eds.).** 1986. Applications of Fluorescence in the Biomedical Sciences. A.R. Liss, New York.
28. **Trainor, G.L.** 1990. DNA sequencing, automation and the human genome. Anal. Chem. *62*:418-426.
29. **Wilson, R.K., C. Chen, N. Avdalovic, J. Burns and L. Hood.** 1990. Development of an automated procedure for fluorescent DNA sequencing. Genomics *6*:626-634.
30. **Wu, S. and N.J. Dovichi.** 1989. High-sensitivity fluorescence detector for fluorescein isothiocyanante derivatives of amino acids separated by capillary zone electrophoresis. J. Chromatogr. *480*:141-155.

Address correspondence to:

Richard A. Mathies
Department of Chemistry
University of California
Berkeley, CA 94720

A System for Rapid DNA Sequencing with Fluorescent Chain-Terminating Dideoxynucleotides

JAMES M. PROBER,* GEORGE L. TRAINOR, RUDY J. DAM, FRANK W. HOBBS, CHARLES W. ROBERTSON, ROBERT J. ZAGURSKY, ANTHONY J. COCUZZA, MARK A. JENSEN, KIRK BAUMEISTER

A DNA sequencing system based on the use of a novel set of four chain-terminating dideoxynucleotides, each carrying a different chemically tuned succinylfluorescein dye distinguished by its fluorescent emission is described. Avian myeloblastosis virus reverse transcriptase is used in a modified dideoxy DNA sequencing protocol to produce a complete set of fluorescence-tagged fragments in one reaction mixture. These DNA fragments are resolved by polyacrylamide gel electrophoresis in one sequencing lane and are identified by a fluorescence detection system specifically matched to the emission characteristics of this dye set. A scanning system allows multiple samples to be run simultaneously and computer-based automatic base sequence identifications to be made. The sequence analysis of M13 phage DNA made with this system is described.

THE DEVELOPMENT OF SEQUENCING METHODS FOR DETERmining the order of nucleotide bases in deoxyribonucleic acid (DNA) has led to rapid advances in our understanding of the organization and processing of information in biological systems. Two methods are available for DNA sequencing: the chemical degradation method of Maxam and Gilbert (*1*), and the dideoxy chain termination method of Sanger (*2*). Traditionally, each approach affords four sets of radioisotopically labeled fragments which are resolved according to their lengths by gel electrophoresis and the resulting autoradiographic pattern is used to obtain the DNA sequence.

The Maxam-Gilbert and Sanger techniques, which are conceptually elegant and efficacious, are in practice time-consuming and labor-intensive, partly because a single radioisotopic reporter is used for detection. Using one reporter to analyze each of the four bases requires four separate reactions and four gel lanes. The resulting autoradiographic patterns, obtained after a delay for exposure and development, are complex and require skilled interpretation and data transcription.

These deficiencies can be corrected by switching from a radioisotopic to a fluorescent reporter. We describe here a system for DNA sequencing in which four chemically related, yet distinguishable, fluorescence-tagged dideoxynucleotides are used to label DNA by a modified Sanger protocol with a suitable chain-extending DNA polymerase. The fluorescent sequencing fragments are resolved temporally rather than spatially in a single lane by conventional polyacrylamide gel electrophoresis. Analysis of the fluorescent emission of each fragment permits us to identify the terminating nucleotide and assign the sequence directly in real time.

Fluorescent tags. We have developed a family of fluorescent dyes with largely overlapping yet distinct emission bands. These dyes are 9-(carboxyethyl)-3-hydroxy-6-oxo-6H-xanthenes or succinylfluoresceins (SF-xxx, where xxx refers to the emission maximum in nanometers) (Fig. 1A). They are readily prepared from succinic anhydride and an appropriately substituted resorcinol by a modification of the procedure cited for the parent dye, SF-505 (*3*). The fluorescent forms of these dyes are the dianions, which predominate in aqueous solution above *p*H 7. The dianion of SF-505 absorbs maximally at 486 nm, a wavelength that is well suited for excitation by an argon ion laser operating at 488 nm. This species shows an absorption coefficient of $72{,}600 M^{-1}$ cm^{-1} at the maximum and fluoresces with an emission maximum at 505 nm with a quantum yield comparable to that of fluorescein. The carboxylic acid functionality is not essential for fluorescence and is used here for covalent attachment to the nucleotides by means of standard methodologies.

The wavelengths of the absorption and emission maxima in the succinylfluorescein system are tuned by changing the substituents $-R_1$ and $-R_2$. The absorption spectra for the four dyes where $-R_1$ and $-R_2$ are $-$H or $-$Me are shown in Fig. 1B. Close spacing of the absorption maxima results in efficient excitation of all dyes by the single emission line of the argon ion laser. (The absorption coefficients at 488 nm of the two most disparate dyes, SF-505 and SF-526, differ only by a factor of 2.) These succinylfluoresceins carry the same charge and are nearly identical in size, minimizing any differential perturbation of the electrophoretic mobilities of the DNA fragments to which they are attached. We observe no differences in the relative mobilities among identical DNA fragments tagged with any of the four dyes.

Labeling strategy. Dideoxy sequencing involves the template-directed, enzymatic extension of a short oligonucleotide primer in the presence of chain-terminating dideoxyribonucleotide triphosphates (ddNTP's). A nested set of DNA fragments is produced

J. M. Prober, R. J. Dam, and C. W. Robertson are with the Engineering Physics Laboratory; G. L. Trainor, F. W. Hobbs, R. J. Zagursky, A. J. Cocuzza, and K. Baumeister are with the Central Research and Development Department (contribution number 4543); and M. A. Jensen is with the Medical Products Department, all of the E. I. du Pont de Nemours & Company (Inc.), Wilmington, DE 19898.
*To whom correspondence should be addressed.

having primer-defined 5′ ends and variable 3′ ends determined by the positions of incorporation of a given base (as ddNMP). Radioisotopic label is generally incorporated by including [α-^{32}P]dNTP or [α-^{35}S]dNTP in the reaction mixture such that internal nucleotides in the newly synthesized portions of the fragments are labeled.

The analogous incorporation of fluorescence-tagged nucleotides may be difficult to achieve enzymatically, and may adversely affect the crucial relation between chain length and electrophoretic mobility, which is essential for accurate sequence determination. We have chosen instead to incorporate a single fluorescent tag by labeling chain-terminating dideoxynucleotide triphosphates. This labeling approach offers several advantages. Generation of all four sets of DNA sequencing fragments can be carried out simultaneously in a single reaction since only the terminating nucleotide carries the tag. In addition, many polymerase pausing artifacts are eliminated since only those fragments resulting from bona fide termination events carry a fluorescent tag.

The set of four fluorescence-tagged chain-terminating reagents we have designed and synthesized is shown in Fig. 2A. These are ddNTP's to which succinylfluorescein has been attached via a linker to the heterocyclic base. (These reagents are designated N-xxx where N refers to the ddNTP and xxx refers to the SF-xxx portion.) The linker is attached to the 5 position in the pyrimidines and to the 7 position in the 7-deazapurines. The 7-deazapurines were used to facilitate stable linker arm attachment at that site. Coupling of the dyes to the nucleotides was found to influence both the wavelengths of the absorption and emission maxima and their relative fluorescence yields. The dyes and bases were therefore paired for maximum distinguishability and for balanced net fluorescence sensitivities.

The synthetic scheme devised for these reagents is highly convergent and general. The preparation of T-526 is illustrative. 5-Iodo-2′,3′-dideoxyuridine was coupled to *N*-trifluoroacetylpropargylamine under palladium(0) catalysis in dimethylformamide (*4*). The resulting derivatized nucleoside was converted to its 5′-triphosphate (*5*) and deacylated to afford 5-(3-amino-1-propynyl)-2′,3′-dideoxyuridine triphosphate. This amine was coupled with an *O*-acetyl–protected form of the SF-526–sarcosine conjugate and deprotected to afford T-526.

The fluorescence-tagged chain-terminators are accepted as alternative substrates by avian myeloblastosis virus (AMV) reverse transcriptase with efficiencies comparable to that of the corresponding unsubstituted ddNTP's. A comparison of the sequencing ladders produced using the ddNTP's and their fluorescent counterparts is shown in Fig. 3. The fidelity of terminator incorporation is maintained. Comparison of lanes 4 and 5, containing ddCTP and C-519, respectively, shows that the fluorescence-tagged fragments run approximately 2 bases slower than their untagged counterparts. This mobility shift is consistent for all four sets of fluorescence-tagged fragments, allowing the sequence ladder to be read and qualifying this set of reagents for single-lane DNA sequencing. These terminators are also substrates for modified T7 DNA polymerase (*6*). They are not, however, substrates for the Klenow fragment of DNA polymerase I from *Escherichia coli*.

Fluorescence detection system. Labeled DNA fragments, produced by the enzymatic chain extension reactions, are separated by polyacrylamide gel electrophoresis, detected, and identified as they migrate past the fluorescence detection system illustrated in Fig. 4. High signal-to-noise ratio is achieved in this system through efficient excitation, optical filtering, and light collection.

Strong excitation is obtained with a laser source that provides most of its output energy at a single wavelength and by matching the dye absorbances to that wavelength. Fluorescence detection is enhanced approximately fourfold by depositing a mirror on the outside surface of the glass gel support plate furthest away from the laser. The excitation beam is thereby returned through the gel, in effect doubling the excitation pathlength, and the fluorescence headed away from the detectors is also returned, increasing the amount of collected light.

In addition to the desired fluorescence from the dye-labeled DNA, light emanating from the excitation region includes scattered laser radiation, Raman scattering, and fluorescence from other sources. Optical filtering and other means are used to reduce these undesired signals. Secondary laser lines are removed with a narrow-band interference filter placed at the source. The reflected component of the 488-nm laser light is eliminated by the mirror, which provides a return path for the beam out of the detectors' field of view. Scattered light is removed by a filter stack consisting of an interference filter, a fiber-optic face plate, and a colored glass absorbing filter. The interference filter is designed to strongly reject the excitation light, pass the dye emission region, and reject Raman scattering and fluorescence above 560 nm. At high angles of incidence, the filter passband is shifted toward the excitation wavelength, thus increasing background levels and associated noise.

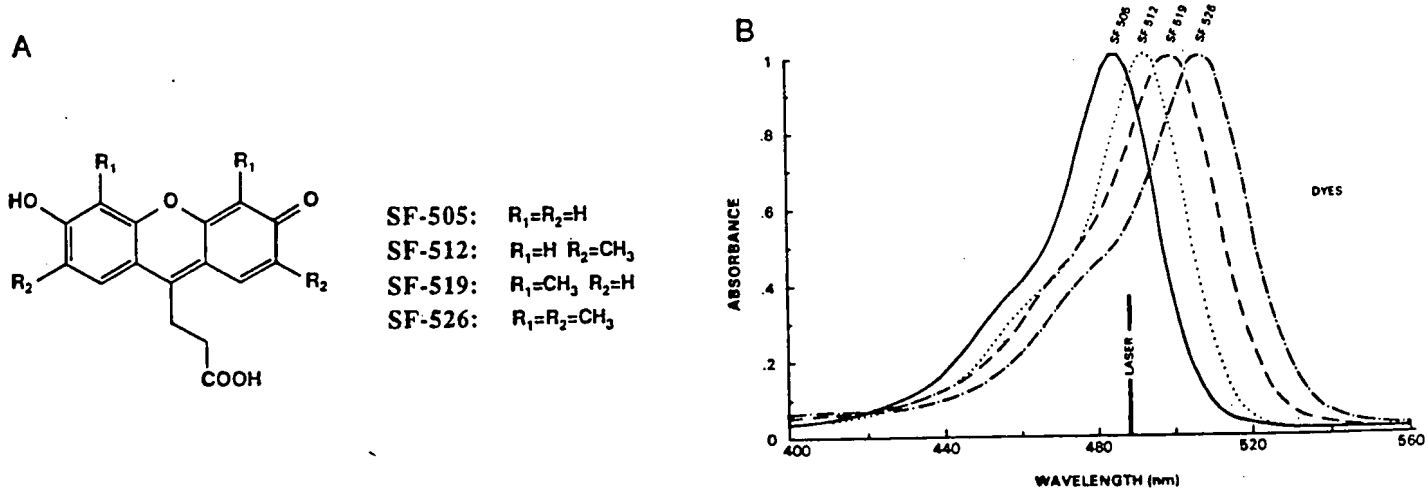

Fig. 1. Succinylfluorescein dyes. (**A**) Chemical structure of the four dyes used to label dideoxynucleotide triphosphates for use as chain-terminators in modified dideoxy DNA sequencing protocols. (**B**) Normalized absorption spectra of the dyes shown in (A). Absorption coefficient at the maximum for SF-505 is 72,600M^{-1} cm^{-1}. Spectra were measured in *p*H 8.2, 50 m*M* aqueous tris-HCl buffer. The other dyes have coefficients within 10 percent of this value. Vertical bar (laser) indicates the position of the argon ion laser line at 488 nm used for fluorescence excitation.

Thus a fiber-optic face plate with extramural absorber is employed as an aperture to restrict entrance angles on the filter. This element absorbs incident rays outside the acceptance angle of the fiber, in this case about 22 degrees. This aperture appears over any point of excitation across the gel.

The dyes that we used are distinguished by small differences in their absorption and emission spectra. Close spacing of the spectra facilitates efficient excitation and simultaneous detection. This contrasts with the use of large differences in emission spectra that one would intuitively select to facilitate discrimination. Figure 2B shows the emission spectra of the fluorescence-tagged chain-terminators that occur in a polyacrylamide gel. In our system, two photomultiplier tube detectors, each with a different filter stack, view the fluorescence simultaneously; one collects light at the low-wavelength side of the emission bands and the other collects light at the high wavelength side. When, for example, G-505–terminated fragments pass the detectors, one detector registers a large signal relative to the other; when T-526–terminated fragments pass, the reverse occurs. The A-512– and C-519–terminated fragments give specific detector signal ratios lying between these two extremes. The ratio of baseline-corrected peak intensities is used to determine the base assignment. This method provides very efficient light collection and obviates the need for more refined spectral analysis.

The scanning mechanism shown in Fig. 4 directs the laser beam to the gel through a periscope mounted on the shaft of a stepper motor. By stepping the periscope, any point in the detection region can be accessed. The detectors span the full width of a gel so that fluorescence is collected and analyzed from wherever the laser is pointed. Directing only the laser beam, rather than any of the major optical elements, results in a low-noise scanning system that is mechanically simple and stable.

Data processing and analysis. Processing of the raw detector data and subsequent nucleotide base assignment is accomplished in several steps. Digitized signals from both detectors are subjected to a peak-finding algorithm to determine the time positions of the DNA bands. Once the DNA peaks are located, the ratios of baseline-corrected peak intensities are calculated along with a statistical calculation of the certainty of those ratios. The 15 percent most certain ratios are displayed as a histogram in Fig. 5. These fall naturally into clusters centered about four values, each defining one of the bases. These reference values can differ slightly from lane to lane due to geometrical effects of the wavelength selection filters. To allow for these variations, the reference values are determined independently for each lane.

The four reference values correspond to peaks in the histogram. Measurement of scatter about the reference values allows the determination of boundaries which are used for base assignment. When DNA peaks are no longer resolvable or when their amplitude falls below the inherent noise level of the detection system, no further bases are assigned. In the current system, this usually occurs between 300 to 400 bases from the 3′ terminus of the primer. Deconvolution, predictive modeling, and digital signal processing are being investigated to extend the readable sequence range.

Nucleotide sequence determination. Raw detector data obtained from the nucleotide sequence of the phage M13*mp*18 during a 6-hour run are shown in Fig. 6. A modified, two-stage dideoxy chain termination protocol (*6*) was used to generate the DNA fragments for fluorescence-based sequence analysis. The data shown correspond to bases 3 to 234 from the 3′ terminus of the primer. Reference values for this sequencing run are established in Fig. 5, which illustrates the principles discussed above for base assignment. Regions of the sequence are shown in greater detail in Fig. 7.

Improvements in sequencing. As illustrated by recent discussions of human genome sequencing, large-scale sequencing projects would require massive resources with current technology (*7*). Programs of intermediate scope, crucial in fundamental research as well as in the development of DNA probes, clinical reagents, and useful genetically engineered organisms, are likewise limited by the speed and ease of DNA sequencing.

Efforts to improve the technology of radioisotopic sequencing have been reviewed (*8*). In one example, a technique of continuous DNA blotting during electrophoresis is described in which the DNA fragments resulting from conventional dideoxy sequencing are separated by electrophoresis and allowed to elute from the bottom of the gel onto a moving membrane (*9*). The membrane is subsequently exposed to film and the resulting autoradiographic band patterns are interpreted in the normal fashion. This technique offers some advantages in readability of the band patterns and in the potential for a degree of automation in sequence analysis. However, the inherent disadvantages of using isotopically labeled reporters in the traditional manner remain and will limit the ultimate utility of this approach. A newer method with potential for genomic sequenc-

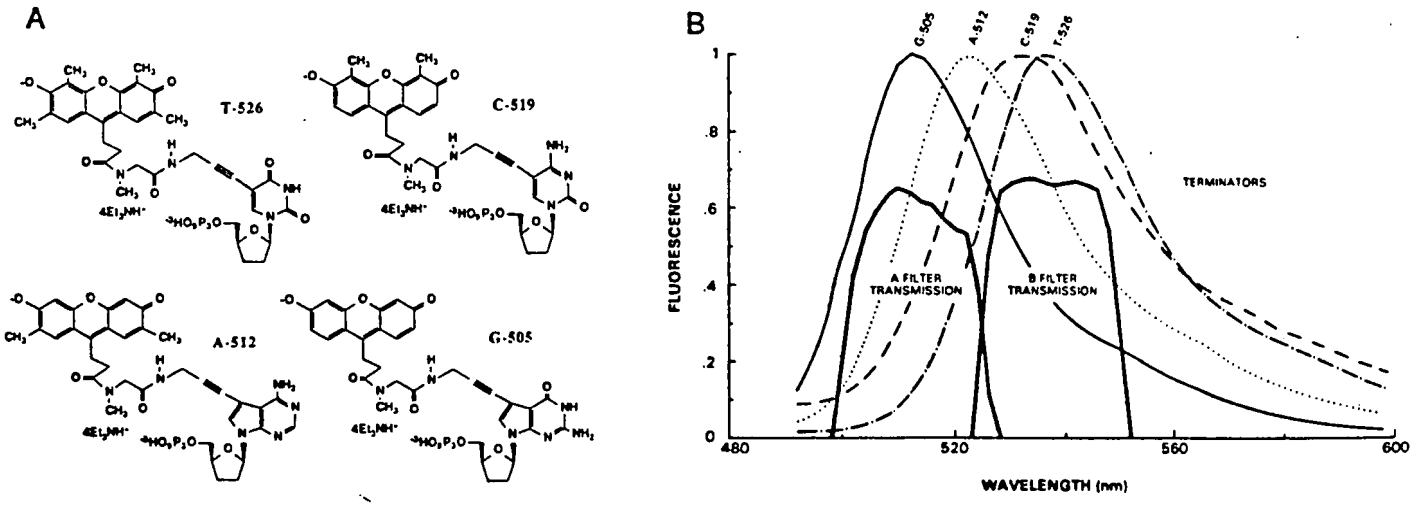

Fig. 2. Fluorescence-tagged chain-terminating reagents. (**A**) Chemical structures of the reagents used in modified dideoxy reactions for DNA sequencing. (**B**) Normalized fluorescence emission spectra of the reagents, measured in an 8 percent w/v polyacrylamide gel (19:1 w/w acrylamide:bis) under electrophoresis conditions similar to those of Fig. 6. The excitation wavelength was 488 nm. The absolute emission intensity values of the four compounds varied relative to each other by less than a factor of 2. Superimposed on the emission spectra are transmission functions of the interference filters used in the fluorescence detection system (Fig. 4). The nucleotide base assignment for each band is achieved by measuring the relative fluorescence signal in two detectors with spectral responses defined primarily by these filter functions.

ing employing radioactively labeled probes has also been described (*10*). This technique may address the problem of low throughput by enabling multiple sequences to be read from a single gel. The method does reduce the amount of gel preparation and electrophoresis required for a given sequencing task; however, sequence data are still obtained from autoradiographs which must be analyzed and transcribed in separate steps.

Advances in fluorescent sequencing have also been reported. The synthesis of oligonucleotides labeled at 5′ ends with fluorescent labels and useful for dideoxy sequencing (*11*), and several systems based on fluorescent primer technology (*12–14*), have been described. These systems successfully reduce or eliminate a number of the deficiencies of the current radioisotope technology. However, the disadvantages of primer labeling remain. In addition to the polymerase pausing problem noted previously, the use of labeled primers requires that oligonucleotides be custom synthesized and purified for each set of sequencing reactions. This restricts the use of sequencing strategies which employ multiple priming sites or different cloning vectors.

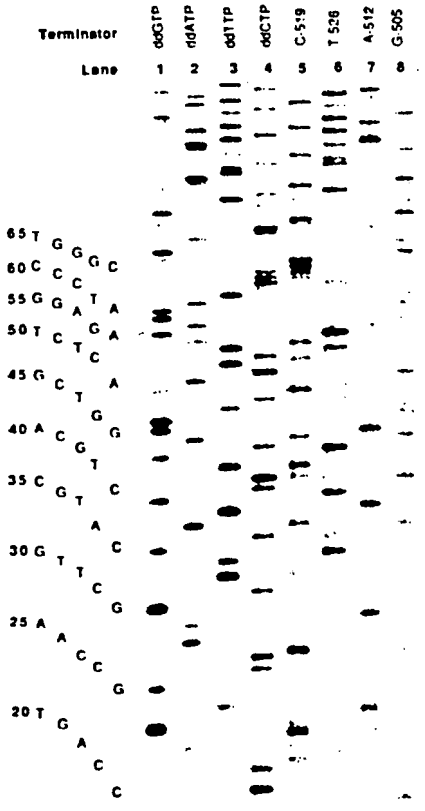

Fig. 3. Comparison of electrophoretic mobilities of DNA sequencing fragments terminated with ddNTP's and with fluorescence-tagged chain-terminators. The dideoxy method of Sanger (*2*) was used to sequence a region of M13*mp*18. A 17-bp oligonucleotide corresponding to the (−40) region of the template was end-labeled with [γ-^{32}P]ATP and polynucleotide kinase. Each reaction mixture contained template (0.1 μg), end-labeled primer (2.5 ng, annealed by heating to 95°C for 2 minutes and slowly cooled to room temperature), 60 m*M* tris-HCl at *p*H 8.5, 7.5 m*M* $MgCl_2$, 75 m*M* NaCl, 0.5 m*M* dithiothreitol, AMV reverse transcriptase (NEN, 20 units), and nucleotides at the following concentrations: lane 1, 2.5 μ*M* ddGTP, 12 μ*M* dGTP, 2.5 μ*M* dATP, 50 μ*M* dCTP and dTTP; lane 2, 0.25 μ*M* ddATP, 2.5 μ*M* dATP, 50 μ*M* dGTP, dCTP, and dTTP; lane 3, 3.0 μ*M* ddTTP, 12 μ*M* dTTP, 2.5 μ*M* dATP, 50 μ*M* dCTP and dGTP; lane 4, 2.5 μ*M* ddCTP, 12 μ*M* dCTP, 2.5 μ*M* dATP, 50 μ*M* dGTP and dTTP; lane 5, as in lane 4 except ddCTP has been replaced with 5.0 μ*M* C-519; lane 6, as in lane 3 except ddTTP has been replaced with 6.0 μ*M* T-526; lane 7, as in lane 2 except ddATP has been replaced with 2.0 μ*M* A-512; lane 8, as in lane 1 except ddGTP has been replaced with 8.0 μ*M* G-505. The primer extensions were carried out at 42°C for 10 minutes, and then unlabeled dNTP's (100 μ*M*) were added and the reaction proceeded for 10 minutes at 42°C. The reactions were stopped by diluting to 60 percent (v/v) formamide and denatured at 65°C for 10 minutes. A portion of each sample (1/8) was loaded onto an 8 percent (w/v) polyacrylamide gel containing urea (8*M*) and TBE buffer (100 m*M* tris-HCl, 83 m*M* boric acid, 1 m*M* Na_2EDTA, *p*H 8.1). The electrophoresis was carried out at 1600 volts.

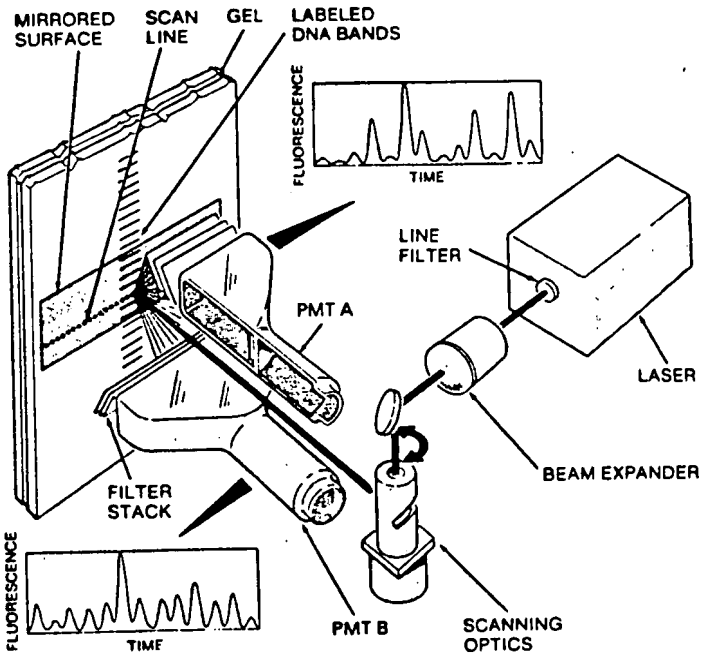

Fig. 4. Fluorescence detection system. Schematic drawing of the optical system used for scanning excitation and for measuring fluorescence from multiple sequencing lanes in an electrophoresis gel. Light from the argon ion laser is filtered to isolate the 488-nm emission line. The beam is deflected by a mirror into the scanning optics which are mounted on the shaft of a digitally controlled stepper motor. A lens focuses the beam into a spot in the plane of the gel. A second mirror directs the beam to a position on the scan line defined by the rotational position of the motor shaft. Sequencing of multiple samples is achieved by directing the beam sequentially to each of the sequencing lanes on the gel. Upon entering the gel, the beam excites fluorescence in the terminator-labeled DNA. Fluorescence is detected by two elongated, stationary photomultiplier tubes (PMT A and PMT B) which span the width of the gel. In front of each PMT, a filter stack is placed with one of the complementary transmission functions (Fig. 2B). Baseline-corrected ratios of signals in the PMT's are used to identify the labeled DNA fragments currently in the excitation region. Excitation efficiency and fluorescence collection are increased by the mirrored outer surface of the glass plate in the electrophoresis gel assembly.

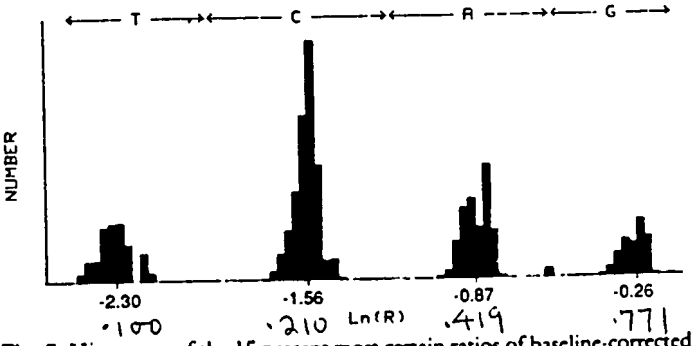

Fig. 5. Histogram of the 15 percent most certain ratios of baseline-corrected peak intensities of detector A to detector B for the run shown in Fig. 6. The natural logarithm of the ratio is used to enhance visual presentation. The ratios cluster about four reference values corresponding to the four bases as shown. The intervals used to assign the base identity of each peak are shown above the histogram. Data acquisition and analysis were performed by a Hewlett-Packard 9000 Model 500 computer.

The use of fluorescence-labeled chain-terminators for DNA sequencing, on the other hand, offers several distinct advantages. Labeled chain terminators afford complete flexibility of sequencing strategy and choice of vectors and allow the sequencing reactions to take place in one vessel. In this method, only true dideoxy terminations result in detectable fluorescent bands. Chain synthesis artifacts may still occur, but they will not be detected since these products are not fluorescent. This results in simplified elution patterns and facilitates data analysis.

We have succeeded in using fluorescence-tagged chain-terminating reagents for DNA sequencing. Structurally, each of the four reagents described here (Fig. 2A) consists of a succinylfluorescein attached to a dideoxynucleoside triphosphate through a novel acetylenic linker. The linker is both sterically compact and synthetically accessible for all four bases. The linker is attached to the 5 position of the pyrimidines and the 7 position of the 7-deazapurines. These positions have been reported in some cases to be acceptable for attaching substituents to chain-propagating substrates (that is, deoxynucleotide triphosphates) for DNA polymerases (*15, 16*). The chain-terminators reported here are incorporated by both AMV reverse transcriptase and modified T7 DNA polymerase (*6*), but they are not accepted by the Klenow fragment of DNA polymerase I from *Escherichia coli*. The reasons for the inability of these terminators to serve as substrates for the Klenow fragment are not understood.

Fluorescent reporters have the potential for imparting differential mobility shifts to the DNA fragments, thus complicating their electrophoretic elution pattern and subsequent base assignments. In the systems previously described employing more than one reporter, this effect is aggravated by the use of structurally dissimilar dyes (*12*). Perturbations to the linker arm structure and software algorithms were used to reconstruct the correct elution order of the fragments (*12*). Since the dyes reported here belong to a single family with only minor substituent differences on the succinylfluorescein moieties, they impart no significant differential mobility shifts to the DNA fragments and the correct elution order is observed in the raw data.

A fundamental criterion for an effective sequencing system is accuracy. Accuracy in detection and data analysis derives primarily from high sensitivity to the reporter, and in systems using multiple reporters, the ability to discriminate one label from another. A dideoxy sequencing system must be capable of detecting 10^{-15} to 10^{-16} mol of DNA per band (*12*). For a given number of reporter molecules, the measured fluorescence intensity is determined by the incident laser power, the optical properties of the reporter, and the efficiency of the detection system. This signal is superimposed on a background of Raman and elastic scattering arising from the interaction of the laser beam with the gel matrix and the glass plates of the electrophoresis assembly. Variation in this background determines the inherent noise in the total signal observed. Depending on lane geometry, gel thickness, and other factors, our system is capable of detecting, in real time, between 10^{-18} and 10^{-17} mol of succinylfluorescein reporter under sequencing conditions. Previously reported sensitivities for fluorescence-based sequencing systems are 3×10^{-18} mol (*14*) and from 10^{-17} to 5×10^{-17} mol (*12*).

Possible errors in sequencing include misidentifying a detected base, inserting a base, or failing to detect a base at all. To eliminate insertions and deletions, advantage can be taken of the uniform local temporal spacing of the DNA bands as they pass the detectors (*9*). The prediction of peak positions results in simplified detection and

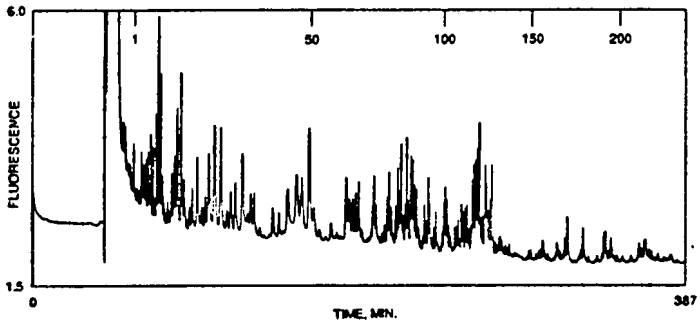

Fig. 6. Detection of fluorescent terminator-labeled DNA fragments from a region of M13*mp*18. Sum of the detector outputs for PMT A and PMT B (in arbitrary units of fluorescence intensity) versus time are shown for a 6-hour sequencing run. The fragments were generated in a two-stage reaction. In one reaction tube were added 3 μg of M13*mp*18 single-stranded DNA and 60 ng of primer (17 bp). This mixture was heated at 95°C for 2 minutes and then placed on ice for 5 minutes to anneal. In the primer extension reaction, 250 pmol each of dATP, dCTP, dTTP, and c^{7}dGTP were added and the reaction incubated at 42°C for 12 minutes in the presence of 60 m*M* tris-HCl, *p*H 8.3, 7.5 m*M* $MgCl_2$, 75 m*M* NaCl, 0.5 m*M* dithiothreitol, and 17 units of AMV reverse transcriptase. The extension reaction was stopped by the addition of a mixture containing 100 pmol of G-505, 800 pmol of A-512, 200 pmol of C-519, and 800 pmol of T-526 and then incubated for an additional 30 minutes at 42°C. Unincorporated fluorescent terminators were removed by gel filtration using a Sephadex G-25 spin column (5′ to 3′ Inc.). The effluent was dried under vacuum, washed with 70 percent ethanol, dried again, and resuspended in 5 μl of 90 percent formamide containing 11 m*M* Na_2EDTA. The sample was then heated to 65°C for 7 minutes and loaded onto an 8 percent w/v polyacrylamide gel (19:1 acrylamide:bis, 20 cm by 40 cm by 0.3 mm) containing 7*M* urea, 100 m*M* tris-HCl, *p*H 8.3, 83 m*M* boric acid, and 11 m*M* Na_2EDTA. The gel was electrophoresed for about 6 hours at 27 watts of constant power. Markers at top show the locations of bands corresponding to the bases.

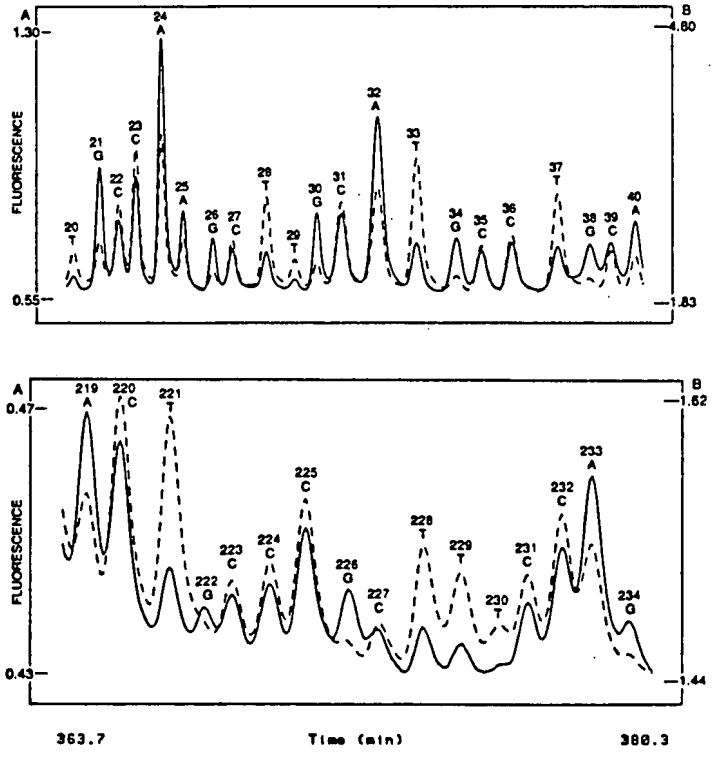

Fig. 7. Sequence of M13*mp*18 showing base assignments. (**Top**) Region of the sequence from base 20 to base 40. Each detector's output (in arbitrary fluorescence intensity units) is plotted as a function of time. Scale factors for the fluorescence are shown independently for the two detectors. Detector A, solid line, left scale; detector B, dashed line, right scale. (**Bottom**) Region of the sequence from base 219 to base 234. Similar data were obtained from base 3 to base 234.

identification of low-intensity peaks. The variation of detector signals across a band helps to identify peaks which are not fully resolved.

The nucleotide sequence of the M13*mp*18 region shown in Fig. 6 was determined by computer algorithms from base 3 to base 234 with no wrong base assignments and no missing or extra bases. Peak intensity variations result from sequence-dependent differences in rates of base incorporation and termination. This distribution is also affected by relative concentrations of dNTP's in the extension reaction and of the terminators in the final chain termination step, as well as by reaction times and conditions. More sequencing experience is required to determine the inherent accuracy in base assignment, but we are encouraged by the absence of errors for peaks above a minimum intensity threshold for discrimination.

In practice there are regions of DNA which are difficult to sequence due to aberrations in electrophoretic mobility caused by secondary structure (*17*). The data analysis system allows the location and extent of such regions to be identified so that flanking sequences remain in frame. 2'-Deoxy-7-deazaguanosine triphosphate has been used (c^7dGTP) in place of dGTP to minimize these effects. A similar technique has been used in fluorescent primer–based sequencing (*18*). For the run of Fig. 6, two regions of GC overlap were assigned by inspection.

A fundamental measure of the utility of an automated sequencer is raw throughput, defined as the sequencing rate per lane times the number of lanes per instrument. In our system 12 lanes are practical. After an initial period of electrophoresis during which the first DNA bands reach the detector, the sequencer is capable of determining approximately 50 bases per hour per lane. A fully loaded gel thus yields a throughput of about 600 bases per hour.

In summary, we have reported advances in chemistry and instrumentation for fluorescent labeling and detection of DNA fragments, and have described a rapid DNA sequencing sytem based on the use of fluorescent chain terminators. Further improvements in the performance of this system, as well as the emergence of other applications requiring sensitive DNA detection, are the subjects of current study.

REFERENCES AND NOTES

1. A. M. Maxam and W. Gilbert, *Proc. Natl. Acad. Sci. U.S.A.* **74**, 560 (1977); *Methods Enzymol.* **65**, 499 (1980).
2. F. Sanger, S. Nicklen, A. R. Coulson, *Proc. Natl. Acad. Sci. U.S.A.* **74**, 5463 (1977).
3. S. Biggs and F. G. Pope, *J. Chem. Soc. (London)* **123**, 2934 (1923).
4. For details on similar couplings see: M. J. Robins and P. J. Barr, *J. Org. Chem.* **48**, 1854 (1983).
5. J. L. Ruth and Y.-C. Cheng, *Mol. Pharmacol.* **20**, 415 (1981).
6. S. Tabor and C. C. Richardson, *Proc. Natl. Acad. Sci. U.S.A.* **84**, 4767 (1987).
7. L. Roberts, *Science* **237**, 358 (1987); *ibid.*, p. 486.
8. W. J. Martin and R. W. Davies, *BioTechnology* **4**, 890 (1986).
9. S. Beck and F. M. Pohl, *EMBO J.* **3**, 2905 (1984).
10. G. M. Church and W. Gilbert, *Proc. Natl. Acad. Sci. U.S.A.* **81**, 1991 (1984).
11. L. M. Smith, S. Fung, M. W. Hunkapiller, T. J. Hunkapiller, L. E. Hood, *Nucleic Acids Res.* **13**, 2399 (1985).
12. L. M. Smith, J. Z. Sanders, R. J. Kaiser, P. Hughes, C. Dodd, C. R. Connel, C. Heiner, S. B. H. Kent, L. E. Hood, *Nature (London)* **321**, 674 (1986).
13. W. Ansorge, B. S. Sproat, J. Stegemann, C. Schwager, *J. Biochem. Biophys. Methods* **13**, 315 (1986).
14. W. Ansorge, B. Sproat, J. Stegeman, C. Schwager, M. Zenke, *Nucleic Acids Res.* **15**, 4593 (1987).
15. R. M. K. Dale, D. C. Livingston, D. C. Ward, *Proc. Natl. Acad. Sci. U.S.A.* **70**, 2238 (1973).
16. P. R. Langer, A. A. Waldrop, and D. C. Ward, *ibid.* **78**, 6633 (1981).
17. N. L. Brown, *Methods Microbiol.* **17**, 259 (1984); N. S. Ambartsumyan and A. M. Mazo, *FEBS Lett.* **114**, 265 (1980); S. Mizusawa *et al.*, *Nucleic Acids Res.* **14**, 1319 (1986).
18. C. Connell *et al.*, *Biotechniques* **5**, 342 (1987).

19. We thank E. R. Adams, J. B. Clemens, D. E. Cope, G. C. Emmett, and R. K. Martin for technical assistance and our colleagues for support that made this research program possible. We especially acknowledge the encouragement provided by M. L. Pearson, F. F. Huppe, and C. T. Sciance.

4 September 1987; accepted 25 September 1987

Electrophoresis, 1992, 13, 18-31

Suraphol Nathakarnkitkool[1]
Peter J. Oefner[2]
Georg Bartsch[2]
Michael A. Chin[3]
Günther K. Bonn[4]

[1]Institute of Radiochemistry, University of Innsbruck
[2]Department of Urology, University of Innsbruck
[3]Applied Biosystems, San Jose, CA
[4]Department of Analytical Chemistry, University of Linz

High-resolution capillary electrophoretic analysis of DNA in free solution

Capillary electrophoretic separations of double-stranded DNA fragments in the size range of 20–2200 base pairs were achieved in less than 20 min with the use of a Tris-borate buffer containing hydroxyethylcellulose. Analyses were carried out in both uncoated and phenylmethyl-coated capillaries of fused silica with internal diameters of 50 and 100 μm, respectively, and an effective column length of 50 cm. The addition of ethidium bromide resulted in an improved resolution of double-stranded DNA fragments, thereby permitting even the separation of fragments differing only 1–2 base pairs in length. Moreover, resolution was found to be linearly proportional to the size of the cation used to adjust ionic strength $Cs^+ > Rb^+ > K^+ > Na^+ > Li^+$. However, the analysis times also increased with increasing cation size due to a decrease in electroosmotic flow. Elution order was verified by spiking restriction digests with slab gel electrophoretically purified components. Subsequently, the described system was applied to the detection and quantitation of an mRNA transcript of the androgen receptor, which had been amplified by polymerase chain reaction and purified by size-exclusion chromatography to avoid peak broadening due to conductivity differences between sample and running buffer. Since the actual amount of DNA introduced into the capillary cannot be defined, molar ratio – peak area ratios of the polymerase chain reaction product to various restriction fragments of known concentration were used to determine the amount of amplified DNA. The coefficient of variation was as small as 3.4 % and the results were in good agreement with a spectrophotometric assay.

1 Introduction

Restriction enzyme mapping and polymerase chain reaction, which is a new and powerful method for the rapid exponential amplification of specific DNA segments, have gained tremendous popularity in molecular biology [1–3] and clinical diagnostics [4–7]. The standard method for separating DNA fragments is electrophoresis in polyacrylamide and agarose gels [8]. Despite impressive advances, modern electrophoresis is still, for the most part, a collection of manually intensive methodologies that cannot be run unattended and that are prone to irreproducibility and poor quantitative accuracy. The use of capillaries as the migration channel in electrophoresis holds the promise of putting electrophoretic separations on the same instrumental footing as high-performance liquid chromatography. Compared with open-bed gel electrophoresis, capillary columns offer several advantages, including higher resolution, improved reproducibility, minute sample requirements, reduced analysis time, and increased sensitivity, as well as the ability to use greater potential fields and to perform on-line sample detection without the need for staining procedures [9–13].

Recently, Karger and co-workers [14, 15] described the use of low- or zero-crosslinked polyacrylamide-filled capillaries for the separation of DNA restriction fragments up to 12 000 base pairs in length within 18 min. The anticonvective properties of the narrow capillaries permitted the application of high electric fields and the realization of up to five million theoretical plates per meter. This allowed the resolution of DNA fragments that differed by only 10 base pairs, if their overall length was not larger than approximately 500 base pairs. However, gel-filled capillaries are difficult to prepare and, due to the destruction of the gel matrix at high current densities, resolving power cannot be maintained for long periods of time. And since sample can only be injected electrokinetically, it is not possible to deliver the same amount of each DNA species. Therefore, several investigators have explored the feasibility of separating DNA fragments in free solution using micellar buffer systems containing either cetyltrimethylammonium bromide [16], which also serves as an ion-pairing reagent, or sodium dodecyl sulfate [17]. Zhu and co-workers [18] used linear polymers such as hydroxypropylmethylcellulose and methylcellulose, which generate a molecular sieving effect. Recently, a more hydrophilic cellulose derivative [19, 20] was introduced, allowing the size-dependent separation of DNA fragments in fused silica capillaries within 20 min. In all instances, however, the resolving power was not as high as that achieved with gel-filled capillaries.

The present study investigates the use of hydroxyethylcellulose (HEC) as a sieving medium for the separation of double-stranded DNA fragments in free solution. Moreover, the impact of several parameters such as capillary surface charge, ethidium bromide concentration, pH, and ionic content on electroendosmosis as well as electrophoretic mobility and resolution of DNA fragments will be evaluated. Finally, the application of capillary electrophoresis to the quantitative analysis of polymerase chain reaction (PCR) products is reported.

Correspondence: Dr. Peter Oefner, Department of Urology, University of Innsbruck, Anichstr. 35, A-6020 Innsbruck, Austria

Abbreviations: bp, base pair; HEC, hydroxyethylcellulose; PBS, phosphate-buffered saline; PCR, polymerase chain reaction; TE, Tris-EDTA; Tris, Tris(hydroxymethyl)aminomethane

0173-0835/92/0102-0018 $3.50+.25

2 Materials and methods

2.1 Instrumentation

Analyses were carried out on an Applied Biosystems (ABI, San Jose, CA, USA) Model 270A capillary electrophoresis system equipped with either a 720-mm fused silica capillary of I.D. 50 µm (Cat. No. 0602-0014, ABI) or a 720-mm phenylmethyl siloxane deactivated fused silica tubing of I.D. 100 µm (Cat. No. 10041, Restek Corporation, Bellefonte, PA, USA). Nucleic acids were detected by means of an on-column UV-monitor at 260 nm. The electropherograms were acquired on a Chromatopac Model C-R6A integrator (Shimadzu, Kyoto, Japan). Flushing of capillary was performed by the built-in vacuum system at a pressure of 67.7 kPa, while the vacuum for injection was adjusted to 16.9 kPa.

2.2 Sample and reagents

2.2.1 Chemicals

HEC (viscosity of a 2% aqueous solution 0.3 Pa·s) was purchased from Serva (Cat. No. 25236, Heidelberg, Germany). Tris and boric acid of electrophoretic purity were obtained from Bio-Rad (Richmond, CA, USA). Ethidium bromide, EDTA and alkali salts were purchased from Sigma (Deisenhofen, Germany). Mesityl oxide was obtained from Merck (Cat. No. 805791, Darmstadt, Germany). Buffer solutions were filtered through a 0.2 µm pore size filter (Schleicher and Schuell, Keene, NH, USA).

2.2.2 Oligonucleotide primers

Oligonucleotide primers were synthesized using phosphoramidite chemistry on an Applied Biosystems DNA Synthesizer (Model 381 A). After their purification by means of oligonucleotide purification cartridges (Cat. No. 400771, ABI), they were stored as lyophilizates or dissolved in Tris-EDTA (TE) buffer (10 mM Tris·HCl, 1 mM EDTA, pH 8.0), aliquoted and frozen at −80°C. The following gene-specific primers were used for PCR amplification: AR 2113/19, 5'-AGCTACTCCGGACCTTACG; AR 2474/22, 5'-GTGGTGCTGGAAGCCTCTCCTT; AR 3294/21, 5'-AAGGTGTGGGTCACTTCGTAA.

2.2.3 DNA size standards

Size standards of double-stranded DNA were purchased from Bio-Rad (pBR322 DNA-*Ava* II/*Eco*RI digest), Boehringer Mannheim (pBR322 DNA-*Hae*III digest and pBR328 DNA-*Bgl*I/*Hin*fI digest, Boehringer Mannheim, Mannheim, Germany), Pharmacia (ϕX-174 RF DNA-*Hae*III digest, Pharmacia, Uppsala, Sweden), and USB (ϕX-174 DNA-*Hin*cII digest, United States Biochemical, Cleveland, OH, USA).

2.3 Procedures

2.3.1 Tissue culture

Fibroblast strains were established from specimens of preputial and scrotal skin obtained surgically. The tissue was chopped finely, the pieces were seeded into cell culture flasks (25 cm² surface, Costar, Cambridge, MA, USA) and covered with a thin film of Dulbecco's modification of Eagle's minimum essential medium (Boehringer Mannheim), such that surface tension held them in place until they adhered spontaneously to the surface. The medium was supplemented with 20% fetal calf serum, penicillin (250 units/mL), streptomycin (250 µg/mL), kanamycin (50 µg/mL), and amphotericin B (2.5 µg/mL). The cells were incubated at 37°C in a humid environment with a 95:5% air-to-carbon dioxide ratio. The medium volume was made up to 5 mL on the next day and changed weekly until outgrowth of fibroblasts was observed. The cells were then detached in 0.05% trypsin-0.02% EDTA in phosphate-buffered saline (PBS) and passed serially into larger flasks (150 cm², Costar) and grown in Dulbecco's modification of Eagle's minimum essential medium supplemented with 10% fetal calf serum.

2.3.2 Isolation of mRNA

mRNA was isolated by means of a commercial mRNA isolation kit (Invitrogen, San Diego, CA, USA). Briefly, six to eight large flasks of confluent fibroblasts were washed with PBS before cells were lysed in 15 mL of lysis buffer. Then the lysate was passed several times through a 10 mL sterile plastic syringe fitted with a 22-gauge needle to shear high-molecular weight DNA. After incubation at 45°C for 2 h, the sodium chloride concentration of the lysate was adjusted to 0.5 M. Then the lysate was added to approximately 60 mg of preequilibrated oligo (dT) cellulose and rocked gently at room temperature for another 60 min. The cellulose was then pelleted at 1000 × g for 3 min, rinsed twice with 10 mL of binding buffer, transferred to a disposable polypropylene column (Cat. No. 731-1550, Bio-Rad) and spun with binding buffer until the $O.D._{260}$ of the eluate was less than 0.05. Finally, mRNA was eluted with elution buffer and precipitated with 0.1 volume of 2 M sodium acetate and 1 volume of isopropanol. The sample was mixed thoroughly, incubated at −30°C for 1 h and spun at 16000 × g for 30 min. The pellet was rinsed twice with 75% ethanol, dried under vacuum and, finally, resuspended in 2 µL of TE buffer.

2.3.3 Synthesis of cDNA

First-strand synthesis of cDNA was accomplished in a 0.6 mL Eppendorf tube by adding 1–2 µg of mRNA to a total volume of 50 µL of 50 mM Tris·HCl (pH 8.3), 75 mM KCl, 3 mM $MgCl_2$, 10 mM dithiothreitol, 50 U ribonuclease inhibitor, 3.3 µg of random hexamers, 0.5 mM deoxynucleotide triphosphates (dNTPs), and 500 U Moloney murine leukemia virus reverse transcriptase (Cat. No. 71053, USB). The reaction mixture was incubated at 37°C for 1 h.

2.3.4 PCR

PCR was performed in a 1.5 mL microcentrifuge tube by adding 2 µL of cDNA to a total volume of 100 µL of 10 mM Tris·HCl (pH 9.0, 25°C), 50 mM KCl, 1.5 mM $MgCl_2$, 0.2 mM dNTPs, 0.1 mg/mL gelatin, 0.1% Triton X-100, 0.5 µM of each oligonucleotide primer, and 2.5 U Taq polymerase (Cat. No. M1861, Promega, Madison, WI, USA). To prevent evaporation, the reaction mixture was sealed with 50 µL of

mineral oil (Cat. No. M5904, Sigma). Thirty cycles of amplification were carried out in a thermocycler (BioMed, Theres, Germany) with a 95 °C denaturation step for 25 s, a 57 °C annealing step for 30 s, and a 73 °C extension step for 60 s. The very first denaturation step was elongated for 2 min, and the last synthesis step for 3 min to ensure completion of the final extension step. Beginning at cycle 16 each following DNA synthesis step was elongated for 5 s. Finally, samples were cooled to room temperature.

2.3.5 Purification of PCR products

PCR products were purified by means of size-exclusion chromatography. Briefly, 0.7 mL of Sephadex G-150 (Cat. No. 17-0070-01, Pharmacia) slurry were filled into a 1 mL syringe and washed two times with TE buffer. Then, 50–70 µL of PCR sample were applied to the top of the gel bed. The column was centrifuged in a swinging bucket at 1100 × *g* for 4 min. This procedure was repeated a second time with 75 µL of TE buffer. The eluted DNA was then precipitated with 0.1 volume of 3 M sodium acetate, pH 5.0, and 1 volume of isopropanol, stored at −30 °C for 1 h, and centrifuged at 16000 × *g* for 30 min. The supernatant was discarded and the pellet was rinsed twice with 75% ethanol, dried under vacuum and usually resuspended in 10 µL of TE buffer prior to analysis.

2.3.6 Restriction endonuclease digestion

A PCR-amplified segment of the androgen receptor was digested with the restriction endonucleases *Eco*RI, *Hpa*II and *Hin*fI (Promega) using the buffers and conditions suggested by the supplier.

2.3.7 Agarose electrophoresis

Ten µL of each PCR sample or restriction digest were separated in a 2% agarose gel (low-melting agarose, Cat. No. 32829, USB) in TBE buffer (90 mM Tris-borate, 1 mM EDTA, pH 8.3). Separations were carried out in a small horizontal agarose submarine unit (Hoefer, San Francisco, CA, USA) at a constant voltage of 80 V. The position of DNA fragments was determined by staining one of the lanes in a solution of 0.5 µg/mL ethidium bromide in TBE buffer. Individual restriction fragments were then isolated by excision from the agarose gel, immersion in liquid nitrogen, and centrifugation at 20000 × *g* for 15 min at 4 °C. The supernatant was transferred to an Eppendorf tube. The pellet was resuspended in 100 µL of TE buffer, immersed in liquid nitrogen, and centrifuged. The supernatants were combined and purified by means of Sephadex G-150 size-exclusion chromatography.

2.3.8 Capillary conditioning

A new fused-silica capillary was flushed with 1 M NaOH for 1 h followed with 0.001 M NaOH for 5 min. Between runs, the capillary was washed first with 1 M NaOH for 2 min, and then with 0.001 M NaOH for 1 min. Finally, it was equilibrated with running buffer until the baseline remained stable. The capillary was stored in 0.001 M NaOH overnight. Phenylmethyl-coated capillaries were flushed with bidistilled water only.

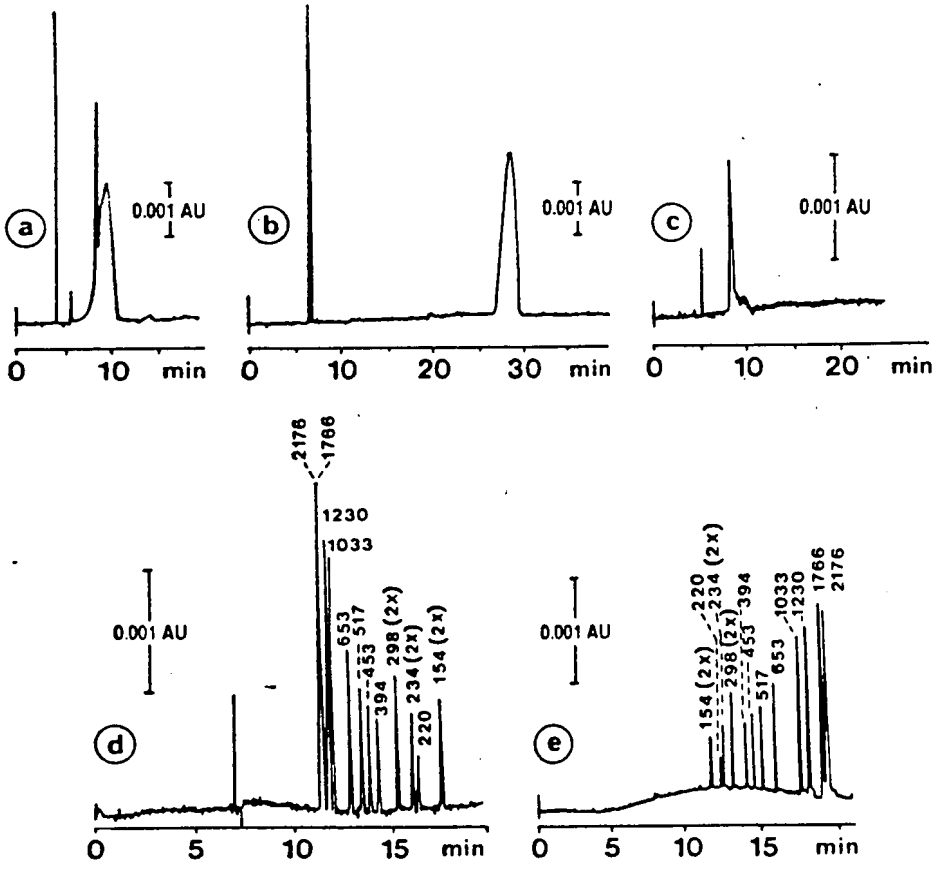

Figure 1. Influence of buffer composition on the separation of a pBR328 DNA-*Bgl*I/*Hin*fI digest (0.25 µg/µL). Buffers: (a) 0.01 M Tris-borate, pH 8.7, 0.1 mM EDTA, (b) 0.01 M Tris-borate, pH 8.7, 0.1 mM EDTA, 25 mM NaCl, (c) 0.01 M Tris-borate, pH 8.7, 0.1 mM EDTA, 0.5% w/v HEC, (d) 0.01 M Tris-borate, pH 8.7, 0.1 mM EDTA, 25 mM NaCl, 0.5% w/v HEC, (e) 0.01 M Tris-borate, pH 8.7, 0.1 mM EDTA, 25 mM NaCl, 0.5% w/v HEC, column: (a)–(d) fused silica 720 × 0.050 mm I.D., effective length 500 mm, (e) phenylmethyl-coated capillary 720 × 0.10 mm I.D., effective length 500 mm; injection: vacuum, (a)–(d) 5 s, (e) 0.5 s; voltage: (a)–(d) + 15 kV, (e) −14 kV; current: (a)–(d) 10 µA, (e) 48 µA; detection: UV, 260 nm; temperature: 35 °C.

3 Results and discussion

3.1 Separation of DNA fragments in free solution

Figure 1 shows the impact of buffer composition on the separation of a pBR328 DNA-*BglI*/*HinfI* digest in a fused silica capillary of an internal diameter of 50 μm using a Tris-borate buffer adjusted to pH 8.7. Tris-borate is preferred to Tris-phosphate because borate complexation with the sugar moieties of nucleic acids has been reported to yield higher resolving power [17]. EDTA was added to protect DNA from nuclease digestion. At the selected pH value, ionization of the surface silanol groups of fused silica capillaries induces the formation of a mobile layer of positive charge in the buffer adjacent to the wall. When an electric field is applied, these mobile charges migrate toward the cathode, entraining a bulk flow of fluid in the same direction. Under alkaline conditions, DNA will migrate upstream against electroosmotic flow due to its negative charge. However, electroendosmosis, with its greater velocity in the opposite direction, causes all DNA to be swept past the detector. Since nucleic acids over twenty base pairs in length have essentially the same charge-to-mass ratio [21], DNA fragments cannot be separated according to differences in electrophoretic mobility alone in free solution (Fig. 1a). Even a decrease in electroosmotic flow caused by the addition of 25 mM of sodium chloride will not allow the separation of the fragments (Fig. 1b). It has been shown that separation of nucleic acids can be achieved by means of various sieving media such as agarose, polyacrylamide, or cellulose derivatives [22]. However, the addition of hydroxyethylcellulose to the Tris-borate buffer did not result in resolution of the restriction fragments because of the overwhelming electroosmotic flow (Fig. 1c). Only upon reduction of electroosmotic flow by the addition of 25 mM of sodium chloride was the successful separation of nucleic acids accomplished (Fig. 1d). Furthermore, in comparison to phosphate buffer, Tris-borate was found to allow better separation of smaller linear DNA fragments ranging from approximately 100–200 bp in length. This effect seems to be related to the use of HEC as a sieving agent, in accordance with various reports on agarose gel electrophoresis of DNA molecules [23–25] describing that the interaction between borate and hydroxyethylated agarose causes an increase in sieving power due to an increase in the apparent agarose bundle radius and a decrease in the inter-fiber spacing. The electropherograms also indicate that apparent mobility of a DNA fragment depends on its length. In an uncoated capillary the largest fragment is detected first since it is less able to migrate upstream through the cellulose derivative. The smallest fragment is detected last due to its greater upstream migration rate. This was verified by spiking a commercial DNA digest with a 154-bp and a 653-bp fragment, which had been isolated from an agarose gel and further purified by size-exclusion chromatography. Electroendosmosis, however, is no prerequisite for the successful separation of DNA fragments. This was corroborated by the analysis of a pBR328 DNA-*BGI*/*HinfI* digest in a phenylmethyl-deactivated fused silica capillary (Fig. 1e). Since the coating depresses electroendosmosis, polarity has to be reversed in order to allow the detection of DNA fragments, which are now separated solely because of differences in solute mobility caused by the sieving effect of HEC.

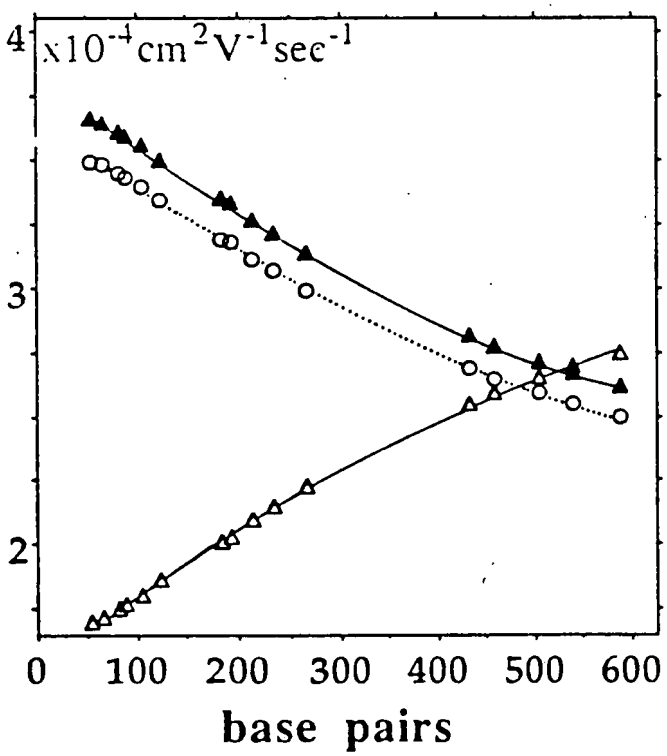

Figure 2. Electrophoretic mobilities (▲,○) and apparent mobilities (△,○) of DNA restriction fragments in a fused silica capillary (– –) and a phenylmethyl-coated capillary (. . . .). Buffer: 0.01 M Tris-borate, pH 8.7, 0.1 mM EDTA, 25 mM NaCl, 0.5% w/v HEC; sample: pBR322 DNA-*HaeIII* (0.25 μg/μL); voltage: −15 kV. Other conditions as in Fig. 1.

Figure 2 illustrates that true electrophoretic mobilities of DNA fragments are identical in both coated and uncoated capillaries. Calculation of true electrophoretic mobility, μ_e, is based on the migration time of the solute and the hold-up time of the neutral marker

$$\mu_e = (L1/V)\ (1/t_m - 1/t_{eo}) \quad (1)$$

where L is the total capillary length (cm), l the capillary length to the detector (cm), V the applied voltage (V), t_m the solute migration time (s), and t_{eo} the hold-up time of the electroosmotic flow-marker mesityl oxide (s). The small difference in true electrophoretic mobility, which can be seen, may be due to incomplete deactivation of fused silica, which causes electroosmotic flow and, hence, reduced solute mobility. But with polarity reversed, electroendosmosis is difficult to measure because the neutral marker will be carried away from the detector. The apparent mobility of a DNA fragment in an uncoated capillary not only depends on its electrophoretic mobility but also on electroosmotic flow. Since it is greater than the size-dependent upstream DNA migration rate, it will cause the smaller fragments to pass the detector later than the largest fragments, which are least able to migrate through the sieving medium against the electroosmotic flow. Therefore, apparent mobility, μ_{app}, is given as the following equation

$$\mu_{app} = \mu_{eo} + \mu_e \quad (2)$$

where μ_{eo} is the mobility of the electroosmotic flow ($\mu_{eo} = 5.36 \cdot 10^{-4}$ cm²/Vs).

The mobility plot might also provide accurate molecular weight determinations for DNA fragments, regardless of the source. This was demonstrated by an experiment in which three unrelated restriction digests were coinjected and separated in a single run. All three sets of restriction fragments nested perfectly and migrated precisely in the order of their known lengths. Checking the reproducibility of electrophoretic mobilities by six repeated determinations, for which the restriction fragments of the ϕX-174 RF DNA-*Hae*III digest were used, a coefficient of variation better than 0.75% was obtained (Table 1). Since the mobility curve has a different slope at each point, uncertainties in the electrophoretic mobilities correspond to an uncertainty in fragment length, which depends upon fragment size. This relationship is shown in the last column of Table 1, which pertains to fragment length values derived from comparisons between runs. As with slab gels, the sizes of small fragments can be measured with the most accuracy. Estimation of fragment length will be more precise if fragment length values are derived from comparisons with internal standards.

3.2 Optimization of operational parameters

3.2.1 Capillary conditioning

The physical and chemical states of the inner capillary surface exert a major impact on electroosmotic flow [26]. Therefore, capillaries of fused silica must be prepared for use prior to any analytical runs by washing for at least 30 min with 1 M NaOH to remove any adsorbed impurities or traces of old sample and to ensure maximum ionization of silanol groups. Following a flush with 0.001 M NaOH, the capillary has to be equilibrated with the running buffer until the baseline remains stable. This procedure was also repeated between runs whenever there was loss of reproducibility or a change in buffer composition. Otherwise, capillaries were flushed first with 1 M NaOH for 2 min, then with 0.001 M NaOH for 1 min. The 2-min rinse with 1 M NaOH was shown to yield optimum resolution, whereas shorter or longer washing periods resulted in lower separation efficiency. The dilute sodium hydroxide flush was preferred to water, which exerted a deteriorating effect on resolution due to reprotonation of the charged silanols on the inner capillary wall. Moreover, it is recommended to replace the cathode reservoir during the sodium hydroxide wash, thereby avoiding a loss of reproducibility and resolution due to a change in buffer composition. Taking these precautions, it suffices to renew the buffer in both reservoirs every 3–4 runs.

Table 1. Reproducibility of electrophoretic mobilities

bp	$cm^2/V.s$ ($\times 10^{-4}$)	SD	CV	SD (bp)
1358	2.310	0.013	0.583	–
1078	2.347	0.015	0.619	67
872	2.402	0.013	0.552	36
603	2.555	0.015	0.590	16
310	2.992	0.019	0.635	6
281	3.078	0.019	0.604	6
271	3.105	0.022	0.707	7
234	3.224	0.022	0.694	7
194	3.351	0.025	0.736	7
118	3.650	0.025	0.682	6
72	3.848	0.024	0.636	–

Phenylmethyl-deactivated fused silica capillaries did not require any conditioning except for short flushes with bidistilled water. The minor peak tailing seen in Fig. 1e might indicate some adsorption of DNA molecules due to hydrophobic interaction. However, it did not have a significant effect on separation efficiency since theoretical plates in excess of 4×10^6 per meter could be realized. Perhaps a more hydrophilic coating, such as the one introduced by Hjertén [27], would eliminate all electrostatic and hydrophobic interactions and remain stable for a longer time.

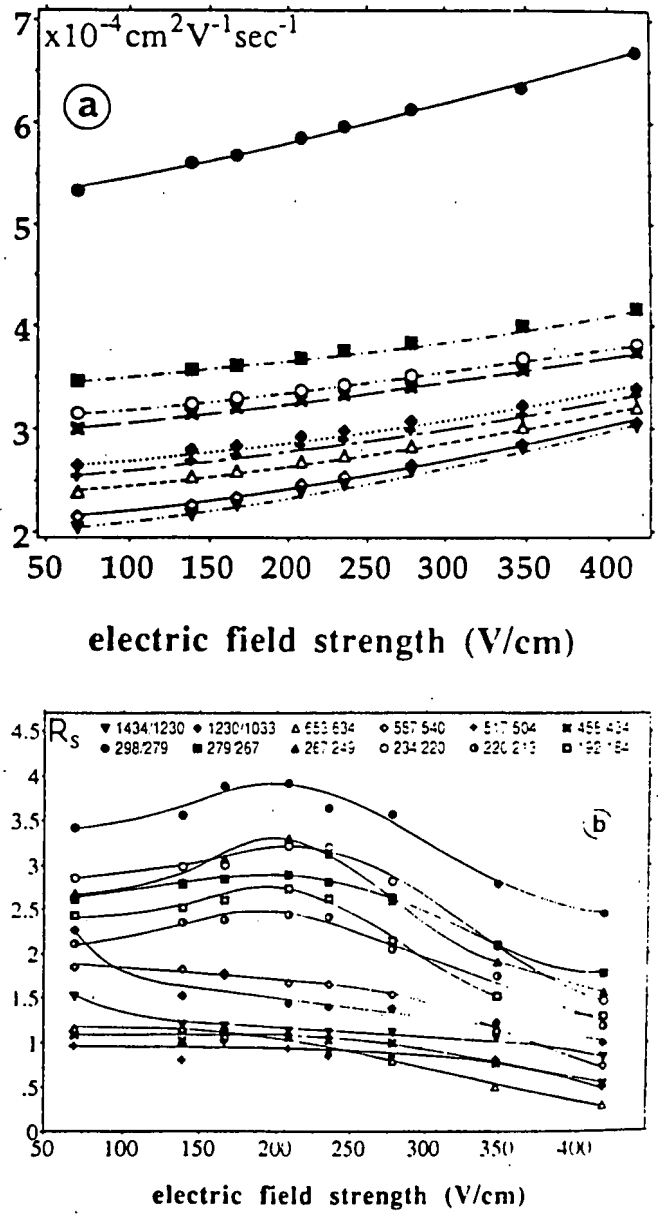

Figure 3. Impact of electric field strength (E) on (a) electroosmotic flow (●) and electrophoretic mobilities as well as (b) resolution (R_s) of DNA restriction fragments: (■) 104 bp, (○) 184 bp, (▽) 213 bp, (◆) 303 bp, (○) 391 bp, (△) 504 bp, (◇) 800 bp, (▼) 1033 bp. Buffer: 0.01 M Tris-borate, pH 8.3, 0.1 mM EDTA, 25 mM NaCl, 1.27 μM ethidium bromide, 0.5% w/v HEC; sample: a mixture of pBR322 DNA-*Aval*I/*EcoR*I (0.2 μg/μL), pBR322 DNA-*Hae*III (0.25 μg/μL) and pBR328 DNA-*Bcl*I/*Hin*dIII (0.25 μg/μL) digests at a ratio 1:2:2; column: fused silica 720 × 0.050 mm I.D., effective length 500 mm; injection: vacuum, 8 s; voltage: 5–30 kV; detection: UV, 260 nm; temperature: 35°C.

3.2.2 Electric field strength

An increase in applied voltage is known to result in a shorter analysis time and higher separation efficiency [28]. Figure 3a shows the impact of the applied electric field on electroosmotic flow and the mobility of DNA fragments ranging in size from 104 to 1033 base pairs. As expected, a nonlinear relationship between electric field strength and electroosmotic flow, as well as true electrophoretic mobilities, is observed [29–31]. However, the more upward curvature in mobility exhibited by the larger DNA molecules results in faster migration of the larger species than the smaller ones and, hence, in a loss of selectivity. This behavior is consistent with known field effects on mobility of DNA molecules in slab gels [32].

Figure 3b depicts the resolution of adjacent pairs of DNA restriction fragments as a function of electric field strength. Since the number of theoretical plates is known to be proportional to the applied voltage [28], resolution was enhanced up to an electric field strength of approximately 200 V/cm. At higher electric field strengths, resolution decreased as a result of increased Joule heat.

3.2.3 Cellulose concentration

Cellulose derivatives have been used as anion exchangers for the separation of DNA fragments in chromatography [33]. In the present study, a hydrophilic cellulose derivative was chosen to generate a molecular sieving effect. Figure 4 shows the impact of cellulose concentration on electroosmotic flow and electrophoretic mobilities of DNA fragments in a 50 µm fused silica capillary. It is evident that the increase in apparent mobilities with increasing cellulose concentration results from the indirectly proportional decrease in solute mobilities, whereas electroosmotic flow is reduced only slightly. Since an increase in temperature will result in decreased viscosity of cellulose and, hence, in an indirectly proportional increase in both electroosmotic flow and electrophoretic mobility, it is important to keep the temperature constant in order to ensure a high degree of reproducibility [34].

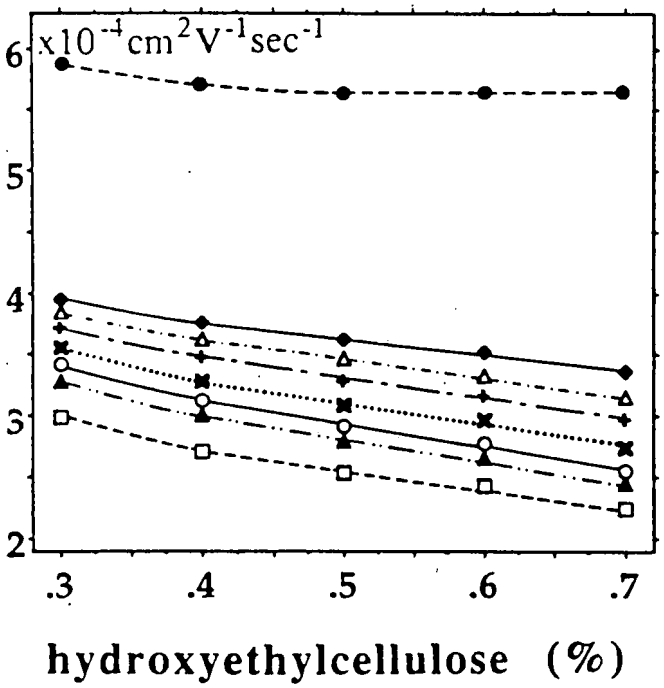

Figure 4. Effect of HEC concentration on electroosmotic flow (▼) and electrophoretic mobilities of DNA restriction fragments: (◆) 154 bp, (△) 220 bp, (+) 298 bp, (✕) 394 bp, (=) 517 bp, (▲) 653 bp, (□) 1230 bp. Buffer: 0.01 M Tris-borate, pH 8.7, 0.1 mM EDTA, 25 mM NaCl, 0.3–0.7% w/v HEC; sample: pBR328 DNA-*Bgl*I/*Hin*fI digest, 0.25 µg/µL; column: fused silica 720 × 0.050 mm I.D., effective length 500 mm; injection: vacuum, 5 s; voltage: 15 kV; current: 16 µA; detection: UV, 260 nm; temperature: 35°C.

3.2.4 pH of the buffer

At low pH, ionization of silanol groups of the inner capillary surface is suppressed and electroosmotic flow approaches zero. At neutral and alkaline pH, the silanol groups are deprotonated to yield a negatively charged surface, which induces electroosmotic flow upon the application of an electric field. Upon complete deprotonization, electroosmotic flow reaches a plateau [29]. Under the present conditions, electroosmotic flow increased from pH 8.0 to 9.5, whereas electrophoretic mobility of DNA fragments was not affected. Therefore, the increase in electroosmotic flow resulted in a decrease of migration time for a DNA fragment (154 base pairs in length) from 61 min at pH 8.0 to 14 min at pH 9.5. However, pH values higher than 9.0 caused only a comparatively small reduction in apparent mobility, and since resolution decreased, a pH value of 8.75 was found to offer optimum resolution within the shortest time of analysis. At a pH value of approximately 7.5, electroosmotic flow became too small to sweep the DNA fragments past the detector.

3.2.5 Ionic strength

A nonbuffering salt, such as sodium chloride, is added to the buffer medium to increase ionic strength. Figure 5a shows the effect of ionic strength on electroosmotic flow as well as electrophoretic mobilities of various DNA size standards at a constant voltage of 15 kV. Under these conditions, current increases linearly with increasing salt concentration. It can be seen that migration time decreased as salt concentration increased; this is because the addition of sodium chloride reduces electroosmotic flow by increasing the thickness of the diffusion double layer at the inner capillary wall, which is a function of the number of valence electrons and the concentration of the electrolyte in water [30]. The addition of sodium chloride to the buffer system, however, also alters the mobility of DNA fragments in a variety of ways, which affect charge, shape, and size. DNA molecules in aqueous solutions are charged highly negatively and produce strong electric field gradients that cause accumulation of small counterions in their vicinity. These interactions have considerable influence on the conformation of DNA. ^{23}Na-NMR studies have shown that DNA in dilute solutions is surrounded by a layer of counterions that are condensed near the polyion surface and that form a double helix external to the cylindrical volume determined by the phosphate groups [35]. Under conditions that are equivalent to the fully hydrated B-DNA, the sodium ions are found to be bridged by water molecules, forming a hydrated bound pair, which also forms a bridge between the phosphate group and the guanine N7, which is another sub-

stantial negative component of the electric field [36]. The ratio of bound counterions to DNA phosphates is estimated to be in the range of 0.5–0.8, with a rapid exchange of sodium ions between free and bound subpopulations. The sodium ion correlation times estimated for dilute DNA solutions are of the order of 2–5 ns [37]. Therefore, it is not surprising that an increase in the concentration of sodium ions in the running buffer causes an increase in the ratio of bound counterions to DNA and, subsequently, a decrease in true electrophoretic mobility. The improved resolution of DNA fragments, which can be observed when the sodium chloride concentration is increased from 20 to 25 mM (Fig. 5b), is a result of the spread in electrophoretic mobilities between the largest and the smallest DNA fragment (Fig. 5a). Thereafter, no further increase in selectivity is observed. Hence, the slight and linear improvement in resolution seen at even higher concentrations of sodium chloride in the running buffer may be due to the increase in current density, which is known to cause a proportional increase in the number of theoretical plates [9].

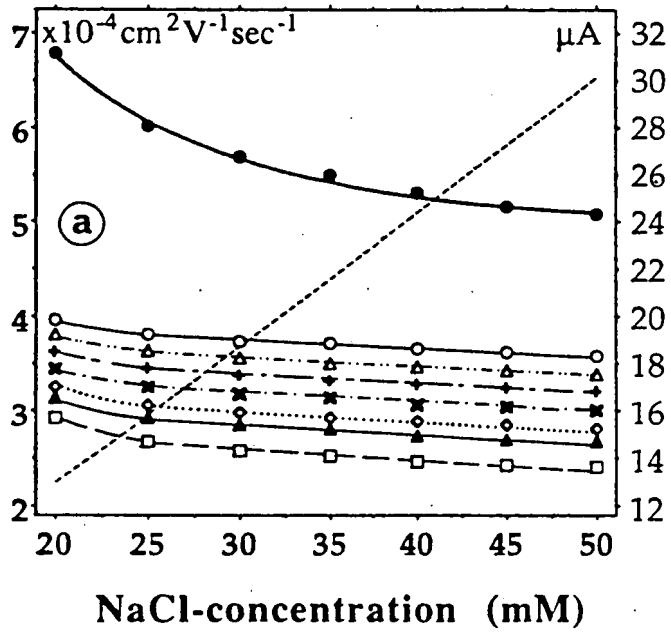

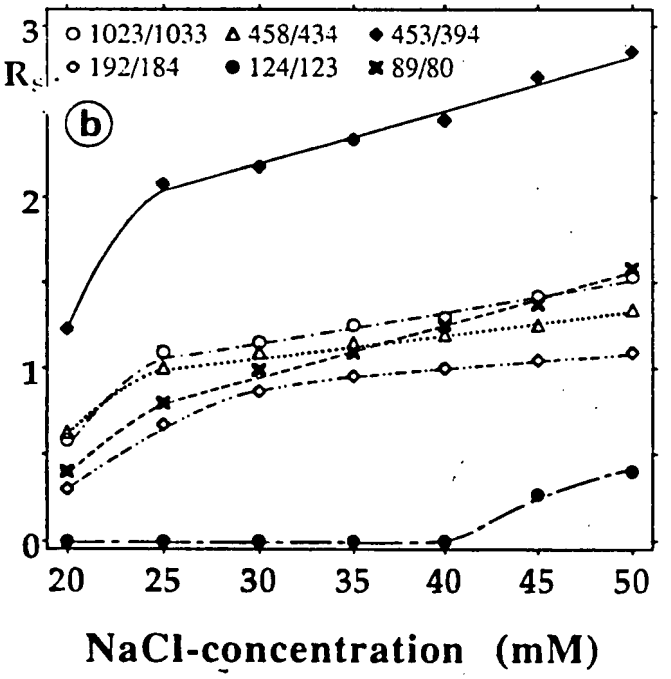

Figure 5. Impact of sodium chloride concentration on (a) current (- - -), electroosmotic flow (●) and electrophoretic mobilities as well as (b) resolution (R_s) of DNA restriction fragments: (○) 154 bp, (△) 220 bp, (+) 298 bp, (✕) 394 bp, (◇) 517 bp, (▲) 653 bp, (□) 1230 bp. Buffer: 0.01 M Tris-borate, pH 8.7, 0.1 mM EDTA, 5–50 mM NaCl, 0.5% w/v HEC. Other conditions as in Fig. 4.

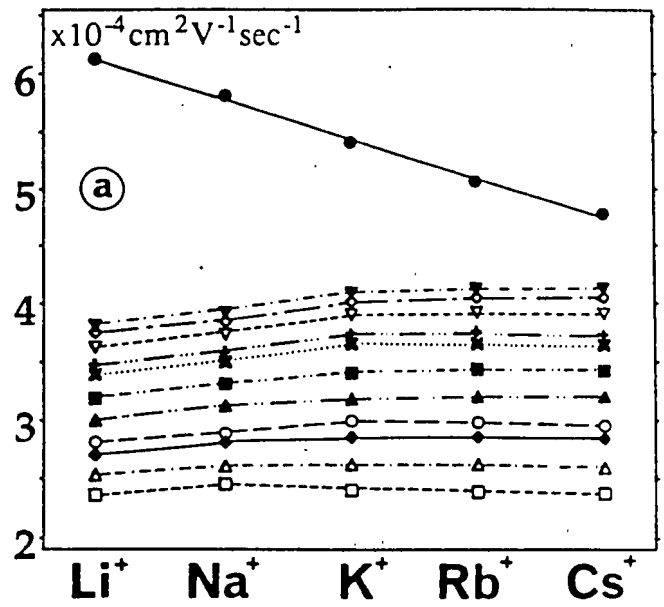

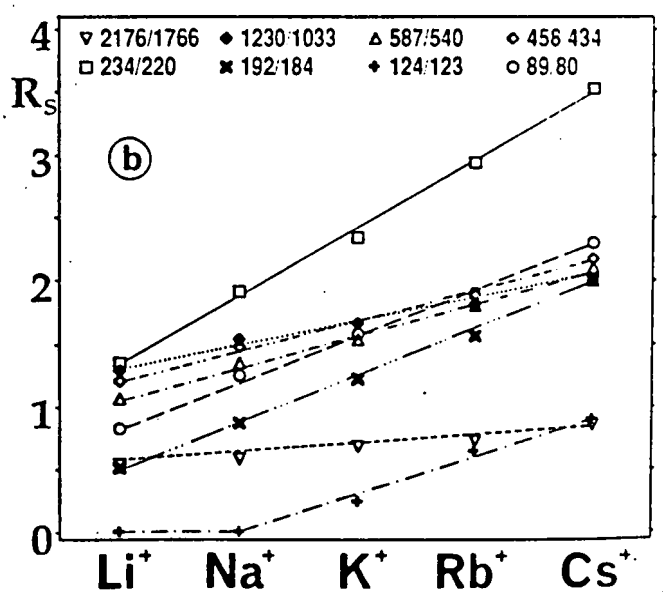

Figure 6. Influence of various cations on (a) electroosmotic flow (●) and electrophoretic mobilities as well as (b) resolution (R_s) of DNA restriction fragments: (▼) 51 bp, (◇) 80 bp, (▽) 124 bp, (+) 184 bp, (✕) 213 bp, (■) 298 bp, (▲) 394 bp, (○) 540 bp, (●) 653 bp, (△) 1033 bp, (□) 2176 bp. Buffer: 0.01 M Tris-borate, pH 8.7, 0.1 mM EDTA, 0.5% w/v HEC, 25 mM of LiCl, NaCl, KCl, RbCl, and CsCl, respectively; sample: pB322 DNA-*Hae*III and pBR328 DNA-*Bgl*I/*Hin*fI digests, 0.25 μg/μL each; injection: vacuum, 5 s; voltage: 17, 15, 13, 12 and 12 kV, respectively; current: 16 μA. Other conditions as in Fig. 4.

The influence of various alkali ions, namely lithium, sodium, potassium, rubidium, and cesium, on electroosmotic flow as well as electrophoretic mobility of DNA restriction fragments is depicted in Fig. 6a. The results show that as the cation size increased the migration times increased. This is mainly due to the decrease in zeta potential, which causes lower electroosmotic flow [38]. The zeta potential is linearly proportional to the charge density, which decreases as the atomic weight of the cation increases [39]. Another observation is that the spread in electrophoretic mobilities between the largest and the smallest fragments increased considerably when lithium or sodium chloride were replaced with potassium chloride. While cesium chloride gave the best separation of DNA fragments, the migration times were five times longer than when lithium chloride was used. Generally, an increase in resolution of all fragments was realized with an increase in the size of the cation (Fig. 6b), but the concomitant increase in migration times might be unacceptable in routine analysis.

3.2.6 Addition of ethidium bromide

Figure 7a shows the analysis of a complex mixture of restriction digests obtained with the use of a Tris-borate buffer containing 25 mM NaCl and 0.5% hydroxyethylcellulose. Upon addition of 1.27 μM of ethidium bromide to the running buffer, a major improvement in resolution can be

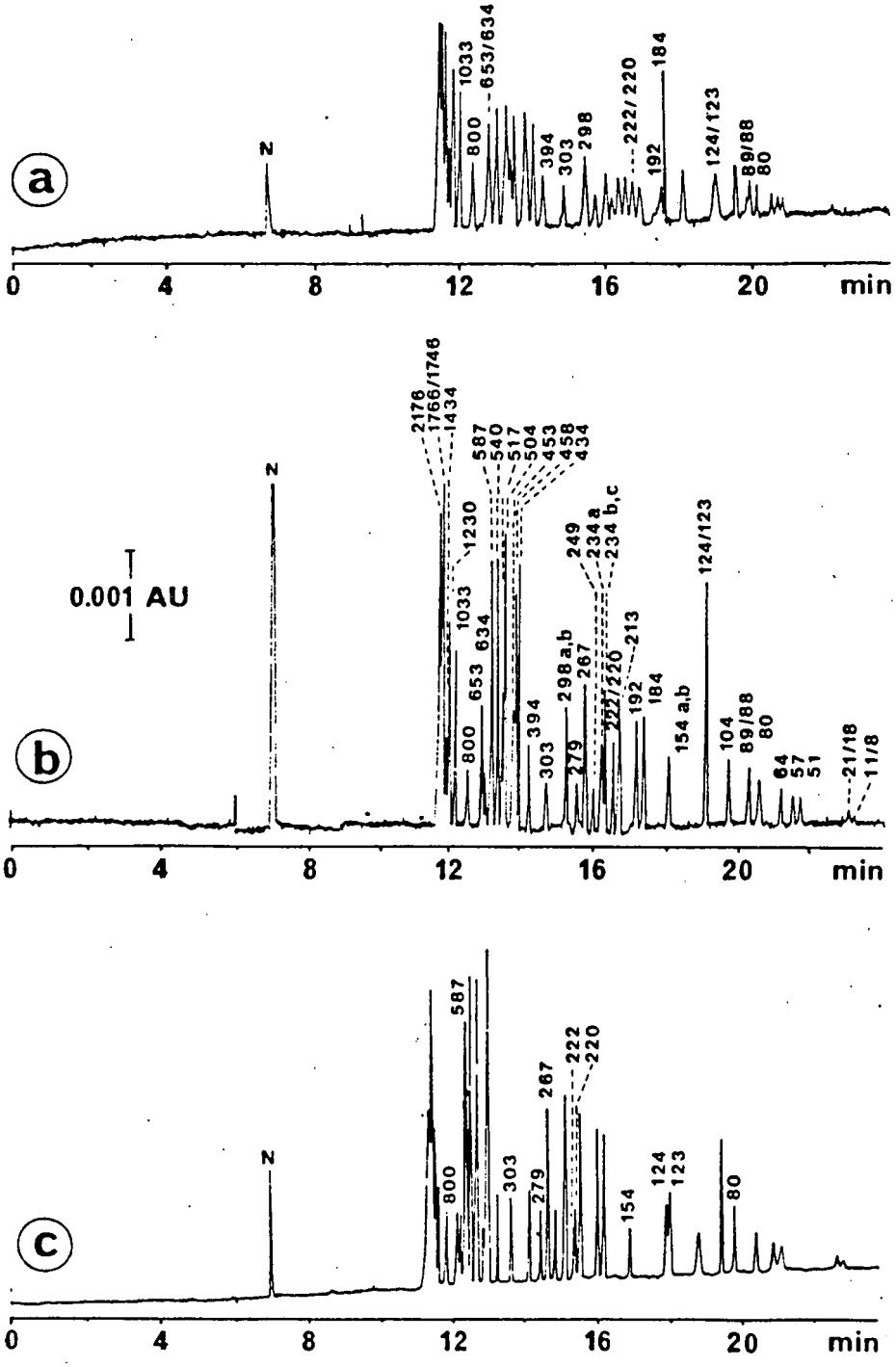

Figure 7. Impact of ethidium bromide on electropherograms of DNA restriction fragments. Buffer: 0.01 M Tris-borate, pH 8.7, 0.1 mM EDTA, 25 mM NaCl, 0.5% w/v HEC, (a) without and with the addition of (b) 1.27 and (c) 5.07 μM of ethidium bromide, respectively; sample: a mixture of pBR322 DNA-*Ava*II/*Eco*RI (0.2 μg/μl), pBR322 DNA-*Hae*III (0.25 μg/μL) and pBR328 DNA-*Bgl*I/*Hin*fI (0.25 μg/μL) digests at a ratio 1:2:2. Injection: vacuum, 8 s. Other conditions as in Fig. 4.

observed, which permits the separation of DNA species that differ only a few base pairs in length (Fig. 7b). While the addition of even more ethidium bromide allows the resolution of DNA fragments which differ in length by only 1–2 base pairs (*i.e.* 123 and 124 bp, or 220 and 222 bp), resolution for DNA molecules longer than approximately 400 base pairs starts to decline again (Fig. 7c). Ethidium bromide causes an almost uniform reduction in true electrophoretic mobilities regardless of the size of the DNA fragments. Therefore, the significant improvement in resolution cannot be attributed to a spread in electrophoretic mobilities (Fig. 8b). Spectroscopic and hydrodynamic studies of complexes of ethidium bromide and DNA suggest that the phenanthidium ring of ethidium bromide intercalates between two adjacent G-C base pairs and, subsequently, derotates the DNA duplex [40]. Each time it becomes inserted into a DNA molecule, ethidium bromide increases the spacing of successive base pairs along the helical axis to roughly 7 Å, almost the distance between phosphate atoms in a fully extended polynucleotide chain. In this situation, little rotation is possible around the helical axis, and therefore ethidium bromide also unwinds the double helix extensively. Thus, every intercalating molecule of ethidium bromide reduces the rotation angle between two adjacent G-C base pairs from 36° to 10°. The fact that intercalation occurs so readily indicates that it must be energetically favored, with the van der Waals bonds (holding the inserted molecules to the base pairs) being stronger than those found between conventionally stacked base pairs. In addition, intercalation is evidence for the ability of the double-helical structure to temporarily assume many inherently unstable configurations that normally quickly revert back to the standard B conformation [41]. Nevertheless, the metastability of DNA may contribute to minor differences in electrophoretic mobility, which may be minimized by the addition of ethidium bromide to the running buffer. Moreover, the cationic-charged nitrogens interact electrostatically with the phosphate group of DNA, which slows the migration rate of DNA by about 10–15%, as can be seen in Fig. 8a. This is further corroborated by a comparison of the pherograms shown in Fig. 9. The obviously higher migration rate of the 458-bp restriction fragment in the presence of 0.635 μM ethidium bromide (Fig. 9b) results from its relatively lower content (23.4%) of adjacent G-C base pairs in comparison to the 434-bp fragment (32.7%). Since less ethidium bromide intercalates with the former fragment, it is more negatively charged than the latter one and, hence, it exhibits a higher electrophoretic mobility.

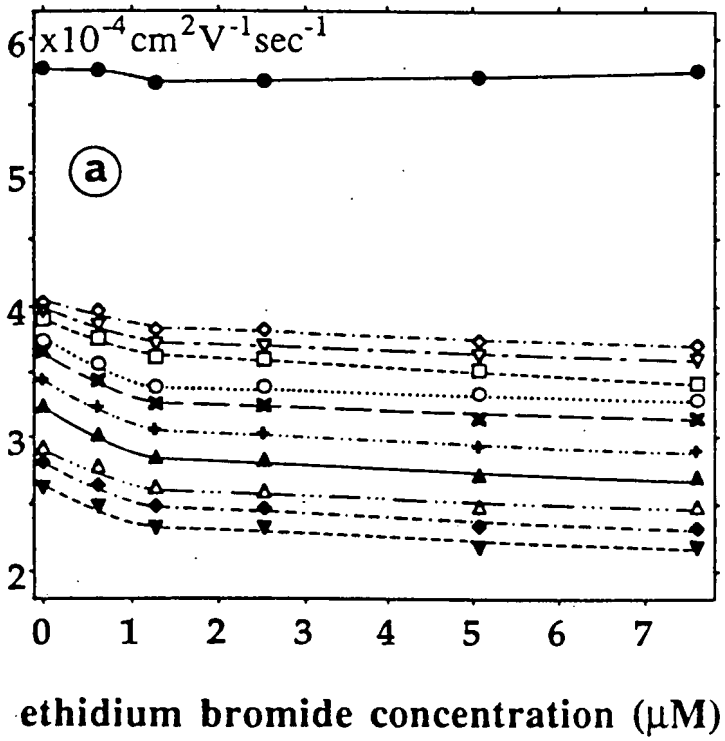

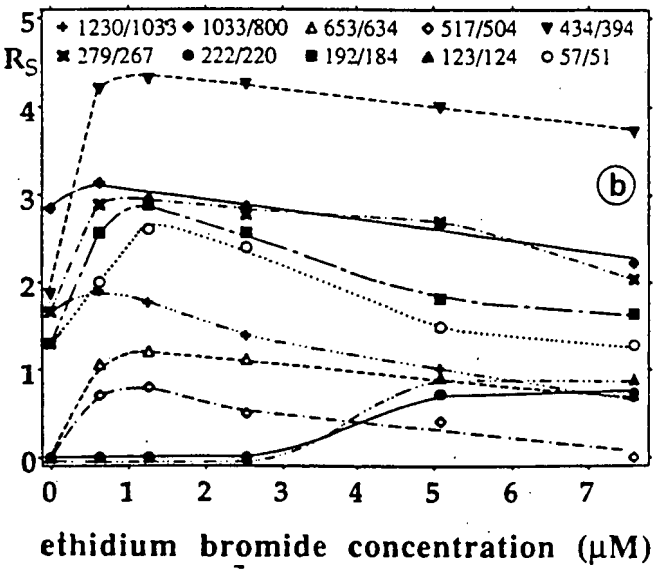

Figure 8. Impact of ethidium bromide concentration on (a) electroosmotic flow (●) and electrophoretic mobilities as well as (b) resolution (R_s) of DNA restriction fragments: (◇) 51 bp, (□) 80 bp, (▽) 104 bp, (○) 154 bp, (×) 192 bp, (+) 267 bp, (▲) 303 bp, (△) 540 bp, (◆) 653 bp, (▼) 1033 bp. Buffer: 0.01 M Tris-borate, pH 8.7, 0.1 mM EDTA, 25 mM NaCl, 0.5% w/v HEC, 0–7.61 μM ethidium bromide. Other conditions as in Fig. 4.

Efficiency is further noted by the larger number of theoretical plates per meter. It became evident that the addition of ethidium bromide to the buffer system at a concentration of 1.27 μM yielded four times the theoretical plates obtained without ethidium bromide. For fragments less than 300 base pairs in length, theoretical plates of up to 2 million per meter could be realized. Upon addition of even more ethidium bromide, the number of theoretical plates declined again. Finally, at a concentration of 7.6 μM the same number of plates per meter was observed as without the addition of ethidium bromide, namely $2–4 \cdot 10^5$ for DNA restriction fragments ranging from 89 to 1230 base pairs in length.

When a phenylmethyl-coated capillary was used, a concentration of only 0.635 μM ethidium bromide in a buffer system, which contained 10 mM of Tris-borate, pH 8.75, 25 mM of NaCl and 0.5% HEC, yielded the highest number of theoretical plates, namely 1.65×10^5 per meter for a DNA fragment 267 bp in length. In this regard, it is important to note that the number of theoretical plates not only depends on fragment length but also on the efficiency of the purification protocol used to remove the restriction endonuclease and the buffer salts upon completion of the digest. An even higher number of theoretical plates in excess of 4 million

plates per meter could be realized for restriction fragments ranging from 220 to 1766 bp in length when the aforementioned buffer system was replaced with 100 mM of Tris-borate, pH 8.7, 0.5% HEC, and 0.635 μM of ethidium bromide. This is in contrast to the observations made with uncoated capillaries. Although 100 mM of Tris-borate generated about the same current density as 10 mM Tris-borate plus 25 mM of NaCl in an unmodified capillary, electroosmotic flow was almost 50% less. This resulted in long migration times and poor resolution.

3.2.7 Sample concentration

To obtain high resolution in capillary electrophoresis, the volume of the injected sample must be very small compared with the volume of the capillary. As a rule, sample volumes should be limited to no more than 1% of the total capillary volume in order to avoid perturbation of the electric field and, consequently, uneven zone migration and zone distortion [42]. As shown in Table 2, both the number of theoretical plates and resolution decreased with increas-

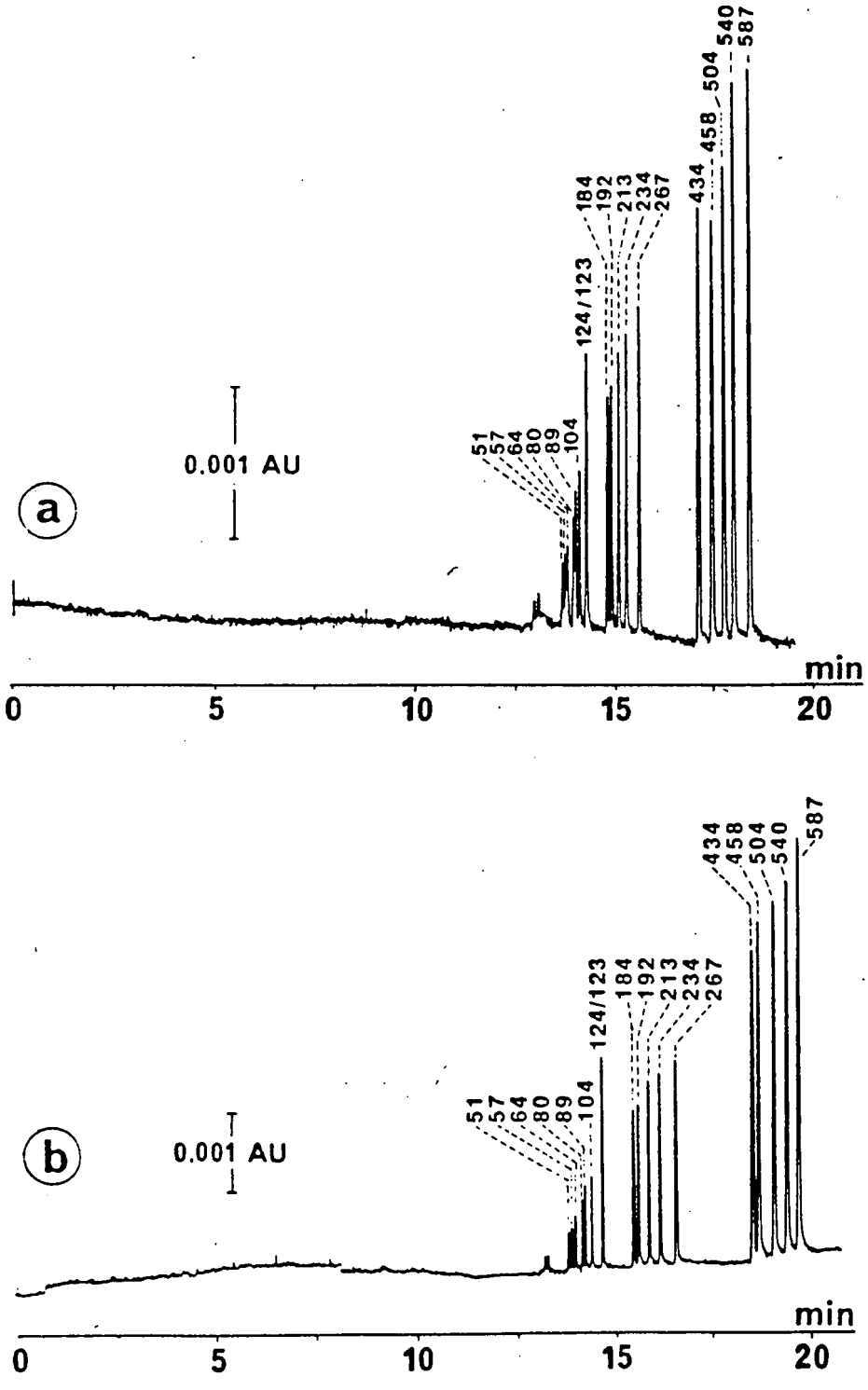

Figure 9. Impact of ethidium bromide on separation of DNA restriction fragments in a phenylmethyl-coated capillary. Buffer: 0.1 M Tris-borate, pH 8.7, 1 mM EDTA, 0.5% w/v HEC. (a) without and (b) with the addition of 0.635 μM of ethidium bromide; sample: pBR322 DNA-*Hae*III digest (0.25 μg/μL); column: 720 × 0.10 mm I.D., effective length 500 mm; injection: vacuum, 0.5 s; voltage: −15 kV; current: 18 μA; detection: UV, 260 nm; temperature: 35°C.

Table 2. Effects of injection time on number of theoretical plates and resolution

Injection time s	Sample concentration µg/mL	Number of theoretical plates ($\times 10^5$)/m		Resolution
3	200	222 bp	3.956	2.27
		249 bp	3.782	
6	100	222 bp	2.826	2.22
		249 bp	2.874	
15	40	222 bp	2.534	2.11
		249 bp	2.656	
30	20	222 bp	1.882	1.90
		249 bp	1.878	

ing injection time, though the actual amount of sample introduced remained constant. Hence, DNA samples of high concentration shall be injected if optimum resolution is required.

3.3 Applications in molecular biology

3.3.1 Analysis of PCR products

The capillary electrophoretic analysis of a PCR-amplified 361-bp segment of an androgen receptor mRNA transcript could be achieved in less than 18 min with a running buffer consisting of 10 mM Tris-borate, 25 mM NaCl, 0.1 mM EDTA, 1.27 µM ethidium bromide, and 0.5% HEC at a constant voltage of 15 kV (Fig. 10a). Figure 10b shows the same segment amplified by 30 cycles of polymerase chain reaction, spiked with DNA size standards derived from a commercially obtained ϕX-174 DNA – *Hin*cII digest and purified by means of Sephadex G-150 size-exclusion chromatography. Purification of PCR products prior to their analysis is recommended because the salts contained in the samples will cause considerable band broadening due to the conductivity difference between the sample zone and the surrounding buffer [9, 15, 43]. The addition of DNA size standards of known concentration allows both the accurate measurement of fragment length as well as the quantitative determination of amplified DNA segments.

3.3.2 Quantitation of PCR products

Quantitation of amplified products allows optimization of the PCR process, which is affected by a number of different parameters such as the source of Taq polymerase, the concentrations of $MgCl_2$, KCl and deoxynucleotide triphosphates, as well as the temperature of the denaturation and annealing steps. Since no appropriate standard PCR products are commercially available, a capillary electrophoretic calibration curve was generated with a 361-bp segment of the androgen receptor, which had been amplified by the described PCR method. The specificity of the amplification was checked using capillary electrophoresis, and since the reaction yielded only one product, a spectrophotometric assay was employed to determine the yield of the purified 361-bp product at a wavelength of 260 nm. The DNA sample had been amplified to 105 µg/mL, a typical value obtained under the PCR conditions used. The sample was then successively diluted to cover a range of concentrations from 5.25 to 31.5 µg/mL. Using a sampling time of 6 s, each diluted sample was injected hydrodynamically into the capillary together with the commercially available ϕX-174 DNA – *Hin*cII digest, the concentration of which was kept constant at 108 µg/mL. Although the relative standard deviation of six peak area measurements was as small as 3.06%, the peak area ratio of the PCR product to a DNA size standard was chosen to generate the calibration curve.

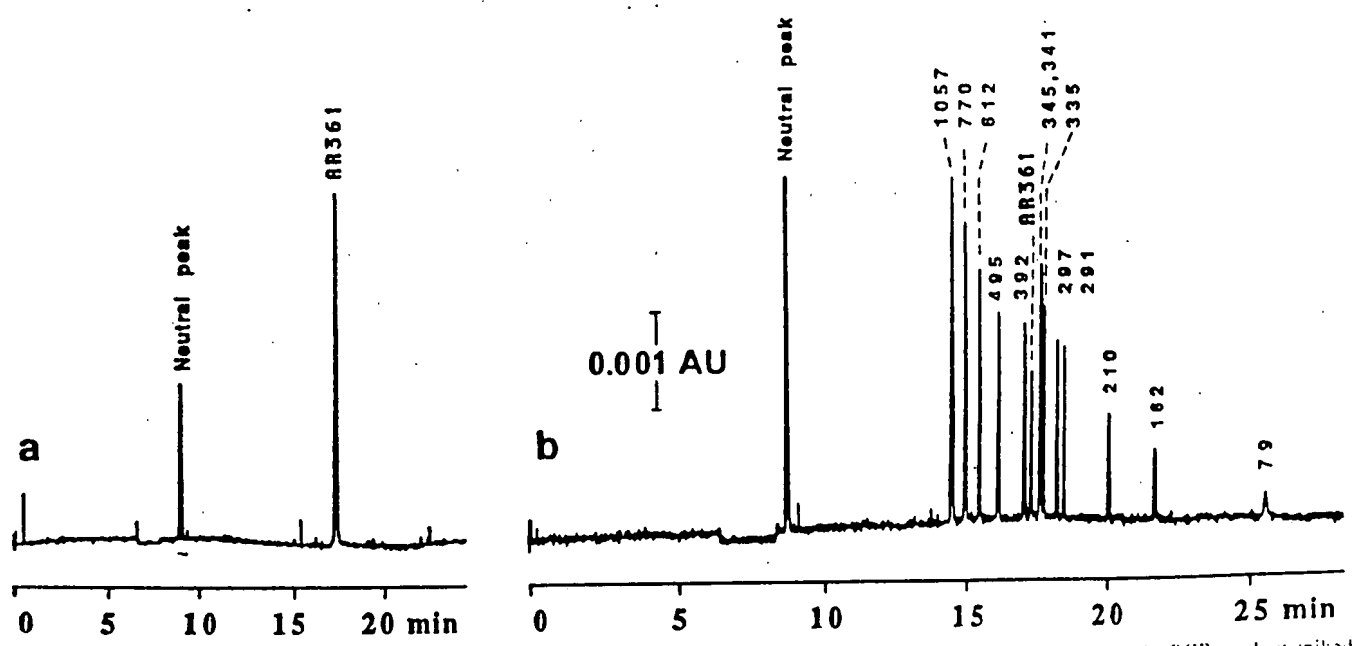

Figure 10. Electropherograms of a purified 361-bp androgen receptor mRNA transcript amplified by 30 cycles of PCR (a) and the PCR product spiked with a ϕX-174 DNA-*Hin*cII digest prior to its purification by size-exclusion chromatography. Buffer: 0.01 M Tris-borate, pH 8.7, 0.1 mM EDTA, 25 mM NaCl, 1.27 µM ethidium bromide, 0.5% w/v HEC. Other conditions as in Fig. 4.

This eliminates any errors resulting from the injection of the samples. Since peak area is related inversely to solute mobility, it should be normalized by dividing peak area with migration time when hydrodynamic sample injection is used. Figure 11 depicts the linear correlation between the concentration of a 361-bp segment of the androgen receptor amplified by the PCR and peak area ratio of the androgen receptor fragment to the 392-bp restriction fragment of the ϕX-174 DNA – *Hinc*II digest ($y = 0.076\ x - 0.148$, $r^2 = 0.991$). Since a restriction digest, the concentration of which is known, contains equimolar amounts of every fragment, quantitation of PCR products may also be accomplished by determining the molar ratio – peak area ratio of an amplified product to a restriction fragment of known molarity. The precision of determination was checked by relating the PCR amplified 361-bp segment of the androgen receptor to seven different DNA size standards of the ϕX-174 DNA – *Hinc*II digest. A coefficient of variation as small as 3.41% was obtained. Further, the result was in good agreement with the value obtained spectrophotometrically.

Quantitation of PCR products has been used, for instance, to measure methylation of DNA [44], to detect allelic loss of the β1-interferon gene [45], as well as to determine the relative and actual amounts of specific mRNA species, such

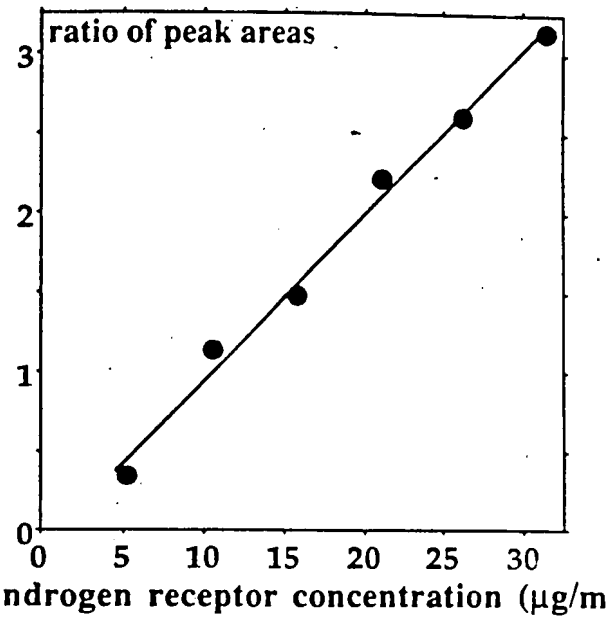

Figure 11. Relationship between amount of a purified 361-bp androgen receptor mRNA transcript amplified by polymerase chain reaction and ratio of peak area of the androgen receptor fragment to peak area of the 392-bp DNA size standard of the ϕX-174 DNA-*Hinc*II digest.

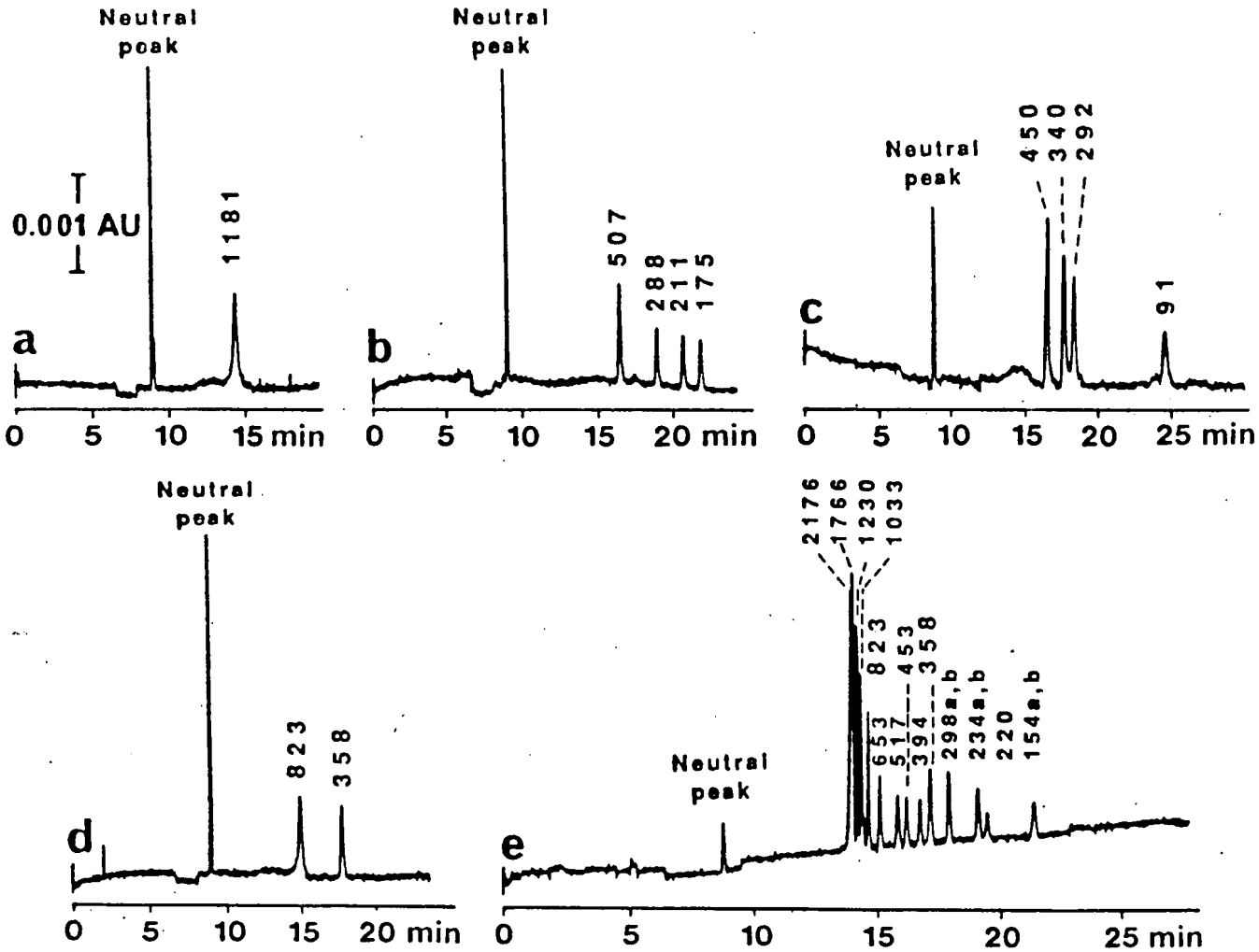

Figure 12. Electropherograms of a purified 1181-bp segment of the androgen receptor amplified by (a) PCR and of various restriction fragments obtained by its digestion with the restriction enzymes (b) *Hin*fI, (c) *Hpa*II and (d) *Eco*RI, respectively. In addition, the *Eco*RI digest was spiked with a commercially obtained pBR328 DNA-*Bgl*I/*Hin*fI digest. Other conditions as in Fig. 10.

as dystrophin [46] and interleukin 2 [47]. Quantification was accomplished by either densitometry of photographic negatives of ethidium bromide-stained gels [44, 45], hybridization with ^{32}P-labeled probes and autoradiography [46], liquid scintillation counting of excised gel bands [47], or high-performance liquid chromatography [48]. However, all these techniques suffer from severe limitations. Accurate quantification of ethidium bromide-stained bands in slab gels, for instance, requires the use of a two-dimensional scanner because of lateral diffusion of the DNA perpendicular to the electric field. However, fluorimetry instruments which accurately excite and quantify the fluorescence from a two-dimensional field are not widely available. Hence, quantification of DNA in ethidium bromide-stained gels has usually been achieved indirectly by the densitometric evaluation of pictures taken from the gels. However, particular care must be taken with several variables such as transillumination, exposure time, temperature, use of filters, and background subtraction, to ensure that one is working in the linear range of the film [49]. On the other hand, quantification of DNA by means of hybridization with radioactive reporter molecules and subsequent autoradiography not only suffers from increasing cost and difficulty of radioactive waste disposal, but also from numerous variables associated with film blackening as a measure of DNA concentration. A far more promising approach seems to be the use of liquid chromatography. Efficient separation and quantitation of PCR products has been achieved in less than 10 min on an anion-exchange column packed with 2.5 µm diethylaminoethyl-bonded nonporous resin particles [48]. Although high-performance liquid chromatography offers the advantage of accurate sample delivery by means of a loop, both peak area reproducibility (which was about 10%) as well as resolution and selectivity do not match the results obtained by capillary electrophoresis. However, one has to remember that the main constraint in obtaining quantitative data is inherent in the amplification process itself [50]. Since small differences in any of the variables that control the rate of amplification are magnified by the exponential behavior of the PCR, the number of cycles should preferentially be kept below 15. Since concentration sensitivity of capillary electrophoresis, which has been found to be 750 ng/mL for a 72-bp restriction fragment using on-column UV absorbance detection, does not exceed that obtained with ethidium bromide-stained slab gels, at least 25 PCR cycles are required for reliable quantification. But due to the lower mass detection limit, which is approximately 3 pg for the 72-bp fragment at a signal-to-noise ratio of 3, only 3–5 nL of sample have to be injected, in contrast to the 10 µL required for an agarose slab gel separation.

3.3.3 Restriction endonuclease digestion of PCR products

Enzymatic digestion of DNA with a restriction endonuclease yields a mixture of well-defined DNA fragments. Therefore, restriction mapping of a PCR product permits both the confirmation of its authenticity as well as the detection of mutations. Capillary electrophoretic analyses of various restriction digests of an 1181-bp transcript of the androgen receptor amplified by PCR are shown in Fig. 12. The digests yielded the expected number of restriction fragments. Moreover, the simultaneous injection of DNA size standards allowed the accurate determination of their length (Fig. 12e).

4 Concluding remarks

The combination of hydroxyethylcellulose and ethidium bromide allows the rapid separation of DNA fragments in both uncoated and coated capillaries with a degree of resolution comparable to that obtained by means of gel-filled capillaries. The described method may be of great value to the analysis of restriction fragment length polymorphisms and PCR products.

The scholarship granted to Mr. Suraphol Nathakarnkitkool by the Austrian Government is gratefully acknowledged. The authors are grateful to Mrs. Gertrude Sierek for her help with cell culture. This work was supported in part by the Ministry of Science, Vienna, Austria (G.Z. 49.685/3-III/A/4/90) and grants from the Austrian National Bank (No. 3533 & 3776).

Received April 24, 1991; in revised form October 15, 1991

5 References

[1] Saiki, R. K., Bugawan, T. L., Horn, G. T., Mullis, K. B. and Erlich, H. A., *Nature* 1986, *324*, 163–166.
[2] Scharf, S. J., Horn, G. T. and Erlich, H. A., *Science* 1986, *233*, 1076–1078.
[3] Saiki, R. K., Gelfand, D. H., Stoffel, S., Scharf, S. J., Higuchi, R., Horn, G. T., Mullis, K. B. and Erlich, H. A., *Science* 1988, *239*, 487–491.
[4] Saiki, R. K., Scharf, S., Faloona, F., Mullis, K. B., Horn, G. T., Erlich, H. A. and Arnheim, N., *Science* 1985, *230*, 1350–1354.
[5] Bos, J. L., Fearon, E. R., Hamilton, S. R., Verlaan de Vries, M., van Boom, J. H., van der Eb, A. J. and Vogelstein, B., *Nature* 1987, *327*, 293–297.
[6] Kwok, S., Mack, D. H., Mullis, K. B., Poiesz, B., Ehrlich, G., Blair, D., Friedman-Kien, A. and Sninsky, J. J., *J. Virol.* 1987, *61*, 1690–1694.
[7] Bernet, C., Garret, M., Debarbeyrac, B., Bebear, C. and Bonnet, J., *J. Clin. Microbiol.* 1989, *27*, 2492–2496.
[8] Stellwagen, N. C., *Adv. Electrophoresis* 1987, *1*, 177–228.
[9] Jorgenson, J. W. and Lukacs, K. D., *Science* 1983, *222*, 266–272.
[10] Foret, F. and Boček, P., *Electrophoresis* 1990, *11*, 661–664.
[11] Wallingford, R. A. and Ewing, A. G., *Adv. Chromatogr.* 1988, *29*, 1–76.
[12] Kuhr, W. G., *Anal. Chem.* 1990, *62*, 403R–414R.
[13] Righetti, P. G., *J. Chromatogr.* 1990, *516*, 3–22.
[14] Guttman, A., Cohen, A. S., Heiger, D. N., and Karger, B. L., *Anal. Chem.* 1990, *62*, 137–141.
[15] Heiger, D. N., Cohen, A. S. and Karger, B. L., *J. Chromatogr.* 1990, *516*, 33–48.
[16] Kasper, T. J., Melera, M., Gozel, P. and Brownlee, *J. Chromatogr.* 1988, *458*, 303–312.
[17] Cohen, A. S., Najarian, D., Smith, J. A. and Karger, B. L., *J. Chromatogr.* 1988, *458*, 323–333.
[18] Zhu, M., Hansen, D. L., Burd, S. and Gannon, F., *J. Chromatogr.* 1989, *480*, 311–319.
[19] Chin, A. M. and Colburn, J. C., *Am. Biotech. Lab.* 1989, 16.
[20] Nathakarnkitkool, S., Oefner, P. J., Chin, A. M., Bonn, G. K. and Bartsch, G., *International Symposium on Capillary Electrophoresis*, Poster No. 8, August 22–24, York, UK 1990.
[21] Serwer, P. and Allen, J. L., *Biochemistry* 1984, *23*, 922–927.
[22] Olivera, B. M., Baine, P. and Davidson, N., *Biopolymers* 1964, *2*, 245–257.
[23] Zernik, J. and Lichter, A., *BioTechniques* 1987, *5*, 411–414.
[24] Peats, S., Nochumson, S. and Kirkpatrick, F. H., *Biophys. J.* 1986, *49*, 91a.
[25] Dumais, M. M. and Nochumson, S., *BioTechniques* 1987, *5*, 62–67.
[26] Lukacs, K. D. and Jorgenson, J. W., *J. High Resolut. Chromatogr. Chromatogr. Commun.* 1985, *8*, 407–411.
[27] Hjertén, S., *J. Chromatogr.* 1985, *347*, 191–198.
[28] Jorgenson, J. W. and Lukacs, K. D., *Anal. Chem.* 1981, *53*, 1298–1302.
[29] Tsuda, T., Nomura, K. and Nakagawa, G., *J. Chromatogr.* 1983, *264*, 385–392.

[30] Tsuda, T., Nomura, K. and Nakagawa, G., *J. Chromatogr.* 1982, *248*, 241–247.
[31] Tsuda, T., *J. Liq. Chromatogr.* 1989, *12*, 2501–2514.
[32] Cantor, C. R., Smith, C. L. and Mathew, M. K., *Annu. Rev. Biophys. Biophys. Chem.* 1988, *17*, 287–304.
[33] Peterson, E. A. and Sober, H. A., *J. Am. Chem. Soc.* 1956, *78*, 751.
[34] Grushka, E., McCormick, R. M. and Kirkland, J. J., *Anal. Chem.* 1989, *61*, 241–246.
[35] Clementi, E. and Corongiu, G., *Biopolymers* 1982, *21*, 763–777.
[36] Lee, W. K., Gao, Y. and Prohofsky, E. W., *Biopolymers* 1984, *23*, 257–270.
[37] Van Dijk, J., Gruwel, M. L. H., Jesse, W., De Bleijser, J. and Leyte, J. C., *Biopolymers* 1987, *26*, 261–284.
[38] Atamna, I. Z., Metral, C. J., Muschik, G. M. and Issaq, H. J., *J. Liq. Chromatogr.* 1990, *13*, 2517–2527.
[39] Chang, R., *Physical Chemistry with Applications to Biological Systems*, 2nd Edit., Macmillan, New York 1977, p. 290.
[40] Long, E. C. and Barton, J. K., *Acc. Chem. Res.* 1990, *23*, 273–279.
[41] Watson, J. D., Hopkins, N. H., Roberts, J. W., Argetsinger-Steitz, J. and Weiner, A. M., *Molecular Biology of the Gene*, Vol. 1, 4th Edit., Benjamin & Cummings, Menlo Park 1987, pp. 254–255.
[42] Mikkers, F. E. P., Everaerts, F. M. and Verheggen, T. P. E. M., *J. Chromatogr.* 1979, *169*, 1–10.
[43] Huang, X., Gordon, M. J. and Zare, R. N., *Anal. Chem.* 1988, *60*, 375–377.
[44] Singer-Sam, J., LeBon, J. M., Tanguay, R. L. and Riggs, A. D., *Nucleic Acids Res.* 1990, *18*, 687.
[45] Neubauer, A., Neubauer, B. and Liu, E., *Nucleic Acids Res.* 1990, *18*, 993–998.
[46] Chelly, J., Kaplan, J. C., Maire, P., Gautron, S. and Kahn, A., *Nature* 1988, *333*, 858–860.
[47] Wang, A. M. and Mark, D. F., in: Innis, M. A., Gelfand, D. H., Sninsky, J. J. and White, T. J. (Eds.), *PCR Protocols: A Guide to Methods and Applications*, Academic Press, San Diego 1990, pp. 70–75.
[48] Katz, E. D., Haff, L. A. and Eksteen, R., *J. Chromatogr.* 1990, *512*, 433–444.
[49] Riberio, E. A., Larcom, L. L. and Miller, D. P., *Anal. Biochem.* 1989, *181*, 197–208.
[50] Gilliland, G., Perrin, S. and Bunn, H. F., in: Innis, M. A., Gelfand, D. H., Sninsky, J. J. and White, T. J. (Eds.), *PCR Protocols: A Guide to Methods and Applications*, Academic Press, San Diego 1990, pp. 60–69.

Petr Boček*
Andreas Chrambach

Section on Macromolecular Analysis, Laboratory of Theoretical and Physical Biology, National Institute of Child Health and Human Development, National Institutes of Health, Bethesda, MD

Capillary electrophoresis in agarose solutions: Extension of size separations to DNA of 12 kb in length

The upper limit of the size range of DNA amenable to separation in agarose solutions above their gelling temperature, using capillary zone electrophoresis apparatus, was increased to 12 kb. The plot of log(bp) *vs.* mobility derived from electrophoresis in 1.7% agarose solution is biphasic, exhibiting higher resolving power for DNA less than 1 kb in size than that of larger sizes. Resolving power for DNA larger than 1 kb increased when the agarose concentration was increased in the range of 1.0–2.6%. It was similar in solutions at 40°C of SeaPrep and SeaPlaque agaroses as well as in Acrylaide (trade names are those of the manufacturer). However, the resolving power of SeaPrep agarose at 25°C was inferior to that at 40°C. Concave plots of log(mobility) *vs.* concentration of the agarose solutions are those predicted under the assumption that the effective "equivalent radius" of the DNA molecule diminishes with increasing agarose concentration in the investigated concentration range up to 2.6%.

1 Introduction

The application of agarose solutions to DNA separations by capillary electrophoresis at 40°C has previously been reported for the size range up to 1 kb [1]. It appeared of interest to investigate the question whether this DNA size range could be extended further, to match the DNA separations in polyacrylamide gels of DNA fragments up to 23 kb (Figs. 1 and 2 of [2]) and the corresponding ones achieved in buffer in the presence of 0.5% methylcellulose (Fig. 5 of [3]). To render separations in agarose solutions more convenient, we also addressed the question whether separations could be achieved by highly substituted agaroses which were soluble at room temperature and could be stored at such temperature.

Correspondence: Dr. Petr Boček, Institute of Analytical Chemistry, Veveri 97, CS-611 42 Brno, Czech and Slovak Federated Republic

Abbreviations: bp, basepair; **cP**, centipoise = 0.001 Pa × s; **Ferguson plot**, log(mobility) *vs.* polymer (agarose) concentration; **kb**, kilo basepair; **Pa**, pascal = Newton × m^{-2}; **r**, fiber radius; **R**, particle radius; **R-plot**, $(K_R)^{0.5}$ *vs.* R; **TBE**, Tris, boric acid, EDTA buffer

* Permanent address: Czechoslovak Academy of Sciences, Institute of Analytical Chemistry, 61142 Brno, Czech and Slovak Federated Republic.

0173-0835/92/0102-0031 $3.50+.25/0

Anal. Chem. 1994, 66, 4063–4067

Separation of Fragments up to 570 Bases in Length by Use of 6% *T* Non-Cross-Linked Polyacrylamide for DNA Sequencing in Capillary Electrophoresis

Norine Best, Edgar Arriaga, Da Yong Chen, and Norman J. Dovichi*

Department of Chemistry, University of Alberta, Edmonton, Alberta T6G 2G2, Canada

Non-cross-linked polyacrylamide is a very convenient medium for the separation of DNA sequencing fragments in capillary electrophoresis. We demonstrate DNA sequencing with this matrix at an electric field of 200 V/cm and at room temperature. Resolution is observed to decrease exponentially with fragment length. Fragments 570 bases in length generate a resolution of 0.5, which is adequate for sequence identification.

DNA sequencing by capillary electrophoresis has attracted much attention over the past five years.[1-11] Most separations are performed with conventional polyacrylamide gels. These materials are not particularly convenient for routine use; gel performance is not outstanding at electric fields much larger than ~200 V/cm. We have reported the use of LongRanger, an alternative cross-linked matrix, at very high electric field and at elevated temperatures.[12-13]

Recently, attention has focused on the use of non-cross-linked polyacrylamide in electrophoresis. These solutions have relatively low viscosity. In principle, they may be pumped from the capillary after use. By refilling the capillary after every separation, it should not be necessary to realign optical systems in automated DNA sequencers.

It may be useful to review the terminology used in describing polyacrylamide. The weight percentage of monomer plus cross-linker in the polymer is denoted % *T*. The mole fraction of cross-linker to monomer is denoted as % *C*. Polymers with no cross-linkers are called entangled polymers, syrupy solutions, linear polymers, or non-cross-linked polymers. We prefer the latter terminology.

Bode first used non-cross-linked polyacrylamide in combination with agarose for separation of proteins and double-stranded oligonucleotides.[14] Crambach and co-workers compared the performance of 0% *C* and 5% *C* gels at various total acrylamide concentrations.[15-17] More recently, Karger and co-workers compared 0, 0.5, and 5% *C* gels for separation of double-stranded DNA in capillary electrophoresis.[18] Bocek and co-workers reported that 0% *C* polyacrylamide could be pumped from a capillary through use of a special high-pressure syringe.[19] However, Righetti has demonstrated that the high viscosity of 10% *T* non-cross-linked polyacrylamide makes refilling of capillaries extremely difficult.[20] Guttman and co-workers reported the use of non-cross-linked polyacrylamide for separation of double-stranded DNA; they claimed that the capillary could be reused 100 times without replacement of the separation medium.[21]

More recently, there have been applications of non-cross-linked polyacrylamide for separation of DNA sequencing fragments. Pentoney and co-workers reported DNA sequencing in 10% *T*, non-cross-linked polyacrylamide at an electric field of 300 V/cm; sequence could not be determined for fragments longer than 300 bases.[22] Similar results have been reported by Mathies' group with 9% *T* non-cross-linked polyacrylamide gels.[23] Karger and co-workers have shown separation of fragments 370 bases in length with 6% *T*, 0% *C* polyacrylamide, again at an electric field of 300 V/cm.[24]

We have reported the effect of cross-linker concentration on separations of single-stranded DNA at an electric field of 300 V/cm.[25] We observed that the resolution of adjacent fragments was on the order of 0.5 for fragments 350 bases in length. This level of resolution marks the limit for convenient sequence determination; it is difficult to determine the sequence of longer fragments with the material at that electric field. Resolution is limited both by peak width, which increases with fragment length, and by the onset of biased reptation. Biased reptation causes longer fragments to coelute, destroying resolution of successive fragments.[26-31]

(1) Dovichi, N. J. In *CRC Handbook of Capillary Electrophoresis*; Landers, E., Ed.; CRC Press, Inc.: Boca Raton, FL, 1993; Chapter 14, pp 369–387.
(2) Swerdlow, H.; Gesteland, R. *Nucleic Acids Res.* 1990, *18*, 1415–1419.
(3) Drossman, H.; Luckey, J. A.; Kostichka, A. J.; D'Cunha, J.; Smith, L. M. *Anal. Chem.* 1990, *62*, 900–903.
(4) Cohen, A. S.; Najarian, D. R.; Karger, B. L. *J. Chromatogr.* 1990, *516*, 49–60.
(5) Swerdlow, H.; Wu, S.; Harke, H.; Dovichi, N. J. *J. Chromatogr.* 1990, *516*, 61–67.
(6) Rocheleau, M. J.; Grey, R. J.; Chen, D. Y.; Harke, H. R.; Dovichi, N. J. *Electrophoresis* 1992, *13*, 484–486.
(7) Chen, D. Y.; Swerdlow, H. P.; Harke, H. R.; Zhang, J. Z.; Dovichi, N. J. *J. Chromatogr.* 1991, *559*, 237–246.
(8) Karger, A. E.; Harris, J. M.; Gesteland, R. F. *Nucleic Acids Res.* 1991, *19*, 4955–4962.
(9) Swerdlow, H.; Zhang, J. Z.; Chen, D. Y.; Harke, H. R.; Grey, R.; Wu, S.; Dovichi, N. J.; Fuller, C. *Anal. Chem.* 1991, *63*, 2835–2841.
(10) Chen, D. Y.; Harke, H. R.; Dovichi, N. J. *Nucleic Acids Res.* 1992, *20*, 4873–4880.
(11) Harke, H. R.; Bay, S.; Zhang, J. Z.; Rocheleau, M. J.; Dovichi, N. J. *J. Chromatogr.* 1992, *608*, 143–150.
(12) Rocheleau, M. J.; Dovichi, N. J. *J. Microcolumn Sep.* 1992, *4*, 449–453.
(13) Lu, H.; Arriaga, E.; Chen, D. Y.; Starke, H.; Dovichi, N. J. *J.Chromatogr.* 1994, *680*, 497–501.
(14) Bode, H. J. *Anal. Biochem.* 1977, *83*, 364–371.
(15) Tietz, D.; Gottleib, M. H.; Fawcett, J. S.; Crambach, A. *Electrophoresis* 1986, *7*, 217–220.
(16) Pulyaeva, H.; Wheeler, D.; Garner, M. M.; Crambach, A. *Electrophoresis* 1992, *13*, 608–614.
(17) Tietz, D.; Aldroubi, A.; Pulyaeva, H.; Guszczynski, T.; Garner, M. M.; Crambach, A. *Electrophoresis* 1992, *13*, 614–616.
(18) Heiger, D. N.; Cohen, A. S.; Karger, B. L. *J. Chromatogr.* 1990, *516*, 33–48.
(19) Sudor, J.; Foret, F.; Bocek, P. *Electrophoresis* 1991, *12*, 1056–1058.
(20) Chiari, M.; Nesi, M.; Fazio, M.; Righetti, P. G. *Electrophoresis* 1992, *13*, 690–697.
(21) Guttman, A.; Wanders, B.; Cooke, N. *Anal. Chem.* 1992, *64*, 2348–2351.
(22) Pentoney, S. L.; Konrad, K. D.; Kaye, W. *Electrophoresis* 1992, *13*, 467–474.
(23) Huang, X. C.; Quesada, M. A.; Mathies, R. A. *Anal. Chem.* 1992, *64*, 2149–2154.
(24) Ruiz-Martinez, M. C.; Berka, J.; Belenkii, A.; Foret, F.; Miller, A. W.; Karger, B.L. *Anal. Chem.* 1993, *65*, 2851–2858.
(25) Figeys, D.; Dovichi, N. J. *J. Chromatogr.* 1993, *645*, 311–317.
(26) Lumpkin, O. J.; Déjardin, P.; Zimm, B. H. *Biopolymers* 1985, *24*, 1573–1593.

0003-2700/94/0366-4063$04.50/0

There are several different versions of reptation theory for DNA sequencing. The recent work of Duke and Viovy on biased reptation with fluctuations seems to provide a particularly accurate description of DNA migration in gels.[28-31] Over the years, a number of other models for DNA separations have been proposed by this group,[11] Crambach,[32-33] Giddings,[34] Smisek,[35] Stellwagen,[36] Rodbard,[37] Southern,[38] Calladine,[39] Smith,[40] and others. The purpose of this paper is not to confirm or reject any particular model. We use the terminology of biased reptation for convenience.

Resolution produced by the non-cross-linked material and the resolution of the cross-linked material approached similar values for longer fragments.[25] Since it is possible to obtain long sequencing reads at lower electric fields with cross-linked gels,[10] we decided to investigate the performance of non-cross-linked polyacrylamide at an electric field of 200 V/cm. While the sequencing rate will decrease at lower electric field, it should be possible to determine sequence for longer fragments. The increase in sequence information at lower electric field is associated with the delayed onset of biased reptation.

EXPERIMENTAL SECTION

Fluorescence Detection. The two-color direct reading fluorescence spectrograph used for DNA sequencing by capillary electrophoresis has been reported elsewhere.[41] It consists of a single helium–neon laser (λ = 543.5 nm) as the excitation source. A postcolumn sheath flow cuvette is used as the detection chamber.[42-45] Fluorescence is collected with a single microscope objective, and a dichroic filter is used as the spectral dispersive element. Two interference filters are used to isolate fluorescence in two bands corresponding to emission from tetramethylrhodamine and sulforhodamine 101 labeled DNA fragments. Photomultiplier tubes detect fluorescence, and a simple electronic bandpass filter is used to condition the signal before digitization by a Macintosh computer.

Electrophoresis. The polyimide-coated fused-silica capillary tubing is 50-μm inner diameter, 145-μm outer diameter, and typically 35 cm long. The non-cross-linked polyacrylamide is prepared from 5 mL aliquots of carefully degassed acrylamide solution (6% *T*), 1× TBE, and 7 M urea. Polymerization is initiated by addition of 2 μL of TEMED and 20 μL of 10% ammonium persulfate. The capillaries are treated with a solution of [(γ-methacryloyloxy)propyl]trimethoxysilane to bind the polyacrylamide to the capillary walls. The capillaries are filled with the acrylamide monomer solution by application of a vacuum. Polymerization occurs within the capillary and appears complete within 30 min; however, capillaries are typically stored overnight before use.

Sample Preparation. The sequencing reaction is carried out in 40 mM MOPS buffer, pH 7.5, 50 mM NaCl, 10 mM $MnCl_2$, and 15 mM sodium isocitrate. For the first reaction, 2 μL of 5 μM tetramethylrhodamine-labeled primer (Applied Biosystems, 21M13 TAMRA) is annealed to 1 μg of M13mp18 single-stranded DNA at 65 °C for 2 min, followed by slow cooling. A mixture of deoxy- and dideoxynucleoside triphosphates is added to give an average nucleoside ratio (dNTP/ddNTP) of 1500:1 with 7-deaza-2′-deoxyguanosine-5′-triphosphate used in place of dGTP. The ratios of dideoxynucleosides are adjusted to yield a nominal peak height ratio of 3:1 for T and G. After the mixture is warmed to 37 °C, 6 units of Sequenase Version 2.0 and 0.006 unit of pyrophosphatase are added. Incubation continues at 37 °C for 30 min, after which the DNA is precipitated with ethanol.[2] Identical experimental conditions are used with a sulforhodamine-labeled primer (Applied Biosystems, 21M13 ROX) to yield a nominal peak height ratio of 3:1 for A and C. The samples are resuspended in a 49:1 mixture of formamide–0.5 M aqueous EDTA. Three-microliter aliquots are taken from the resuspended samples, heated to 95 °C for 2 min, and injected onto the capillary by applying a 150 V/cm electric field for 60 s.

Data Processing. The data from the electropherograms are convoluted with a 2-s wide Gaussian peak to smooth high-frequency noise; the width of this Gaussian peak was chosen to match the width of early-eluting peaks. The signals are set to zero baseline, and the two spectral channels are normalized to generate similar amplitude peaks.

Some of the emission from the TAMRA-labeled fragments overlaps with the emission from the ROX-labeled fragments. TAMRA-labeled fragments generate peaks in both spectral channels, whereas ROX-labeled fragments only generate signal in the red spectral channel. To simplify data analysis, a fraction of the signal from the green spectral channel is subtracted from the red spectral channel to eliminate spectral cross-talk.

Last, we noticed that ROX- and TAMRA-labeled fragments tended to demonstrate a slight mobility shift; the TAMRA fragments tended to elute slightly later than expected, based on the position of the ROX-labeled fragments. To correct for this mobility shift, the signal from the red spectral channel is offset by 5 s. This mobility shift is a significant fraction of the ~10-s peak spacing.

RESULTS AND DISCUSSION

The top panel of Figure 1 presents the separation of a typical M13mp18 sequencing reaction. There is roughly exponential decrease in signal with time. This decrease in signal presumably is due to the first-order kinetics that describe the incorporation of chain-terminating dideoxynucleotides into

(27) Slater, G. W.; Noolandi, J. *Biopolymers* **1985**, *24*, 2181–2184.
(28) Duke, T. A.; Semenov, A. N.; Viovy, J. L. *Phys. Rev. Lett.* **1992**, *69*, 3260–3263.
(29) Duke, T. A.; Viovy, J. L.; Semenov, A. N. *Biopolymers* **1994**, *34*, 239–247.
(30) Heller, C.; Duke, T. A.; Viovy, J. L. *Biopolymers* **1994**, *34*, 249–259.
(31) Duke, T.; Viovy, J. L. *Phys. Rev. E* **1994**, *49*, 2408–2416.
(32) Rodbard, D.; Chrambach, A. *Proc. Natl. Acad. Sci. U.S.A.* **1970**, *65*, 970–977.
(33) Lunney, J.; Chrambach, A.; Rodbard, D. *Anal. Biochem.* **1971**, *40*, 158–173.
(34) Giddings, J. C.; Kucera, E.; Russell, C. P.; Marcus, M. N. *J. Phys. Chem.* **1968**, *72*, 4397–4408.
(35) Smisek, D. L.; Hoagland, D. A. *Science* **1990**, *248*, 1221–1223.
(36) Holmes, D. L.; Stellwagen, N. C. *Electrophoresis* **1990**, 11, 5–15.
(37) Oerter, K. E.; Munson, P. J.; McBride, W. O.; Rodbard, D. *Anal. Biochem.* **1990**, *189*, 235–243.
(38) Southern, E. M. *Anal. Biochem.* **1979**, *100*, 319–323.
(39) Calladine, C. R.; Collis, C. M.; Drew, H. R.; Mott, M. R. *J. Mol. Biol.* **1991**, *221*, 981–1005.
(40) Luckey, J. A.; Smith, L. A. *Anal. Chem.* **1993**, 65, 2841–2850.
(41) Lu, H.; Arriaga, E.; Chen, D. Y.; Figeys, D.; Dovichi, N. J. *J. Chromatogr.* **1994**, *680*, 503–510.
(42) Dovichi, N. J.; Martin, J. C.; Jett, J. H.; Keller, R. A. *Science* **1983**, *219*, 845–847.
(43) Cheng, Y. F.; Dovichi, N. J. *Science* **1988**, *242*, 562–567.
(44) Wu, S.; Dovichi, N. J. *J. Chromatogr.* **1989**, *460*, 141–155.
(45) Cheng, Y. F.; Wu, S.; Chen, D. Y.; Dovichi, N. J. *Anal. Chem.* **1990**, *62*, 496–503.

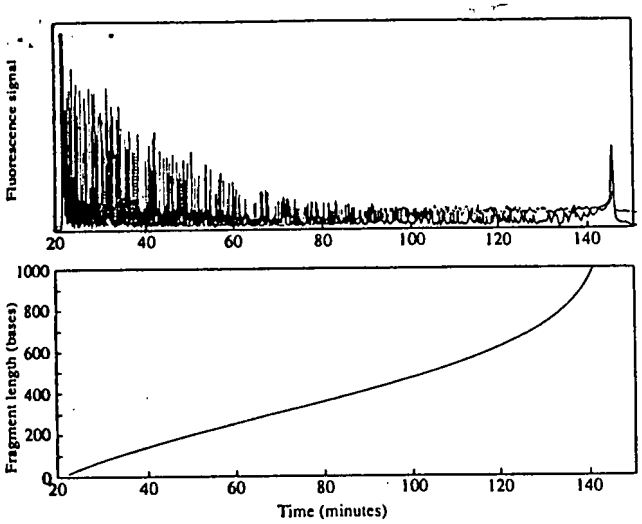

Figure 1. Separation of M13mp18 in 6% *T* non-cross-linked polyacrylamide at an electric field of 200 V/cm. Both channels of the two-color peak height encoded sequence are superimposed in the top panel. The bottom panel presents the fragment length eluting as a function of temperature. Note that the horizontal axes of the two panels are aligned.

the growing sequencing fragment. The decrease in signal is not due to biased injection because of different mobility of DNA fragments; the mobility of DNA in free solution is nearly independent of fragment length, and there should be little if any bias in injection amount.

The bottom panel of Figure 1 presents the observed fragment length as a function of retention time. Retention time is roughly linear up to ~100 min,[11] corresponding to fragments that are 500 bases in length. Longer fragments tend to coelute, ultimately reaching an asymptotic limit at 145 min, by which time all fragments have eluted. This asymptotic elution of long fragments is the hallmark of biased reptation; it is this asymptotic elution that limits the amount of sequence information that can be determined in a single separation.[26-31] As fragments coelute, it is no longer possible to resolve adjacent peaks.

Figure 2 presents a detailed view of the separation. At the electric field of 200 V/cm, the primers elute in ~22 min. Fragment spacing is quite uniform up to ~500 bases, where the onset of biased reptation causes the peaks to crowd together. The sequencing data are easily read beyond 500 bases; the sequence can be identified with the known sequence of M13mp18[46] for fragments 1000 bases in length.

The excellent resolution produced by non-cross-linked polyacrylamide at 200 V/cm is demonstrated by Figure 3. A portion of the sequence corresponding to bases 567–571 is shown. The fragments are well resolved, and automated peak-calling algorithms should have little difficulty dealing with data of this quality.[47] Note that successive bases are observed as peaks in alternate spectral channels. The T's are two bases apart and the resolution of each pair of T's is ~1, corresponding to a resolution of 0.5 for adjacent peaks. In this portion of the electropherogram, adjacent peaks present in the same spectral channel are more difficult to distinguish. The use of a four-color sequencing protocol will provide more information to help identify these late-eluting peaks.[9]

Plate counts were determined by use of a nonlinear regression algorithm to fit a Gaussian function to individual peaks. In a few cases where peaks overlapped, the data were fit with two Gaussian functions. Figure 4 presents the observed separation efficiency as a function of fragment length. Plate counts ranged from 1×10^6 to 4×10^6 plates for fragments ranging from 25 to 600 bases in length. There was a trend toward lower plate counts for the longer fragments; the line is the least-squares linear regression fit to the data. However, plate counts do not change dramatically for these fragments. This result is consistent with our data obtained at 300 V/cm.[25] As pointed out earlier, plate count is related to the ratio of mobility and diffusion coefficient.[11] The slow variation in plate count with fragment length suggests that mobility and diffusion coefficients are highly correlated. This result is expected based on the Stokes–Einstein formula for diffusion coefficient and the Debye–Hückel–Henry theory for mobility; both diffusion and mobility are expected to depend on the particle radius. The ratio of mobility and diffusion coefficient should be independent of fragment size, which is consistent with our data. However, the weak dependence of plate count with fragment length implies that peak width increases with fragment length.

Resolution for adjacent bases was also determined by use of nonlinear regression analysis. Fragments were fit with a pair of Gaussian functions, and resolution was calculated on the basis of the peak width and spacing. In a few cases, peaks separated by several bases were used in the resolution calculation; the resolution was normalized by the number of bases separating the fragments. Figure 5 presents the resolution as a function of fragment length. Resolution showed a pronounced decrease with fragment length. The smooth curve in Figure 5 is a least-squares fit of an exponential decay to the observed resolution. The data appear to be consistent with a factor of 2 decrease in resolution for every 250 bases in fragment length. Resolution drops from 2 for early-eluting peaks to 0.5 for fragments 600 bases in length. This decrease in resolution arises because both peak width increases and peak spacing decreases with fragment length.

We earlier reported resolution for DNA sequencing fragments separated in 6% *T* non-cross-linked polyacrylamide at an electric field of 300 V/cm.[25] Resolution was 2 for fragments less than 100 bases and dropped to 0.5 for fragments that were ~375 bases in length. This limiting value of resolution is related to the phenomenon described by biased reptation, which predicts that the onset of biased reptation scales inversely with electric field.[28-31,36] The 50% increase in sequence obtained at 200 V/cm compared with the results at 300 V/cm is consistent with the predictions of biased reptation. Of course, it may be possible to obtain very long sequencing reads at lower electric fields. A study of the variation in read length with electric field should be profitable.

Finally, the data presented in this paper were obtained at room temperature. We have shown that mobility increases dramatically with temperature in cross-linked polyacrylamide.[13] Similar results are expected with the non-cross-linked material. However, the onset of biased reptation moved to shorter fragments as temperature increased. We assume

(46) Yanisch-Perron, C.; Vieira, J.; Messing, J. *Gene* **1985**, *33*, 103–119.
(47) Giddings, M. C.; Brumley, R. L.; Haker, M.; Smith, L. M. *Nucleic Acids Res.* **1993**, *21*, 4530–4540.

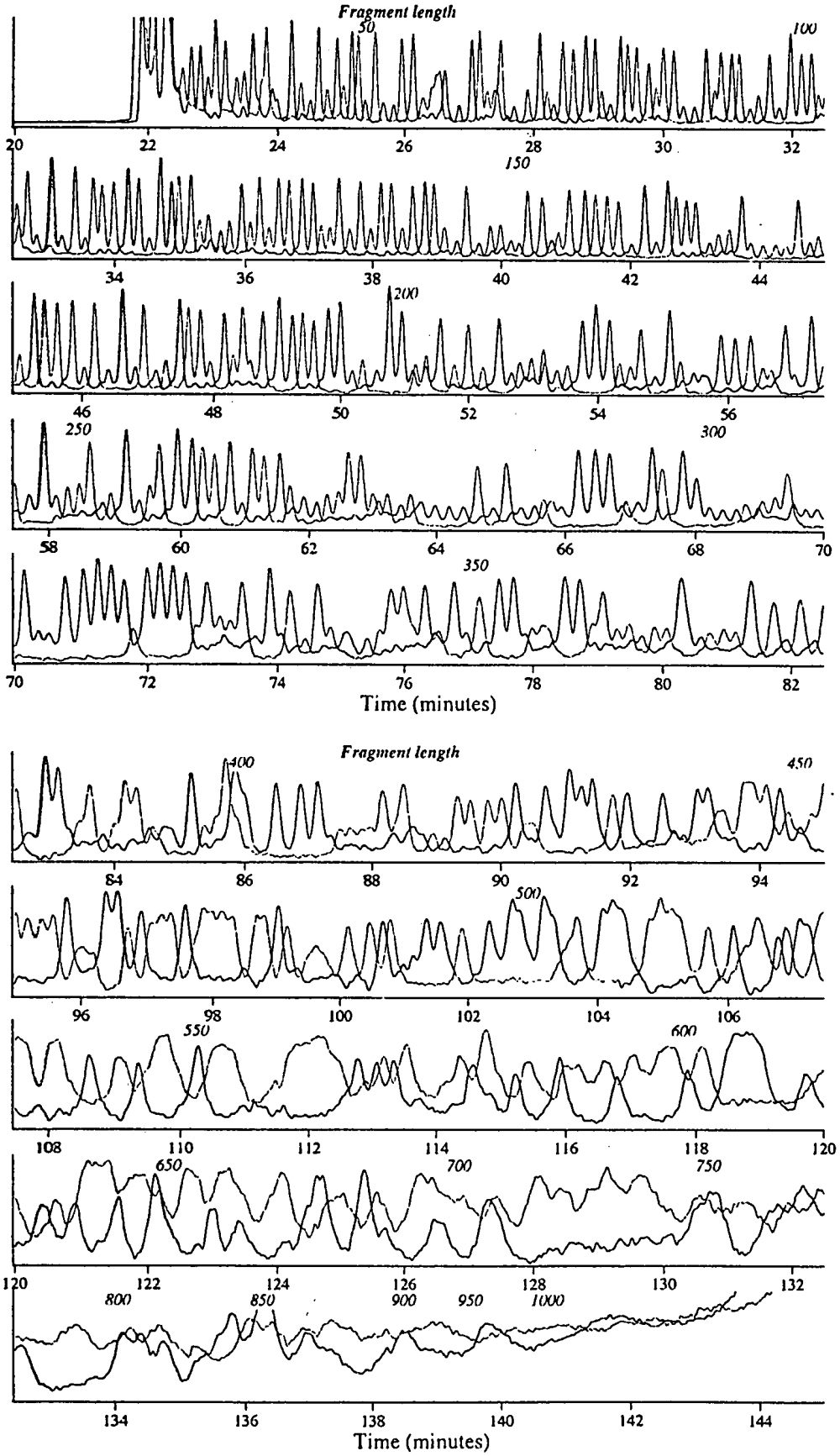

Figure 2. Two-color peak height encoded sequencing of M13mp18 in non-cross-linked polyacrylamide. The red trace corresponds to the signal generated by ROX-labeled fragments; large peaks are A and small peaks are C. The blue trace corresponds to TAMRA-labeled fragments; large peaks are G and small peaks are T. The fragment length is denoted in italics at the top of each panel.

that similar results will be observed with non-cross-linked polyacrylamide.

The long sequencing reads reported in this paper should be compared with results reported elsewhere with non-cross-

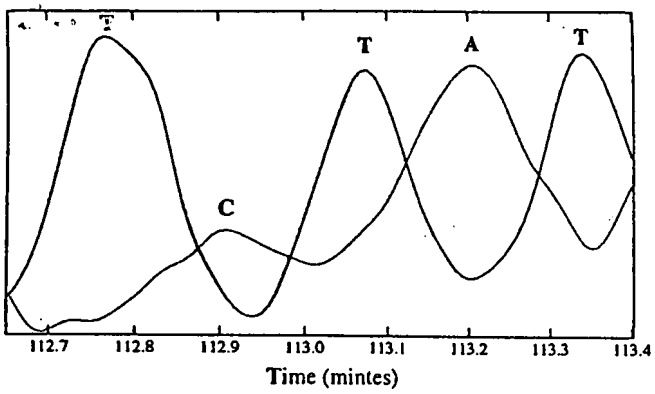

Figure 3. Separation of fragments 567–571 bases in length. The identity of each peak is denoted above.

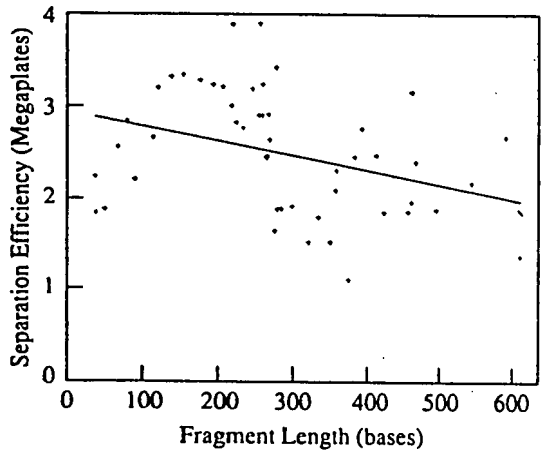

Figure 4. Separation efficiency as a function of fragment length. The number of theoretical plates is plotted as a function of fragment length. The line is the least-squares regression fit of a straight line to the data.

linked polyacrylamide. We demonstrate separation of fragments over 550 bases in length; previous workers have achieved separations of fragments ~370 bases in length. There are four important reasons for the difference in sequence length. First, we used a separation potential of 200 V/cm; earlier workers used an electric field of 300 V/cm. The inverse dependence of the onset of biased reptation with electric field accounts for most of the improvement in sequence length reported here. Second, our separation was performed at room temperature; most earlier work had been performed at elevated temperature, where the effects of biased reptation are expected to be more serious. Third, the earliest work with non-cross-linked polyacrylamide used very high concentration material. We suspect that the small effective pore size produced by the high concentration material will exacerbate the effects of biased reptation. Decreased total acrylamide concentration is known to increase sequencing rates for short sequencing fragments in cross-linked gels.[11] Fourth, high-sensitivity detection is required for determination of large amounts of sequence. As we pointed out above, there is an exponential decrease in fluorescence signal with fragment length; longer fragments generate lower amplitude signals. It is likely that part of the difficulty in obtaining long reads from some of the early workers was poor signal-to-noise ratio, so that the smaller amplitude, later eluting fragments were buried in noise. Our postcolumn sheath-flow cuvette produces extremely high sensitivity. We have reported detection limits of a few molecules of both tetramethylrhodamine and sulforhodamine 101;[48,49] these results were obtained with a low-power helium–neon laser and a postcolumn sheath flow cuvette. This high sensitivity generates very high signal-to-noise ratio for the late-eluting peaks.

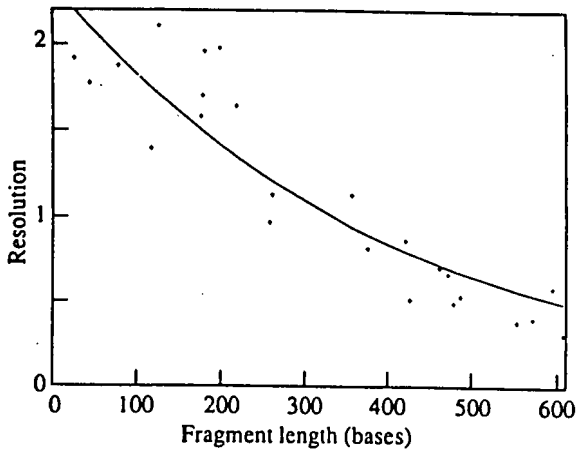

Figure 5. Resolution as a function of fragment length. The smooth curve is an exponential decay that was fit to the data.

ACKNOWLEDGMENT

This work was supported in part by the Department of Energy—Human Genome Initiative Grant DE-FGO2-91ER61123. Support by DOE does not constitute an endorsement of the views expressed in this article. This work was also supported by the Natural Sciences and Engineering Research Council of Canada (NSERC) and the Department of Chemistry of the University of Alberta. N.J.D. acknowledges a Steacie fellowship from NSERC.

Received for review March 17, 1994. Accepted July 8, 1994.[⊗]

[⊗] Abstract published in *Advance ACS Abstracts*, September 15, 1994.

(48) Chen, D. Y.; Adelhelm, K.; Cheng, X. L.; Dovichi, N. J. *Analyst* 1994, *119*, 349–352.
(49) Zhao, J. Y.; Dovichi, N. J.; Hindsgaul, O.; Gosselin, S.; Palcic, M. M. *Glycobiology* 1994, *4*, 239–242.

Harold Swerdlow[1]
Kerry E. Dew-Jager[1]
Kevin Brady[1]
Ronda Grey[2]
Norman J. Dovichi[2]
Raymond Gesteland[3]

[1]Department of Human Genetics, University of Utah
[2]Department of Chemistry, University of Alberta
[3]Howard Hughes Medical Institute, University of Utah

Stability of capillary gels for automated sequencing of DNA

Recent interest in capillary gel electrophoresis has been fueled by the Human Genome Project and other large-scale sequencing projects. Advances in gel polymerization techniques and detector design have enabled sequencing of DNA directly in capillaries. Efforts to exploit this technology have been hampered by problems with the reproducibility and stability of gels. Gel instability manifests itself during electrophoresis as a decrease in the current passing through the capillary under a constant voltage. Upon subsequent microscopic examination, bubbles are often visible at or near the injection (cathodic) end of the capillary gel. Gels have been prepared with the polyacrylamide matrix covalently attached to the silica walls of the capillary. These gels, although more stable, still suffer from problems with bubbles. The use of actual DNA sequencing samples also adversely affects gel stability. We examined the mechanisms underlying these disruptive processes by employing polyacrylamide gel-filled capillaries in which the gel was not attached to the capillary wall. Three sources of gel instability were identified. Bubbles occurring in the absence of sample introduction were attributed to electroosmotic force; replacing the denaturant urea with formamide was shown to reduce the frequency of these bubbles. The slow, steady decline in current through capillary sequencing gels interferes with the ability to detect other gel problems. This phenomenon was shown to be a result of ionic depletion at the gel-liquid interface. The decline was ameliorated by adding denaturant and acrylamide monomers to the buffer reservoirs. Sample-induced problems were shown to be due to the presence of template DNA; elimination of the template allowed sample loading to occur without complications. The improved samples permitted multiple consecutive DNA sequencing runs on the same capillary.

1 Introduction

In the 1930s, Tiselius [1] inaugurated the modern science of electrophoresis with an elegant series of experiments in a tube apparatus. Tiselius showed that protein molecules from human serum could be separated in free solution on the basis of differences in charge and mass, under the influence of an electric field. In free zone electrophoresis, Joule heating causes convective disturbances, which severely reduce resolution. To overcome this problem, many workers employed solid supports, namely paper, starch, cellulose acetate, agarose and polyacrylamide. An exciting alternative has been popularized recently by Jorgensen and Lukacs [2], capillary zone electrophoresis (CZE, also called capillary electrophoresis – CE, and high performance capillary electrophoresis – HPCE). The high surface-to-volume ratio of micro-bore (25–100 μm i.d. typically) fused silica capillaries obviates the need for an anticonvective medium, and allows for efficient electrophoretic separations in free solution. The high surface-to-volume ratio also provides a rapid transfer of Joule heat generated during electrophoresis. This has allowed investigators in the last decade to increase the electric fields used for separations. Recent work has demonstrated that the high voltages used in capillaries (typically 10–30 kV) can produce both rapid separations and outstanding resolution [3]. Additionally, the use of capillaries has promoted electrophoresis into an instrumental technique. Capillary electrophoresis is now a true counterpart to high performance liquid chromatography and gas chromatography, the more traditional automated analytical methods [4].

The Human Genome Project has created a need for sophisticated tools to perform DNA sequencing. The potential for capillary electrophoresis to lessen the labor involved in conventional sequencing methods has been shown recently by several groups [5–7]. Sequencing DNA in capillaries depends upon augmenting the free solutions used in CZE with a sieving matrix – capillary gel electrophoresis (CGE). A suitable DNA sequencing gel system must be capable of resolving fragments differing in length by only one nucleotide. Polyacrylamide gel electrophoresis was first described in the early 1960s [8–10]. About a decade later, Reijnders [11] began using urea and high temperatures to denature RNA. Also popular at this time were gels based on the nonaqueous solvent formamide [12]. Formamide gels showed promising results for RNA, but faded from popularity [13]. The work of Maxam and Gilbert [14] and of Sanger [15], in the late 1970s, both relied on denaturing urea slab gels for DNA separations. The use of thin slab gels (0.4 mm thick) for DNA sequencing was first introduced by Sanger and Coulson [16] in 1978. Ansorge [17] and Smith [18] have been having success recently with gels only 10–100 μm in thickness. The advantages proposed for thin slab gels are exactly those of capillaries, *i.e.*, increased speed and better resolution, due to enhanced heat dissipation [19]. There are some major problems to be overcome in the automation of thin slab techniques. The thickness of glass plates precludes the rapid heat transfer possible in capillaries. A decided advantage of thin slab gels over capillary gels is the ability to run multiple samples in parallel, in a simple geometry.

Correspondence: Dr. Harold Swerdlow, 6160 Eccles Genetics Bldg., University of Utah, Salt Lake City, UT 84112, USA

Abbreviations: TBE, Tris-borate EDTA buffer; UDG, uracil DNA glycosylase

0173-0835/92/0808-0475 $3.50+.25/0

Capillary gel electrophoresis had its roots in experiments of Edström [20] and Matioli and Niewisch [21] in the 1950s and 1960s. They performed separations on 5–50 μm diameter polymer fibers. In 1983, Hjertén [22] reported protein separations in 150 μm i.d. capillaries filled with polyacrylamide. Capillary gel electrophoresis in the more recent past has been popularized by Karger [23–26], in numerous reports of separations of both proteins and nucleic acids, on polyacrylamide gels. Karger has reported the highest known efficiency of any separation method, 15 million theoretical plates for a 160 mer oligonucleotide [23]. Gesteland's, Smith's and Karger's groups showed that capillary gel electrophoresis could successfully be used for separation of products from DNA sequencing reactions [5–7].

The adaptation of capillary gel electrophoretic techniques to DNA sequencing has been hampered by the difficulty of pouring gels and by the instability of the medium during prolonged runs at high voltage [5, 6, 27–30]. Reproducible pouring of capillary gels appears to have been solved by many researchers using polymeric additives [30], high pressure during polymerization [31], alternative polymerization methods [32], and good laboratory practice [5, 6, 23, 27, 30, 33]. Gel instability during electrophoresis can be observed by a decrease in current (at constant voltage) [6] and by a loss of resolution [5, 7, 23, 28]. It is usually accompanied by production of bubbles near the injection (negative) end of the capillary gel. These bubbles can be visualized by examination under a microscope [28, 29].

Solutions that have been employed to increase gel stability include use of a bifunctional reagent (usually 3-methacryloxypropyl-trimethoxysilane) [6, 7, 23, 27, 30, 34] to secure the gel to the capillary wall, limiting the electric field during electrophoresis to 300 V/cm or less [5–7, 23, 27, 29] and trimming the injection end of the capillary to remove the damaged portion of the gel [5, 7, 27]. The use of gels attached to the silica surface of the capillary has allowed researchers to perform remarkable separations; however, the resolution benefits of higher electric fields have remained elusive [29]. This is partly a result of gel instability. The common practice of trimming the injection end of the capillary virtually eliminates any possibility of automating the technique. This provides a major stumbling block to application of capillary gel electrophoresis to large-scale DNA sequencing endeavors, such as the Human Genome Project.

In reports in which 50 or more runs were performed on a single capillary, the samples used were oligonucleotides or mixtures of oligonucleotides [23, 27, 33, 35]. The use of DNA sequencing samples creates additional problems [5–7, 28, 36]. Stability of the gel is reduced and the resolution for subsequent separations is compromised. Attempts to load increasing amounts of such samples, in order to increase the readability of the sequence, resulted in diminished resolution and reproducibility, especially for large molecular weight fragments [6, 28]. Often, the gel must be trimmed immediately after injection of the sample [5, 7, 36]. Full automation of capillary DNA sequencing technology would benefit substantially from the ability to load and analyze multiple samples on a single gel-filled capillary. The complications which arise from loading real samples preclude this possibility.

To our knowledge, consideration of the fundamental processes causing gels to fail has not yet been reported. Basic experiments are described here addressing these issues. Solutions to the key instability phenomena have been achieved. This has allowed multiple DNA sequencing runs with highly concentrated samples on a single capillary, without trimming the end of the capillary, and without a decrease in the current passing through the capillary at constant electric field.

2 Materials and methods

2.1 Apparatus

The apparatus employed for capillary electrophoresis was essentially as described [5], with a few modifications. A 0.75 mW green helium-neon laser (543 nm Melles-Griot, Irvine, CA) was focused by a 6.3 × microscope objective for excitation. Fluorescence was collected with a 20 × 0.4 numerical aperture microscope objective and passed through a spatial filter followed by a 610 nm center wavelength, 10 nm bandwidth interference filter and an OG-590 colored glass filter (Omega Optical, Brattleboro, VT). A Hamamatsu (Bridgewater, NJ) R1477 photomultiplier tube was employed to detect the emitted light. The photomultiplier signal was converted from current to voltage, passed through a 1 Hz analog low-pass filter and digitally sampled at 2 Hz. Electric field was set with three significant figure precision by applying a digital multimeter to the voltage monitor output of the high voltage power supply (MJ30N0400, Glassman instruments, Whitehead Station, NJ). The analog meters on most power supplies are not precise enough for studies of gel stability. Current was monitored as voltage, measured across a 1 Mohm resistor placed in series with the capillary at the grounded (+) side of the high voltage circuit. The current signal was low-pass filtered at 0.7 Hz and digitally sampled at 1 Hz. A 12-bit analog-to-digital converter was used to allow at least three significant figures on measurements of current (better than 0.01 μA precision).

2.2 Gel preparation

Urea gels were made from 89 mM Tris-borate–2 mM EDTA buffer, pH 8.3 (1 × TBE), with 7 M urea (ultra pure, BRL, Gaithersburg, MD), 5.7% acrylamide, 0.3% *N,N'*-methylene bisacrylamide (19:1 premixed electrophoresis purity, Bio-Rad, Richmond, CA), 0.05% w/v ammonium persulfate and 0.05% v/v *N,N,N',N'*-tetramethylethylenediamine (TEMED) (electrophoresis purity, Bio-Rad). Formamide gels consisted of 1 × TBE buffer, 50% formamide (ultra pure, United States Biochemicals, Cleveland OH), 5.7% acrylamide, 0.3% *N,N'*-methylenebisacrylamide, 0.15% w/v ammonium persulfate and 0.15% v/v TEMED. The polymerization solutions were degassed with an aspirator for 20 min prior to addition of the initiator and catalyst. Fused silica capillaries (50 μm i.d., 375 μm o.d. Polymicro Technologies, Phoenix, AZ) were used without any pretreatment and were filled with the monomer solution by a syringe. Shrinkage was measured by polymerization of 10 mL of gel in a 10 mL pipette.

2.3 Running buffers and preelectrophoresis

Running buffers consisted of 1 × TBE or 1 × TBE with 50% formamide and added acrylamide monomers (4–5%T = total acrylamide concentration of 4–5% w/v were used with 5%C = a crosslinking concentration of 5% w/w or an acrylamide:*N,N'*-methylenebisacrylamide ratio of 19:1). Before running, both ends of the capillary gels were trimmed with a sapphire cutter (Lee Scientific, Salt Lake City, UT) and examined under water with a microscope to insure that bubbles were not introduced while cutting. This step was found to be essential for producing accurate, reproducible results with the gel stability experiments described here. All gels were prerun for 2 h at 100–150 V/cm before loading samples or performing stability experiments.

2.4 Sample preparation

Samples were prepared as described [5] using 7.3 µg of Amber m13mp11 control DNA containing uracil (Bio-Rad special order # 999-1412-001; concentration was estimated from the optical density of the solution at 260 nm). The primer employed was an 18-nucleotide-long m13 universal primer (–21) fluorescently tagged with the ROX fluor–610 nm maximum emission (Applied Biosystems, Foster City, CA). Sequenase version 2 (United States Biochemicals) was used for all reactions. After ethanol precipitation, the samples and controls were dissolved in 70 µL uracil DNA glycosylase (UDG) buffer (70 mM Hepes-KOH, pH 8.0, 1 mM dithiothreitol, 1 mM EDTA) [37]. To the samples, 5 µL of UDG (Bethesda Research Laboratories) was added while the controls received 5 µL of 50% glycerol. After a 2 h incubation period at 37°C the samples were brought to pH 10 by the addition of 1 N KOH and heated to 94°C for 10 min. They were then subjected to phenol extraction and ethanol precipitation, and dissolved in 4 µL of loading buffer (10 mM EDTA, pH 8.0, 98% formamide). Samples were heated to 94°C for 2 min and loaded electrokinetically, by lowering the electrode and capillary into the sample, for 10 s at 150 V/cm.

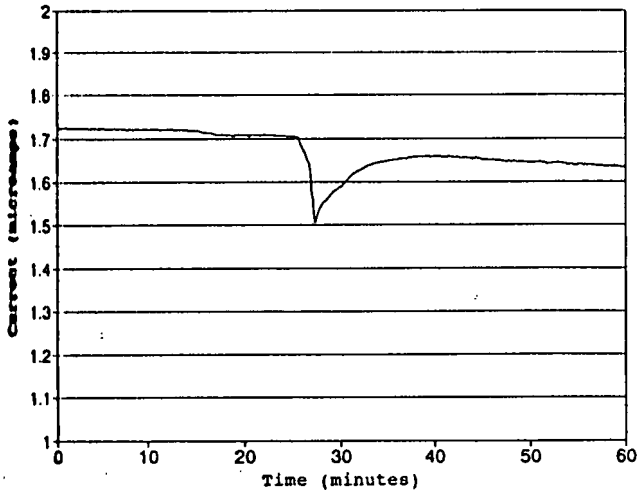

Figure 1. Typical current *vs.* time graph for a bubble. The current is monitored at a constant electric field of 150 V/cm. After the prerun, the current should be stable. The 6%T, 5%C urea gel was electrophoresed in standard 1 × TBE buffer as described in Section 2.2 for urea gels. Data shown are a seven-point moving average of the original 1 Hz current data.

2.5 Electroosmotic mobility measurements

Measurements of electroosmotic mobility were performed on a Beckman P/ACE capillary electrophoresis instrument (Beckman Instruments, Palo Alto, CA). A cartridge was assembled using 57 cm of the same 50 µm i.d. capillary that was used for gel experiments. Riboflavin was dissolved at 100 µg/mL in running buffer (either 1 × TBE with 7 M urea or 1 × TBE with 50% formamide) and was injected with pressure for 5 s. Electrophoresis was under normal polarity for capillary zone electrophoresis (injection end positive), at 11.4 kV = 200 V/cm; UV detection was employed at 254 nm. Electrophoretic mobility (µ = velocity / electric field) was calculated simply as the distance to the detector (50 cm) divided by the retention time in seconds and by the electric field in V/cm.

3 Results and discussion

3.1 Phenomena of gel breakdown

Representative examples of the phenomena being studied are illustrated in Fig. 1–3. Graphs of capillary current *vs.* time are shown, under a constant applied electric field. A 2 h prerun is performed to remove ions remaining from polymerization. After this prerun, the current through a capillary gel should stabilize. Additionally, the cross section of the gel and its resistivity remain constant for a given gel/buffer recipe. Ohm's law predicts that the current should then be constant from run to run.

Figure 1 depicts the typical type of bubble that appears at the injection end of the capillary. The bubble dramatically increases the local resistance of the capillary and produces a small increase in the resistance of the entire gel. There is a sudden precipitous drop in current, followed by a rise in current to a level somewhat below the starting value. Since the region containing the bubble has a higher resistivity than the remainder of the capillary, Joule heating is locally increased, leading to formation of additional bubbles and eventually to a catastrophic breakdown of the gel. If the

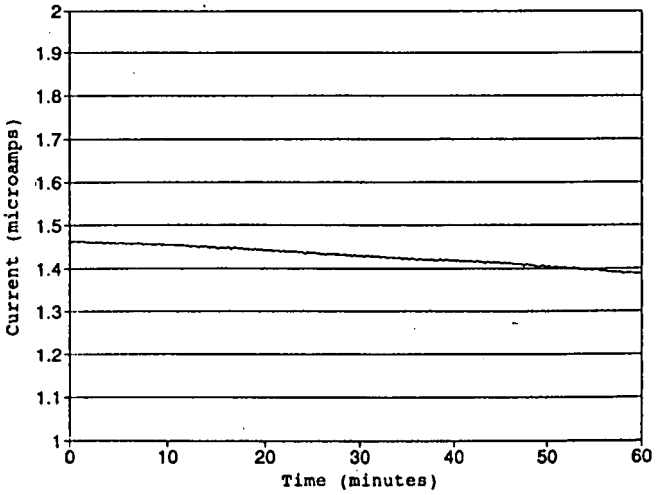

Figure 2. Current *vs.* time graph showing a typical steady decrease. All conditions were as described in the legend to Fig. 1. The data, taken for 1 h about 2 h into the run, are a seven-point moving average of the original 1 Hz current data.

damage is minimal in extent, removal by trimming the injection end of the capillary can often be accomplished satisfactorily.

The slow decline in current visible in Fig. 2 is seen in all types of gels we have studied. This phenomenon could easily be overlooked. The decline does not appear to be a major contributor to loss of resolution or to major catastrophic breakdown of the gel; however, if the gel is run continuously for long periods of time, gel stability will suffer. This effect is of interest because it confuses the analysis of other sources of gel breakdown. The increased gel resistance is local to the injection end of the capillary and can be ameliorated by trimming that end of the gel (data not shown). It is therefore not a bulk degradation process of the gel matrix. It is also not attributable to buffer changes brought on by electrophoresis.

Using fairly concentrated DNA sequencing samples, a third gel anomaly can be observed. Immediately after loading, the samples induce a rather large drop in current through the capillary (Fig. 3). This current decrease is often accompanied soon thereafter by formation of bubbles (see arrows). Correction of the problem can be accomplished by trimming a small portion of the injection end of the capillary (see Fig. 3), and proceeding with the run (typically 1–3 mm will suffice, if the gel is trimmed within the first min). This phenomenon limits the amount of DNA that can be loaded onto a capillary gel, thereby limiting signal and readability of the sequence. Resolution and run-to-run reproducibility are probably affected by sample overloading in slab gels as well as capillary gels.

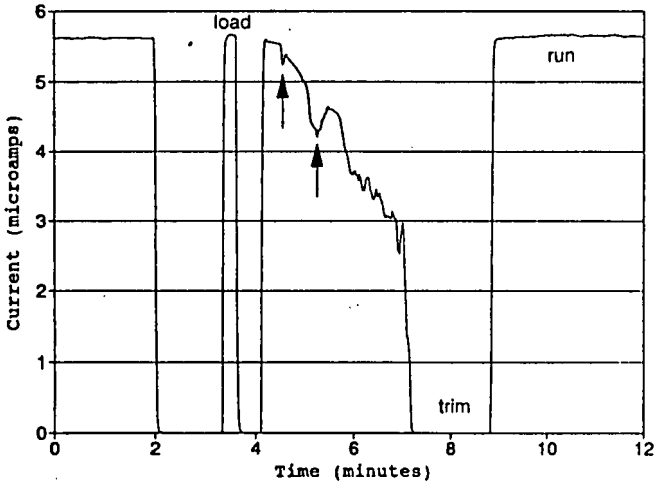

Figure 3. Sample-induced drop in current. The gel was a 30.1 cm 50% formamide, 6%T, 5%C gel, run in 1 × TBE, 50% formamide, 4%T, 5%C acrylamide monomers at 200 V/cm as described in Section 2.2. Data shown are a seven-point moving average of the original 1 Hz current data. The gel was run for 2 min to verify stability. The voltage was turned off, and a UDG "-"-control sample (containing template DNA) was loaded for 15 s at 200 V/cm ("load"). The running buffer was replaced, and the voltage was turned on. Two bubbles that formed soon afterwards are indicated by the arrows. After 3 min of running, the current had dropped to 1.27 μA, or 23% of its starting value. At this point, the voltage was turned off, and 3.2 cm of the gel was trimmed as described ("trim"). The voltage was reapplied at 200 V/cm, and the current was shown to be steady ("run").

All of the observed gel breakdown phenomena limit the ability to reuse the gels for DNA sequencing, especially in an automated fashion. For shorter runs and for oligonucleotide samples, the phenomena described above may not be as serious.

3.2 Bubbles

The onset of a bubble at the injection end of the capillary during electrophoresis appears to occur randomly in time. This complicates analysis of the underlying cause(s) of this problem. Nonetheless, the possible role of electroosmotic force in bubble production can be considered. Electroosmotic force arises as a result of the presence of negative charges on the capillary inner wall, due to ionization of surface silanol groups by the aqueous buffer. Electroosmotic force is directed from the positive to the negative end of the capillary due to the excess of cations in the mobile phase of the double layer [38]. Although a gel-filled capillary provides a substantial hydrodynamic resistance, thereby essentially eliminating electroosmotic flow, the force remains. At the negative (injection) end of the capillary gel, the electroosmotic force is no longer balanced by gel-silica adhesion, and the matrix may therefore be especially susceptible to damage. A displacement toward the negative electrode (*i.e.*, out of the capillary) of a small portion of the gel could lead to the formation of a bubble in its wake. Even a small defect in the gel will cause localized heating of the capillary and, possibly, the production of a bubble.

Evidence for this model stems from the observation that the occurrence of bubbles can be shifted from the injection end to the detection end of the capillary using a surfactant (data not shown). This reagent, cetyltrimethylammonium bromide (CTMAB) [39], is known to reverse the direction of electroosmotic flow in capillary electrophoresis. Using a three-day-old gel, voltage was applied until a bubble formed, as demonstrated by a sudden drop in current. Restoration of current through the capillary occurred when a portion of the injection end was cut. When the same gel was equilibrated in running buffer supplemented with 1 mM CTMAB, current was restored by trimming the detection end. This concentration of CTMAB was much higher than the concentration known to cause reversal of electroosmotic flow (about 50 μM) [39].

In addition to the bubble problem discussed above, it is well known that gels can extrude from capillaries at high voltages [27]. This phenomenon has also been attributed to electroosmotic force. It is not a simple matter to eliminate electroosmotic force in a reproducible, stable manner. One approach to solving this problem, first employed by Karger's group, has been to covalently link the gel to the wall of the capillary using bifunctional silane compounds [6, 7, 23, 27, 30]. The coating employed does not eliminate the electroosmotic force but provides a gel-capillary interaction to oppose it. The silane coupling is fairly unstable under the conditions normally used for DNA sequencing, pH 8.3–9.0 [40]. Additionally, the gels which are attached to the wall of the capillary are somewhat difficult to pour, as tears develop in the gel matrix as the gelling solution shrinks during polymerization [31]. Further improvements on this methodology have been described. Novotny's group [40] replaced the standard siloxane linkage (Si-O-Si-C) with more

stable (Si-C) bonds, increasing the ability of the coating to withstand hydrolysis at elevated pH. Hjertén [41] published a method for eliminating electroosmotic flow by coating the wall of the capillary with a linear polyacrylamide monolayer. As demonstrated by Schomburg's group [27], a capillary coated in this manner can support a polyacrylamide gel without inducing tears in the gel upon polymerization. The application of Novotny's novel silane linkage to Schomburg's method of preparing gels could further increase gel stability by decreasing bubble production.

Another approach to increasing gel stability has been to change the physical properties of the matrix. Whatever the source(s) of stress in the gel material, softening of the gel should allow it to deform to relieve this stress without tearing. Karger [30] has added hydrophilic polymers to eliminate the bubbles produced by use of the bifunctional silane reagent. He has demonstrated a concomitant improvement in the ability of these gels to withstand high voltages. We have attempted a different solution, using an organic solvent to plasticize or soften the gel [42]. An obvious choice for such a solvent was formamide. Formamide has been used in the past in gels to denature nucleic acids, usually RNA [12, 43–45]. The results of a direct comparison between a 7 M urea-containing gel and a 50% formamide-containing gel are shown in Fig. 4. The traces in this figure represent current profiles, at constant electric field, from two consecutive 2 h runs with both gels. The formamide-containing gels routinely give higher current, primarily a result of ionic breakdown species in the formamide buffers, although these gels also have a larger effective pore size [12]. The higher inherent instability of urea gels is clearly indicated by their erratic current toward the end of each run. Formamide gels were found to be very stable at 150–200 V/cm and, interestingly, resistant to extrusion of the gel from the capillary at higher voltages (data not shown) [27]. To determine the origin of the stability and extrusion resistance of formamide gels, electroosmotic flow rates were measured and compared for the buffers containing formamide and urea. The electroosmotic mobility (velocity/electric field) was measured using a neutral riboflavin marker in a capillary zone electrophoresis instrument [46]. The electroosmotic mobility in the 1 × TBE, 7 M urea buffer was found to be 2.7×10^{-4} cm²/V·s, while for the 1 × TBE, 50% formamide-containing buffer the value obtained was 2.1×10^{-4} cm²/V·s. This small difference in electroosmotic mobility cannot explain the observed results. The large increase in stability of formamide gels at high voltages is probably due to the less brittle nature of formamide solvated polyacrylamide chains [12].

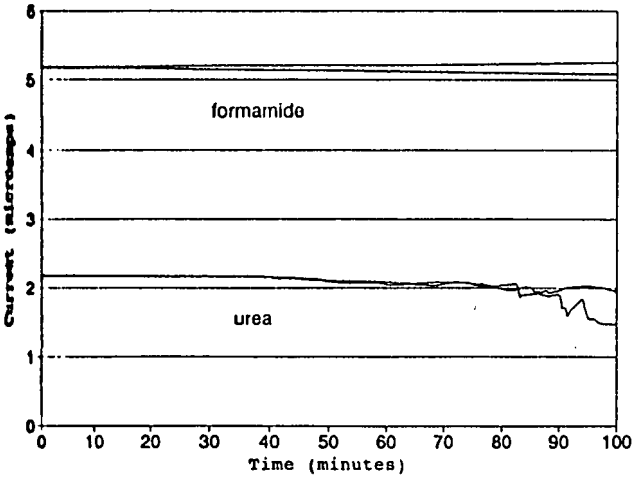

Figure 4. Current profiles for formamide and urea gels. Preparation of the gels was as described. Both gels were run in 1 × TBE running buffer at 200 V/cm. After an initial prerun, and between runs, both ends of both gels were trimmed to eliminate bubbles. The higher current seen in the formamide gel is probably due to the presence of ionic breakdown products in the formamide-containing buffer.

3.3 Declining current

The steady decline in current in a capillary gel run at constant voltage (Fig. 2) can be attributed to the difference between the gel environment and that of the running buffer. The model for the current decline depends on depletion of ions at the injection-end, liquid-gel interface. Depletion of ions is due to the difference in transference (or transport) numbers of the ions between the gel and the buffer. The transference number, an electrochemical property of solutions, is a measure of the fraction of the total electrical current carried by each ionic species [47]. The transference number for a given ion can change, depending on its organic environment [48]. In a standard DNA sequencing gel, the gel itself contains polyacrylamide and urea, while the running buffer contains only 1 × TBE. If the transference number for H^+ cations is greater in the running buffer than in the gel, H^+ ions will migrate to the cathode from the gel in a higher proportion than they are being transported through the gel from the anode. This will deplete the H^+ ions at the injection (cathode) liquid-gel interface. Similarly, since the sum of transference numbers for all ions is 1, the anions will have a greater transference number in the gel than in the buffer, causing more ions to move away from the same interface than are moving toward it. The anions will also be depleted at the injection end of the gel. The net result is a local decrease in current carrying species, an increase in local electrical resistance and an overall decrease in current through the capillary. At the opposite end of the capillary, the ions will be accumulating at the liquid-gel interface, producing a region of lower resistance than the rest of the gel. This accumulation will not change the total resistance of the gel significantly, and therefore will not be observed.

Support for this model is based upon several facts: (i) Depletion potentials are well described at liquid-liquid interfaces in electrochemistry [49]. (ii) The kinetics, on the order of hours, are similar to what is expected [50]. (iii) The effect is confined to the tip of the capillary, *i.e.*, it is not due to a bulk condition of the gel or the buffer. If the injection end is trimmed, the current can be restored. (iv) The phenomenon is observed only at the injection-end interface. If the detection end is trimmed, there is no observable increase in current. (v) After a significant drop in current, there are no bubbles visible upon microscopic examination of the entire gel. (vi) The decrease in current is reversible; either by switching polarity on the gel, or by allowing the ions to diffuse for several hours without an electric field applied.

A solution to this problem might be to add denaturant and polymer to the running buffer to match transference numbers with that of the gel; however, crosslinked polymer cannot be incorporated into the running buffer without complicating the loading of samples. If denaturant and acryl-

amide monomers are added to the running buffer, in the same concentration as in the gel, it is found that the conductivity does not quite match that of the gel. An assumption that can be made from this observation is that the transference numbers of the buffer and the gel are still unequal. To offset the effect of polymerization, a lower percentage of monomer is used in the buffer than the gel polymer percentage. The measured percentage of shrinkage for a 6%T, 5%C gel was found to be 1.6% (see also [31]). Using this shrinkage value, and the density of acrylamide (1.122 g/cc), the volume fraction occupied by acrylamide was calculated for a 6% polyacrylamide gel, and found to be equal to a 4.2% monomer solution. Empirically, the conductivity of a 4–5% acrylamide monomer solution matches that of a 6% polyacrylamide gel (19:1 acrylamide:bisacrylamide).

Figure 5 shows the effect of these buffer additives on the current profile of a gel containing formamide. The direct comparison, under constant electric field, of a 6%T, 5%C gel run in standard 1 × TBE and one run in 1 × TBE, 50% formamide, 5%T, 5%C acrylamide monomers is shown after an initial prerun. The slopes of the current *vs.* time graphs of Fig. 5, obtained by fitting a straight line to the observed data, are 720 pA/min for the 1 × TBE buffer, and 120 pA/min for the buffer containing formamide and acrylamide. The current through the gel in the latter buffer may actually increase with time, due to breakdown of formamide to formic acid and ammonia.

3.4 Sample effects

The sudden drop in current depicted in Fig. 3 has been attributed, by sample reconstruction experiments, to the presence of template DNA in the sequencing reaction. In order to observe this effect, fairly concentrated samples are used (5 µg = 2 pmoles of m13 single-stranded DNA in 4 µL of loading buffer or 0.5 µM DNA). Concentrated template DNA, by virtue of its very low electrophoretic mobility in a gel, probably creates a region of high electrical resistivity.

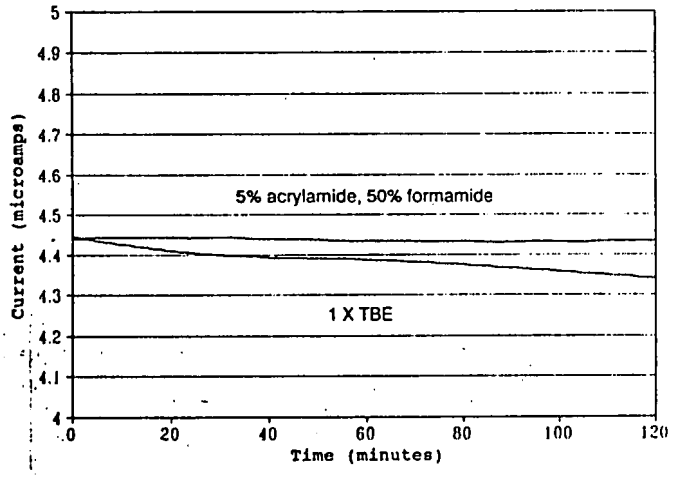

Figure 5. Buffer additives improve gel stability. Two formamide gels were run simultaneously in different buffers at 200 V/cm. The lower trace corresponds to a gel run in 1 × TBE. The buffer used for the upper trace contains, in addition, 50% formamide and 5%T, 5%C acrylamide monomers. For the sake of comparison, the lower trace has been shifted upward 2.55 µA; the initial current for the lower trace was 1.89 µA, while the upper trace started at 4.44 µA. Runs were for 2 h following a 2 h prerun. The data shown are a seven-point moving average of the initial 1 Hz data.

Such a region could cause the observed sudden sharp drop in the current passing through the capillary and increase local heating. If this condition is not corrected immediately, secondary bubbles soon produce irreversible damage to the gel. The effect can be corrected by trimming a small region of the injection end of the gel soon after loading, or reduced by reversing the polarity of the power supply briefly. The gel instability, created by the DNA template, is dependent upon its size (in the same volume, 5 µg quantities of smaller double-stranded DNA fragments, 72–1353 base pairs in length, do not produce the phenomenon), and its concentration (less is better). It is not known whether increased local resistance is due to the low mobility of large template molecules, or if it is the result of large DNA clogging the polyacrylamide gel pores.

Our attempts to solve this problem by reduction of the mass of template DNA used in a sequencing reaction, by cycle sequencing [51], or elimination of the template after the reaction, using magnetic bead technology [52], have met with limited success. We have turned to a method based on *E. coli* UDG [37]. UDG is an enzyme that edits DNA, to eliminate occasional uracil residues, which may be inadvertently incorporated by DNA polymerase, or produced by deamination of cytosine [53]. In a cell line deficient in both UDG and deoxyuridine 5′-triphosphate nucleotidohydrolase (ung⁻ dut⁻), a large number of uracil residues (normally associated with RNA) are incorporated into replicated DNA in place of thymidines [54, 55]. Phage or plasmid DNA, replicated in this strain, will also contain a large number of uracil residues. A sequencing reaction was performed using uracil-containing m13 single-stranded

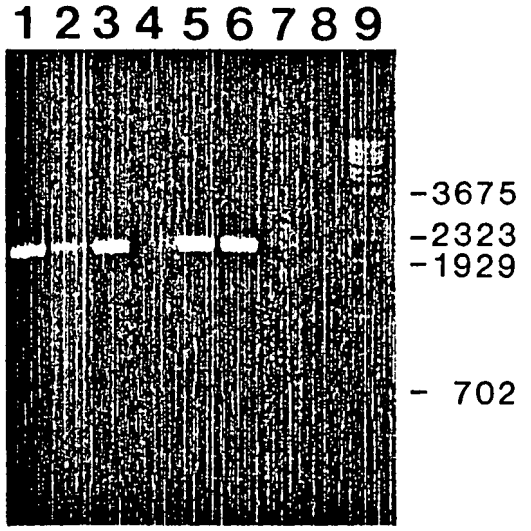

Figure 6. Samples of UDG-cut DNA run on a 1% agarose, 1 × TBE ge Single-stranded m13 DNAs, about 7250 base pairs long, migrate as if they were a 2000 bp double-stranded DNA. Markers (lane 9) are lambda DNA cut with *Bst*EII, sizes are indicated on the right. All samples contain 1 µ of m13 DNA and were treated as described in Section 2.4. Lanes (1), (3) (5) and (7) are control reactions. Lanes (2), (4), (6), (8) are depyrimidi nated with UDG. Lanes (1) and (2) contain uracil DNA treated with UDG only. Lanes (3) and (4) were additionally treated with high pH a high temperature. Lanes (5) and (6) were m13mp18 control DNA add tionally treated with high pH and high temperature. Lanes (7) and (8 were DNA sequencing reactions performed with uracil DNA and treated additionally at high pH and high temperature. The smearing of the DNA in lane (7) is probably attributable to residual protein and/or salt in the se quencing samples.

DNA template and standard DNA monomers. Thus the template DNA alone is susceptible to depyrimidination by the UDG enzyme. A similar scheme has been used to eliminate polymerase chain reaction (PCR) carry-over contamination [56]. Lanes 1–2 of Fig. 6 show the agarose gel pattern of uracil-containing DNA, without and with treatment with UDG. Lanes 3–4 represent the same samples, additionally incubated at high temperature and high pH, following the UDG treatment. In the same experiment, m13 control DNA (containing only thymidine) was unaffected by the UDG, high temperature, and high pH procedure (lanes 5–6). The results of performing the complete UDG protocol on an actual DNA sequencing reaction are shown in Fig. 6, lanes 7–8. The reactions were prepared using uracil-containing m13 DNA and fluorescent primers; the hydrolysis of the template DNA to small fragments of widely varying sizes can be seen in lane 8.

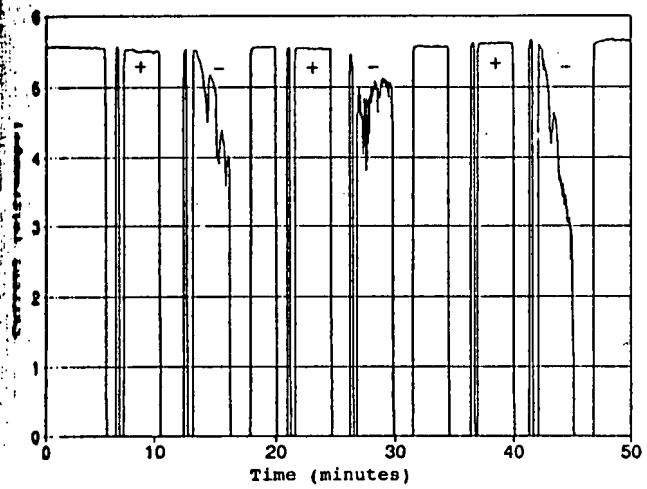

Figure 7. Current profiles for repetitive sample loadings with and without UDG treatment. The formamide gel was run in 1 × TBE, 50% formamide, 4%T, 5%C acrylamide monomers at 200 V/cm. Samples were loaded for 15 s at 200 V/cm. Samples were treated as described in Section 2.4. The "+" samples were treated with UDG and contain virtually no detectable intact template DNA; "–" samples were control reactions containing template DNA. The interpretation of these current profiles is described in the legend to Fig. 3. The gel was trimmed each time, after running the "–" samples for 3 min.

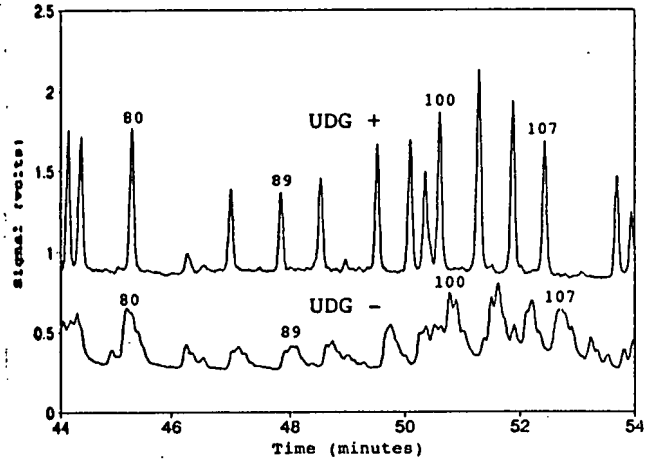

Figure 8. Comparison of signal from sequencing reactions with and without UDG treatment. The formamide gel was run in 1 × TBE, 50% formamide, 5%T, 5%C acrylamide monomers at 150 V/cm. Samples were loaded for 10 s at 150 V/cm. The upper trace represents the UDG-treated sample, while the lower trace was a control reaction. Template DNA has been essentially eliminated in the sample corresponding to the upper trace. Sequence is shown for the dideoxy TTP reaction only. The detection scheme is described in Section 2.1. The ordinate, measured in volts, represents arbitrary units of fluorescent light intensity. Representative peaks are numbered according to the length of DNA, including the primer. Time is measured from injection.

The sequencing reactions shown in Fig. 6 were loaded onto a capillary gel, as shown in Fig. 7. The current profiles of 6 loadings are shown, three with the UDG-treated sample (+) and three with the control sample, containing intact template DNA (–). The UDG treatment overcomes the problem of the presence of template DNA in the sample. The separation of the same two reaction products on a formamide gel-filled capillary was compared. Results are shown in Fig. 8. There is a loss of both signal and resolution

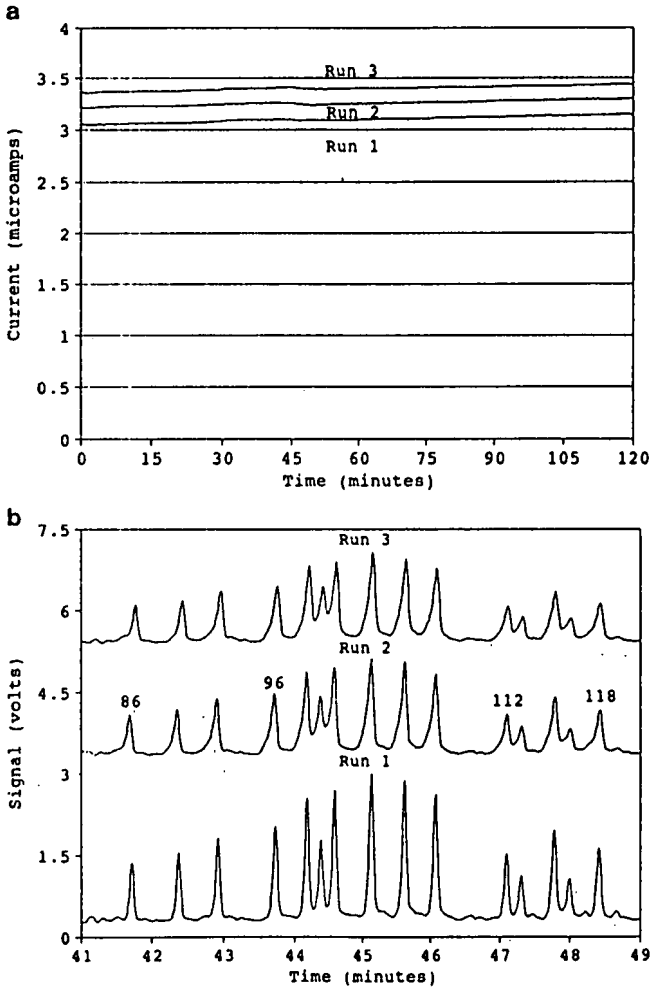

Figure 9. Current and signal profiles from multiple runs on a single gel-filled capillary. The formamide gel was run in 1 × TBE, 50% formamide, 5%T, 5%C acrylamide monomers at 150 V/cm. The UDG, high pH, high temperature sample was loaded for 10 s at 150 V/cm. No trimming of the capillary gel was performed either during or after the runs. After each run (3 h), the next sample was loaded on the gel. (a) 2 h current profiles from each of the 3h long runs. The current steadily increased during the three runs due to formamide hydrolysis. Data displayed are a seven-point moving average of the original 1 Hz data obtained about 15 min after sample injection. (b) Signal obtained from the three consecutive runs. The sequence shown is a dideoxy TTP reaction prepared and detected as described. The traces for runs 2 and 3 have been offset by 3 and 5 V, respectively, for clarity. The time axes have been shifted by less than 1/2 min to align the traces.

visible for the sample containing intact template DNA (–). Other investigators have also noted decreased signal [57] or resolution [6] associated with overloading. The reduction or elimination of template DNA will allow an increase in the amount of sample that can be loaded onto a capillary gel, and should therefore simultaneously improve gel stability, signal-to-noise ratios, resolution, and accuracy of DNA sequencing.

3.5 Multiple runs

The ability to load multiple DNA samples sequentially on a single capillary, without trimming the end of the capillary, has eluded us for some time. Figure 9 displays the profiles of (a) the current and (b) the signal from three consecutive runs on a single capillary gel. The formamide gel was run in a buffer containing 50% formamide and 5% acrylamide monomers. The sample was treated with UDG and high pH/high temperature before loading. Increased stability of the gel is visible from the traces in Fig. 9a; during 9 h of continuous electrophoresis the current increased slowly, rather than dropping. This current increase is probably a result of formamide breaking down into ionic species. There is a significant loss in signal and resolution from the first to the third loading. This may be a result of traces of large DNA species present in the sample, which accumulate in the capillary. The resolution and the current degraded rapidly during the fourth run (data not shown). We are currently pursuing the use of other methods for sample production, either alone or in concert with the UDG procedure to improve the gel stability and resolution for extended multiple runs.

4 Concluding remarks

The practice of sequencing DNA on capillary gels promises faster, more accurate determination of sequence, and resolution further out than slab gel data [3, 5]. The speed of single capillary runs is certainly higher than conventional slab gel separations; however, the throughput of a multiple-well slab gel system is probably still greater [29]. Further improvements in gel stability will increase speed by allowing gels to be run at higher voltages, increasing single capillary sequencing rates. Beyond this point, improvements in capillary sequencing throughput will certainly require an instrument capable of running multiple capillaries simultaneously. The latter will also require stable, reproducible gels. Instrument efficiency will improve substantially if gels can be reused, reducing the time of pouring and setting up gels. In order to reuse gels, reproducibility of sample injections will need to be improved. The methodology reported here may help improve run-to-run reproducibility, and propel capillary gel electrophoresis with actual DNA sequencing samples into a useful analytical technique.

Sequencing accuracy is dependent on large signals and minimal noise. One way to achieve this is the design of better detectors, such as the sheath flow cuvette-based instruments employed by Dovichi's group [36]. Another approach relies on loading more sample, as addressed in this study. A third possibility is the design of better fluors and more efficient sequencing reactions [51, 58].

Resolution of capillary gels has been shown to be better than conventional slab gels, at least for the first few hundred nucleotides [5, 29]. The ability to clearly resolve peaks beyond about 300 nucleotides in length has been somewhat elusive. At least three factors may contribute to the observed loss in resolution. As shown on slab gels, resolution between consecutive peaks decreases inversely with the number of bases [59]. This occurs because the time between peaks passing a fixed point is nearly constant, while the peak width, in time, increases for large molecules. Secondly, the alignment of double-stranded DNA molecules in an electric field limits resolution for large species on agarose gels [60]. This so-called "reptation with stretching" phenomenon is exacerbated by high electric fields, and limits the fields that can be used. A similar mechanism may account for the poorer resolution seen for large single-stranded DNA species, on polyacrylamide capillary gels, when compared to slab gels run at lower electric fields. Gel instability is a third source of resolution loss on capillary gels. The elimination of this latter problem should improve capillary gel methodology.

The results reported here for gels in uncoated capillaries can almost certainly be improved by incorporating recent advances in capillary and gel preparation technology [27, 30, 40]. Having reduced some of the major problems limiting gel stability, optimization of capillary coatings, testing other gel recipes, and consideration of alternative polymers can more easily be accomplished. Further, the origin and nature of the injection-end bubbles still needs to be addressed more systematically.

Note that some of the techniques reported in this paper may be applicable to slab gels. In particular, we are looking into the use of buffer additives to stabilize slab gels run for long periods of time. In addition, we are attempting multiple runs on a slab gel-based automated sequencing instrument. The latter improvement would markedly reduce the time and expense of automated fluorescent DNA sequencing technology.

The authors wish to thank Jeff Ives for stimulating discussions and critical review of the manuscript and Robert Weiss and P. Vanysek for advice during the course of the work. Dr. Johann van de Sande kindly supplied a gift of uracil DNA glycosylase. H. S. acknowledges a Graduate Research Fellowship from the National Science Foundation. This work was supported in part by grants from the National Institutes of Health, the Department of Energy, and the Natural Sciences and Engineering Research Council of Canada, and the Howard Hughes Medical Institute.

Received January 9, 1992

5 References

[1] Tiselius, A., *Trans. Faraday Soc.* 1937, *33*, 524–531.
[2] Jorgensen, J. W. and Lukacs, K. D., *Science* 1983, *222*, 266–272.
[3] Karger, B. L., *Nature* 1989, *339*, 641–642.
[4] Eby, M. J., *BioTechnology* 1989, *7*, 903–911.
[5] Swerdlow, H. and Gesteland, R., *Nucleic Acids Res.* 1990, *18*, 1415–1419.
[6] Drossman, H., Luckey, J. A., Kostichka, A. J., D'Cunha, J. and Smith, L. M., *Anal. Chem.* 1990, *62*, 900–903.
[7] Cohen, A. S., Najarian, D. R. and Karger, B. L., *J. Chromatogr.* 1990, *516*, 49–60.

[8] Raymond, S. and Weintraub, L. S., *Science* 1959, *130*, 711–713.
[9] Ornstein, L., *Annals NY Acad. Sci.* 1964, *121*, 321–349.
[10] Davis, B. J., *Annals NY Acad. Sci.* 1964, *121*, 404–427.
[11] Reijnders, L., Sloof, P., Sival, J. and Borst, P., *Biochim. Biophys. Acta* 1973, *324*, 320–333.
[12] Staynov, D. Z., Pinder, J. C. and Gratzer, W. B., *Nature (New Biology)* 1972, *235*, 108–110.
[13] Pinder, J. C., Staynov, D. Z. and Gratzer, W. B., *Biochemistry* 1974, *13*, 5373–5378.
[14] Maxam, A. and Gilbert, W., *Proc. Natl. Acad. Sci. USA* 1977, *74*, 560–564.
[15] Sanger, F., Nicklen, S. and Coulson, A. R., *Proc. Natl. Acad. Sci. USA* 1977, *74*, 5463–5467.
[16] Sanger, F. and Coulson, A. R., *FEBS Lett.* 1978, *87*, 107–110.
[17] Garoff, H. and Ansorge, W., *Anal. Biochem.* 1981, *115*, 450–457.
[18] Smith, L. M., Brumley, R. L., Buxton, E., Drossman, H., Kostichka, A. J., Luckey, J. A. and Mead, D. A., in: *Abstracts, Genome Mapping and Sequencing*, Cold Spring Harbor Laboratory, Cold Spring Harbor, New York 1991, p. 250.
[19] Stegemann, J., Schwager, C., Erfle, H., Hewitt, N., Voss, H., Zimmerman, J. and Ansorge, W., *Nucleic Acids Res.* 1991, *19*, 675–676.
[20] Edström, J. E., *Nature* 1953, *172*, 809.
[21] Matioli, G. T. and Niewisch, H. B., *Science* 1965, *150*, 1824–1826.
[22] Hjertén, S., *J. Chromatogr.* 1983, *270*, 1–6.
[23] Guttman, A., Cohen, A. S., Heiger, D. N. and Karger, B. L., *Anal. Chem.* 1990, *62*, 137–141.
[24] Cohen, A. S. and Karger, B. L., *J. Chromatogr.* 1987, *397*, 409–417.
[25] Cohen, A. S., Paulus, A. and Karger, B. L., *Chromatographia* 1987, *24*, 15–24.
[26] Cohen, A. S., Najarian, D. R., Paulus, A., Guttman, A., Smith, J. A. and Karger, B. L., *Proc. Natl. Acad. Sci. USA* 1988, *85*, 9660–9663.
[27] Yin, H. F., Lux, J. A. and Schomburg, G., *J. High Resol. Chromatogr.* 1990, *13*, 624–627.
[28] Swerdlow, H., Wu, S. Harke, H. and Dovichi, N. J., *J. Chromatogr.* 1990, *516*, 61–67.
[29] Luckey, J. A., Drossman, H., Kostichka, A. J., Mead, D. A., D'Cunha, J., Norris, T. B. and Smith, L. M., *Nucleic Acids Res.* 1990, *18*, 4417–4421.
[30] Karger, B. L. and Cohen, A. S., *US Patent* # 4,865,706 and 4,865,707, 1989.
[31] Bente, P. F. III, Myerson, J., *US Patent* # 4,810,456, 1989.
[32] Lux, J. A., Yin, H. F. and Schomburg, G., *J. High Resol. Chromatogr.* 1990, *13*, 436–437.
[33] Baba, Y., Matsuura, T., Wakamoto, K. and Tsuhako, M., *Chem. Letters* 1991, 371–374.
[34] Radola, B. J., *Electrophoresis* 1980, *1*, 43–56.
[35] Beckman Instruments eCAP U100P product literature, Beckman Instruments, Palo Alto, CA.
[36] Swerdlow, H., Zhang, J. Z., Chen, D. Y., Harke, H. R., Grey, R., Wu, S., Dovichi, N. J. and Fuller, C., *Anal. Chem.* 1991, *63*, 2835–2841.
[37] Lindahl, T., Ljungquist, S., Siegert, W., Nyberg, B. and Sperens, B., *J. Biol. Chem.* 1977, *252*, 3286–3294.
[38] Jorgensen, J. W. and Lukacs, K. D., *Science* 1983, *222*, 266–272.
[39] Altria, K. D. and Simpson, C. F., *Anal. Proc.* 1988, *25*, 85.
[40] Cobb, K. A., Dolnik, V. and Novotny, M., *Anal. Chem.* 1990, *62*, 2478–2483.
[41] Hjertén, S., *J. Chromatogr.* 1985, *347*, 191–198.
[42] Mascia, L., *The Role of Additives in Plastics*, John Wiley & Sons, New York 1974, p. 61.
[43] Gould, H. and Matthews, H. R., in: Work, T. S. and Work, E. (Eds.), *Laboratory Techniques in Biochemistry and Molecular Biology: Separation Methods for Nucleic Acids and Oligonucleotides*, North-Holland Publishing Company, Amsterdam 1976, pp. 350–351.
[44] Helmkamp, G. H. and Ts'o, P. O. P., *J. Amer. Chem. Soc.* 1961, *83*, 138–142.
[45] Maniatis, T. and Ptashne, M., *Proc. Natl. Acad. Sci USA* 1973, *70*, 1531–1535.
[46] VanOrman, B. B., Liversidge, G. G., McIntire, G. L., Olefirowicz, T. M. and Ewing, A. G., *J. Microcol. Sep.* 1990, *2*, 176–180.
[47] Goodisman, J., *Electrochemistry: Theoretical Foundations. Quantum and Statistical Mechanics, Thermodynamics, the Solid State*, John Wiley & Sons, New York 1987, pp. 33–35.
[48] Izutsu, K., Nakamura, T. and Yamashita, T., *J. Electroanal. Chem.* 1988, *256*, 43–50.
[49] Girault, H. H. J. and Schiffrin, D. J., in: Bard, A. J. (Ed.), *Electroanalytical Chemistry*, Vol. 15, Marcel Dekker, New York 1989, pp. 1–141.
[50] Izutsu, K., Nakamura, T. and Yamashita, T., *J. Electroanal. Chem.* 1987, *225*, 255–262.
[51] Cathcart, R., *Nature* 1990, *347*, 310.
[52] Hultman, T., Stahl, S., Hornes, E. and Uhlen, M., *Nucleic Acids Res.* 1989, *17*, 4937–4946.
[53] Duncan, B. K., *The Enzymes*, 3rd Edit., Part A, Academic Press, New York 1981, pp. 565–586.
[54] Tye, B., Chien, J., Lehman, I. R., Duncan, B. K. and Warner, H. R., *Proc. Natl. Acad. Sci. USA* 1978, *75*, 233–237.
[55] Kunkel, T., *Proc. Natl. Acad. Sci. USA* 1985, *82*, 488–492.
[56] Longo, M. C., Berninger, M. S. and Hartley, J. L., *Gene* 1990, *93*, 125–128.
[57] Connell, C., Fung, S., Heiner, C., Bridgham, J., Chakerian, V., Heron, E., Jones, B., Menchen, S., Mordan, W., Raff, M., Recknor, M., Smith, L., Springer, J., Woo, S. and Hunkapiller, M., *Biotechniques* 1987, *5*, 342–348.
[58] Mead, D. A., McClary, J. A., Luckey, J. A., Kostichka, A. J., Witney, F. R. and Smith, L. M., *BioTechniques* 1991, *11*, 76–87.
[59] Kambara, H., Nishikawa, T., Katayama, Y. and Yamaguchi, T., *Biotechnology* 1988, *6*, 816–821.
[60] Slater, G. W., Rousseau, J., Noolandi, J., Turmel, C. and Lalande, M., *Biopolymers* 1988, *27*, 509–524.

Three DNA Sequencing Methods Using Capillary Gel Electrophoresis and Laser-Induced Fluorescence

Harold Swerdlow,[1] Jian Zhong Zhang, Da Yong Chen, Heather R. Harke, Ronda Grey, Shaole Wu,[2] and Norman J. Dovichi*

Department of Chemistry, University of Alberta, Edmonton, Alberta T6G 2G2, Canada

Carl Fuller

United States Biochemical Corporation, Cleveland, Ohio 44128

Capillary gel electrophoresis is demonstrated for the four-spectral-channel sequencing technique of Smith, the two-spectral-channel sequencing technique of Prober, and the one-spectral-channel sequencing technique of Richardson and Tabor. Sequencing rates up to 1000 bases/h are obtained at electric field strengths of 465 V/cm. At lower electric field strengths, capillary electrophoresis produces useful data for fragments greater than 550 nucleotides in length with 2 times better resolution than slab gel electrophoresis. An on-column detector produces detection limits of 200 zmol (1 zmol = 10^{-21} mol = 600 molecules) for the four-spectral-channel technique. A postcolumn detector, based on the sheath flow cuvette, produces detection limits of 20 and 2 zmol for the two- and one-spectral-channel techniques, respectively.

DNA sequencing is a fundamental tool in the biological sciences. Two powerful sequencing techniques were reported in 1977, one a chemical degradation method developed by Maxam and Gilbert and the other an enzymatic method developed by Sanger's group (*1*). In both cases, a nested set of radioactively labeled DNA fragments is generated in four reactions. The reaction products are separated by size in adjacent lanes of a high-resolution polyacrylamide gel and detected by use of autoradiography. The sequence is interpreted from the pattern of alternating bands in the lanes corresponding to the terminal base of the fragment. Sequence determination by these now classic techniques is an important, albeit tedious and labor intensive, task.

An advance in sequencing technology occurred in 1986–87 when Smith and co-workers in Hood's laboratory, workers in Ansorge's group, and Prober and co-workers at Du Pont reported DNA sequencers that replaced the radioactive labels and autoradiography in Sanger's method with fluorescent labels and laser-based detection (*2*). In Smith's four-spectral-channel, single-lane sequencer, four fluorescently labeled primers are associated with the terminating dideoxynucleotide through use of separate chain-terminating reactions. Fluorescence, excited by two laser lines and detected in four spectral channels, is used to identify the terminal nucleotide. In Ansorge's single-spectral-channel, four-lane sequencer, a single fluorescent label is used with each dideoxynucleotide chain-terminating reaction and the products are run on separate lanes of a slab gel; sequence identification is similar to the classic autoradiography technique. In Prober's two-spectral-channel, single-lane sequencer, one of four fluorophores is associated with the terminating dideoxynucleotide through use of distinctly labeled dideoxynucleotides in a single reaction mixture. Fluorescence, excited by a single laser line and detected in two spectral channels, is used to identify the terminal nucleotide. Smith's, Ansorge's, and Prober's fluorescence sequencers have been commercialized by Applied Biosystems, Pharmacia, and Du Pont, respectively; as an example, the Applied Biosystems Model 373A instrument runs 24 lanes simultaneously on a slab gel to produce sequencing rates of 50 bases/(h/lane) or 1200 bases/(h/slab). Similar sequencing rates are produced by other instruments. Sequence may be determined, by use of computer algorithms, to about 450 bases, which is limited by the resolution of the gel. The separation efficiency may be characterized in terms of chromatographic resolution, defined as the peak spacing divided by 4 times the standard deviation of the Gaussian-shaped peaks.

Increased sequencing rate is produced by operating the gels at high electric field strength. Unfortunately, the finite resistance of the separation buffer leads to unacceptable heating of conventional 200 to 400 μm thick gels at electric field strengths much greater than 50 V/cm. Gel-filled capillaries have attracted interest because their high surface-to-volume ratio provides excellent heat transport properties, allowing use of very high electric field strength. Typical capillaries are 50–75-μm i.d. and 25–100 cm long, although early work on RNA separations used cellulose fibers of 10-μm diameter and 25-mm length (*3*). More recently, Hjertén's and Karger's groups have reported the use of gel-filled capillaries for protein separations (*4*). Karger's group and others have reported the use of gel-filled capillaries for separation of oligonucleotide standards with detection by ultraviolet absorbance (*5*). An important issue is the performance of the gel-filled capillaries under high electric field strength; patents have been issued on the use of a bifunctional silane reagent to bind the acrylamide to the wall of the capillary to improve the gel stability (*6*).

Capillary gel electrophoresis has been applied to the separation of fluorescently labeled DNA sequencing fragments. Swerdlow and Gesteland reported the separation of a single dideoxynucleotide reaction mixture with a single spectral channel laser-induced fluorescence detector (*7*). Resolution of the capillary-based system was superior to that of a slab gel by a factor of 2.4. Drossman and co-workers in Smith's laboratory reported the separation of a single reaction mixture in gel-filled capillaries (*8*). When operated at 400 V/cm, the system produced sequencing rates of 1000 bases/h after elution of the primer, a roughly 25 times higher sequencing rate than produced by conventional slab gel electrophoresis. A subsequent report from Smith's laboratory described the use of capillary gel electrophoresis for the separation of the reaction products of the four-spectral-channel, single-lane sequencing system (*9*). Karger's laboratory reported separation of DNA fragments, labeled with a single fluorophore, at 350 V/cm, yielding sequencing rates of 450 bases/h, base line

* To whom correspondence should be addressed.
[1] Visiting scholar from the Department of Human Genetics, University of Utah, Salt Lake City, UT 84132.
[2] Present address: Chemistry Division, Alberta Environment Centre, Vegreville, Alberta T0B 4L0, Canada.

0003-2700/91/0363-2835$02.50/0

resolution was obtained for fragments up to 330 nucleotides in length (*10*).

Laser-induced fluorescence detection in slab-gel electrophoresis requires low detection limits, typically on the order of 1–100 amol/band (*2*). However, the detection requirements in capillary gel electrophoresis are more severe. On the basis of a comparison of the cross section of a 50-μm capillary with the cross section of a loading well in a slab-gel, Smith has estimated that the sample loading in capillary gel electrophoresis will be on the order of 1–10 amol of DNA/band (*8*). Detection limits in the zeptomole range (1 zmol = 10^{-21} mol = 600 molecules, ref 11) are necessary for accurate DNA sequence determination by capillary gel electrophoresis. Detector design is complicated further by the requirement that the detection volume be less than 1 nL to preserve the separation efficiency of the nanoscale electrophoresis technique. Swerdlow and Gesteland's system used an on-column laser-induced fluorescence detector with detection limits of 200 zmol of fluorescently labeled product (*7*). Smith and co-workers described the use of one- and four-spectral-channel on-column fluorescence detectors; both the single- and four-spectral-channel detectors produced detection limits of about 100 zmol of labeled fragments (*8*, *9*); Karger's group has reported similar detection limits for their single spectral channel detector (*10*). We have reported a postcolumn single-spectral-channel fluorescence detector in the gel electrophoresis separation of the products of a single chain-terminating reaction; detection limits were 10 zmol (*12*).

This paper demonstrates three different methods of DNA sequencing by capillary gel electrophoresis. These systems do not define the global optimum in sequencing by capillary electrophoresis; an optimized system can only be designed after much more experience is generated with these sequencing technologies. However, the three systems presented in this paper may be used to guide future developments in capillary sequencing.

Four-Spectral-Channel Sequencing. The technology developed by Smith et al. and marketed by Applied Biosystems uses four dyes, FAM, JOE, TAMRA, and ROX, to label primers to be used with each dideoxynucleotide reaction (*7*). These dyes have relatively widely spaced absorbance and emission spectra. Two lines from an argon ion laser (514.5 and 488 nm) are used to excite fluorescence; interference filters are used to isolate emission at 540, 560, 580, and 610 nm, corresponding to the wavelength of maximum emission for the four dyes. While excitation at 488 nm is well suited for excitation of FAM and JOE, excitation of TAMRA and ROX at 514.5 nm produces water Raman scatter that interferes with emission at 610 nm. The green helium–neon laser ("Gre-Ne", λ = 543.5 nm) is an interesting alternative for excitation of TAMRA and ROX. The wavelength of this laser provides better overlap with the excitation spectra of the dyes, and more importantly, the main water Raman band produced by the laser at 670 nm does not interfere with fluorescence detection. Although the laser produces a low-power beam (750 μW), the intensity generated at the beam waist is sufficient to photobleach many fluorophores (*13*, *14*). The relatively low linear velocity of analyte in gel electrophoresis (~4 mm/min for fragments 300 bases long) produces a long illumination time (~0.5 s) and observable photobleaching of fluorescein labeled primer at a few hundred microwatts of laser power. Higher laser power does not produce a linear increase in fluorescence signal.

Our four-spectral-channel, laser-induced detector for capillary gel electrophoresis is based on an on-column detector where the capillary serves as the detection chamber (Figure 1). To produce an observation window, a portion of the polyimide coating of the quartz capillary is removed with a gentle flame before the capillary is filled. An intense fan of scattered laser light can be observed at right angles to the capillary, particularly if the beam spot size approaches the capillary inner diameter (*15*); this fan is attenuated if the beam is tightly focused and if the capillary is tilted with respect to the incident laser beam by greater than ~15°. To attenuate the scattered laser light further, colored glass filters with high optical density at the excitation wavelength are used in the optical train. Finally, the illuminated capillary is imaged onto a pinhole of sufficient size to pass most of the fluorescence while blocking much of the residual light scatter. A filter wheel is rotated to transmit sequentially fluorescence intensity in four spectral bands to a single photomultiplier tube. This detector design offers the advantage of low component count and simple alignment compared with a beam-splitter arrangement based on four photomultipliers (*9*). A 150-mer peak passes the detector region in 5 s; the filter wheel is rotated at 2 Hz, providing 10 data points per spectral channel per peak, which is sufficient to reconstruct the electrophoretic data. A sector wheel is rotated at the same rate as the filter wheel to block alternately the two laser beams; excitation at 488 nm is associated with measurement of emission at 540 and 560 nm while excitation at 543.5 nm is associated with measurement of emission at 580 and 610 nm. This combination of excitation/emission channels not only eliminates interference by Rayleigh scatter of the 543.5-nm excitation wavelength with the 540-nm emission channel but also eliminates interference by Raman scatter due to the 488-nm excitation wavelength with the 580-nm emission channel. Synchronization of the sector and filter wheels is achieved through use of stepper motors and a single digital controller.

Detection limits (the amount of analyte that produces a signal that is 3 times the standard deviation of the background signal) are 200 zmol for all four of the labeled primers. The similar detection limit for each dye, despite the 20-fold difference in laser intensity between 488 and 543.5 nm, reflects both the superior fluorescent properties of the red-emitting

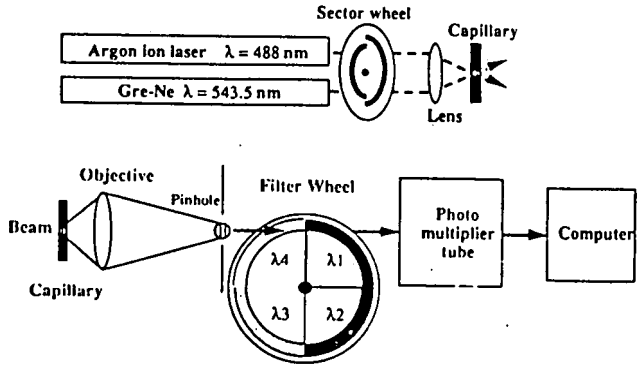

Figure 1. Laser-induced fluorescence detector for four-spectral-channel sequencing. A 19-mW argon ion laser beam (λ = 488 nm) and a 0.75-mW helium–neon laser beam (λ = 543.5 nm) were combined coaxially with a dichroic beam splitter. A two-sector chopping wheel was used to block alternately the two beams. The beams were brought to a common focus with a 4× microscope objective. The 50-μm-i.d. fused-silica capillary was placed at the beams' foci and was tilted ~30° with respect to them. Fluorescence was collected at right angles by a 32×, 0.6 numerical aperture microscope objective and imaged onto a pinhole of 1.6-mm diameter. A rotating filter wheel, synchronized with the sector wheel, was fitted with the following pairs of filters: a 535–545 nm band-pass interference filter with an OG-515 colored glass filter, a 555–565 nm band-pass interference filter with an OG-530 colored glass filter, a 575–585 nm band-pass interference filter with an OG-570 colored glass filter, and a 605–615 nm band-pass interference filter with an OG-590 colored glass filter. The signal from the Hamamatsu R1477 photomultiplier tube, operated at 1050 V, was filtered with a 70-Hz four-pole filter. A computer was used to digitize, average, and store data at 2 Hz/channel. The data are further treated to a 7 point moving average before display.

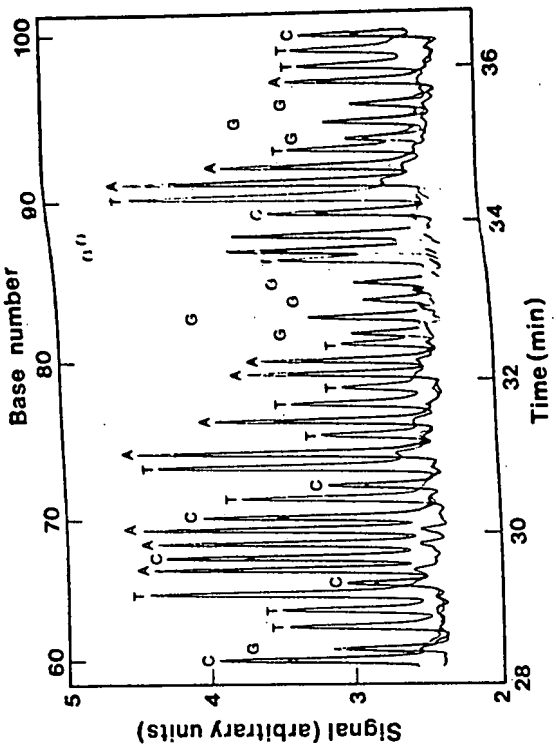

Figure 2. Four-spectral channel sequencing of M13mp18 with a histidine tRNA insert: (a, left) extended run; (b, *right*) expanded region corresponding to nucleotides 60–100; the known sequence is printed above (*8*). Samples were prepared as in Sanger, Nicklen, and Gesteland, except four reactions were performed and pooled in the ratio C:A:T:G 1:2:1:1 (*8*). The 41 cm long (27 cm to the detector), 50-μm i.d., 375-μm o.d. capillary was filled with 6% T, 5% C gel and prerun for 60 min at 150 V/cm at room temperature (*18*). The sample was introduced electrophoretically for 30 s at 150 V/cm; after injection, the sample was replaced with a fresh vial of 1× TBE. The gel was run for 1 min, trimmed at the injection end by 2 mm, and the run was continued at 150 V/cm. Time is measured from the injection; the numbers at the top of the figure correspond to the nucleotide length including the universal −21 18-mer primer. The blue, green, yellow, and red traces correspond to emission centered at 540, 560, 580, and 610 nm, respectively.

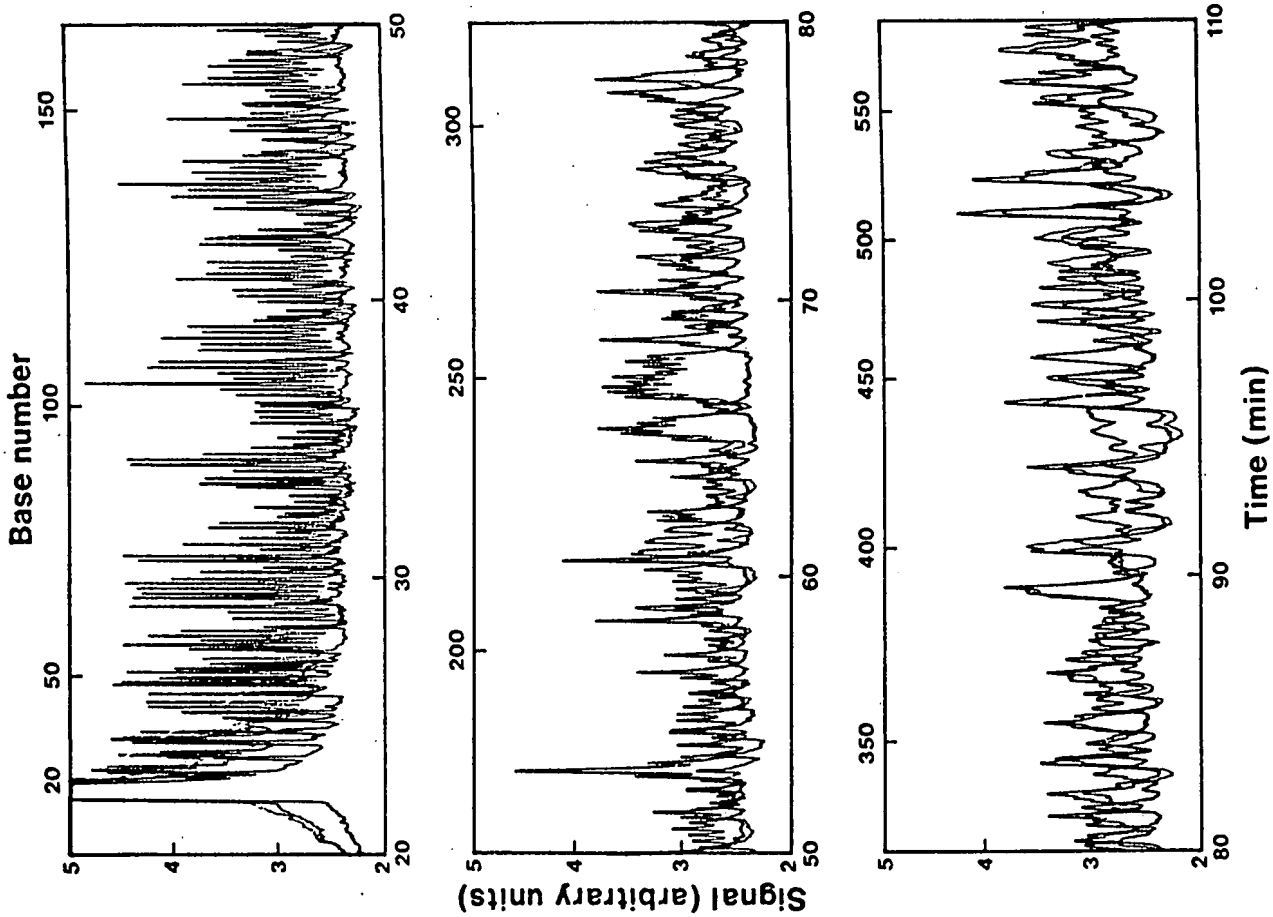

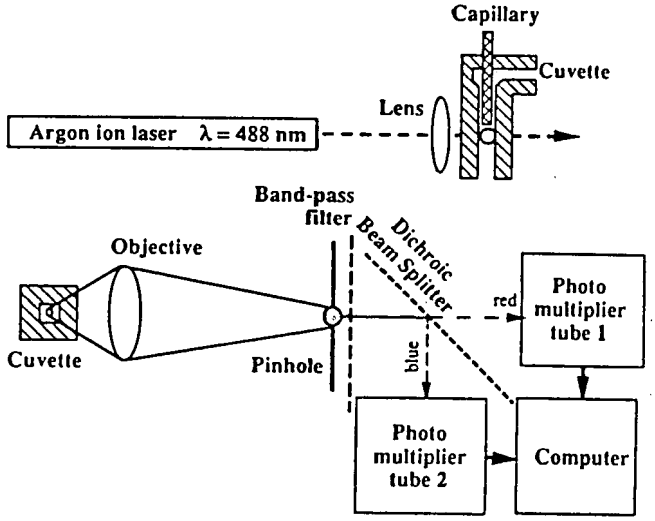

Figure 3. Laser-induced fluorescence detector for two-spectral-channel sequencing. A 5-mW argon ion laser beam (λ = 488 nm) was focused with a 4× microscope objective about 200 μm below the exit of the capillary in a sheath flow cuvette with 200-μm square flow chamber and 2 mm thick windows (*10*). Fluorescence was collected at right angles with a 32×, 0.6 numerical aperture microscope objective and imaged onto a 0.75-mm-diameter pinhole. A single interference filter (525-nm center wavelength, 40-nm band-pass) transmitted fluorescence. A dichroic filter, centered at 525 nm, was used to direct fluorescence in two spectral channels to two R1477 photomultiplier tubes operated at 1200 V; the transmitted light was centered at 535 nm (red) and the reflected light was centered at 515 nm. The photomultiplier tubes' signals were passed through a 1-Hz low-pass filter, digitized at 10 Hz with a computer, and passed through a quadratic-cubic polynomial filter before display.

dyes and the effect of photobleaching, which levels the fluorescent intensity produced by each dye. These detection limits are equivalent to those produced by Luckey et al. in the only other report of sequencing by capillary gel electrophoresis (*9*).

Capillary gel electrophoresis separation of the pooled reaction products from DNA sequencing of an M13mp18-histidine tRNA clone is shown in Figure 2. The 6% T, 5% C gel is run at a modest electric field strength, 150 V/cm, and produces sequencing rates of ~300 bases/h after elution of the primer and sequencing data beyond 550 bases (Figure 2a). In the region of highest resolution, from 60 to 100 bases (Figure 2b), the peaks are nearly base line resolved. Resolution of adjacent peaks ranges between 1 and 2.5, typically is 1.5, and is typical for separations at modest electric field, 150 V/cm. Similar resolution has been reported by Luckey for fragments 100 bases in length at 300 V/cm in a 3% gel (*9*) and by Swerdlow for fragments 150 bases in length at 180 V/cm in a 6% gel (*8*). Except for modest digital smoothing, the data have not been treated to account for the overlap between spectral channels.

Two-Spectral-Channel Sequencing. The Du Pont sequencing technique uses succinylfluorescein dyes to label the four dideoxynucleotides. These dyes have relatively closely spaced absorbance and emission bands. As a result, a single excitation wavelength, 488 nm, is used to excite fluorescence from all dyes. Emission is distributed between two spectral channels centered at 510 and 540 nm. The ratio of the fluorescence intensity in the two spectral channels is used to identify the terminating dideoxynucleotide.

Our two-spectral-channel capillary gel electrophoresis detector is based on a post-column sheath flow detector to reduce the background signal (Figure 3). In this detector, similar to that used in flow cytometry, the sample passes as a narrow stream in the center of a square flow chamber, surrounded by a sheath stream consisting of conducting buffer, typically 1X TBE. The high optical quality quartz windows of the cuvette produce much less light scatter than does an on-column detector. Also, by transferring the analyte to the moving sheath stream, the linear velocity and, hence, the illumination time of the analyte are independent of fragment length. The extent of photobleaching, which depends on illumination time, is independent of fragment length. We have reported the use of a single-spectral-channel fluorescence detector based on the cuvette for capillary zone electrophoresis separation of zeptomole quantities of fluorescently labeled amino acids and for capillary gel electrophoresis separation of zeptomole quantities of the products of a single dideoxynucleotide reaction (*12*, *14*, *16*); Keller's group has reported high-sensitivity fluorescence detectors based on the cuvette (*17*). That group has demonstrated, and Mathies' group has confirmed, detection of single phycoerythrin molecules with a single-spectral-channel fluorescence detector (*18*).

Fluorescence is collected with a high-efficiency microscope objective and imaged onto a pinhole to restrict the field of view of the photodetector to the illuminated sample stream. A single band-pass filter is used to block scattered laser light while a dichroic filter is used to split the fluorescence into two spectral channels, followed by detection with two photomultiplier tubes. The detection limit for this instrument is 20 zmol for a labeled dideoxynucleotide triphosphate and 5 zmol (3000 molecules) for a 100-mer fluorescein-labeled oligonucleotide. The difference in detection limit between the monomer and a 100-mer fragment is related to the behavior of the sheath flow cuvette when applied to gel electrophoresis. A very low sheath flow rate is employed to transport analyte from the capillary to the illumination region. During the transit time, analyte can diffuse an appreciable amount, decreasing the effective concentration of analyte in the detector. However, higher molecular weight fragments undergo less diffusion and are more concentrated in the illumination volume. As a result, the detection limit for the system improves for large DNA fragments, which are typically produced in sequencing reactions at lower concentration compared with early eluting fragments.

A typical separation on a 4% T gel, at 465 V/cm, of the fragments from an M13mp18 template yields sequencing rates of 1000 bases/h (Figure 4a); early termination of the sequence is an artifact of the reaction. In the region from 60 to 100 nucleotides, the peaks are nearly base line resolved (Figure 4b). To perform separations at this high electric field strength, the gel must be chemically bound to the capillary wall; unbound gels extrude from the capillary at electric fields much greater than 250 V/cm, presumably due to electroosmosis. Resolution in Figure 4b ranges from 1 to 2 and typically is 1.5. Comparison with Figure 2 reveals that the resolution is similar but the sequencing rate is much higher at higher electric field.

One-Spectral-Channel Sequencing. In 1990, Richardson and Tabor and, independently, Ansorge reported a sequencing technique based on a single fluorophore; by variation of the amount of dideoxynucleotide in the reaction mixture, each base is identified with a particular fluorescence peak height during separation in a single lane of an acrylamide gel (*19*). This technique relies on uniform labeling of the reaction products through use of the manganese/T7 polymerase reaction. In the work that has been published, a fluorescein labeled primer is excited with an argon ion laser at 488 nm; emission is detected in a single spectral band.

In our single-spectral-channel sequencer, a TAMRA-labeled primer is excited by a green helium–neon laser (λ = 543.5 nm) (Figure 5). As in the two-spectral-channel sequencer, a sheath flow cuvette is used as a postcolumn fluorescence detector to minimize background light scatter. Further reduction in the

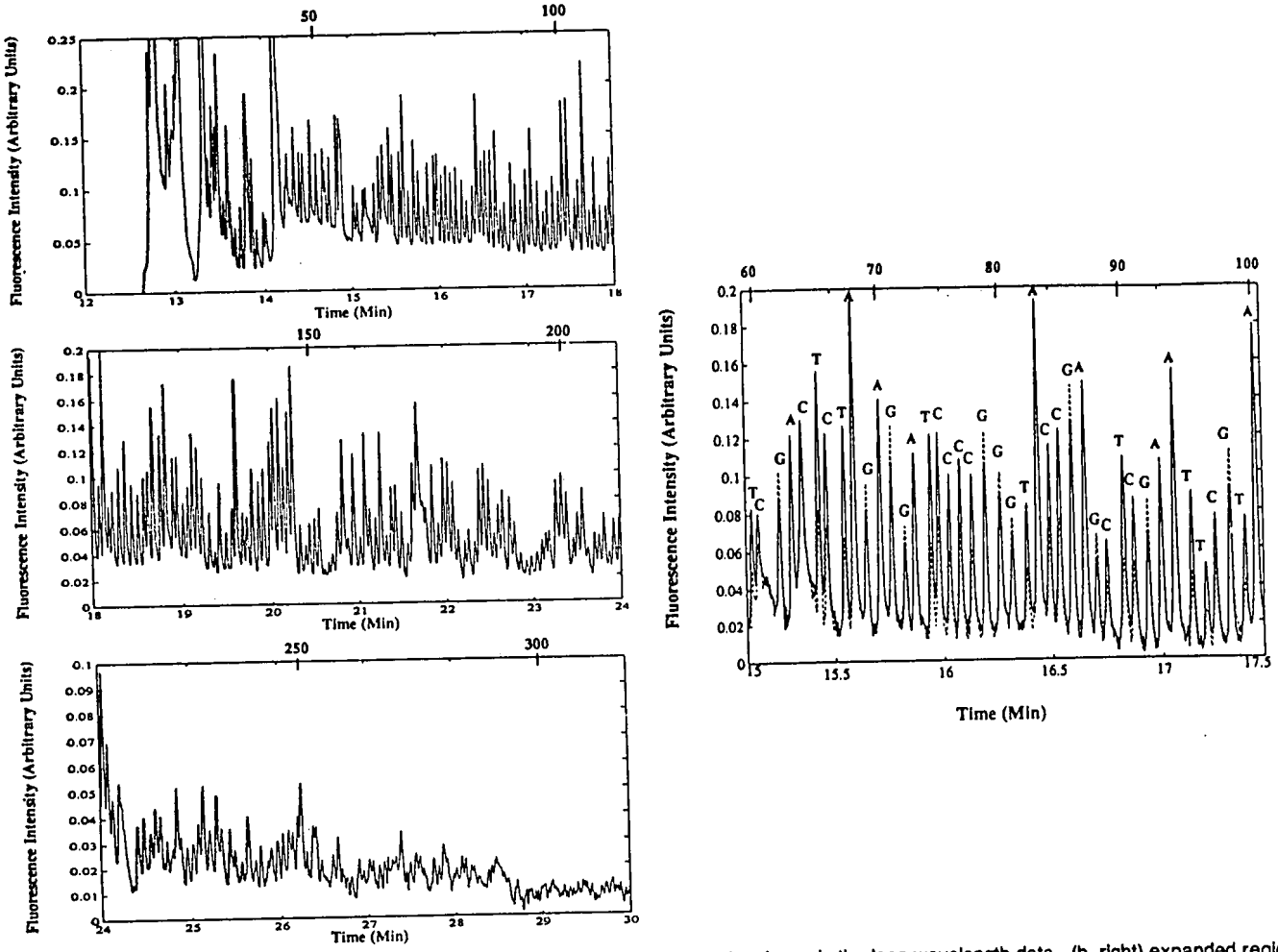

Figure 4. Two-spectral-channel sequencing of M13mp18: (a, left) extended run showing only the long wavelength data. (b, right) expanded region corresponding to nucleotides 60–100 with the known sequence printed above. The sample was prepared from a Du Pont Genesis 2000 protocol using 3 μg of M13mp18 single-stranded DNA, 15 ng of ~40 17-mer M13 primer, and 1 μL of Sequenase (U.S. Biochemicals) in a standard reaction mix. They were ethanol precipitated and washed and resuspended in 3 μL of a 49:1 mixture of formamide:0.5 M EDTA at pH 8.0. The 34 cm long, 50-μm-i.d. 190-μm-o.d. capillary was filled with 4% T, 5% C acrylamide gel that was covalently bound to the capillary wall through use of γ-[(methacryloxy)propyl]trimethoxysilane (*6*). The sample was injected at 100 V/cm for 30 s; after injection, the sample was replaced with a fresh vial of 1× TBE. The electrophoresis continued for 1 min at 100 V/cm. The capillary was then trimmed at the injection end by 1 mm, and the voltage was increased in 1-kV increments over a 14-min period to a total electric field strength of 465 V/cm. The sheath stream was 1× TBE at a flow rate of 0.16 mL/h. Time is measured from the injection; the numbers at the top of the figure correspond to the nucleotide length including the 17-mer primer. The solid trace corresponds to emission at wavelengths longer than 525 nm and the dashed trace corresponds to emission at wavelengths shorter than 525 nm.

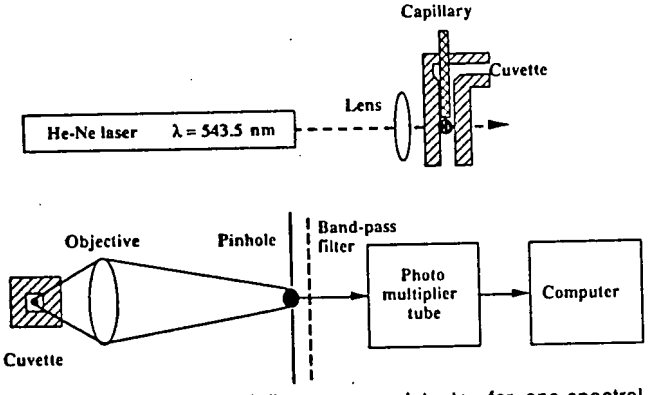

Figure 5. Laser-induced fluorescence detector for one-spectral-channel sequencing. A 0.75-mW helium–neon laser beam (λ = 543.5 nm) was focused with a 4× microscope objective about 200 μm below the exit of the capillary in a sheath flow cuvette. The cuvette had a 200-μm square flow chamber and 2 mm thick window. Fluorescence was collected at right angles with an 18×, 0.45 numerical aperture objective and imaged onto a 0.8-mm-diameter pinhole. A single interference filter (590-nm center wavelength, 40-nm band-pass) was used to block scattered laser light. Fluorescence was detected with an R1477 photomultiplier tube, cooled to −25 °C. The photomultiplier tube output was passed through a 1-s RC low-pass filter and digitized by a computer. The signal is digitized at 2 Hz and passed through a quadratic-cubic polynomial filter before display.

background signal comes from the relatively long excitation wavelength and low-power excitation beam (750 μW). In fact, the major contribution to background signal often is dark current produced by the photomultiplier tube. This contribution to the background signal is minimized by cooling the photomultiplier tube to −25 °C.

The standard deviation in the background signal for this system corresponds to 700 ymol (1 ymol = 10^{-24} mol, ref 11) of labeled primer introduced onto the capillary; detection limits are, by definition, a factor of 3 higher (1200 molecules). As with the two-spectral-channel detector, detection limits improve for higher molecular weight fragments. These detection limits, produced by a very low power laser, are associated with the excellent spectral properties of the TAMRA–fluorophore and reflect the simple detector design allowed by the single-spectral-channel sequencing technique.

This single-spectral-channel sequencing protocol, when applied to M13mp18, produces compressions in our standard capillary sequencing gels at room temperature. To minimize compressions, 30% by volume formamide was incorporated in the 6% T, 5% C, 7 M urea gel for separation of the sequencing products (Figure 6a). Figure 6b presents an expanded region corresponding to the elution of fragments ranging from 60 to 100 nucleotides in length. The data, obtained at modest electric field strength, 200 V/cm, suffers from

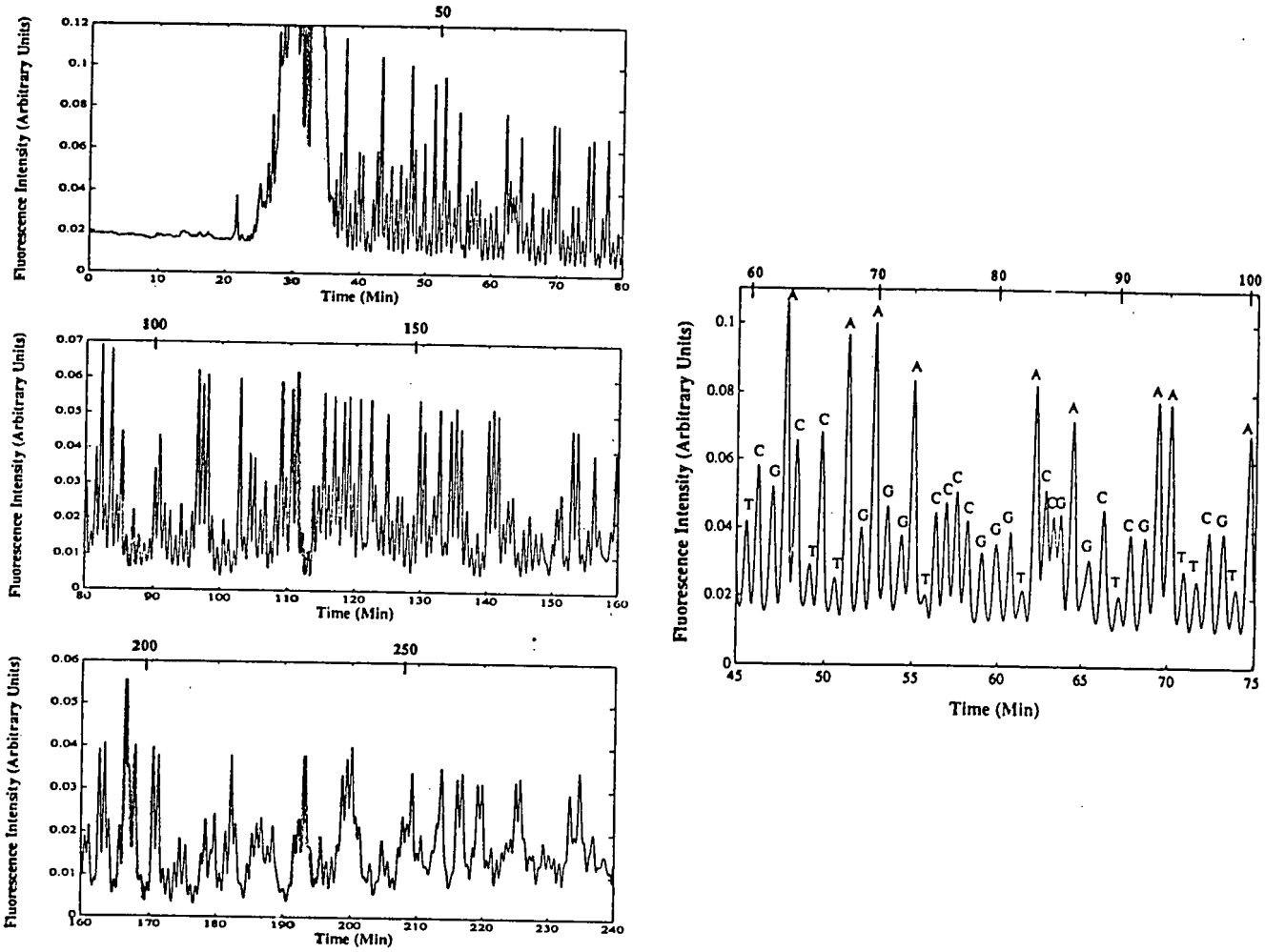

Figure 6. One-spectral-channel sequencing of M13mp18: (a, left) extended run; (b, right) expanded region corresponding to nucleotides 60–100. The sequencing reaction was carried out in 40 mM MOPS buffer, pH 7.5, 50 mM NaCl, 10 mM $MgCl_2$, and 15 mM sodium isocitrate. Dye-labeled primer (Applied Biosystems 21M13 TAMRA, 1.6 pM) was annealed to 1 μg of M13mp18 single-stranded DNA at 65 °C for 2 min followed by slow cooling. A mixture of deoxy- and dideoxynucleoside triphosphates was added to give an average nucleotide ratio (dNTP/ddNTP) of 1200:1 with 7-deaza-2′-deoxyguanosine 5′-triphosphate used in place of dGTP. The ratios of nucleotides were adjusted to yield a nominal peak height ratio of 8:4:2:1 for A:C:G:T. The mixture was warmed to 37 °C and 6 units of Sequenase Version 2.0 and 0.006 units of pyrophosphatase were added. Incubation continued at 37 °C for 30 min, after which the DNA was precipitated with ethanol (*19*). The 37 cm long, 50-μm-i.d., 190-μm-o.d. capillary was filled with 6% T, 5% C, 30% formamide, 7 M urea gel that was covalently bound to the capillary wall through use of γ-[(methacryloxy)propyl]trimethoxysilane. The sample was injected at 200 V/cm for 30 s; after injection, the sample was replaced with a fresh vial of 1× TBE. The capillary tip was not trimmed after injection, and separation proceeded at 200 V/cm. The sheath stream was 1× TBE at a flow rate of 0.16 mL/h. The numbers at the top of the figure correspond to the nucleotide length including the −21 18-mer primer.

Table I. Information Content in Bits for Three Different Detectors[a]

			information content			
			sample size			
detector	noise	detn limit, zmol	10 amol	1 amol	100 zmol	10 zmol
four-channel	70 zmol	200	29	15	2	
two-channel	7 zmol	20	21	14	8	1
one-channel	700 ymol	2	14	10	7	4

[a] zmol = 10^{-21} mol; ymol = 10^{-24} mol. A bit (binary digit) is the basic unit of information. A minimum of two bits are required to identify the terminal base in a DNA fragment.

low migration rate, 80 bases/h, and reflects the low mobility of DNA in the formamide–urea gels. The peaks across this region are nearly base line resolved; the resolution ranges from 1.2 to 1.8, with an average of about 1.5. This recipe reduced greatly the compressions but yielded a relatively slow separation rate. The sequencing accuracy of this gel appears to be poor, particularly with respect to C and G discrimination, reflecting difficulties in the reaction chemistry. Improved performance should be possible with elimination of ghost peaks and optimization of the dideoxynucleotide ratios.

CONCLUSIONS

These results, along with work performed in Smith's laboratory, define four points in the global optimization of capillary sequencing technology. They should be interpreted with regard to the entire system and not as characterizing a particular sequencing chemistry. For example, it is clear that use of a sheath flow cuvette would improve dramatically the performance of the four-spectral-channel system. Similarly, different electrophoresis conditions are used for each separation; the electrophoretic performance is characteristic of the gels and the sample but not the sequencing chemistry. Sequencing rate increases with electric field strength and sequencing rates of 1000 bases/h are produced at 465 V/cm; the sequencing rate for a single capillary is similar to that produced by a 24-lane slab gel.

A postcolumn detector produces lower background signal and superior detection limits to an on-column fluorescence detector. In the best case, the detector performance is dominated by dark current; cooling the PMT produces a factor

of 2 improvement in detection limit. Photobleaching is important for these fluorescent dyes; microwatt-power lasers produce outstanding detection limits.

Detection limit is not sufficient to compare the performance of the three laser-induced fluorescence detectors; it is necessary also to consider the number of spectral channels used by each technique. The information content of a signal, I, may be used to compare the detectors. Information is expressed in units of bits (binary digits) and is linearly related to the number of independent spectral channels, n, and logarithmically related to the signal-to-noise ratio of the measurement.

$$I = n \log_2 (\text{signal/noise}) = \log_2 (\text{signal/noise})^n$$

Two bits are the minimum necessary to distinguish four signals corresponding to the four dideoxynucleotides, assuming that there is no spectral overlap in the four- and two-spectral-channel sequencers and that the signal levels are quantized into discrete levels in the one-spectral-channel sequencer. Clearly, real samples will require more than two bits of information to determine accurately the sequence.

A simplistic comparison of the information content of our three detectors is provided in Table I, under the assumption that each spectral channel is independent. The noise value will change with analyte concentration; for convenience, this calculation uses the noise value associated with the blank. Also, the conservative detection limit of 20 zmol is used for the two-spectral-channel detector. Our four-spectral-channel detector produces a huge amount of information, nearly 30 bits, for relatively large amounts of sample, 10 amol, but rapidly loses information as the quantity of sample approaches the detection limit. On the other hand, the two- and one-spectral-channel detectors operate well above their detection limit at the 100 zmol level and produce sufficient information for peak identification. As the sample level drops to the low-zeptomole range, the information content produced by the one-spectral-channel detector becomes highest.

It seems that all three detectors provide sufficient information to identify DNA sequences with high accuracy for all but the smallest sample loadings, assuming that the spectral channels are independent. Certainly, a redesigned four-spectral channel detector, based on a sheath flow cuvette, would generate greater information for small sample loadings. The one-spectral-channel data suffer from poor peak-height resolution, particularly with respect to C–G discrimination; careful enzymology is required to produce accurate sequencing information. Routine use of this sequencing technology will require careful preparation and characterization of the reaction mixture. Similarly, the four- and two-spectral-channel data suffer from spectral overlap; the simple calculation presented above overestimates the information content of the fluorescent signal.

Finally, several additional issues must be addressed in the development of capillary gel electrophoresis for high-speed DNA sequencing. Either gel stability must be increased or the cost and time associated with capillary replacement must be reduced so that unattended, automated runs are possible. It will be necessary to operate several capillaries simultaneously to produce enhanced sequencing rates for large-scale sequencing projects; this laboratory has proposed the development of a 32-capillary instrument to produce sequencing rates approaching 64 000 bases/h. Automated base calling algorithms must be incorporated into the sequencing instrumentation. Last, the instrumentation must be evaluated with a large number of samples to assess and improve the sequencer accuracy.

ACKNOWLEDGMENT

R. Gesteland of the University of Utah provided advice and encouragement during this work.

LITERATURE CITED

(1) (a) Maxam, A. M.; Gilbert, W. *Proc. Natl. Acad. Sci U.S.A.* **1977**, *74*, 560–564. (b) Sanger, F.; Nicklen, S.; Coulson, A. R. *Proc. Natl. Acad. Sci. U.S.A.* **1977**, *74*, 5463–5467.
(2) (a) Smith, L. M.; Sanders, J. Z.; Kaiser, R. J.; Hughes, P.; Dodd, C.; Connell, C. R.; Heiner, C.; Kent, S. B. H.; Hood, L. E. *Nature* **1986**, *321*, 674–679. (b) Ansorge, W.; Sproat, B. S.; Stegemann, J.; Schwager, C. *J. Biochem. Biophys. Methods* **1986**, *13*, 315–317. (c) Prober, J. M.; Trainor, G. L.; Dam, R. J.; Hobbs, F. W.; Robertson, C. W.; Zagursky, R. J.; Cocuzza, A. J.; Jensen, M. A.; Baumeister, K. *Science* **1987**, *238*, 336–341.
(3) (a) Edström, J. E. *Nature* **1953**, *172*, 809. (b) Edström, J. E. *Biochim. Biophys. Acta* **1956**, *22*, 378–388.
(4) (a) Hjertén, S. *J. Chromatogr.* **1983**, *270*, 1–6. (b) Cohen, A. S.; Karger, B. L. *J. Chromatogr.* **1987**, *397*, 409–417.
(5) (a) Cohen, A. S.; Najarian, D. R.; Paulus, A.; Guttman, A.; Smith, J. A.; Karger, B. L. *Proc. Natl. Acad. Sci. U.S.A.* **1988**, *85*, 9660–9663. (b) Guttman, A.; Cohen, A. S.; Heiger, D. N.; Karger, B. L. *Anal. Chem.* **1990**, *62*, 137–141. (c) Paulus, A.; Gassmann, E.; Field, M. J. *Electrophoresis* **1990**, *11*, 702–708. (d) Yin, H. F.; Lux, J. A.; Schomburg, G. *J. High Resolut. Chromatogr.* **1990**, *13*, 624–627.
(6) (a) Bente, P. F.; Myerson, J. *U.S. Pat.* 4,810,456, 1989. (b) Karger, B. L.; Cohen, A. S. *U.S. Pat.* 4,865,706, 1989. (c) Karger, B. L.; Cohen, A. S. *U.S. Pat.* 4,865,707, 1989.
(7) Swerdlow, H.; Gesteland, R. *Nucleic Acids Res.* **1990**, *18*, 1415–1419.
(8) Drossman, H.; Luckey, J. A.; Kostichka, A. J.; D'Cunha, J.; Smith, L. M. *Anal. Chem.* **1990**, *62*, 900–903.
(9) Luckey, J. A.; Drossman, H.; Kostichka, A. J.; Mead, D. A.; D'Cunha, J.; Norris, T. B.; Smith, L. M. *Nucleic Acids Res.* **1990**, *18*, 4417–4421.
(10) Cohen, A. S.; Najarian, D. R.; Karger, B. L. *J. Chromatogr.* **1990**, *516*, 49–60.
(11) Zepto, $z = 10^{-21}$, and yocto, $y = 10^{-24}$, were accepted as prefixes by the Comité International des Poids et Mesures in Oct./90 to be put forward to the Conférence Générale des Poids et Mesures for adoption in Oct./91. See: Sweedler, J. V.; Shear, J. B.; Fishman, H. A.; Zare, R. N.; Scheller, R. H. *Anal. Chem.* **1991**, *63*, 496–502.
(12) Swerdlow, H.; Wu, S.; Harke, H.; Dovichi, N. J. *J. Chromatogr.* **1990**, *516*, 61–67 ().
(13) (a) Hirshfeld, T. *Appl. Opt.* **1976**, *15*, 3135–3139. (b) Mathies, R. A.; Peck, K.; Stryer, L. *Anal. Chem.* **1990**, *62*, 1786–1791.
(14) Wu, S.; Dovichi, N. J. *J. Chromatogr.* **1989**, *480*, 141–155.
(15) Lyons, J. W.; Faulkner, L. R. *Anal. Chem.* **1982**, *54*, 1960–1964.
(16) (a) Cheng, Y. F.; Dovichi, N. J. *Science* **1988**, *242*, 562–567. (b) Cheng, Y. F.; Wu, S.; Chen, D. Y.; Dovichi, N. J. *Anal. Chem.* **1990**, *62*, 496–503.
(17) (a) Dovichi, N. J.; Martin, J. C.; Jett, J. H.; Keller, R. A. *Science* **1983**, *219*, 845–847. (b) Dovichi, N. J.; Martin, J. C.; Jett, J. H.; Trkula, M.; Keller, R. A. *Anal. Chem.* **1984**, *56*, 348–354.
(18) (a) Nguyen, D. C.; Keller, R. A.; Jett, J. H.; Martin, J. C. *Anal. Chem.* **1987**, *59*, 2158–2160. (b) Peck, K.; Stryer, L.; Glazer, A. N.; Mathies, R. A. *Proc. Natl. Acad. Sci. U.S.A.* **1989**, *86*, 4087–4091.
(19) (a) Tabor, S.; Richardson, C. C. *J. Biol. Chem.* **1990**, *265*, 8322–8329. (b) Ansorge, W.; Zimmermann, J.; Schwager, C.; Stegemann, J.; Erfle, H.; Voss, H. *Nucleic Acids Res.* **1990**, *18*, 3419–3420.

RECEIVED for review June 6, 1991. Accepted September 5, 1991. This work was supported in part by the Department of Energy-Human Genome Initiative (U.S.A.) Grant No. DE-FGO2-91ER61123. Support by DOE does not constitute an endorsement of the views expressed in this article. This work was also supported by the Natural Sciences and Engineering Research Council of Canada, the Department of Chemistry of the University of Alberta, Pharmacia Inc., Waters Division of Millipore Inc., and U.S. Biochemical Corp. H.S. acknowledges a predoctoral fellowship from the National Science Foundation and H.H. acknowledges a predoctoral fellowship from the Alberta Heritage Foundation for Medical Research. J. E. Bertie of the University of Alberta kindly loaned the photomultiplier cooler. G. Tice of Du Pont kindly supplied the sample used to generate Figure 4.

R.A. Mathies et al., Abstract 133, DOE Human Genome Workshop IV, Santa Fe, NM, November 13-17, 1994

NEW DIRECTIONS IN HIGH-SENSITIVITY FLUORESCENCE DETECTION OF DNA AND CAPILLARY ARRAY ELECTROPHORESIS*

Richard A. Mathies, Jingyue Ju[1], Huiping Zhu, Steven M. Clark, Adam T. Woolley, Yiwen Wang, Scott C. Benson and Alexander N. Glazer, Chemistry Department and Department of Cell and Molecular Biology, University of California, Berkeley CA 94720.

Capillary Array Electrophoresis, coupled with confocal fluorescence detection,[2] is a valuable new technique for performing high-speed, high-throughput DNA sequencing[3,4] and fragment sizing.[5] In current implementations, up to 50 capillaries can be run in parallel and separations are complete ~10 times faster than slab gels. Our recent efforts have focused on (i) the development of improved fluorescence reagents for DNA sequencing, (ii) the development of methods for using intercalating dyes for double-stranded DNA fragment detection in CE, (iii) and the development of methods for microfabricating capillary arrays.

To improve the spectroscopic properties of the labels used in DNA sequencing, we have synthesized sequencing primers labeled with pairs of dyes that are coupled by fluorescence energy transfer (ET).[6] The donor is chosen to provide intense absorption at the laser wavelength (488 nm) while the acceptors are chosen to provide large Stokes shifts and distinctive emission spectra. The spacing of the dyes along the primer is selected to provide efficient energy transfer with no quenching. The mobility shifts of the ET primers are less than those observed using current commercial dye-labeled primers and the fluorescence intensities are as much as 5 times stronger. Results using these ET dye-labeled primers for 4-color DNA sequencing (collaboration with Dr. Carl Fuller at U. S. Biochemical) and for 2-color allelic fragment detection will be presented.

A variety of monomeric and dimeric intercalating dyes have been used to improve the sensitivity and versatility of DNA fragment detection in CE.[7] The monomeric intercalating dyes TO, TO6, YO, Propidium 2 and Propidium 3 have been used for on-column staining. TO and TO6 are able to detect as little as 1 fg/μL of a 600 bp fragment in the initial sample. Separations of DNA precomplexed with the dimeric intercalating dyes EthD, TOTAB, and YOYO have also been successful, although it is important to work at low dye:DNA ratios and to use 9-aminoacridine in the running buffer to achieve high-resolution separations.

In a continuing effort to miniaturize DNA analysis systems, we have used photolithographic techniques to microfabricate capillary arrays.[8] These arrays were fabricated on planar glass slides by first etching channel patterns, and then forming the capillaries by thermally bonding the etched substrate to a top glass plate. The channels have an effective length of 3.5 cm and the 10 micron deep channels ranged from 30-120 μm in width. Using these CAE chips, high-resolution separations of double-stranded ΦX/HaeIII DNA have been performed from 70-1000 bp in only 120 seconds! Since up to 100 such channels can be fabricated on a single glass slide, this work establishes the feasibility of developing miniaturized DNA analysis chips.

*Supported by a grant from the Director, Office of Energy Research, Office of Health and Environmental Research of the U.S. Department of Energy under contract DE-FG-91-61125.

[1]DOE Human Genome Distinguished Postdoctoral Fellow

[2]R.A. Mathies et al., *Rev. Sci. Instrum.* **65**, 807-812 (1994).

[3]R.A. Mathies and X.C. Huang, *Nature (London)* **359**, 167-168 (1992).

[4]R.A. Mathies and X.C. Huang, *Automated DNA Sequencing and Analysis*, eds. M.D. Adams, C. Fields & J. C. Venter, Academic Press, pp. 17-28 (1994).

[5]S.M. Clark and R.A. Mathies, *Anal. Biochem.* **215**, 163-170 (1993).

[6]J. Ju, C. Fuller, C. Ruan, A.N. Glazer and R.A. Mathies, Fluorescence Energy Transfer Primers for DNA Sequence Analysis, in preparation.

[7]H. Zhu, S.M. Clark, S.C. Benson, H.S. Rye, A.N. Glazer and R.A. Mathies, *Analytical Chemistry* **66**, 1941-1948 (1994).

[8]A.T. Woolley and R.A. Mathies, Ultra-High-Speed DNA Fragment Separations Using Microfabricated Capillary Array Electrophoresis Chips, *Proc. Natl. Acad. Sci. U.S.A.*, in press.

J. Balch et al., Abstract 134, DOE Human Genome Workshop IV, Santa Fe, NM, November 13-17, 1994.

Sequencing of DNA by Gel Electrophoresis in Micromachined Channels

Joe Balch[1], Courtney Davidson[1], Jeff Gingrich[1], Muhammad Sharaf[2], Larry Brewer[1], Jackson Koo[1] Doug Smith[2], Michael Albin[2], and Anthony Carrano[1]

[1]Human Genome Center, L-452, Biology and Biotechnology Research Program, Lawrence Livermore National Laboratory, Livermore California. 94550, [2]Perkin Elmer Corporation, Applied Biosystems Division, Foster City, California 94404.

Sequencing of DNA by gel electrophoresis is typically performed in slab gel systems. Efforts to increase sequencing rates have generally relied on increasing sample load capacity (higher lane density or multiple capillary systems) and increasing the electric field to obtain faster fragment separation (requiring the use of thinner gels or capillaries to reduce heat dissipation). As an alternative to slab and capillary systems, we are investigating a hybrid technique based upon a high density array of electrophoresis channels fabricated using micromachining technologies on a single, large substrate at fixed locations. Furthermore, standard polyacrylamide gel (PAG) compositions can be poured into the channels using conventional techniques without the problem of bubble formation and other defects commonly incurred in PAG filled capillaries.

We have found that electrophoretic resolution is dependent upon the surface finish of the micromachined channels. We have developed and refined fabrication techniques that result in electrophoretic resolution in microchannels comparable to the electrophoresis resolution measured in standard slab gels formed between two flat glass plates. We have obtained resolution that results in accurate base calling to greater than 500 DNA bases per channel (200 micrometer deep by 1 mm wide by 25 cm long microchannels filled with 6% PAG). Present efforts are underway to develop large electrophoresis channel arrays on a single glass substrate for high throughput DNA sequencing.

This work was performed under a Cooperative Research and Development Agreement (CRADA) between Perkin-Elmer Corporation, Applied Biosystems Division and by Lawrence Livermore National Laboratory under the auspices of the U.S. Department of Energy contract no. W-7405-Eng-48.

0033863
IDENTIFYING NO.: 24328; OHER-RPIS 4922 AGENCY CODE: ENRGY
Quantitation in Electrophoresis Based on Lasers
PRINCIPAL INVESTIGATOR: Yeung, E.S.
ADDRESS: Ames IA 50011
PERFORMING ORG.: Ames Laboratory, Iowa State University, Department of Chemistry
PROJECT MONITOR: Wood, R.W.
SPONSORING ORG.: USDOE Energy Research
TO 931231

SUMMARY: This project develops novel detection and quantitation techniques in gel and capillary electrophoresis to increase the cost efficiency, reliability, convenience, sensitivity, and speed of processing DNA fragments. One technique used is indirect fluorometry, in which a fluorescing ion is used to elute the sample, resulting in a large fluorescence background signal throughout the gel. When a component of the sample appears, the fluorescing ion is displaced, and a lower fluorescence signal is observed. This negative signal allows nonfluorescing species, such as DNA fragments, to be detected with the high sensitivity normally associated only with fluorescing species. Migration errors are eliminated because tags are absent. Sample preparation for electrophoresis and sample collection for subsequent sequencing are also simplified. Researchers have demonstrated that restriction fragments in the range of 0.1–23 kb can be (1) separated by this method and (2) detected down to the pg level in capillary electrophoresis and down to the ng level in slab gel electrophoresis. A complete electrophoretogram can be obtained in a few minutes using capillary electrophoresis. Novel ways to improve the speed and reliability of imaging schemes for use in mapping and sequencing are also being explored. A charged-coupled detection device and a unique background correction algorithm can be employed to image native DNA in slab gels, using the intrinsic ultraviolet absorption of the bases at concentration levels comparable to those in standard protocols. This technique is being applied to the real-time monitoring of pulsed-field gel electrophoresis so that interactive control can be implemented by field programming during the separation. For sensitive laser-excited fluorescence detection in capillary electrophoresis, a multiplex approach that does not require critical optical alignment is being developed. Hundreds of parallel capillaries can be monitored at the same time, thus speeding up DNA sequencing. (RPIS 4922)

DESCRIPTORS: OLIGONUCLEOTIDES/electrophoresis ;DNA SEQUENCING; FLUORESCENCE SPECTROSCOPY; RFLPS; OPTIMIZATION; OLIGONUCLEOTIDES; ELECTROPHORESIS; MONITORS; FLUORIMETERS; DESIGN; DNA; EMISSION SPECTROSCOPY; MEASURING INSTRUMENTS; NUCLEIC ACIDS; ORGANIC COMPOUNDS; SPECTROSCOPY; STRUCTURAL CHEMICAL ANALYSIS

0038411
IDENTIFYING NO.: 79345; WPAS-93/CH-AMES/00 AGENCY CODE: ENRGY
Genome
PRINCIPAL INVESTIGATOR: Yeung, E.S.
ADDRESS: Iowa State University Ames IA 50011
PERFORMING ORG.: Ames Laboratory, Iowa State University
PROJECT MONITOR: Galas, D.
SPONSORING ORG.: USDOE Energy Research
DATES: 820122 TO 931231
SUMMARY: Electrophoresis is one of the most powerful proven techniques available for gene mapping and sequencing. Separation efficiencies and information content in 2-D gels easily outperform other techniques as judged by the number of possible resolution elements. Electrophoresis in capillary tubes is another important recent development. The potential for substantially increased speed and extended size range in sequencing runs has been demonstrated recently. The major problem is that of detection of the separated components. Typically, a tag is introduced to allow measurement by absorption, fluorescence, or radiography. At best, only semiquantitative results are obtained because of unreliable chemistry and difficulties in probing a 2-D spot that can be distorted. Staining can also affect the migration of the components, leading to errors in sequencing. Novel separation, detection, and imaging techniques for real-time monitoring in electrophoresis will be developed. Emphasis will be on schemes that allow multiplexing and methods that do not require specialized fluorescent or radioactive tags. These techniques will be used to substantially increase the speed, reliability, and sensitivity in gene mapping and in DNA sequencing applications, both in slab gels and in capillary gels.
DESCRIPTORS: ELECTROPHORESIS/sensitivity; DNA SEQUENCING/optimization;ELECTROPHORESIS; SENSITIVITY; OPTIMIZATION

stimulation of hepatocyte replication through partial hepatectomy 30 minutes after injection.[68] Definite evidence of integration of the transgene could not be shown, however. The endocytosed DNA persists in a cytoplasmic vesicular pool[69] after partial hepatectomy with concomitant disappearance of microtubules. A blockade of translocation of endosomes to lysosomes and thus delivery of endosomal contents for degradation is a possible explanation for the previously observed persistence and transgene expression.[70]

In vivo transfer of the structural gene for human serum albumin to hepatocytes in Nagase analbuminemic rats has been achieved using an asialoglycoprotein-polycation conjugate.[71] Forty-eight hours after injection and two-thirds partial hepatectomy, human albumin could be detected in serum at 0.05 μg/mL. By 2 weeks, the level had increased to 34 μg/mL; it remained stable through 4 weeks after initial gene transfer.[71]

Selected Models for Clinical Applications

Liver

The liver has proven to be a suitable target for gene delivery. With hepatocytes playing an integral role in protein synthesis and homeostasis, it is not surprising that liver-directed gene therapy has many potential clinical applications.

LDL receptor deficiency. Homozygous low-density lipoprotein (LDL) receptor deficiency leads to familial hypercholesterolemia (FH) and the associated premature development of atherosclerotic cardiovascular disease. Although LDL receptors are expressed on most cells, it is the hepatic expression of these receptors that regulates cholesterol homeostasis in the body.[72,73] The clinical importance of hepatocyte LDL receptor expression has been shown through successful treatment, resulting in marked reduction in total (76%) and LDL (83%) cholesterol concentrations, with liver transplantation in a patient with FH.[74] This was also accompanied by almost total regression of xanthomas, a usually slow process, in 6 months.[74] Transfer of LDL receptor genes to hepatocytes offers a more practical method to treat FH when compared with the problems associated with liver transplantation, especially organ procurement.

The Watanabe heritable hyperlipidemic (WHHL) rabbit is an animal model for homozygous familial hypercholesterolemia, showing similar clinical and metabolic abnormalities when compared with the human disease.[75] Using this model, ex vivo gene transfer using retroviral vectors to deliver the human LDL receptor gene to WHHL rabbit hepatocytes resulted in infection of about 20% of cells.[76] Transduced cells expressed receptor levels 4–5 times the levels found in normal hepatocytes.[76] It is felt that clinical benefit can be attained by replacing only a few percent of normal LDL receptor activity.[77] Injection of transduced hepatocytes into the portal vein of subject rabbits resulted in cell engraftment in periportal areas.[78] More importantly, recipient animals showed a decrease in total serum cholesterol of 30%–50% that persists for at least 4 months.[79] Evaluation of hepatocytes 6.5 months after transplantation showed no decrease in recombinant-derived LDL receptor RNA.[79]

The WHHL rabbit has also been used to study in vivo LDL receptor gene transfer targeted to hepatocytes using an asialoglycoprotein-polylysine carrier. Successful delivery of the genetic material resulted in a 25% decrease in total serum cholesterol for 5 days, followed by a return to pretreatment levels.[80] Recombinant adenoviruses have also been used to transfer the LDL receptor gene in vivo to WHHL rabbits with dramatic, though transient, decreases in plasma cholesterol.[81]

Clinical studies in humans have begun using a retroviral vector and ex vivo methods to deliver the LDL receptor gene to hepatocytes in patients with familial hypercholesterolemia.[51]

Hemophilia B. Hemophilia B, Christmas disease, is an x-linked coagulation disorder stemming from deficient or functionally defective clotting factor IX, which is synthesized in the liver. Current treatment centers around transfusion of factor IX concentrates in patients with evidence of bleeding.[82] Although current preparations can be stringently tested and treated to eliminate impurities,[82,83] there still remains the risk of transfusion-transmitted diseases such as hepatitis C and human immunodeficiency virus. In addition, because of the short half-life of factor IX (24 hours), repeated transfusions are often necessary, especially after major trauma and surgery.[84] Gene therapy would eliminate these transfusion-associated risks and inconveniences.

The gene for factor IX has been delivered to hepatocytes both in vitro[85] and in vivo.[33] Retroviruses have been used to infect primary rabbit liver cells with the gene for human factor IX, leading to a 20% cellular infection rate.[85] Factor IX production by transduced hepatocytes, however, is 10 times that of normal cells.[85] Canine factor IX, attached to a replication-defective herpes simplex virus (HSV)-1 vector, injected directly into mouse liver or portal vein, also results in production of circulating factor IX.[33] However, although serum levels reached normal values 1 day after injection, they quickly dropped to background levels within 1 week.[33]

The levels of expression in a target organ can be influenced by a number of factors. At a transcriptional level, the regulatory elements built into the construct[86] are important. The use of short-term in vitro assays to identify optimal regulatory elements for use in vivo can be misleading because of the phenomenon of extinction of gene expression that can occur in vivo. In these cases, loss of expression was observed without loss of introduced genes.[87] In general, regulatory elements specific for the target tissue have had the longest duration of expression.[42] In addition to transcriptional elements that can

affect expression, the lack of targetability of injected retrovirus to parenchymal liver cells even when introduced directly into the portal vein results in another level of inefficiency.

Even if transfection efficiency is limited, factor IX production by infected hepatocytes may be sufficient clinically. Spontaneous bleeding episodes in hemophiliacs can be alleviated with only 1%–2% of normal levels of factor IX.[85] Twenty-five percent of normal levels are needed to maintain adequate hemostasis.

Metabolic disorders. Severe phenylalanine hydroxylase (PAH) deficiency leads to phenylketonuria, an inborn error of metabolism affecting about 1 in every 10,000 births.[88] In humans, PAH is expressed only in the liver. Traditional therapy for phenylketonuria consists of restriction of phenylalanine intake. However, gene therapy for this disease may become possible; efficient transfer of the human PAH gene to rat hepatocytes in culture using a retroviral vector has been achieved.[89]

Similarly, the gene for ornithine transcarbamylase (OTC) can be transferred to primary hepatocytes using a retroviral vector. Transfected cells exhibit OTC levels equivalent to those present in normal human liver.[90]

Hepatitis B. Chronic infection with the HBV leads to substantial morbidity and mortality. To date, there remains no definitive therapy, though interferon alfa is helpful in many cases. Some preliminary work suggests that gene therapy may prove to be a possible mode of treatment.

Using asialo-orosomucoid coupled with poly-L-lysine, double-stranded DNA have been delivered specifically to hepatocytes by targeting their asialoglycoprotein receptors. Similarly, single-stranded DNA can be delivered using this same vehicle.[91] For example, an oligodeoxynucleotide (antisense sequence) complementary to the polyadenylation signal for human hepatitis B virus was introduced into a hepatoma cell line, HepG2 (2.2.15). This cell line had been previously permanently transfected with a complete human hepatitis B viral genome and secretes complete, infectious virions into culture medium. Twenty-four hours after exposure to the antisense sequence in the form of a targetable complex, measurement of HBV DNA levels were 80% lower than controls. Repeat evaluation 7 days after exposure showed 95% inhibition of HBV DNA when compared with controls.[91] These findings suggest that delivery of antisense oligonucleotides to infected hepatocytes with a soluble DNA-carrier system can inhibit HBV gene expression and replication.

In vivo inhibition of hepatitis B viral replication has also been achieved using antisense oligodeoxynucleotides. Antisense sequences were injected intravenously into infected Peking ducks, an animal model for hepatitis B infection. Comparison with controls after incubation revealed that viral replication was inhibited by greater than 90% by two different antisense oligodeoxynucleotides.[92]

Despite these early successes, it should be kept in mind that, as with any therapy, there are potential drawbacks such as limited uptake,[93] short half-life, and nonspecific binding to other (nontarget) messenger RNAs (mRNAs).[94]

Liver tumors. *Hepatoma.* Gene therapy methods are also being explored to treat hepatocellular carcinoma. Carrier systems[95] and retroviruses bearing genes under the regulation of albumin enhancer and promoter[96] have been shown to successfully deliver genetic material to hepatoma cells in culture. Hepatocellular carcinoma cells can be killed in vitro using a gene transfer method termed "virus-directed enzyme/prodrug therapy".[97] A retroviral vehicle chosen to preferentially infect rapidly dividing neoplastic cells containing a varicella zoster virus thymidine kinase gene and the nontoxic prodrug 6-methoxypurine arabinonucleoside (araM) was introduced to hepatoma cells in vitro. Selective uptake by these cells resulted in selective destruction after the thymidine kinase metabolically activated the araM to adenine arabinonucleoside triphosphate, a cytotoxic anabolite.[97,98]

Metastatic disease. A method to destroy cells transduced with genes from a retroviral vector has been developed by inserting the gene for herpes virus thymidine kinase into the transferred genetic material. The exposure of these cells to ganciclovir resulted in cell destruction. Although this "suicide vector" was initially developed to provide a method to eliminate cells infected by retroviruses, especially should undesirable results occur, it also has therapeutic applications. Rapidly dividing adenocarcinoma cells transduced in vivo with this suicide retroviral vector were eliminated by subsequent administration of ganciclovir.[99,100] Similarly, this suicide vector can be used to treat tumors by making them susceptible to ganciclovir through delivery of the thymidine kinase gene to tumor cells.[101] Tumors representing liver metastases of a colon cancer were induced in rats by direct injection of tumor cells under the liver capsule. Then, a retroviral vector carrying the gene for HSV type 1 thymidine kinase was later injected into the tumor. Preferential uptake into tumor cells, as opposed to normal hepatocytes, was accomplished because of the need for active cell division for retroviral gene transfer. Intraperitoneal administration of ganciclovir 5 days later resulted in a decrease in mean cancer cell mass 60-fold when compared with controls. Pathological examination revealed fibrotic scars devoid of any cancer cells in 4 of 13 treated animals.[102]

Cystic fibrosis. Cystic fibrosis (CF) is a common, autosomal recessive genetic syndrome involving multiple organ systems. The fundamental genetic defect has been identified and cloned. The product of the gene is termed the cystic fibrosis transmembrane conductance regulator (CFTR); the CFTR functions primarily as a cyclic adenosine monophosphate–activated chloride channel in epithelial cells.[103] CF-induced chronic pulmonary disease

contributes to much of the morbidity and mortality associated with CF beyond the neonatal period.[104] Multiple gene therapy trials using adenoviral vectors to deliver normal CFTR DNA to respiratory epithelium have been approved and are in progress.

CF can also involve the gastrointestinal tract, pancreas, and hepatobiliary system.[104] Studies of rat liver have revealed that the endogenous CFTR gene is expressed primarily in intrahepatic biliary epithelial cells; no significant gene activity was found in other liver cells, including hepatocytes.[105] This finding is consistent with clinical findings of CF-induced biliary damage.[104,105] Thus, attempts have been made to transfer the CFTR gene into biliary epithelial cells in vivo using adenoviruses. During laparotomy, injection of the vector directly into the common bile duct resulted in delivered gene expression in essentially all intrahepatic bile duct epithelial cells initially.[105] After 21 days, gene activity had diminished in large biliary ducts but remained stable in epithelial cells of the small bile ducts.[105] These results offer encouraging hope for the treatment of CF-induced hepatobiliary disease in vivo, especially with the availability of endoscopic retrograde cholangiopancreatography to deliver material into the common bile duct without the need for surgery.

α_1-antitrypsin deficiency. α_1-antitrypsin deficiency is another inherited disease with multiple organ involvement. Most of the current efforts to use gene therapy as treatment for α_1-antitrypsin deficiency have concentrated on pulmonary disease. Adenoviral vectors are being used in efforts to prevent the development of chronic obstructive pulmonary disease through transfer of an α_1-antitrypsin gene into respiratory epithelial cells.[106] In addition, retroviral vectors have been successful in delivering the desired gene to hepatocytes in dogs with production of significant amounts of alpha 1-antitrypsin for 1 month.[107]

Intestine

The intestinal epithelium is an attractive target for gene therapy because it is readily accessible, has a large tissue mass, and contains stem cells with known locations.[108] Although few studies have targeted the intestine, marker genes have been transferred into intestinal epithelium successfully using retroviral vectors in experimental animals.[108,109] Although preliminary attempts to transfer genetic material into intestinal epithelial cells have shown some promise, the relatively rapid turnover of the epithelium would limit long-term clinical benefits of delivered genes unless they were delivered successfully to stem cells.

In addition, the gene for human ornithine decarboxylase has been shown to be expressed in small intestinal epithelium after direct microinjection into fertilized oocytes of sparse fur mice, an animal model for human X-linked OTC deficiency.[110] This method resulted in high levels of gene expression in the small bowel and very low levels in the liver.[110] Studies of orotic acid concentration in urine proved metabolic correction of OTC deficiency as well.[110] Thus, gene therapy for OTC deficiency can be targeted to intestinal epithelium or the liver, as discussed above.

Colon Cancer

Treatment for colorectal cancer using gene therapy methods has also met with some success. One such method, using a retroviral vector to deliver the human granulocyte colony-stimulating factor (GCSF) gene to colon adenocarcinoma cells in vitro, resulted in the inability of transduced cells to develop tumors.[111] This finding suggests that GCSF may have antitumor properties when released at tumor sites. The antitumor effect probably occurs due to recruitment and targeting of neutrophils to GCSF-releasing cells.[111]

Another potential method to treat colorectal carcinoma focuses on the tumor suppressor gene, p53. Normal cells contain two alleles of the p53 gene. Transformed cells, in contrast, most commonly have lost one of the alleles while the remaining allele is defective, resulting in loss of tumor suppressor function. Loss of wild-type p53 gene function may be the most common event in human carcinogenesis[112] and has been estimated to occur in 20%-69% of colon cancer patients.[112] Thus, transfer of the p53 gene to cancer cells could potentially lead to tumor suppression. This hypothesis has been tested with human colorectal cell lines in vitro. These cells were transfected with wild-type or mutant human p53 genes. The cells expressing wild-type p53 formed colonies 5- to 10-fold less efficiently than those expressing mutant p53.[113]

Conclusions

Gene therapy is a relatively young, though rapidly advancing field in medicine. Progress in genetic engineering has made the transfer of genetic material into cells possible using many different methods. Digestive organs offer attractive targets for somatic gene therapy because of the numerous disease entities that affect them. Indeed clinical trials using ex vivo and in vivo methods have begun in earnest. Other potential clinical applications of gene therapy include the treatment of cancer by delivering antitumor cytokines such as interleukin 2, tumor necrosis factor, or GCSF to neoplastic cells.[114-116] Genes can also be transferred into vascular endothelial cells,[117-119] fibroblasts,[120] synoviocytes,[121] as well as many other cell lines, making potential clinical applications for gene therapy quite diverse.

References

1. Verma IM. Gene Therapy. Sci Am 1990;263:68-84.
2. Frohman MA, Martin GR. Cut, paste and save: new approaches to altering specific genes in mice. Cell 1989;56:145-147.
3. Roemer K, Friedmann T. Concepts and strategies for human gene therapy. Eur J Biochem 1992;208:211-225.

4. Blaese RM, Culver KW. Prospects for gene therapy of human disease. Allergol Immunopathol 1991;19:25–28.
5. Blaese RM. Progress toward gene therapy. Clin Immunol Immunopathol 1991;61:S47–S55.
6. Miller AD. Human gene therapy comes of age. Nature 1992;357:455–460.
7. Abbot A. German state unexpectedly approves first gene trials. Nature 1992;360:702.
8. Thompson L. Healy approves an unproven treatment. Science 1993;259:172.
9. Adams RM, Soriano HE, Wang M, Darlington G, Steffen D, Ledley FD. Transduction of primary human hepatocytes with amphotropic and xenotropic retroviral vectors. Proc Natl Acad Sci USA 1992;89:8981–8985.
10. Leffert HL, Koch KS, Skelly H. Primary cultures of hepatocytes. In: Barnes DW, Sirbasku DA, Sato GH, eds. Methods for serum-free culture of epithelial and fibroblastic cells. New York: Alan R. Liss, 1984:43–55.
11. Grossman M, Raper SE, Wilson JM. Towards liver-directed gene therapy: retrovirus-mediated gene transfer into human hepatocytes. Somat Cell Mol Genet 1991;17:601–607.
12. Friedman T, Xu L, Wolff J, Yee JK, Miyanohara A. Retrovirus vector-mediated gene transfer into hepatocytes. Mol Biol Med 1989;6:117–125.
13. Mito M, Kusano M, Kawaura Y. Hepatocyte transplantation in man. Transplant Proc 1992;24:3052–3053.
14. Graham FL, Van Der Eb AJ. A new technique for the assay of infectivity of human DNA. Virology 1973;52:456–467.
15. Makdisi WJ, Wu CH, Wu GY. Methods of gene transfer into hepatocytes: progress toward gene therapy. In: Boyer JL, Ockner RK, eds. Progress in Liver Diseases Philadelphia: WB Saunders Co., 1992;10:1–24.
16. Versland MR, Wu CH, Wu GY. Strategies for gene therapy in the liver. Semin Liver Dis 1992;12:332–339.
17. Chen CA, Okayama H. Calcium phosphate-mediated gene transfer: a highly efficient transfection system for stably transforming cells with plasmid DNA. Biotechniques 1988;6:632–638.
18. Gregoriadis G, Leathwood P, Ryman B. Enzyme entrapment in liposomes. FEBS Lett 1971;14:95–99.
19. Fraley RT, Fornari CS, Kaplan S. Entrapment of a bacterial plasmid in phospholipid vesicles: potential for gene transfer. Proc Natl Acad Sci USA 1979;76:3348–3352.
20. Nicolau C, Legrand A, Grosse E. Liposomes as carriers for in vivo gene transfer and expression. Methods Enzymol 1987;149:157–176.
21. Gopal TV. Gene transfer method for transient gene expression, stable transfection, and cotransfection of suspension cell cultures. Mol Cell Biol 1985;5:1188–1190.
22. Ding JL. Stellate- and foci-formation of mouse fibroblast cells transfected with various cancer cell DNA. Cytobios 1989;59:101–114.
23. Tur-Kaspa R, Teicher L, Levine BJ, Skoultchi AI, Shafritz DA. Use of electroporation to introduce biologically active foreign genes into primary rat hepatocytes. Mol Cell Biol 1986;6:716–718.
24. Anderson GL, Evans GA. Introduction and expression of DNA molecules in eukaryotic cells by electroporation. Biotechniques 1988;6:650–660.
25. Potter H, Weir L, Leder P. Enhancer-dependent expression of human k immunoglobulin genes introduced into mouse pre-B lymphocytes by electroporation. Proc Natl Acad Sci USA 1984;81:7161–7165.
26. Fechheimer M, Boylan JF, Parker S, Sisken JE, Patel GL, Zimmer SG. Transfection of mammalian cells with plasmid DNA by scrape loading and sonication loading. Proc Natl Acad Sci USA 1987;84:8463–8467.
27. Luzzatto L. Frontiers in medicine—gene transfer and gene therapy. J Intern Med 1992;231:3–6.
28. Wilson JM, Jefferson DM, Chowdhury JR, Novikoff PM, Johnston DE, Mulligan RC. Retrovirus-mediated transduction of adult hepatocytes. Proc Natl Acad Sci USA 1988;85:3014–3018.
29. Coffin JM. Retroviridae and their replication. In: Fields BN, Knipe DM, eds. Virology. New York: Raven Press, 1990:1437–1500.
30. Muzyczka N. Use of adeno-associated virus for mammalian cells. Curr Top Microbiol Immunol 1992;158:97–129.
31. Friedmann T. Progress toward human gene therapy. Science 1989;244:1275–1281.
32. Dienes HP, Ramadori G, Falke D, Thoenes W. Electron microscopic observations on primary hepatocyte cultures infected with herpes simplex virus types I and II. Virchows Arch B 1984;46:321–332.
33. Miyanohara A, Johnson PA, Elam RL, Dai Y, Witztum JL, Verma IM, Friedmann T. Direct gene transfer to the liver with herpes simplex virus type 1 vectors: transient production of physiologically relevant levels of circulating Factor IX. New Biol 1992;4:238–246.
34. Horwich A, Furtak K, Pugh J, Summers J. Synthesis of hepadnavirus particles that contain replication-defective duck hepatitis B virus genomes in cultured HuH7 cells. J Virol 1990;64:642–650.
35. Chang C, Ganem DE, Lavine JE. Foreign gene delivery and expression in hepatocytes using a hepatitis B virus vector (abst.). Hepatology 1991;14:124A.
36. Demetriou AA, Whiting JF, Feldman D, Levenson SM, Chowdhury NR, Moscioni AD, Kram M, Chowdhury JR. Replacement of liver function in rats by transplantation of microcarrier-attached hepatocytes. Science 1986;233:1190–1192.
37. Demetriou AA, Reisner A, Sanchez J, Levenson SM, Moscioni AD, Chowdhury JR. Transplantation of microcarrier-attached hepatocytes into 90% partially hepatectomized rats. Hepatology 1988;8:1006–1009.
38. Bosman DK, de Haan JG, Smit J, Jorning GGA, Maas MAW, Chamuleau RAFM. Metabolic activity of microcarrier attached liver cells after intraperitoneal transplantation during severe liver insufficiency in the rat. J Hepatol 1989;9:49–58.
39. Kasai S, Sawa M, Hirai S, Nishida Y, Onodera K, Yamamoto T, Mito M. Beneficial effect of hepatocyte transplantation on hepatic failure in rats. Transplant Proc 1992;24:2990–2992.
40. Miyanohara A, Elam RL, Witztum JL, Friedmann T. Long-term transgene expression from genetically modified hepatocytes grafted to the rat liver. New Biol 1992;4:261–267.
41. Gupta S, Aragona E, Vemuru RP, Bhargava KK, Burk RD, Chowdhury JR. Permanent engraftment and function of hepatocytes delivered to the liver: implications for gene therapy and liver repopulation. Hepatology 1991;14:144–149.
42. Ponder KP, Gupta S, Leland F, Darlington G, Finegold M, De Mayo J, Ledley FD, Chowdhury JR, Woo SLC. Mouse hepatocytes migrate to liver parenchyma and function indefinitely after intrasplenic transplantation. Proc Natl Acad Sci USA 1991;88:1217–1221.
43. Vemuru RP, Davidson A, Aragona E, Chowdhury JR, Burk RD, Gupta S. Immune tolerance to a defined heterologous antigen after intrasplenic hepatocyte transplantation: implications for gene therapy. FASEB J 1992;6:2836–2842.
44. Kato K, Hodgson WJB, Onodera K, Matsuda M, Kusano M, Mito M. Developmental regulation of cytochrome P-450 of intrasplenically transplanted fetal hepatocytes in spontaneously hypertensive rats. Transplant Proc 1992;24:2956–2959.
45. Onodera K, Ebata H, Sawa M, Katoh K, Kasai S, Mito M, Nozawa M. Comparative effects of hepatocellular transplantation into the spleen, portal vein, or peritoneal cavity in congenitally ascorbic acid biosynthetic enzyme-deficient rats. Transplant Proc 1992;24:3006–3008.

46. Inagaki M, Ogawa K, Mito M. Retroviral-mediated gene transfer to neonatal rat hepatocytes and intrasplenic transplantation of the transduced hepatocytes. Transplant Proc 1992;24:2969–2970.
47. Sutherland DER, Numata M, Matas AJ, Simmons RL, Najarian JS. Hepatocellular transplantation in acute liver failure. Surgery 1977;82:124–132.
48. Soriano HE, Gest A, Bair D, Vander Straten M, Lewis D, Brandt M, Finegold M, Ledley FD. Hepatocellular transplantation via the umbilical vein in fetal and newborn lamb. Transplant Proc 1992;24:2964–2965.
49. Fuller BJ. Transplantation of isolated hepatocytes. J Hepatol 1988;7:368–376.
50. Gupta S, Chowdhury JR. Hepatocyte transplantation: back to the future. Hepatology 1992;15:156–162.
51. Grossman M, Wilson JM, Raper SE. A novel approach for introducing hepatocytes into the portal circulation. J Lab Clin Med 1993;121:472–478.
52. Dubensky TW, Campbell BA, Villarreal LP. Direct transfection of viral and plasmid DNA into the liver or spleen of mice. Proc Natl Acad Sci USA 1984;81:7529–7533.
53. Benvenisty N, Reshef L. Direct introduction of genes into rats and expression of the genes. Proc Natl Acad Sci USA 1986;83:9551–9555.
54. Yang NS, Burkholder J, Roberts B, Martinell B, McCabe D. In vivo and in vitro gene transfer to mammalian somatic cells by particle bombardment. Proc Natl Acad Sci USA 1990;87:9568–9572.
55. Nicolau C, Le Pape A, Soriano P, Fargette F, Juhel MF. In vivo expression of rat insulin after intravenous administration of the liposome-entrapped gene for rat insulin I. Proc Natl Acad Sci USA 1983;80:1068–1072.
56. Kaneda Y, Iwai K, Uchida T. Increased expression of DNA cointroduced with nuclear protein in adult rat liver. Science 1989;243:375–378.
57. Ferry N, Duplessis O, Houssin D, Danos O, Heard JM. Retroviral-mediated gene transfer into hepatocytes in vivo. Proc Natl Acad Sci USA 1991;88:8377–8381.
58. Markowitz D, Geoff S, Bank A. A safe packaging line for gene transfer: separating viral genes on two different plasmids. J Virol 1988;62:1120–1124.
59. Hersdorffer C, Ward M, Markowitz D, Bank A. Efficient gene transfer in live mice using a unique retroviral packaging line. DNA Cell Biol 1990;9:717–723.
60. Drazan KE, Wu L, Bullington D, Jurin O, Graham F, Berk A, Busuttil RW, Shaked A. In vivo gene transfer to the liver using adenoviral vectors results in high transfection efficiency (abstr). Gastroenterology 1993;104:A897.
61. Wall DA, Wilson G, Hubbard AL. The galactose-specific recognition system of mammalian liver: the route of ligand internalization in rat hepatocytes. Cell 1980;21:79–93.
62. Schwartz A. Trafficking of asialoglycoproteins and the asialoglycoprotein receptor. In: Wu G, Wu C, eds. Liver diseases: targeted diagnosis and therapy using specific receptors and ligands. New York: Marcel Dekker, 1991:3–40.
63. Wu G, Wu C, Rubin M. Acetaminophen hepatotoxicity and targeted rescue: a model for specific chemotherapy of hepatocellular carcinoma. Hepatology 1985;5:709–713.
64. Wu G, Wu C, Stockert R. Model for specific rescue of normal hepatocytes during methotrexate treatment of hepatic malignancy. Proc Natl Acad Sci USA 1983;80:3078–3080.
65. Wu G, Keegan-Rogers V, Franklin S, Midford S, Wu CH. Targeted antagonism of galactosamine toxicity in normal rat hepatocytes in vitro. J Biol Chem 1988;263:4719–4823.
66. Wu GY, Wu CH. Delivery systems for gene therapy. Biotherapy 1991;3:87–95.
67. Wu GY, Wu CH. Receptor-mediated gene delivery and expression in vivo. J Biol Chem 1988;263:14621–14624.
68. Wu CH, Wilson JM, Wu GY. Targeting genes: delivery and persistent expression of a foreign gene driven by mammalian regulatory elements in vivo. J Biol Chem 1989;264:16985–16987.
69. Chowdhury NR, Wu CH, Wu GY, Yerneni PC, Bommaneni VR, Chowdhury JR. Fate of DNA targeted to the liver by asialoglycoprotein receptor-mediated endocytosis in vivo: prolonged persistence in cytoplasmic vesicles after partial hepatectomy. J Biol Chem 1993;268:11265–11271.
70. Chowdhury JR, Hays RM, Wu CH, Bommaneni VR, Yernini PC, Mukhopadhyay B, Wu GY, Chowdhury NR. Disruption of microtubules results in prolonged persistence and expression of genes targeted to the liver in vivo by receptor-mediated endocytosis (abstr). Gastroenterology 1993;104:A981.
71. Wu GY, Wilson JM, Shalaby F, Grossman M, Shafritz DA, Wu CH. Receptor-mediated gene delivery in vivo—partial correction of genetic analbuminemia in Nagase rats. J Biol Chem 1991;266:14338–14342.
72. Grossman M, Wilson JM. Frontiers in gene therapy: LDL receptor replacement for hypercholesterolemia. J Lab Clin Med 1992;119:457–460.
73. Turley SD, Dietschy JM. The metabolism and excretion of cholesterol by the liver. In: Arias IM, Jakoby WB, Popper H, Schachter D, Shafritz DA, eds. The liver: biology and pathobiology. 2nd ed. New York: Raven Press; 1988:617–641.
74. Hoeg JM, Starzl TE, Brewer, Jr. HB. Liver transplantation for treatment of cardiovascular disease: comparison with medication and plasma exchange in homozygous familial hypercholesterolemia. Am J Cardiol 1987;59:705–707.
75. Watanabe Y. Serial inbreeding of rabbits with hereditary hyperlipidemia (WHHL rabbit). Atherosclerosis 1980;36:261–268.
76. Wilson JM, Johnston DE, Jefferson DM, Mulligan RC. Correction of the genetic defect in hepatocytes from the Watanabe heritable hyperlipidemic rabbit. Proc Natl Acad Sci USA 1988;85:4421–4425.
77. Wilson JM, Chowdhury JR. Prospects for gene therapy of familial hypercholesterolemia. Mol Biol Med 1990;7:223–232.
78. Wilson JM, Chowdhury NR, Grossman M, Wajsman R, Epstein A, Mulligan RC, Chowdhury JR. Temporary amelioration of hyperlipidemia in low density lipoprotein receptor-deficient rabbits transplanted with genetically modified hepatocytes. Proc Natl Acad Sci USA 1990;87:8437–8441.
79. Chowdhury JR, Grossman M, Gupta S, Chowdhury NR, Baker, Jr. JR, Wilson JM. Long-term improvement of hypercholesterolemia after ex vivo gene therapy in LDLR-deficient rabbits. Science 1991;254:1802–1805.
80. Wilson JM, Grossman M, Wu CH, Chowdhury NR, Wu GY, Chowdhury JR. Hepatocyte-directed gene transfer in vivo leads to transient improvement of hypercholesterolemia in low density lipoprotein receptor-deficient rabbits. J Biol Chem 1992;267:963–967.
81. Kozarsky K, Wilson JM. Liver-directed gene therapy of LDL receptor-deficient rabbits using recombinant adenovirus. In: Cold Spring Harbor Symposium on "Regulation of Liver Gene Expression in Health and Disease." Cold Spring Harbor, NY: Cold Spring Harbor Laboratory, 1993:197.
82. Goldsmith JC. Steps toward improved safety of treatment in hemophilia B. J Lab Clin Med 1993;121:370–371.
83. Herring SW, Abildgaard C, Shitanishi KT, Harrison J, Gendler S, Heldebrant CM. Human coagulation factor IX: assessment of thrombogenicity in animal models and viral safety. J Lab Clin Med 1993;121:394–405.
84. Thompson AR. Status of gene transfer for hemophilia A and B. Thromb Haemost 1991;66:119–122.
85. Armentano D, Thompson AR, Darlington G, Woo SLC. Expression of human factor IX in rabbit hepatocytes by retrovirus-

mediated gene transfer: potential for gene therapy of hemophilia B. Proc Natl Acad Sci USA 1990;87:6141–6145.
86. Ponder KP, Dunbar RP, Wilson DR, Darlington GJ, Woo SL. Evaluation of relative promoter strength in primary hepatocytes using optimized lipofection. Hum Gene Ther 1991;2:41–52.
87. Palmer TD, Rosman GJ, Osborne WR, Miller AD. Genetically modified skin fibroblasts persist long after transplantation but gradually inactivate introduced genes. Proc Natl Acad Sci USA 1991;88:1330–1334.
88. Horwich AL. Inherited hepatic enzyme defects as candidates for liver-directed gene therapy. Curr Top Microbiol Immunol 1991;168:185–200.
89. Peng H, Armentano D, MacKenzie-Graham L, Shen RF, Darlington G, Ledley FD, Woo SLC. Retroviral-mediated gene transfer and expression of human phenylalanine hydroxylase in primary mouse hepatocytes. Proc Natl Acad Sci USA 1988;85:8146–8150.
90. Grompe M, Jones SN, Loulseged H, Caskey CT. Retroviral-mediated gene transfer of human ornithine transcarbamylase into primary heptocytes of spf and spf-ash mice. Hum Gene Ther 1992;3:35–44.
91. Wu GY, Wu CH. Specific inhibition of hepatitis B viral gene expression in vitro by targeted antisense oligonucleotides. J Biol Chem 1992;267:12436–12439.
92. Offensperger WB, Offensperger S, Walter E, Teubner K, Igloi G, Blum HE, Gerok W. In vivo inhibition of duck hepatitis B virus replication and gene expression by phosphorothioate modified antisense oligodeoxynucleotides. EMBO J 1993;12:1257–1262.
93. Loke SL, Stein CA, Zhang XH, Mori K, Nakanishi M, Subasinghe C, Cohen J, Neckers LM. Characterization of oligonucleotide transport into living cells. Proc Natl Acad Sci USA 1989;86:3474–3478.
94. Woolf TM, Melton DA, Jennings, CGB. Specificity of antisense oligonucleotides in vivo. Proc Natl Acad Sci USA 1992;89:7305–7309.
95. Liang TJ, Makdisi WJ, Sun S, Hasegawa K, Zhang Y, Wands JR, Wu CH, Wu GY. Targeted transfection and expression of hepatitis B viral DNA in human hepatoma cells. J Clin Invest 1993;91:1241–1246.
96. Kuriyama S, Yoshikawa M, Ishizaka S, Tsujii T, Ikenaka K, Kagawa T, Morita N, Mikoshiba K. A potential approach for gene therapy targeting hepatoma using a liver-specific promoter on a retroviral vector. Cell Struct Funct 1991;16:503–510.
97. Huber BE, Richards CA, Krenitsky TA. Retroviral-mediated gene therapy for the treatment of hepatocellular carcinoma: an innovative approach for cancer therapy. Proc Natl Acad Sci USA 1991;88:8039–8043.
98. Askari F, Wilson J. Provocative gene therapy strategy for the treatment of hepatocellular carcinoma. Hepatology 1992;16:273–274.
99. Plautz G, Nabel EG, Nabel GJ. Selective elimination of recombinant genes in vivo with a suicide retroviral vector. New Biol 1991;3(7):709–715.
100. Erickson E. Genes to order. Sci Am 1992;266:112–114.
101. Watson T. Gene therapy research is spread across many disciplines and institutes at NIH. Nature 1992;359:188–189.
102. Caruso M, Panis Y, Gagandeep S, Houssin D, Salzmann JL, Klatzmann D. Regression of established macroscopic liver metastases after in situ transduction of a suicide gene. Proc Natl Acad Sci USA 1993;90:7024–7028.
103. Marino CR, Gorelick FS. Scientific advances in cystic fibrosis. Gastroenterology 1992;103:681–693.
104. Park RW, Grand RJ. Gastrointestinal manifestations of cystic fibrosis: a review. Gastroenterology 1981;81:1143–1161.
105. Yang Y, Raper SE, Cohn JA, Engelhardt JF, Wilson JM. An approach for treating the hepatobiliary disease of cystic fibrosis by somatic gene transfer. Proc Natl Acad Sci USA 1993;90:4601–4605.
106. Rosenfeld MA, Siegfried W, Yoshimura K, Yoneyama K, Fukayama M, Stier LE, Paakko PK, Gilardi P, Stratford-Perricaudet LD, Perricaudet M, Jallat S, Pavirani A, Lecocq JP, Crystal RG. Adenovirus-mediated transfer of a recombinant α-1-antitrypsin gene to the lung epithelium in vivo. Science 1991;252:431–434.
107. Kay MA, Baley P, Rothenberg S, Leland F, Fleming L, Ponder KP, Liu TJ, Finegold M, Darlington G, Pokorny W, Woo SLC. Expression of human α-1-antitrypsin in dogs after autologous transplantation of retroviral transduced hepatocytes. Proc Natl Acad Sci USA 1992;89:89–93.
108. Noel RA, Perez-Rossello J, Henning SJ. Enhancement of gene transfer into intestinal epithelial cell lines (IEC-6 and RIE-1) . an ecotropic retroviral vector (abstr). Gastroenterology 1993; 104:A269.
109. Soriano-Brucher H, Lau C, Hourigan T, Finegold M, Ledley F, Henning SJ. Gene transfer into the intestinal epithelium (abstr). Gastroenterology 1991;100:A252.
110. Jones SN, Grompe M, Munir MI, Veres G, Craigen WJ, Caskey CT. Ectopic correction of ornithine transcarbamylase deficiency in sparse fur mice. J Biol Chem 1990;265:14684–14690.
111. Colombo MP, Ferrari G, Stoppacciaro A, Parenza M, Rodolfo M, Mavilio F, Parmiani G. Granulocyte colony-stimulating factor gene transfer suppresses tumorigenicity of a murine adenocarcinoma in vivo. J Exp Med 1991;173:889–897.
112. Ozturk M, Ponchel F, Puisieux A. p53 as a potential target in cancer therapy. Bone Marrow Transplant 1992;9(Suppl 1):164–170.
113. Baker SJ, Markowitz S, Fearon ER, Willson JKV, Vogelstein B. Suppression of human colorectal carcinoma cell growth by wild-type p53. Science 1990;249:912–915.
114. Colombo MP, Parmiani G. Tumor-cell-targeted cytokine gene therapy. Immunol Today 1991;12:249–250.
115. Gansbacher B, Zier K, Daniels B, Cronin K, Bannerji R, Gilboa E. Interleukin 2 gene transfer into tumor cells abrogates tumorigenicity and induces protective immunity. J Exp Med 1990; 172:1217–1224.
116. Blankenstein T, Qin ZH, Uberla K, Muller W, Rosen H, Volk HD, Diamantstein T. Tumor suppresion after tumor cell-targeted tumor necrosis factor α gene transfer. J Exp Med 1991;173:1047–1052.
117. Zwiebel JA, Freeman SM, Kantoff PW, Cornetta K, Ryan US, Anderson WF. High-level recombinant gene expression in rabbit endothelial cells transduced by retroviral vectors. Science 1989;243:220–222.
118. Nabel EG, Plautz G, Boyce FM, Stanley JC, Nabel GJ. Recombinant gene expression in vivo within endothelial cells of . arterial wall. Science 1989;244:1342–1344.
119. Wilson JM, Birinyi LK, Salomon RN, Libby P, Callow AD, Mulligan RC. Implantation of vascular grafts lined with genetically modified endothelial cells. Science 1989;244:1344–1346.
120. Taniguchi H, Nakauchi H, Iwata H, Amemiya H, Fukao K. Treatment of diabetic mice with encapsulated fibroblasts producing human proinsulin. Transplant Proc 1992;24:2977–2978.
121. Evans CH, Bandara G, Mueller G, Robbins P, Glorioso JC, Georgescu HI. Synovial cell transplants for gene transfer to joints. Transplant Proc 1992;24:2966.

Received July 6, 1993. Accepted October 19, 1993.

Address requests for reprints to: George Y. Wu, M.D., Ph.D., Department of Medicine, Division of Gastroenterology-Hepatology, University of Connecticut Health Center, Room AM-044, 263 Farmington Avenue, Farmington, Connecticut 06030. Fax: (203) 679-3159.